ISSN: 2958-8995. 2958-8987
Doi: 10.59799/APPP6605
No: 7 Val:1 /12/ 2024

Journal of Natural and Applied Sciences URAL

A Quarterly Multidisciplinary Scientific Journal Issued by European Academy for Development and Research / Brussels and Center of Research and Human Resources Development Ramah- Jordan

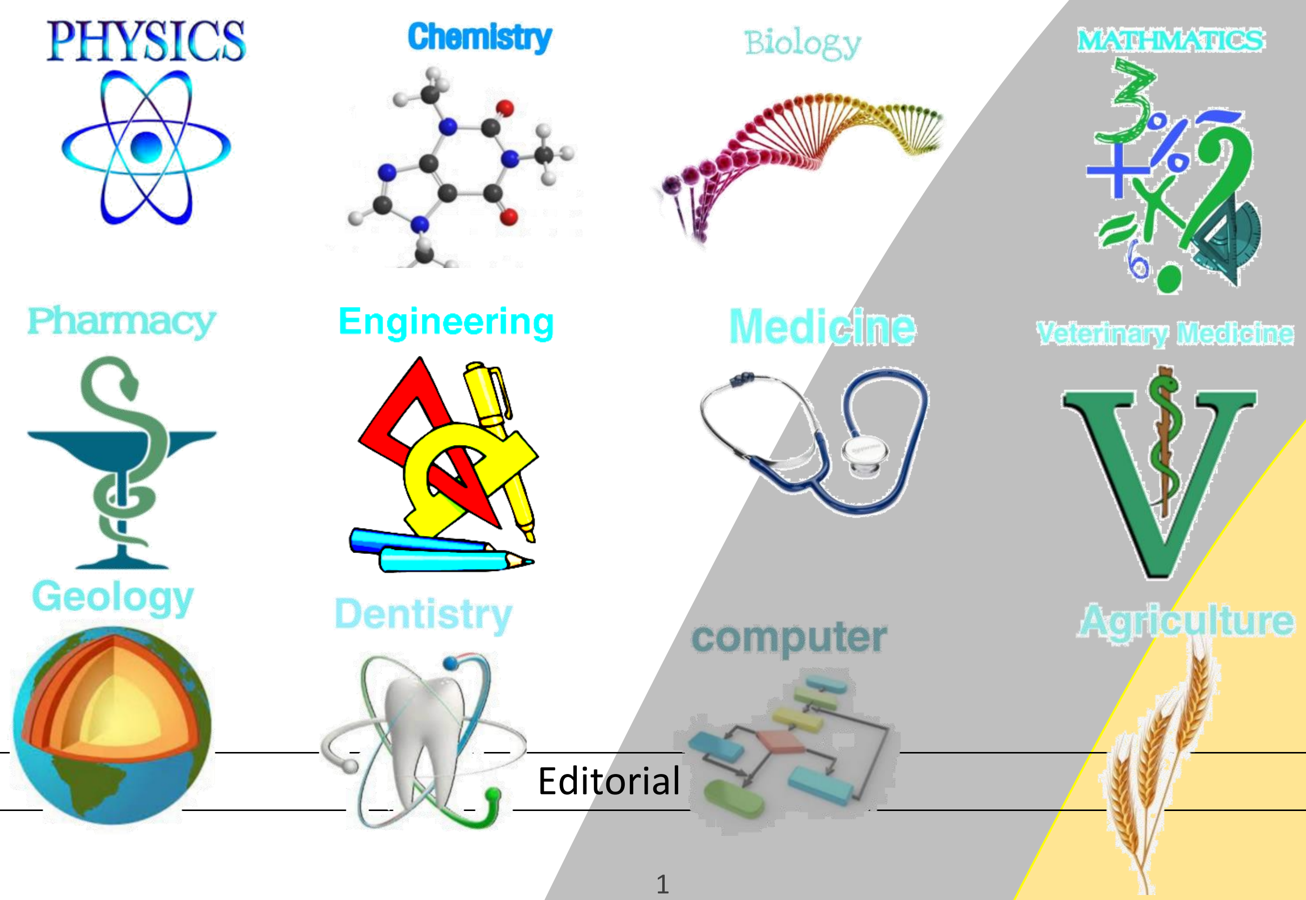

Editorial

Focus & Scope:

Journal of Natural and Applied Sciences URAL

Journal welcomes high quality contributions investigating topics in the fields of Biology, physics, computer science, Engineering, chemistry, Geology, Agriculture, Medicine, Mathematics, Pharmacy, Veterinary, Nursing, Dentistry, and Environment.

Publication specializations in the journal	
Biology	**Chemistry**
Physics	**Geology**
Computer	**Agriculture**
Engineering	**Mathematics**
Medicine	**Pharmacy**
Veterinary	**Dentistry Veternity,**
Environment	**Nursing**

The Journal is Published in English and Arabic

General Supervisor of the Journal

Prof. Dr. Khalid Ragheb Ahmed Al-Khatib

Administrative Title of the Journal:

Amman\ Jordan\ Wasfi Al-Tal \ Gardens

Phone: +962799424774

Index			
No.	Research Title	Researcher	Page No.
1	Oscillation and stability of the solution of some second-order delay differential equations	Raaja Younis Mhoo[1], Their Younis Thanon[2]	6-21
2	Evaluation of CA15-3 Level with Some Immunological and Biochemical Variables in the Blood Serum of Women with Breast Cancer in Kirkuk Governorate.	[1]Zina Abdulmunem Abdulrazaaq Al-doory, [2]Hanan Shihab Ahmad, [3]Esraa Ali Abdul kareem Al-Samarai	22-35
3	Enhance Penetration Testing Techniques to Improve Cybersecurity with NetLogo, Nmap, and Wireshark	Huthaifa Mohammed Kanoosh[1] Mohammed Muayad Sultan[2] Ammar Farooq Abbas[3]	36-48
4	The Zagreb index of the idempotent divisor graph of commutative ring	Luma Ahmed Khaleel	49-57
5	دراسة عدد من العوامل المؤثرة على كفاءة ازالة صبغة الليشمانيا من محاليلها المائي بطريقة التلبيد الكهربائي باستخدام اقطاب الستانلس استيل	يوسف صباح رضوان(1) , احمد سعيد(2) عثمان	58-80
6	Finding Ideal Points in PG(3,2), PG(3,3)	Hajir Hayder Abdullah[1]*, Sahbaa Abd alstar Younus[2], Wafa Younus Yahya[3]	81-97
7	On Some Mappings in Intuitionistic Topological Spaces	[1]Saleh,B.H, [2]Yassen, S.R, [3]Amina, K. H	98-115
8	On ∗-I-open and -I-open Sets in Ideal Topological Spaces	1,*Ali Shaker Mahmoud 2,*Yassen, S.R	116-125
9	The effect of bio-prepared zinc nanoparticles from the fungus Verticillium lecanii on combating third-instar larvae of the date moth Ephestia cautella	**1** Doaa Abdulmajeed Mohamed Hisham naji hameed2	126-143
10	Study on the Existence of Solutions for Some Singular Nonlinear Equations on Exterior Domain	Mageed Hameed Al ,O1thman Mahmood Alwan 2 Sinan Omar Ibrahim3^	144-155
11	Solve System of Nonlinear Fredholm Integro-Differential Equations of Second Kind by using Quintin B-Spline	Yusr Hamad Jassim1, Borhan F. Jumaa2 and Ghassan E. Arif3	156-175
12	Some Properties on Infra Soft Nano Open(Closed) Sets	L1eqaa M. Saeed Hussein, E2, * kram A. Saleh, S3abih W. Askandar	176-185

Oscillation and stability of the solution of some second-order delay differential equations

Raaja Younis Mhoo[1], Their Younis Thanon[2]
[1,2]Department of Mathematics, College of Computer Sciences and Mathematics, University of Mosul, Mosul, Iraq
Corresponding author: [1]rajaamhoo@uomosul.edu.iq, [2]thairyounis59@uomosul.edu.iq

Oscillation and stability of the solution of some second-order delay differential equations

Raaja Younis Mhoo[1], Their Younis Thanon[2]
[1,2]Department of Mathematics, College of Computer Sciences and Mathematics, University of Mosul, Mosul, Iraq
Corresponding author:[1]rajaamhoo@uomosul.edu.iq, [2]thairyounis59@uomosul.edu.iq

Abstract:

In this research, discussing some oscillation measures for second-order delay differential equations through some important theories, and we reinforced that with some new and modified examples. We also studied the stability of this type of equations and used the Laplace method and its inverse, where we reached accurate results. These types of equations were in the form of:

$[r(t)\big(x(t)\big) + p(x)x(t-\tau))']' + q(t)f\big(x(t-\delta)\big) = 0,$

Where, $t \geq t_0$, τ and δ are nonnegative constants, $r, p, q \in C([t_0, \infty), R)$, and $f \in C(R, R)$

Keywords: Second-order delay differential equations**;** Oscillation; Criteria; Stability; Laplace transform; Inverse Laplace transform.

1.Introduction

Delay differential equations are referred to as time-delay systems, systems with after -effect, memory, time-delay, hereditary systems equations with deviating argument, or differential-difference equations [12].

Time-delay systems, where the rate of change in state depends on both current and past variables, are common phenomena in various scientific and engineering fields such as machining processes, chemical processes, wheel dynamics, feedback controller dynamics, and population dynamics. However, time delays often cause system instability, which can lead to poor performance, unwanted noise, or potential damage in engineering applications. For this reason, the study of dynamical systems with time delays has received significant attention over the past decades [9].

Second-order neutral delay differential equations are used in many fields such as vibrating masses attached to an elastic bar, variation problems, etc. (See [1].)

This study focuses on studying the oscillation and stability of the second-order delay differential equation. Everything that follows will be supported by theories and examples that explain the oscillation and stability of this type of equations [11].

Consider the second-order neutral delay differential equation

$$[r(t)\big(x(t)\big) + p(x)x(t-\tau))']' + q(t)f\big(x(t-\delta)\big) = 0, \qquad (1.1)$$

Where, $t \geq t_0$, τ and δ are nonnegative constants, $r, p, q \epsilon C([t_0, \infty), R)$, and $f \in C(R, R)$
Now, we will assume that

$$(a)\ q(t) \geq 0; r(t) > 0, \int_0^{\infty} (1/r(s))ds = \infty; f(x)/x \geq \gamma > 0\ for\ x \neq 0.$$

And we will mention some special cases oscillation criteria of eq. (1.1) as follows:

i. delay equation $(p(t) \equiv 0)$:

$$[r(t)x'(t)]' + q(t)f\big(x(t-\delta)\big) = 0, \qquad (1.2)$$

ii. ordinary differential equation$(p(t) \equiv 0, \delta)$:

$$[r(t)x'(t)]' + q(t)f\big(x(t)\big) = 0, \qquad (1.3)$$

The eq. (1.2) and eq. (1.3) are changed in to eq. (1.4) and eq. (1.5) respectively as follows, if

$r(t) = 1, f\big(x(t)\big) = x(t)$

$$\acute{x}(t) + q(t)x(t-\delta) = 0, \qquad (1.4)$$

$$\acute{x}(t) + q(t)x(t) = 0, \qquad (1.5)$$

With respect to eq. (1.5) there is some important oscillation criteria among them:

- eq. (1.5) is oscillatory (See Leighton [2]) if:

$$\int_{t_0}^{\infty} q(s)ds = \infty \qquad (1.6)$$

- eq. (1.5) is oscillatory (See Wintner [3]) if:

$$lim_{t\to\infty} \frac{1}{t} \int_{t_0}^{t} \int_{t_0}^{s} q(u)duds = \infty. \qquad (1.7)$$

- eq. (1.5) is oscillatory (See Hartman [4]) if:

$$lim_{t\to\infty} inf \frac{1}{t} \int_{t_0}^{t} \int_{t_0}^{s} q(u)duds < lim_{t\to\infty} sup \frac{1}{t} \int_{t_0}^{t} \int_{t_0}^{s} q(u)duds \leq$$
$$-\infty < \infty, \qquad (1.8)$$

- eq. (1.5) is oscillatory (See Kamenev [5]) if:

$$lim_{t\to\infty} sup \frac{1}{t^n} \int_{t_0}^{t} (t-s)^n q(u)ds = \infty, \qquad (1.9)$$

for some integer $n > 1$

For the oscillation of the nonlinear differential eq. (1.3), one can see [7] and references cited therein, with respect to eq. (1.4), in [8], Waltman generalized Leighten's criterion of eq. (1.4) and showed that eq. (1.4) is oscillatory if $q(t) \geq 0$ and

$$\int_{t_0}^{\infty} q(s)ds = \infty$$

2. Some oscillation criteria.

Theorem 1. Let assumption (a) hold. And suppose that for each $T_0 \geq t_0$, there exist some $H \in K, g \in C^1([t_0, \infty), R),\ and\ a, b, c \in R\ \ with\ T_0 \leq a < c < b$ such that one of the following conditions is satisfied:

(W_1) $-1 < \alpha \leq p(t) \leq 0$ and the following inequality holds:

$$\frac{1}{H(c,a)} \int_a^c H(s,a)\emptyset_2(s)ds + \frac{1}{H(b,s)} \int_c^b H(b,s)\emptyset_2(s)ds$$
$$> \frac{1}{4}(\frac{1}{H(c,a)} \int_a^c r(s-\delta)v(s)h_1^2(s,a)ds$$
$$+ \frac{1}{H(b,s)} \int_c^b r(s-\delta)v(s)h_1^2(b,c)ds \qquad (2.1)$$

(W_2) $0 \leq p(t) \leq 1$ and the following inequality holds:

$$\frac{1}{H(c,a)} \int_a^c H(s,a)\emptyset_1(s)ds + \frac{1}{H(b,s)} \int_c^b H(b,s)\emptyset_1(s)ds$$
$$> \frac{1}{4}(\frac{1}{H(c,a)} \int_a^c r(s-\delta)v(s)h_1^2(s,a)ds$$
$$+ \frac{1}{H(b,s)} \int_c^b r(s-\delta)v(s)h_1^2(b,c)ds \qquad (2.2)$$

Then the neutral eq. (1.1) is oscillatory.

Theorem 2. Suppose that for each $T_0 \geq t_0$, and let (a) hold. Then there exist some $H \in K, g \in C^1([t_0, \infty), R),\ and\ a, c \in R\ \ with\ T_0 \leq a < c$ such that one of the following conditions is satisfied:

(W_3) the following inequality holds when $0 \leq p(t) \leq 1$

$$\int_a^c H(s-a)\{\emptyset_1(s) + \emptyset_1(2c-s)\}ds$$
$$> \frac{1}{4} \int_a^c [r(s-\delta)v(2s-s-\delta)v(2c-\delta)]h^2(s-a)ds. \qquad (2.3)$$

(W_4) the following inequality holds when $-1 < \alpha \leq p(t) \leq 0$

$$\int_a^c H(s-a)\{\emptyset_2(s) + \emptyset_2(2c-s)\}ds$$
$$> \frac{1}{4} \int_a^c [r(s-\delta)v(2s-s-\delta)v(2c-\delta)]h^2(s$$
$$-a)ds. \qquad (2.4)$$

Hence, eq. (1.1) is oscillatory.

Proof. Let $b = 2c - a$. Then $H(b-a) = H(c-a) = H((b-a)/2)$, and for any $f \in L[a,b]$, we have

$$\int_c^b f(s)ds = \int_c^b f(2s-s)ds \tag{2.5}$$

Hence,

$$\int_c^b H(b-s)\emptyset_1(s)ds = \int_c^b H(s-a)\emptyset_1(2s-s)ds \tag{2.6}$$

And

$$\int_c^b r(s-\delta)v(s)h^2(b-s)ds = \int_c^b r(2c-s-\delta)v(2c-s)h^2(s-a)ds \tag{2.7}$$

It follows that if (W_3) holds, then, by implication, (W_2) holds for $H \in K_0$ and $g \in C^1([t_0,\infty),R)$

Hence, by theorem 1 the eq. (1.1) is oscillatory

Theorem 3. Assumption (a) and $lim_{t\to\infty} R(t) = \infty$ hold. Then the neutral eq. (1.1) is oscillatory If for each $l \geq t_0$ and there exists $\omega > 1$ one of the following conditions is satisfied.

(Y_5) the following inequality holds when $0 \leq p(t) \leq 1$

$$lim_{t\to\infty} sup \frac{1}{t^{\omega-1}} \int_l^t [R(s) - R(l)]^\omega \gamma q(s)[1 - p(s-\delta)]\, ds > \frac{\omega^2}{2(\omega-1)} \tag{2.8}$$

and

$$lim_{t\to\infty} sup \frac{1}{t^{\omega-1}} \int_l^t [R(t) - R(s)]^\omega \gamma q(s)[1 - p(s-\delta)]\, ds > \frac{\omega^2}{4(\omega-1)} \tag{2.9}$$

(Y_6) the following inequality holds when $-1 < \alpha \leq p(t) \leq 0$

$$lim_{t\to\infty} sup \frac{1}{t^{\omega-1}} \int_l^t [R(s) - R(l)]^\omega \gamma q(s)\, ds > \frac{\omega^2}{4(\omega-1)} \tag{2.10}$$

And

$$lim_{t\to\infty} sup \frac{1}{t^{\omega-1}} \int_l^t [R(t) - R(s)]^\omega \gamma q(s)\, ds > \frac{\omega^2}{4(\omega-1)} \tag{2.11}$$

Theorem 4. Suppose (a), $0 \leq p(t) \leq 1$, and the following inequality holds:

$$\lim_{t\to\infty} inf R(t) \int_t^\infty \gamma q(s)[1 - p(s - \delta)]ds > \frac{1}{4}, \tag{2.12}$$

where $R(t) = \int_{t_0}^t 1/r(s-\delta))ds$. Then every solution of eq. (1.1) is oscillatory.

3. Stability of the solution of some second-order delay differential equations:

Let's concentrate on determining the inverse Laplace transform of $X(s)$ to finding the solution $x(t)$ in lag domain. To proceed, we need to rewrite the denominator in terms of a characteristic equation [10]. Let's define:

$$h(s,p) = s^2 + 2\zeta s + 1 + p - pe^{(-s\tau)} \quad (3.1)$$

The characteristic equation becomes $h(s,p) = 0$.

Now, we can factorize the denominator as follows:

$$s^2 + 2\zeta s + 1 + p - pe^{(-s\tau)} = (s - s_1)(s - s_2) \quad (3.2)$$

Where, s_1 and s_2 are the roots of the characteristic equation $h(s,p) = 0$.

using partial fraction decomposition, we can express $X(s)$ as:

$$X(s) = A/(s - s_1) + B/(s - s_2) \quad (3.3)$$

to find the values of A and B, we multiply both sides by the denominator $(s - s_1)(s - s_2)$ and then substitute $s = s_1$ and $s = s_2$:

$$(s - s_1)(s - s_2)X(s) = A(s - s_2) + B(s - s_1) \quad (3.4)$$

Next, we can solve for A and B by evaluating the equation at $s = s_1$ and $s = s_2$:

$$A(s_1 - s_2) = (s_1 - s_2)X(s_1) \quad (3.5)$$

$$B(s_2 - s_1) = (s_2 - s_1)X(s_2) \quad (3.6)$$

Simplifying, we find:

$$A = (s_1 - s_2)X(s_1) \;/(s_1 - s_2) \quad (3.7)$$

$$B = (s_2 - s_1)X(s_2) \,/\, (s_2 - s_1) \quad (3.8)$$

Now, we can rewrite $X(s)$ as:

$$X(s) = [(s_1 - s_2)X(s_1) \,/\, (s_1 - s_2)] \,/\, (s - s_1) + [(s_2 - s_1)X(s_2) \,/\, (s_2 - s_1)] \,/\, (s - s_2) \quad (3.9)$$

To find the inverse Laplace transform of $X(s)$ as $\mathcal{L}^{-1}[X(s)] = r$, where

$$r = \sum[i = 1\ to\ r]\sum[k = 1\ to\ m_i]R_{ik} * \tau^{(k-1)} * (k - 1)! * e^{(p_{i\tau})}, \quad (3.10)$$

We can use the knowledge that the inverse Laplace transform of $e^{(p_{i\tau})}$ is $\delta(t - \tau)$, where $\delta(t)$ is the Dirac delta function.

The expression for the inverse Laplace transform can be rewritten as:

$$\mathcal{L}^{-1}[X(s)] = \sum[i = 1\ to\ r]\sum[k = 1\ to\ m_i]R_{ik} * \tau^{(k-1)} * (k - 1)! * e^{(p_{i\tau})} \quad (3.11)$$

Where, τ_i denotes the specific value of τ associated with each term.

Therefore, the inverse Laplace transform of $X(s)$ that satisfies $\mathcal{L}^{-1}[X(s)] = r$ is given by:

$$x(t) = \sum[i = 1\ to\ r]\sum[k = 1\ to\ m_i]R_{ik} * \tau^{(k-1)} * (k - 1)! * \delta(t - \tau_i), \tag{3.12}$$

where each term in the double summation corresponds to a specific pole p_i, its multiplicity m_i, and the corresponding residue R_{ik}. The term $\tau^{(k-1)} * (k - 1)!$ accounts for the power and factorial associated with each delay term.

By evaluating the residue R_{ik} for each term and plugging them into the above expression, we can find the solution $x(t)$ in the time domain that satisfies $\mathcal{L}^{-1}[X(s)] = r$.

4. Applications:

Example 1: Consider the following neutral delay equation:

$$[y(t) + y(t - 1)]'' + 2y(t - 2)e^{(t-1)} = 0, \tag{4.1}$$

Where, the delay terms are $t - 1\ and\ t - 2$.

To determine the oscillatory behavior of eq. (4.1), we will apply theorem 2. Let's go through the steps:

Step 1: Verify assumption (a).
Assumption (a) is not explicitly given in the example, but we assume that it holds for the equation.

Step 2: Define the functions and parameters.
Let $\gamma = 1, g(t) = 0, k(t) = 1, and\ R(t) = \int_4^t (1 / r(s - \delta))\,ds = t - 4$. Thus,
$v(t) = 1\ and\ H(t,s) = [R(t) - R(s)]^\lambda = (t - s)^\lambda$.

Step 3: Evaluate the limits.
We need to evaluate the following limit:

$$lim_{t\to\infty}[1 / (t - 4)^{(\lambda-1)}] \int_i^t (s - l)^\lambda * 2 * e^{(t-1)} / \sqrt{(t^3(t - 1))}\,ds,$$

where i is a constant.

To evaluate the limit
$lim_{t\to\infty}[1 / (t - 4)^{(\lambda-1)}] \int_i^t (s - l)^\lambda * 2 * e^{(t-1)} / \sqrt{(t^3(t - 1))}\,ds,$ we can apply the limit properties and integration techniques. Let's proceed with the evaluation:

Step 1: Rewrite the integral in terms of a new variable.
Let $u = s - l, so\ du = ds$. The integral becomes:

$$\int_{0}^{(t-l)} u^{\lambda} * 2 * e^{(t-1)} / \sqrt{(t^{3}(t-1)} du.$$

Step 2: Substitute the new variable back into the limit expression.
the limit becomes:

$$lim_{t\to\infty} [1 / (t - 4)^{(\lambda-1)}] \int_{0}^{(t-l)} u^{\lambda} * 2 * e^{(t-1)} / \sqrt{(t^{3}(t-1)} du.$$

Step 3: Evaluate the limit and integral separately.
First, let's focus on the integral part. Evaluate the integral:

$$I = \int_{0}^{(t-l)} u^{\lambda} * 2 * e^{(t-1)} / \sqrt{(t^{3}(t-1)} du. \quad (4.2)$$

Step 4: Simplify the integral.
Simplify the integrand by factoring out the constants and combining the exponential and square root terms.

$$I = 2 * e^{(t-1)} * \int_{0}^{(t-l)} u^{\lambda} / \sqrt{(t^{3}(t-1)} du \quad (4.3)$$

Step 5: Evaluate the integral.
Evaluate the integral I using appropriate integration techniques or numerical methods.

Once we have obtained the value of the integral I, we can proceed to evaluate the limit:

$$lim_{t\to\infty} [1 / (t - 4)^{(\lambda-1)}] \int_{i}^{t} (s - l)^{\lambda} * 2 * e^{(t-1)} / \sqrt{(t^{3}(t-1))} ds,$$

Finally,

Step 4: Verify the conditions (W_3) and (W_4).

To verify the conditions (W_3) and (W_4) of theorem 2, we need to examine certain properties of the functions involved. Let's go through each condition:

Condition (W_3):
The condition (W_3) requires that the function $q(t)$ satisfies the following inequality for some positive constant M:
$|q(t)| \leq M / t^{a}$

To check this condition, we need to analyze the properties of the function q(t) and determine if its magnitude is bounded above by M / t^{a} for all t.

1. Examine the function q(t) and determine if it is bounded above by M / t^{a}, where $M\ and\ \alpha$ are positive constants.

2. If there exist positive constants $M \; and \; \alpha$ such that $|q(t)| \; \leq \; M \,/\, t^{a}$, then condition (Y_3) is satisfied.

Condition (W_4):
The condition (W_4) requires that the function $f(x)$ satisfies the following inequality for some positive constant N:
$|f(x)| \leq \; N \; * \; x^{\beta}$

To verify this condition, we need to analyze the properties of the function $f(x)$ and determine if its magnitude is bounded above by $N \; * \; x^{\beta}$ for all x.

1. Examine the function $f(x)$ and determine if it is bounded above by $N \; * \; x^{\beta}$, where N and β are positive constants.
2. If there exist positive constants $N \; and \; \beta$ such that $|f(x)| \; \leq \; N \; * \; x^{\beta}$, then condition (Y_4) is satisfied.

Therefore, theorem 2 are satisfied. If we can find suitable values for λ and the constants in the inequalities, and if the conditions are satisfied, then we can conclude that eq. (4.1) is oscillatory.

Example 2: Consider the neutral delay equation:

$$[x(t) \; + \; a\,x(t \; - \; \tau)]'' \; + \; q(t)\,x(t \; - \; \delta) \; = \; 0, \qquad (4.4)$$

Where, $-1 \; < \; a \; < \; 1, \tau \; = \; 3, \delta \; = \; 1$, and the functions and parameters are defined as follows:

$p(t) \; = \; p, \tau \; = \; 3, \delta \; = \; 1,$
$r(t) \; = \; 1 \,/\, (2(t \; + \; 1)),$
$q(t) \; = \; 2\alpha t \,/\, (t^{2} \; - \; 1)^{2},$

We will apply theorem 4 to determine the oscillatory behavior of eq. (4.4). Here are the steps:

Step 1: Verify Assumption (a).
Assumption (a) is assumed to hold for the equation.

Step 2: Define the functions and parameters.
Let $R(t) \; = \; \int_1^t t(1 \,/\, r(s \; - \; \delta)) \, ds \; = \; t^{2} \; - \; 1$. Additionally, we have $p(t) \; = \; p$, where $0 \; \leq \; p \; \leq \; 1$, and $\gamma \; > \; 0$.

Step 3: Evaluate the limit.
We need to evaluate the following limit:

$$lim_{t\to\infty} \, R(t) \int_t^{\infty} \gamma q(s)[1 \; - \; p(s \; - \; \delta)] \, ds.$$

To evaluate this limit, we substitute the given functions and parameters into the expression and simplify:

$$lim_{t\to\infty}\,(t^2\,-\,1)\int_t^{\infty}\gamma q(s)[1\,-\,p(s\,-\,\delta)]\,ds$$

$$=lim_{t\to\infty}\,(t^2\,-\,1)\int_t^{\infty}\,\gamma(2\alpha s\,/\,(s^2\,-\,1)^2)[1\,-\,0.5(s\,-\,1)]\,ds$$

$$=\,\gamma\alpha lim_{t\to\infty}\,(t^2\,-\,1)\int_t^{\infty}\,(2s\,/(s^2\,-\,1)^2)[1\,-\,0.5s\,+\,0.5]\,ds$$

$$=\,\gamma\alpha\,lim_{t\to\infty}\,(t^2\,-\,1)\int_t^{\infty}\,(2s\,/\,(s^2\,-\,1)^2)(1\,+\,0.5s\,-\,0.5)\,ds$$

$$=\,\gamma\alpha\,lim_{t\to\infty}\,(t^2\,-\,1)\int_t^{\infty}\,(s\,/\,(s^2\,-\,1)^2)(2\,+\,s\,-\,1)\,ds$$

$$=\,\gamma\alpha\,lim_{t\to\infty}\,(t^2\,-\,1)\int_t^{\infty}\,(s\,/\,(s^2\,-\,1)^2)(s\,+\,1)\,ds \qquad (4.5)$$

Step 4: Verify the inequality
$p(t) = p = 0.5, \tau = 3, \delta = 1,$
$r(t) = 1\,/\,(2(t + 1)),$
$q(t) = 2\alpha t\,/\,(t^2 - 1)^2,$

The inequality above is:

$$(lim\,inf)_{\top}(t\to\infty)\,R(t)\int_t^{\infty}\,\gamma q(s)[1-p(s-\delta)]ds\,>\,1/4.$$

Substituting the expressions for $R(t), \gamma, p$, and $q(t)$, we get:

$$lim_{t\to\infty}inf\,(t^2\,-\,1)\int_t^{\infty}\,\gamma(2\alpha s\,/\,(s^2\,-\,1)^2)[1\,-\,0.5(s\,-\,1)]\,ds\,>\,1/4.$$

Simplifying further, we have:

$$lim_{t\to\infty}inf\,(t^2\,-\,1)\int_t^{\infty}\,\gamma(2\alpha s\,/\,(s^2\,-\,1)^2)(0.5s\,+\,0.5)\,ds\,>\,1/4.$$

Expanding and rearranging the terms, we obtain:

$$lim_{t\to\infty}inf\,(t^2\,-\,1)\int_t^{\infty}\,(\alpha\gamma s^2+\alpha\gamma s)\,/\,(s^2\,-\,1)^2\,ds\,>\,1/4.$$

To verify the inequality, we need to evaluate the integral and the limit. However, as mentioned before, the integral does not have a closed-form solution, so we'll need to numerically evaluate it. Similarly, the limit requires numerical approximation.

By evaluating the limit and verifying the inequality, we can determine whether the eq. (4.4) is oscillatory according to theorem 4.

Example 3: Consider the following delay differential equation:

$$\ddot{x}(t) + 2\zeta \dot{x}(t) + (1 + p)x(t) = qe^{(-st-\tau)} \quad (4.6)$$

Where, ζ, p and q are constants and τ is delay value.
To solve this equation using Laplace transforms, we can apply the Laplace transform to both sides of the equation. The Laplace transform of a derivative $\dot{x}(t)$ is denoted as $sX(s) - x(0)$, where $X(s)$ is the Laplace transform of $x(t)$ and $x(0)$ is the initial condition of $x(t)$. Similarly, the Laplace transform of the second derivative $\ddot{x}(t)$ is $s^2X(s) - sx(0) - \dot{x}(0)$.

Taking the Laplace transform of both sides of the equation, we have:

$$\mathcal{L}[\ddot{x}(t)] + 2\zeta\mathcal{L}[\dot{x}(t)] + (1 + p)\mathcal{L}[x(t)] = \mathcal{L}\left[qe^{(-st-\tau)}\right] \quad (4.7)$$

Using the properties of Laplace transforms, we have:

$$s^2X(s) - sx(0) - \dot{x}(0) + 2\zeta(sX(s) - x(0)) + (1 + p)X(s) = Q/(s + s') \quad (4.8)$$

Where, $X(s)$is the Laplace transform of $x(t), x(0)$ is the initial value of $x(t), \dot{x}(0)$ is the initial value of $\dot{x}(t), Q$ is the Laplace transform of $qe^{(-s\tau)}$, and $s' = s + \zeta$. Rearranging the equation:

$$(s^2 + 2\zeta s + 1 + p)X(s) - sx(0) - \dot{x}(0) - 2\zeta x(0) = Q/(s + s') \quad (4.9)$$

Now, let's consider the initial conditions. Assuming $x(0) = a$ and $\dot{x}(0) = b$, we can substitute these values into the equation:

$$(s^2 + 2\zeta s + 1 + p)X(s) - sa - b - 2\zeta a = q/s + s/(s + s) \quad (4.10)$$

Now, we can solve for X(s):

$$X(s) = [sx(0) + \dot{x}(0) - 2\zeta x(0) + Q/(s + s')] / [s^2 + 2\zeta s + (1 + p)] \quad (4.11)$$

let's rewrite the expression for $X(s)$ as:

$$X(s) = [sx(0) + \dot{x}(0) - 2\zeta x(0) + Q/(s + s')] / [s^2 + 2\zeta s + (1 + p)] \quad (4.12)$$

To decompose this expression into partial fractions, we assume that the denominator factors into linear factors. The decomposition has the form:

$$X(s) = A/(s - \alpha) + B/(s - \beta) + \ldots$$

Where, $A, B, \ldots$ are the coefficients to be determined, and $\alpha, \beta, \ldots$ are the roots of the denominator polynomial. To determine the coefficients $A, B, \ldots$, we need to perform the partial fraction decomposition. To do this, we need to get the roots of the denominator polynomial $s^2 + 2\zeta s + (1 + p)$.

The roots can be found by solving the quadratic equation:

$$s^2 + 2\zeta s + (1 + p) = 0 \qquad (4.13)$$

let's denote the roots as α and β:

$$s^2 + 2\zeta s + (1 + p) = (s - \alpha)(s - \beta) = 0 \qquad (4.14)$$

Once we have the roots, we can express the inverse Laplace transform of $X(s)$ in terms of these roots and the initial conditions $x(0)$ and $x^{\cdot}(0)$.

To determine the coefficients A and B, we can use the method of partial fractions. multiplying both sides of the equation by the denominator (s - α) (s - β), we have:

$[s^2 + 2\zeta s + (1 + p)]X(s) = (A/ (s - \alpha) + B/ (s - \beta)) * (s - \alpha) (s - \beta)$

Expanding and simplifying the right side, we get:

$s^2X(s) + 2\zeta sX(s) + (1 + p) X(s) = A (s - \beta) + B (s - \alpha)$

Now, we substitute the expression for $X(s)$ and rearrange the equation:

$$[s^2 + 2\zeta s + (1 + p)](A/(s - \alpha) + B/(s - \beta)) = A(s - \beta) + B(s - \alpha) \qquad (4.15)$$

Next, we equate the coefficients of corresponding powers of s on both sides. The coefficient of s^2 on the left side is 1, and on the right side, it is $A + B$. The coefficient of s is 2ζ on the left side, and on the right side, it is $-A\alpha - B\beta$. The constant term on the left side is $(1 + p)$, and on the right side, it is $-A\beta - B\alpha$.

Setting up the equations based on the coefficients:

$$A + B = 1$$
$$-A\alpha - B\beta = 2\zeta$$
$$-A\beta - B\alpha = 1 + p \qquad (4.16)$$

Solving these equations will give us the values of A and B, which we can then use to compute the inverse Laplace transform.

So determine A and B, we need to find the values of α and β. These roots can be obtained by solving the quadratic equation:

$$s^2 + 2\zeta s + (1 + p) = 0 \qquad (4.17)$$

Using the quadratic formula, the roots α and β can be expressed as:

$$\alpha = (-2\zeta + \sqrt{(4\zeta^2 - 4(1 + p)))} / 2$$

$$\beta = (-2\zeta - \sqrt{(4\zeta^2 - 4(1 + p)))} / 2$$

Once we have the roots α and β, we can substitute them back into the equation for $X(s)$ and find the coefficients A and B using algebraic methods or simultaneous equations.

Substituting α and β into this equation, we have:

$$X(s) = A / (s - (-2\zeta + \sqrt{}(4\zeta^2 - 4(1 + p))) / 2) + B / (s - (-2\zeta - \sqrt{}(4\zeta^2 - 4(1 + p))) / 2) \qquad (4.18)$$

Simplifying the expressions:

$$X(s) = A / (s + 2\zeta - \sqrt{}(4\zeta^2 - 4(1 + p)) / 2) + B / (s + 2\zeta + \sqrt{}(4\zeta^2 - 4(1 + p)) / 2) \qquad (4.19)$$

Combining the fractions:

$$X(s) = (A * (s + 2\zeta + \sqrt{}(4\zeta^2 - 4(1 + p))) + B * (s + 2\zeta - \sqrt{}(4\zeta^2 - 4(1 + p)))) / (s + 2\zeta - \sqrt{}(4\zeta^2 - 4(1 + p))) * \left(s + 2\zeta + \sqrt{4\zeta^2 - 4(1 + p)}\right) \qquad (4.20)$$

let's proceed with the partial fraction decomposition:

$$X(s) = (A * (s + 2\zeta + \sqrt{(4\zeta^2 - 4(1 + p))}) + B * (s + 2\zeta - \sqrt{(4\zeta^2 - 4(1 + p))})) / ((s + 2\zeta - \sqrt{(4\zeta^2 - 4(1 + p))}) * (s + 2\zeta + \sqrt{(4\zeta^2 - 4(1 + p))}))$$

$$= A / (s + 2\zeta + \sqrt{(4\zeta^2 - 4(1 + p))}) + B / (s + 2\zeta - \sqrt{(4\zeta^2 - 4(1 + p))}) \quad (4.21)$$

Now, we can find the inverse Laplace transform of each term using standard Laplace transform tables or formulas. The inverse Laplace transform of $A / (s + 2\zeta + \sqrt{(4\zeta^2 - 4(1 + p))})$ and $B / (s + 2\zeta - \sqrt{(4\zeta^2 - 4(1 + p))})$ can be computed separately.

let's denote the inverse Laplace transform of $A / (s + 2\zeta + \sqrt{(4\zeta^2 - 4(1 + p))})$ as $x_1(t)$ and the inverse Laplace transform of $B / (s + 2\zeta - \sqrt{(4\zeta^2 - 4(1 + p))})$ as $x_2(t)$.

Once these inverse Laplace transforms are computed, the overall inverse Laplace transform of X(s) can be written as:

$$x(t) = x_1(t) + x_2(t) \quad (4.22)$$

To study the stability of the given differential equation using Laplace transforms, we need to analyze the poles of the transfer function obtained from the Laplace transform.

The transfer function is given by:

$$H(s) = X(s) / F(s) = [(sa + b + 2\zeta a) / [(s^2 + 2\zeta s + 1 + p) - q/s - s/(s + s)]] \quad (4.23)$$

To study stability, we need to analyze the poles of the transfer function $X(s)$.

the transfer function $X(s)$ can be written as:

$$X(s) = (A * (s + 2\zeta + \sqrt{(4\zeta^2 - 4(1 + p))}) + B * (s + 2\zeta - \sqrt{(4\zeta^2 - 4(1 + p))})) / ((s + 2\zeta - \sqrt{(4\zeta^2 - 4(1 + p))}) * (s + 2\zeta + \sqrt{(4\zeta^2 - 4(1 + p))})) \quad (4.24)$$

To assess stability, we need to examine the location of the poles of $X(s)$ in the complex plane. Stability is typically determined by the real parts of the poles.

let's denote the roots of the denominator as $s_1 = -2\zeta - \sqrt{(4\zeta^2 - 4(1 + p))}$ and

$s_2 = -2\zeta + \sqrt{(4\zeta^2 - 4(1 + p))}$.

To determine the stability of the system, we need to examine the real parts of the poles. let's denote the roots of the denominator as $s_1 = -2\zeta - \sqrt{(4\zeta^2 - 4(1 + p))}$ and

$s_2 = -2\zeta + \sqrt{(4\zeta^2 - 4(1 + p))}$.

For stability, we need both s_1 and s_2 to have negative real parts. This means that both $-2\zeta - \sqrt{(4\zeta^2 - 4(1 + p))}$ and $-2\zeta + \sqrt{(4\zeta^2 - 4(1 + p))}$ should be negative.

To simplify the stability analysis, let's focus on the expression inside the square root:

$4\zeta^2 - 4(1 + p)$

To calculate the value of $4\zeta^2 - 4(1 + p)$, we can follow these steps:

1. Start with the expression $4\zeta^2 - 4(1 + p)$.
2. Simplify the expression by performing the multiplication and addition/subtraction operations.
3. Substitute the specific values of ζ and p into the expression.
4. Evaluate the expression to obtain the numerical value.

let's go through an example to illustrate the calculation:

Suppose we have $\zeta = 0.5$ and $p = 2$. We can calculate $4\zeta^2 - 4(1 + p)$ as follows:

$$4\zeta^2 - 4(1 + p) = 4(0.5)^2 - 4(1 + 2)$$
$$= 4(0.25) - 4(3)$$
$$= 1 - 12$$
$$= -11 \quad (4.25)$$

So, in this example, the value of $4\zeta^2 - 4(1 + p)$ is -11.

By substituting the specific values of ζ and p into the expression and evaluating it, we can calculate the value of $4\zeta^2 - 4(1 + p)$ for particular case. This value will help to determine the stability of the system, we need to evaluate the value of $4\zeta^2 - 4(1 + p)$. If this value is negative or zero, both roots of the denominator will have negative real parts, indicating stability.

Therefore, if $4\zeta^2 - 4(1 + p)$ is negative or zero, it means that the system is stable. However, if $4\zeta^2 - 4(1 + p)$ is positive, the system will be unstable.

REFERENCES

1. Hale, J. K., (1977) "Theory of Functional Differential Equations", Springer-Verlag, New York.
2. Leighton, W. (1950). The detection of the oscillation of solutions of a second order linear differential equation.
3. Wintner, A. (1949). A criterion of oscillatory stability. *Quarterly of Applied Mathematics*, *7*(1), 115-117.
4. Hartman, P. (1952). On non-oscillatory linear differential equations of second order. *American Journal of Mathematics*, *74*(2), 389-400.
5. Kamenev, IV., (1978)"An integral criterion for the oscillation of linear differential equations", Mat. Zametki. 23, 249-251.
7. Wong, J. S. (2000). Oscillation criteria for second order nonlinear differential equations involving general means. *Journal of mathematical analysis and applications*, *247*(2), 489-505.
8. Waltman, P. (1968). A note on an oscillation criterion for an equation with a functional argument. *Canadian Mathematical Bulletin*, *11*(4), 593-595.
9. Jin, G., Zhang, X., Zhang, K., Li, H., Li, Z., Han, J., & Qi, H. (2020). Stability Analysis Method for Periodic Delay Differential Equations with Multiple Distributed and Time-Varying Delays. *Mathematical Problems in Engineering*, *2020*(1), 1982363.
10. Kalmár-Nagy, T. (2009). Stability analysis of delay-differential equations by the method of steps and inverse Laplace transform. *Differential Equations and Dynamical Systems*, *17*, 185-200.
11. Jasim, A. H. (2023). Delay differential equation of the 2nd order and it's an oscillation yardstick. *Baghdad Science Journal*, *20*(3 (Suppl.)), 1116-1116.
12. Rihan, F. A. (2021). *Delay differential equations and applications to biology* (pp. 123-141). Singapore: Springer.

التذبذب والاستقرارية لحل بعض المعادلات التفاضلية ذات التأخير من الرتبة الثانية

الملخص

في هذا البحث، تم مناقشة بعض مقاييس التذبذب للمعادلات التفاضلية من الدرجة الثانية مع تأخير من خلال بعض النظريات المهمة، وقمنا بتعزيز ذلك ببعض الأمثلة الجديدة والمعدلة. كما قمنا بدراسة استقرار هذا النوع من المعادلات واستخدمنا طريقة لابلاس ومعكوسها، حيث توصلنا إلى نتائج دقيقة. كانت هذه المعادلات على الشكل التالي:

$$[r(t)\big(x(t)\big) + p(x)x(t-\tau))']' + q(t)f\big(x(t-\delta)\big) = 0$$

حيث

$t \geq t_0$, [τ ,δ(اعداد موجبة)], $r, p, q \in C([t_0, \infty), R), f \in C(R, R)$

Evaluation of CA15-3 Level with Some Immunological and Biochemical Variables in the Blood Serum of Women with Breast Cancer in Kirkuk Governorate.

*[1]Zina Abdulmunem Abdulrazaaq Al-doory, [2]Hanan Shihab Ahmad, [3]Esraa Ali Abdul kareem Al-Samarai

*[1]Department of Biology, College of Education for Women, University of Kirkuk,Kirkuk, Iraq.

[2]Door Technical Institute, Northenrn Technical University, Mosul .Iraq.

[3] College of Applied Science University of Samarra , Saleh Aden, Iraq.

***1- zinaabd@uokirkuk.edu.iq**

2-israa.a@uosamarra.edu.iq

3-hanan.sha@ntu.edu.iq

Evaluation of CA15-3 Level with Some Immunological and Biochemical Variables in the Blood Serum of Women with Breast Cancer in Kirkuk Governorate.

[*1]Zina Abdulmunem Abdulrazaaq Al-doory, [2]Hanan Shihab Ahmad, [3]Esraa Ali Abdul kareem Al-Samarai

[*1]Department of Biology, College of Education for Women, University of Kirkuk,Kirkuk, Iraq.

[2]Door Technical Institute, Northenrn Technical University, Mosul .Iraq.

[3] College of Applied Science University of Samarra , Saleh Aden, Iraq.

***1- zinaabd@uokirkuk.edu.iq**

2-israa.a@uosamarra.edu.iq

3-hanan.sha@ntu.edu.iq

Abstract

Samples for the current research were collected from women with cancer in the second stage of infection with breast cancer who were taking two doses of chemotherapy in Kirkuk Governorate for the period from (January to the end of February) of the year 2024. 80 blood samples, whose ages ranged between (25-45) years, were collected from clinic visits. . External samples were divided into two groups:

- Patients group: It included (50) samples of blood from women with breast cancer with treatment 2 doses of chemotherapy.

- Control group: It included (30) blood samples from healthy women.

Then, blood was collected from a group of patients and healthy women and was separated by a centrifuge. Then the studied variables were measured, which included (cancer antigen- CA15-3 , interleukin-10- IL-10 , CXCL12, calcium, zinc, iron, estrogen, progesterone, and Xanthine oxidase). Current research results showed a significant elevated in each of the levels (cancer antigen- CA15-3, interleukin-10, CXCL12, calcium, iron, Estrogen, progesterone, and Xanthine oxidase) also the result

showed a significant decrease in progesterone hormone and zinc level in blood serum of patients with B.C simile to the healthy women .

Keywords: Breast cancer, interleukin 10, progesterone and estrogen, mineral

1-Introduction

Cancer is one of the diseases resulting from abnormal growth of cells and thus leads to the formation of cells that do not obey the normal rules of cell division. In addition, cancer is a disease in which it is difficult to control cell proliferation [(1)]. Cancer, as it is known, is an umbrella term for more than 100 unique types of malignant tumors in various tissues throughout the human body .Breast cancer is one of the diseases that results in cell division, and these cells can spread to different parts of the body. More than 1,668 cases were diagnosed in Baghdad Governorate in 2018 for breast cancer patients. (3).

The cancer antigen CA15-3 is a protein that is a natural product of breast tissue. In the event of a cancerous tumor in the breast, the concentration of CA15-3 may rise as the number of cancer cells in the body increases .In many patients with breast cancer, there is an increase in CA15. -3 When it passes into the bloodstream, it is identified, which makes it useful as a tumor marker to monitor tumor development. The normal level of CA 15-3 is less than 25 units/cm3. It is elevated with tumors, diseases, or other conditions, such as colon tumor, rectal tumor. Lung tumor, hepatitis, and benign breast diseases [(4)].

IL-10 is an essential cytokine for regulating lymphatic homeostasis. These cytokines stimulate similar responses from lymphocytes, but play markedly divergent roles in lymphatic biology in vivo. It is an anti-inflammatory cytokine that regulates the immune response ·that IL-10 expression in metastatic cancer cells can regulate the function of cell-mediated inflammatory responses. IL-10 can be considered a potential biomarker for the prediction and prognosis of human cancers [(5)].

Stromal cell-derived factor-1 (SDF1), also known as CXCL12, is a biomarker for the diagnosis of breast cancer. In addition to high expression of CXCL12, it is positively related to estrogen receptor-positive status, human epidermal growth factor receptor-negative status, and small body size. Tumor (6) Primarily by bone marrow stromal cells, it has thus been named stromal cell-derived factor-1 (SDF-1) · On the other hand, calcium has been found to be related to breast cancer, as it was found that the cancer cells themselves affect calcium metabolism, leading to an increase in its levels in the blood. Also it has been found that zinc, which is one of the minerals necessary for growth and has a relationship with breast cancer, must be available in food or nutritional supplements to reduce the incidence of chronic diseases, including cancer [7]. It has been found that zinc has an immune function linked to cellular signaling pathways, which provides an important role for zinc in cancer patients, as its function lies in controlling tumors [8].

Through the high level of immune variables and minerals, the aim of current research is detremantion the level of cancer antigen CA15-3 along with some immune and biochemical variables in the serum of patients with breast cancer in Kirkuk Governorate.

2-Materials and Methods

1-2-Collection of specimens

The samples for the current research were collected from women in Kirkuk Governorate for the period from (January to the end of February) of the year 2024. 80 samples, whose ages ranged between (25-45) years, were collected from visits to outpatient clinics, and the samples were divided into two groups:

• Patients group: It included (50) samples of blood from women with breast cancer-B.C with treatment 2 doses of chemotherapy.

• Control group: It included (30) blood samples from healthy women.

After that, blood was collected from both groups (patients and healthy people) and separated using a centrifuge. Then the biochemical and immunological variables were measured, which included (CA15-3, IL-10, CXCL12 , Ca , Zn , Iron , estrogen , progesterone , Xanthine oxidase).

2-2-Estimation the level of CA15-3 in a group of patients and healthy people

The Sandwich ELISA method was used as a method to measure the level of CA15-3, using a measurement kit designated for them and from the Chinese company Sun Long Biotech

2-3-Estimation the levels of (IL-10, CXCL12, estrogen, progesterone, and Xanthine oxidase in a group of patients and healthy people)

The level of inflammatory cytokines (IL-10, CXCL12), and the level estrogen and progesterone hormone , and Xanthine oxidase were estimated, According to the ELISA

Sandwich approach, the ELISA technique was utilized to measure the quantity of variables. from the Chinese company (Melsin Medical).

2-4-Estimation of calcium concentration in a group of patients and healthy people

The calcium level was estimated according to a kit prepared by ASSEL S.R.I an Italian company.

2-5-Estimation of zinc concentration in blood serum in a group of patients and healthy controls

A concentration of zinc in the serum of blood was estimated using a diagnostic kit prepared by Biovision.

2-6-Estimation of iron concentration in a group of patients and healthy people

The iron level was calculated using a colorimetric method that converts trivalent iron ions into ferric ions in a weakly acidic medium. It forms a colored complex of the iron (II) ion with Ferrozine [9].

2-7-analysis Statistic

SPSS statistical program was used to find a mean ± SD. The averages were also determined for a group of patients with B.C compared to the (healthy people) using a T-test and at the probability level ($P \leq 0.001$).

4-Results and Discussion

4-1Estimation of levels of immunological and biochemical variables for samples studied in both groups:

1-The table below shows mean ± S.D of the immunological and physiological parameters for samples studied in both groups.

Groups / Parameter	Mean ± SD	
	Control n=30	Patients n=50
CA15-3 (U/ml)	8.01±0.47	34.24±10.92
IL-10 (Pg/ml)	139.70±35.51	257.52±79.93
CXCL12 (Pg/ml)	154.48±75.22	693.04±233.13
Ca (mg/dl)	7.86 ± 0.49	12.16 ± 1.22

Zn (mg/dl)	**67.94 ± 4.36**	**45.10 ± 4.27**
Iron (µmol/L)	**140.95±25.13**	**195.11±43.21**
Estrogen (pg/ml)	**235.512± 50.231**	**145.678±30.412**
Progesterone (pg/ml)	**0.412±0.0561**	**1.043±0.302**
XO ng/ml	**5.714±1.l23**	**10.231±2.421**

P ≤ 0.001

The results of present study showed a significant rise in each of the levels (CA15-3, IL-10, CXCL12, Ca , Iron, xanthine oxidase, progesterone) and a significant decrease in the concentration of estrogen and zinc level in blood serum of patients with women infected breast cancer simile control group at its level probability P ≤ 0.001, as in the following figures.

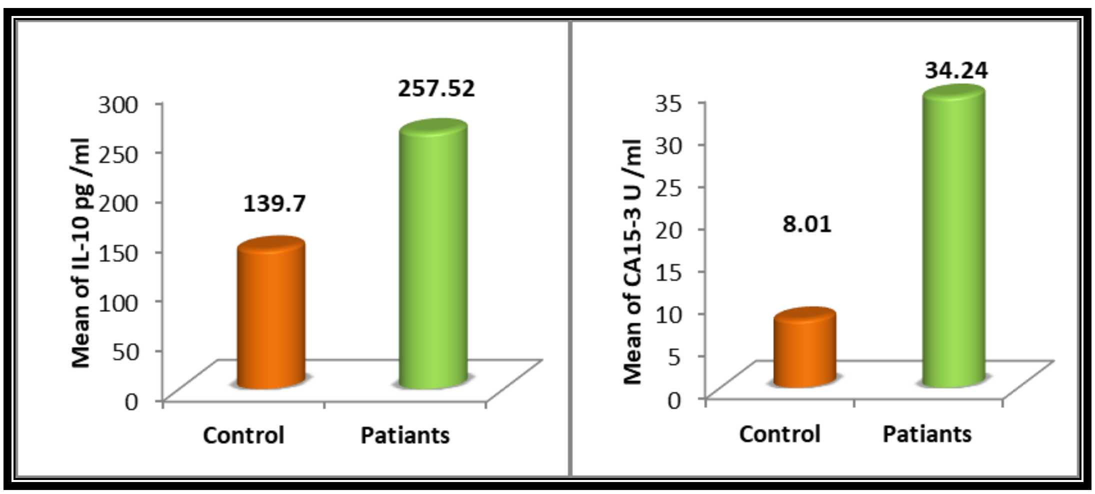

Fig (1):-Level of CA15-3 in all group **Fig (2)**:-Level of IL-10 in all group

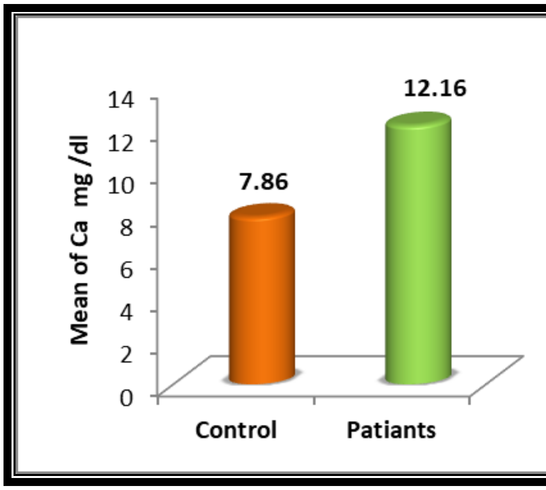

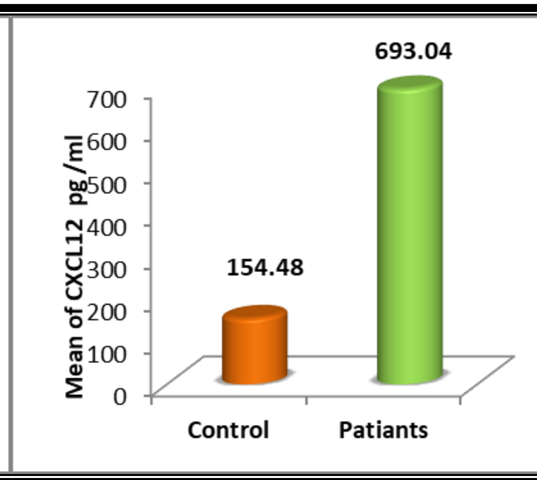

Fig(3):-Level of CXCL12 in all group

Fig(4):-Level of Ca in all group

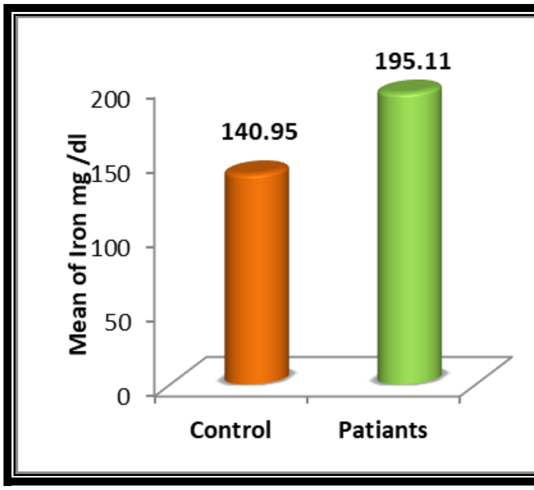

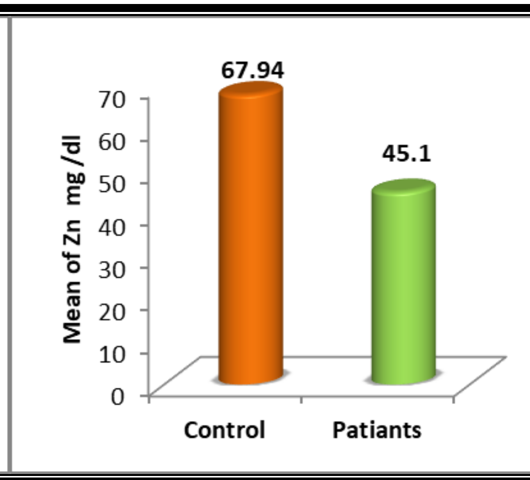

Fig(5):-Level of Zn in all group

Fig(6):-Level of Iron in all group

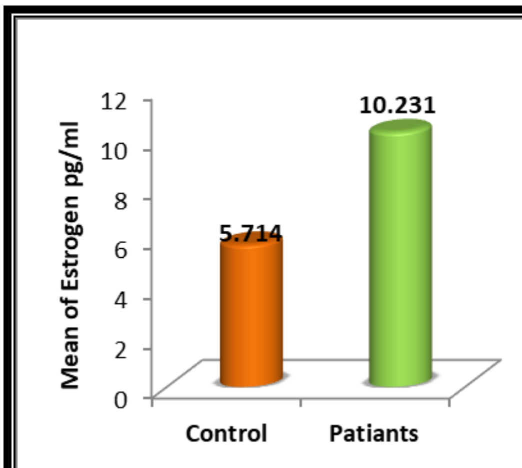

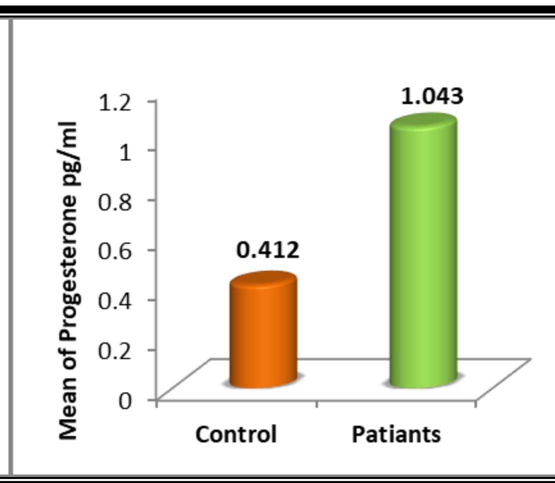

Fig(7):-Level of Estrogen in all group

Fig(8)**:-**Level of progesteron in all group

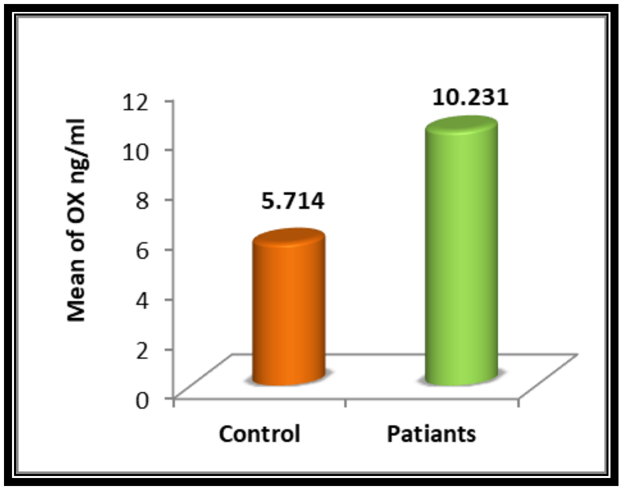

Fig(8):-Level of XO in all grou

Discussion

Cancer antigen (CA15-3)is one of the important diagnostic variables for breast cancer . The results of the research are consistent with the results of [10] who indicated high levels of cancer antigen in patients suffering from breast cancer, as it is considered the most important diagnostic variable and can be used as one of the tumor markers, so it is a marker with high specificity and sensitivity for the disease, as most Studies have shown that it is a biochemical marker for breast cancer patients [11].

As for IL-10, it is considered a cytokine that has been known for a long time in immunology, Particularly concerning its impact on T and B cells, not to mention that its absence results in the death of immature immune cells and that it is essential for the growth of both B and T cells. It's interesting to note that some research has strongly implied that IL-10 could have a function in immunology as well as potentially having a direct or indirect impact on cancer. [12], especially breast cancer, through its work to inhibit apoptosis and stimulate the formation of blood vessels. In tumors. IL-10 is an anti-inflammatory cytokine and can inhibit inflammatory responses by antagonizing co-stimulatory molecules expressed in APC. In addition, IL-10 may contribute to the development of breast cancer [13].

In addition, the concentration of the chemokine CXCL12 increased in female patients simile to a healthy women , as results of a this study agree with a findings of Emilia [14], Marina [15], and Dinesh [16]. In their study, they confirmed the elevated concentration of chemokines in patients with breast cancer, especially the chemokine CXCL12, which regulates breast tumor growth and enhances a entry of cancer cells by increasing blood vessel permeability and expanding leaky tumor blood vessels. Overexpression of

CXCL12 by breast cancer cells can promote in vivo invasion and recruitment of macrophages to the underlying tumor. CXCL12 overexpression also leads to increased microvascular density, which may also be mediated by Connective tissues are associated with the tumor and contribute to changing tumor architecture [17].

As for calcium, it showed a significant increase, as our results agree with Hassan (2011) [18], who discovered that breast cancer patients had higher Ca concentrations than those in the control healthy. The majority of observational studies assessing dietary calcium intake provide evidence for the preventive effect of calcium against breast cancer[19]. Controlled trials revealed that Ca supplementation did not lower postmenopausal women's overall risk of benign proliferative breast disease, which is a precursor to breast cancer. [20]. It has been demonstrated that circulating calcium, which is involved in numerous biological functions, can support the hypothesis that Ca protects against breast cancer, is inversely associated with breast cancer risk. Increased cellular calcium levels after an rise in serum calcium may account for this protective effect. Serum calcium may have an impact on several cellular processes, such as the cell cycle and cell death. [21].

As for zinc, it showed a significant decrease, as the results agree with the results of Arooj and others (2012) [22], .They found that zinc levels decreased in women with B.C compared to healthy group. Zinc deficiency can be linked with malignant tumors [23], and precise function of zinc in cancer [39]. However, zinc is known to be essential for over 100 different metabolic role [24]. It is required for DNA synthesis by altering binding of histones F and F3 to DNA to affect RNA synthesis [25] Whereas Zn deficiency and Zn supplements indicate inhibition and stimulation responses to tumor growth, adding to this funaction of zinc in human cancer. It turns out that there is a significant decrease in the concentration of zinc in the serum of women with breast cancer compared to the control group. This low in zinc concentration can be explained by an elevated demand on cancerous tissue due to increased cellular uptake and enzymatic activity by tumors [26].

In addition, iron showed a significant rise in the group of patients, as its results are consistent with the findings of Rozoqi [27] and Salih [28], who showed in their study a higher concentration of iron in patients with breast cancer simile to the healthy women . One indicator of cancer, according to studies, is an abnormal iron balance. Cancer cells require a lot more iron than regular cells do because they have greater metabolic and reproductive rates than normal cells. This increases oxidative stress in the cells. Moreover, concurrent modulation of antioxidant defenses by cancerous cells may be necessary for their survival. This regulation may include increased expression of several antioxidant genes and the activation of antioxidant transcription factors. [29].

Increased iron metabolism depletes intracellular iron stores by either employing iron-chelating compounds or by mimicking self-regulatory mechanisms, including microRNAs, and is linked to malignant transformation, cancer growth, and medication resistance. Furthermore, hepatitis, a virus that can be generated in cancer cells and provide an alternate anti-cancer strategy, can be brought on by iron overload and result in controlled cell death [30].

Also a results showed a reducation in estrogen hormone in the sera of women patiants , and this may be due to the treatment. It was found that a subgroup of patients with a high concentration of estrogen receptor protein and HER2 negative benefited from the drug tamoxifen, which may lead to a decrease in total cholesterol, which is the main source of estrogen [31]. Therefore, estrogen receptor status may be altered in 5% of chemotherapy groups. Ghufran [32] also indicate that there was an rise in estrogen level before treatment, but it decreased after radiotherapy. The results of a study are also consistent with a results of Wassan [33], and Mousa [34]. In their study, they showed an increase in the level of progesterone in sera of patients with B.C compared with the healthy women , as a reason for the increase is due to the changes that occur in the secretory phase preceding the menstrual cycle, and periodic changes occur in the lining of the uterus and cervix, while the follicle-stimulating hormones and estradiol regulate the secretion of progesterone in a way. Indirectly, it increases luteinizing hormone receptors on ovarian cells responsible for secreting progesterone [35‘36].

On the other hand, it was found through results of current research that there was elevated in the levels of xanthine oxidase, as results of study agree with Thamers results [37], who indicated an increase in the effectiveness of the enzyme thymine oxidase. Therefore, the reason for the increase in the enzyme may be the result of an imbalance of redox and oxidation in the cells that occurs as a result of Oxidative stress is found in many cancer cells compared to normal cells, and thus the imbalance of oxidative stress may be related to the stimulation of tumors [38] The research results of Ismail et al. demonstrated that surface cell markers CD86/CD80 play an active role in the development of certain types of cancers, including brain cancer. [39] Nanoparticles can also be used on MCF-7 breast cancer cell lines, similar to zinc oxide (ZnO) nanoparticles, which have shown clear results on cancer cells. [40]

Conclusion :- It is concluded from the results of the current research that breast cancer is one of the types of cancers widespread in the world and causes death for many women, as it was found to have a correlation with inflammatory cytokines, including interleukin 10 and chemokines, as increasing their levels may be considered a diagnostic variable for B.Cr, in addition to the level of hormones. The female sex hormones, including progesterone and estrogen, have a relationship with breast cancer, in addition to the activity of the enzyme xanthine oxidase, which may be an important diagnostic indicator for the development of the disease.

References

1- Matthews; H. K.; Bertoli; C.; & de Bruin; R. A(2022).Cell cycle control in cancer. Nature Reviews Molecular Cell Biology; 23(1): 74-88.

2- Yadav AR, Mohite SK.(2020). Cancer-A silent killer: An overview. Asian Journal of Pharmaceutical Research. 10 (3):213-6.

3- Iraqi Cancer board. Annual Report Iraqi : Cancer Registry 2018. Iraqi Cancer registry center,Ministry of Health and Inviroment.(Baghdad, Iraq).

4- Shitrit, D.; Zingerman, B.; Shitrit, A.B. *et al*. (2005).Diagnostic value of CYFRA 21-1, CEA, CA 19-9, CA 15-3, and CA 125 assays in pleural effusions: analysis of 116 cases and review of the literature. Oncologist. 10(7):501–7.

5- Acuner-Ozbabacan ES, Hatice Engin B, Emine Guven-Maiorov E, Guray Kuzu G, Muratcioglu S, Baspinar A.(2014). The structural network of Interleukin-10 and its implications in inflammation and cancer. BMC Genomics. 15:S2–S5.

6- Liu, Heyang, et al. (2018)."Prognostic and clinicopathological value of CXCL12/SDF1 expression in breast cancer: a meta-analysis." Clinica Chimica Acta 484 72-80.

7- Lin, Shuai, et al.(2022). "Associations of CXCL12 polymorphisms with clinicopathological features in breast cancer: a case-control study." Molecular Biology Reports 1-9.

8- Janssens, Rik, Sofie Struyf, and Paul Proost. (2018)."The unique structural and functional features of CXCL12." Cellular & molecular immunology 15.4: 299-311.

9- Tietz N.W(1999). .Text book of cinical chemistry,3rd Ed. C.A. Burtis ER Ashwood W.B Seunders .;p 1699-1703.

10- Mohammed , F. Z. Lamis Gamal , Mohamed Farouk Mosa, Mohamed Ibraheim Aref .(2012).Assessment of CA15-3 and CEA as Potential markers for Breast carcinoma prognosis in Egyptian Females. AJBAS Volume 2, Issue 1,

11- Hamdi .E. T , Alsamarai A.T, Ali . A.A .(2020). The relationship between vitamin D with breast Cancer. Medical Science. 24(104).

12-Braihan Hamdi Hameed 1*, Izzat Abdulsatar Al-Rayahi1, Salwa S. Muhsin2 22-(2022).Evaluation of Preoperative CA15-3 Level and its Relationship with Clinico-Pathological Characteristics in Primary Breast Cancer Patients Journal of Techniques, ISSN: 2708-8383, Vol. 4, No. 2, June 30, Pages 21-26

13- Paluskievicz CM, Cao X, Abdi R, Zheng P, Liu Y, Bromberg JS. T(2019). regulatory cells and priming the suppressive tumor microenvironment. Front Immunol. 10:2453.

14- Dąbrowska, Emilia, et al.(2020). "Possible Diagnostic Application of CXCL12 and CXCR4 as Tumor Markers in Breast Cancer Patients." Anticancer Research 40.6: 3221-3229.

15- Okuyama Kishima, Marina, et al. (2015)."Immunohistochemical expression of CXCR4 on breast cancer and its clinical significance." Analytical Cellular Pathology 2015 (2015).

16- Ahirwar, Dinesh K., et al.(2018). "Fibroblast-derived CXCL12 promotes breast cancer metastasis by facilitating tumor cell intravasation." Oncogene 37.32:4428-4442.

17- Boimel, Pamela J., et al. (2012)."Contribution of CXCL12 secretion to invasion of breast cancer cells." Breast Cancer Research 14.1 (2012): 1-14.

18-Zainab Ahmad Hasaan (2011). Study of physiological , biochemical and hormones of women affected by breast cancer in Kirkuk city , College of Science – Tikrit University.

19- Hutchison, A. J. (2009). Oral phosphate binders. Kidney international, 75(9), 906-914.

20- Aziz Mahmood, A., Masood Bilal, K., & Talib Ibrahim, R. (2012). Influence of some Trace Elements and Biochemical Parameters on Breast Cancer. JOURNAL OF EDUCATION AND SCIENCE, 25(1), 34-43.

21- Arooj, B., Ahmed, S., Saleem, M., Khurshid, R. and Zia, M., (2012). Serum trace elements in diagnosis of breast malignancy. *Jour. of Ayub Med. College Abbottabad*, *24*(2), pp.62-64.

22-Arinola, O. G., & Charles-Davies, M. A. (2008). Micronutrient levels in the plasma of Nigerian females with breast cancer. African Journal of Biotechnology, 7(11).

23-Rizk, S. L., & Sky-Peck, H. H. (1984). Comparison between concentrations of trace elements in normal and neoplastic human breast tissue. Cancer research, 44(11), 5390-5394.

24-Prasad, A. S. (1991). Discovery of human zinc deficiency and studies in an experimental human model. The American journal of clinical nutrition, 53(2), 403-412.

25-Drake, E. N., & Sky-Peck, H. H. (1989). Discriminant analysis of trace element distribution in normal and malignant human tissues. Cancer research, 49(15), 4210-4215.

26- Wu, X., Tang, J., & Xie, M. (2015). Serum and hair zinc levels in breast cancer: a meta-analysis. Scientific reports, 5(1), 1-8.

27- Rozoqi, Shahlaa Shafiq. (2021)."Evaluation of Ceruloplasmin Oxidase Activity in Sera of Breast Cancer Individuals in Kurdistan Region/Iraq." Ibn AL-Haitham Journal For Pure and Applied Sciences 2021: 68-75.

28-Salih, Nadya Ahmed, and Moayad M. Yonis Al-Anzy. (2007)."Serum Alkaline Phosphatase, Iron and Calcium Levels in BreastCancer and Leukemia Patients in Salah Al-Din Province." Tikret Journal of Pharmaceutical Sciences 3.2 .

29-Ismail, A., El-Awady, R., Mohamed, G., Hussein, M., & Ramadan, S. S. (2018). Prognostic significance of serum vitamin D levels in Egyptian females with breast cancer. Asian Pacific journal of cancer prevention: APJCP, 19(2), 571.

30-Lee, M. M., & Lin, S. S. (2000). Dietary fat and breast cancer. Annual review of nutrition, 20(1), 221-

31-Brown, Rikki AM, et al.(2020). "Altered iron metabolism and impact in cancer biology, metastasis, and immunology." Frontiers in oncology 10: 476.

32-Ghufran Saad Nsaif 1*, Amer Hassan Abdallah2, Najwa Shehab Ahmed3 and Wafaa Raji Alfatlawi4(2018).. Evaluation of Estridiol and Some Antioxidant in Breast Cancer Iraqi Women. Journal of Al-Nahrain University.;.21 (1):.35-40.

33- Wassan K. Ali, Tareq Y.(2007). Ahmad. Some Biochemical Parameters In Breast Cancer (Part I). Rafidain journal of science, 18(2): 46-57.

34- Mousa Jasim Mohammed AL-Humesh .(2013).Study of The changes in Sexual hormones levels and a number of immune parameters of Women with Brest Cancer and Ovary Cancer. Tikrit Journal of Pure Science, 18 (1): 95-102.

35-Gottlieb, B.; Teifor, M.; Lumbrosa, B. and Pinsky L. (1997).The androgen receptor gene mutation data, Nucleic Acids Res; 25:158 .

36- Albain, K. S.; Barlow, W. E.; Shak, S.; Hortobagyi, G. N.; Livingston, R. B.; Yeh, I. T. et al. (2010).Prognostic and predictive value of the21-gene recurrence score assay in postmenopausal women with nodepositive, oestrogen-receptor-positive breast cancer on chemotherapy: a retrospective analysis of a randomised trial. *The lancet* oncology, 11(1): 55-65.

37. Thamer NA.(2018). Detection of xanthine oxidase in breast cancer. Iraqi Journal of Cancer and Medical Genetics.;6(2)

38. Valko M, Rhodes C, Moncol J, Izakovic MM, Mazur M. (2006).Free radicals, metals and antioxidants in oxidative stress-induced cancer. Chemico-biological interactions. 160(1):1-40.

39-Ismael, Athraa and Jabbar ,Shilan. (2024). Expressions of CD80 and CD86 in Cancer Patients and Its Prognostic Significance. Journal of Pioneering Medical Sciences. 13(1): 127.

40-Husam Al-Hraishawi, Namariq Al-Saadi; Shilan Jabbar.(2023).In Vitro Analysis: The Anticancer Activity of Zinc Oxide Nanoparticales from Cinnamomum Verum. Journal of Nanostructures. 13(1): 146-150.

Enhance Penetration Testing Techniques to Improve Cybersecurity with NetLogo, Nmap, and Wireshark

Huthaifa Mohammed Kanoosh[1] Mohammed Muayad Sultan[2] Ammar Farooq Abbas[3]

[1,3] Department of Computer Science, College of Computer Science and Mathematics, Tikrit University, Tikrit, Iraq.

[2] Mathematics Department, Tikrit University, College of Education of Girls, Tikrit University, Tikrit, Iraq.

[1]E-mail: huthife@tu.edu.iq, [2] E-mail: Mmsultan@tu.edu.iq, [3] E-mail: ammar.abbas@tu.edu.iq

Enhance Penetration Testing Techniques to Improve Cybersecurity with NetLogo, Nmap, and Wireshark

Huthaifa Mohammed Kanoosh[1] Mohammed Muayad Sultan[2] Ammar Farooq Abbas[3]

[1,3] Department of Computer Science, College of Computer Science and Mathematics, Tikrit University, Tikrit, Iraq.

[2] Mathematics Department, Tikrit University, College of Education of Girls, Tikrit University, Tikrit, Iraq.

[1]E-mail: huthife@tu.edu.iq, [2] E-mail: Mmsultan@tu.edu.iq, [3] E-mail: ammar.abbas@tu.edu.iq

Abstract

This study will try to address the complex network security dimensions using a multidimensional approach involving a NetLogo simulation, Nmap scanning, and Wireshark analysis. The NetLogo simulation model ensures an accurate insight into the dynamics of penetration testing and defense strategies of networks thereby allowing a better understanding of interactions amongst different elements in the network and how they affect security from practice (defensive and offensive) to comprehensive security. Information provided by Nmap scanning is used for hosts and services on the network in detail these aid in identifying and assessing potential vulnerabilities as well as enhancement of security strategies. Wireshark analysis focuses on packet transfer behaviors, describing ways communication patterns are identified as well as how to detect suspicious activities: and possible intrusions. At its core, findings accentuate network security as complex, digital assets needing protection through robust defense mechanisms.

Keywords: Cybersecurity, Ethical hacking, network security, NetLogo, Nmap, and Wireshark.

Introduction

In the modern digital age, our daily life and business continuity highly depend on interconnected systems and electronic platforms. Due to this increasing dependence on technology, new advanced cyber threats have evolved that can harm data security and system integrity. Cybersecurity is the practice of protecting information and systems from these digital attacks which could cause large financial losses as well as damage the reputation of organizations, or even governments. Ethical hacking has now become one of the most important tools in cybersecurity by which security vulnerabilities in systems are identified before they are attacked by a hacker so that such operations are performed with the permission network or system owner to enhance security by managing networks to find vulnerabilities early [1][2]. The study is based on how well-advanced tools can be used in the operation of ethical hacking, specifically NetLogo, Nmap, and Wireshark. NetLogo contributes to capturing a vision of systems' behavior and pre-visioning how various systems will act in response to different conditions, thus shedding light on potential vulnerabilities. Nmap proves to be a robust network finding and auditing tool that aids in listing down all connected devices as well as open services that would be possible targets for attacks. However, in this paper, we used Wireshark as a tool to help view data packets as they move across the network and identify any malicious activity that could be an attempt to hack [3]. The widespread use of sensitive data in networks has highlighted the difficulties faced by cybersecurity researchers, especially in defending against cyberattacks on their systems, which have been increasing in recent years. For this reason, experts have had to implement complex, adaptable, and changeable defense plans to keep up with the threats [4]. The process of integrating ethical hacking with advanced technologies can greatly help organizations secure their data and systems. This paper aims to provide comprehensive insights into enhancing cybersecurity with the aforementioned tools and guide researchers and professionals to adopt more adaptable and efficient tactics to confront the growing threats [5].

Research problem

Cyberattacks pose a real and growing threat to information infrastructure in all sectors. The number of cyberattacks has reportedly increased significantly [6]. The company said in its study that cybercrime growth in some countries around the world exceeded 50% between 2016 and 2023, and pointed out the prevalence of cyberattacks, especially ransomware attacks, in its published research. The study showed that the number of ransomware attacks in 2021 increased by 64% compared to the previous year [7]. This growth is because it is becoming easier to carry out these attacks and the availability of attack tools on the dark web at reasonable prices, which has led to a very rapid growth in such attacks. Organizations have suffered significant financial losses due to these attacks. This problem is compounded by the inadequacy of traditional tools and strategies in the face of these sophisticated attacks. This is where the role of ethical hackers proves to be an effective tool in identifying security vulnerabilities before attackers exploit them [8].

Research objectives

This research delves into facets of network security. It centers on three tools: NetLogo, for simulating networks, Nmap for scanning networks and detecting vulnerabilities, and Wireshark for analyzing network traffic. The study investigates the security hurdles faced by networks and aims to offer insights and actionable approaches to enhance network security. Furthermore, it assesses the efficiency of the tools employed. Offers suggestions, for enhancing security protocols.

Previous studies

Mirjalili et al. (2021) explored the concept of penetration testing, in web development underscoring the significance of identifying security weaknesses in web applications to safeguard data. They also pointed out methods like SQL injection and cross-site scripting (XSS). How they can be used to exploit vulnerabilities in web apps. The findings of this research help shed light on the importance of penetration testing in web applications ensuring an environment for users. This study extends its focus beyond web development to networking aspects by utilizing tools, like Nmap and Wireshark [9]. Zhang et al. (2021) researchers examined the vulnerabilities in industrial control systems (ICS) and highlighted the unique challenges these systems face due to their sensitive nature. The study proposed models and techniques to assess and enhance the security of these systems. Through analyzing real-world cases the study showcased how cyberattacks can lead to harm to industrial control systems. It underscores the importance of conducting security assessments for intricate systems. Subsequent research has leveraged these insights to expand security evaluations to enterprise networks offering an understanding of security risks and diverse preventive measures [10]. Saravanan et al. (2021), A research study delved into how mobile technology affects security emphasizing that mobile devices serve as targets for cyberattacks. The research revealed the vulnerabilities of applications to attacks when lacking proper security measures. Ongoing investigations address these risks. Employ tools, like Wireshark to scrutinize transmission patterns and detect any dubious activities potentially stemming from mobile devices [11]. Yunita et al. (2022), examined soil resilience in the context of infrastructure development and pointed out the importance of improving security in digital infrastructure projects.

Although the focus was on physical infrastructure, the study highlighted the need for strong security in all aspects of large projects. Although the research primarily addresses infrastructure its principles are also relevant, to infrastructure. Recent studies utilize these findings to strengthen security measures, in networks emphasizing the significance of implementing comprehensive defense tactics [12]. Altulaihan et al. (2023), Explored the significance of safeguarding web applications. Highlighted the growing vulnerabilities stemming from input verification. The research outlined methods to mitigate these weaknesses and enhance security an aspect of networks. Building upon these tactics the ongoing study extends their application to enhance network security overall by leveraging tools, like Nmap and Wireshark [13]. Leroy (2024), The article discusses the expanding role of intelligence, in cybersecurity. It focuses on introducing ReaperAI, an AI agent created to simulate and carry out cyberattacks. Developed with the help of language models like GPT 4, it showcases its capability to independently identify, exploit, and assess vulnerabilities. The study also introduces methods to enhance the effectiveness and performance of this agent including utilizing task-oriented testing frameworks AI-powered command generation and enhanced prompting techniques. Testing conducted on platforms like Hack the Box has revealed ReaperAIs proficiency in exploiting known vulnerabilities underscoring its potential, in cybersecurity [14].

Conclusion of previous studies

Prior research has highlighted the significance of cybersecurity, across domains spanning from web apps to platforms and mobile devices. Building upon this existing knowledge the present study introduces an approach that incorporates tools, for evaluating and bolstering network security. The findings derived from these investigations offer insights aimed at enhancing measures and mitigating cyber risks effectively.

Research Methodology

The research process involves planning how the study will be conducted, gathering data in ways analyzing the data collected, considering aspects, and acknowledging any limitations, in the research. Tools like NetLogo, Nmap, and Wireshark are used to help achieve research goals. NetLogo is utilized for simulating network behavior, Nmap for identifying vulnerabilities in networks, and Wireshark for analyzing transmissions. Data is gathered through simulations, network scans, and direct observations with precision. Statistical and qualitative analysis methods are applied to uncover patterns and connections, among factors while upholding standards by ensuring data confidentiality and privacy protection.

Tools used in the current research

NetLogo

NetLogo serves as a versatile simulation platform enabling users to construct and execute models that mimic the behaviors of systems. It is utilized for developing models offering users the ability to directly modify and interact with models fostering an engaging learning experience that aids in deepening comprehension of scientific concepts. Additionally, it facilitates the creation of an interactive and adaptable learning environment. Known for being user-friendly and open-source, NetLogo empowers researchers to tailor models to explore scenarios. Researchers can adjust variables within the model or network such, as the rate of news dissemination, credibility fact-checking probability, and user (agent) forgetfulness rate [15].

Nmap

Nmap, also known as Network Mapper, is a tool that helps in exploring networks and recognizing both hosts and security weaknesses within the network. It can conduct security scans, locate devices, on the network uncover open ports, and reveal services accessible through those ports. Additionally, this tool offers flexibility by enabling users to tailor scans according to their requirements either through commands or by creating scripts, to automate the process entirely [16]. Nmap sends data packets to designated targets, within the network assessing the ensuing responses to extract details about said targets. This tool proves valuable and user-friendly for conducting network security analysis and monitoring emphasizing its importance, as a component of organizations' information security strategies [17].

Wireshark

Wireshark is a tool that allows for the examination and monitoring of data transmitted through network packets. It is instrumental in analyzing the behaviors of transfers including details like source, destination, and the type of protocol utilized thereby aiding in the detection of suspicious activities. The tool proves beneficial in identifying and studying attacks associated with protocols enabling users to filter, search, and generate statistics for an analysis of captured data. Being source and user-friendly Wireshark supports network protocols and seamlessly integrates with systems, like intrusion detection systems to pinpoint potential threats and enhance network security [18], [19], [20].

Methods Generally Used Currently and Previously

Traditional methods of penetration testing

At times penetration testing methods depend a lot on tools and basic techniques to discover vulnerabilities. Testers had to scan networks and search for vulnerabilities without the aid of advanced tools to make the process easier.

Modern and advanced tools

With the progress of technology, new and improved tools for penetration testing and security analysis like Metasploit, Nessus, and Burp Suite have been developed. These tools offer enhanced functionalities to detect vulnerabilities and conduct network analysis, with precision and efficiency. Their capabilities encompass identifying vulnerabilities, scanning networks, and performing automated penetration tests.

Research Results

Network simulation using NetLogo:

- The simulation illustrated the interactions, among network components. Highlighted the impact of security measures on network security. Through this simulation, valuable insights were gained on enhancing network infrastructure, for security. Based on Figure 1, we have a space filled with creators of red and blue characters.

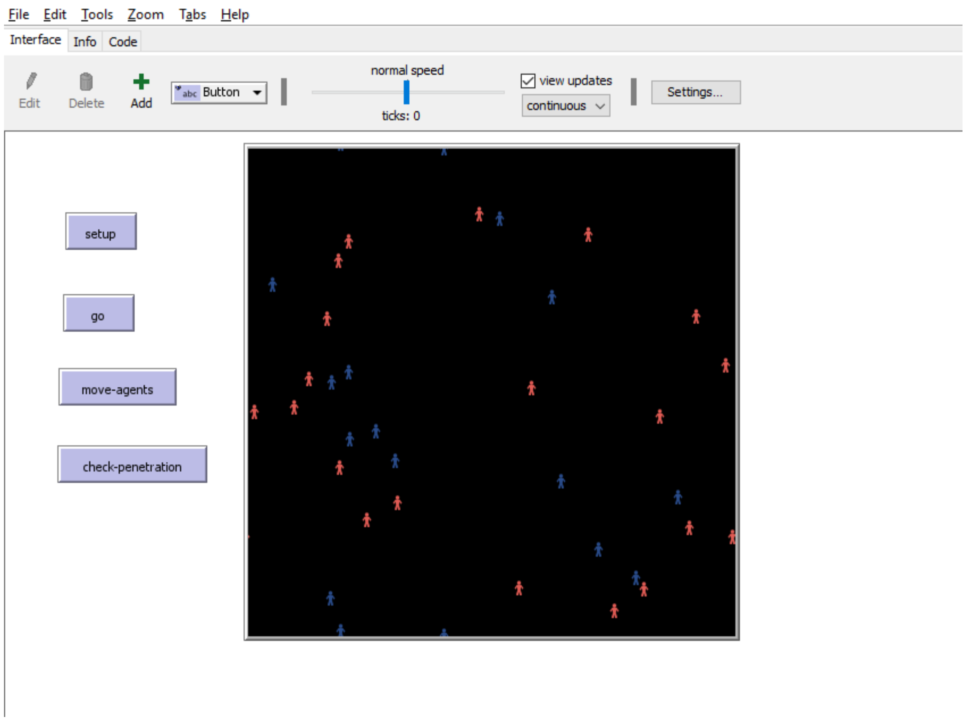

Figure 1 ***Error! No text of specified style in document.*** **Netlogo space and User-**

Red characters refer to the attackers on the network, while the blue refer to the defenders of the network is:

Global Variables:

hackers: This variable stores the number of hacker turtles (Software objects, virtual elements, or the basic element used in the simulation environment) in the simulation.

defenders: This variable stores the number of defender turtles in the simulation.

Setup Procedure (setup):

Clear All: Clear the current state of the world.

Set Default Turtle Shape to "Person": Set the default turtle shape to "Person".

Set Intruders 20: Set the number of Intruders to 20**.**

Set Defenders 15: Set the number of Defenders to 15.

Create Hacker Turtles [...]: Creates Hacker Turtles based on the value stored in the Hacker variable. Each Hacker Turtle is assigned a red + 1 color and placed in a random location in the world.

Create Defender Turtles [...]: Creates Defender Turtles based on the value stored in the Defenders variable. Each Defender Turtle is assigned a blue color - 1 and placed in a random location in the world.

Reset Marks: Resets the mark counter to zero, indicating that the simulation has started.

Go action:

- **Move-Agents:** Call the move-agents procedure to move all turtles.
- **Check-Penetration:** Call the check-penetration procedure to detect and handle hacking attempts.
- **Tick: I**ncrements the tick counter by one, which advances the simulation by a one-time step.

Move-Agents: Call the move-agents action to move all turtles.

This action is responsible for moving all turtles (intruders and defenders) randomly.

Each turtle rotates at a random angle between 0 and 50 degrees (rt random 50) and moves forward by one step (fd 1).

Check Penetration Procedure (check-penetration): Call the check-penetration action to detect and handle hacking attempts.
This procedure is called to check if the intruders are within range to attack the defenders.
It first selects all the intruder turtles as red + 1.
For each intruder turtle, it selects potential defender targets within a radius of 3.
If there are potential targets, it randomly selects one target using one of them and calls the attack procedure on that target.
Tick: Increment the tick counter by one, which advances the simulation by a one-time step.

Attack Procedure (attack):
This procedure is called to simulate an attack by a hacker on a defender.

It takes the target defender turtle as a parameter (**[target]**).

It kills the target defender turtle by calling the **die** procedure on it.

Set Hackers and Set Defenders Procedures:
These procedures allow you to dynamically change the number of hackers and defenders during the simulation by setting the values of the **hacker's** and **defender's** global variables.

The global variables for attackers and defenders act as parameters that define the initial conditions of the simulation. These variables determine the number of attackers and defenders in the environment. The setup process begins by initializing the simulation environment by scanning the world and setting the default appearance of the turtles to "person". It then determines the initial number of attackers and defenders using global variables. Attackers and defenders are generated and randomly distributed across the world.

Once setup is complete, the move action governs the progress of the simulation over time. It calls two sub-actions: move agents and check attack, before advancing the simulation time with a single click. The move agent's action determines the movement behavior of the turtles in the simulation. Each turtle, whether attacker or defender, rotates randomly at a specified angle (between 0 and 50 degrees) and moves forward one step. This random movement creates dynamic interactions between agents in the environment.

The optional hack maneuver is, in charge of spotting attacks that assailants could carry out against protectors. Initially, it pinpoints all assailants. Then locates targets for protectors within a designated range. If potential targets are discovered one target is chosen randomly. The assault maneuver is executed. This maneuver imitates an attack by a hacker on a protector. Upon activation, it utilizes the target turtle, as input. Eliminates it from the simulation by executing the dice move.

Finally, the set penetration maneuvers and designated defenders offer the ability to adapt the quantity of hackers and defenders in time during the simulation. This functionality enables users to experiment with scenarios and tactics, within the simulated setting. Essentially the code manages the engagement between hackers and defenders, in an environment, where hackers strive to breach and assail defenders while defenders work to safeguard themselves. The actions defined for each entity drive their behavior leading to an understanding of penetration testing dynamics.

Scan the network using Nmap:

Network scanning revealed multiple security vulnerabilities in corporate networks. The results showed the importance of using advanced tools such as Nmap to identify and remediate these vulnerabilities before they can be exploited by attackers.

As shown in Figure 2 The results of the Nmap scanning reveal detailed information about the network hosts and the services running on them. Here's a breakdown of the findings:

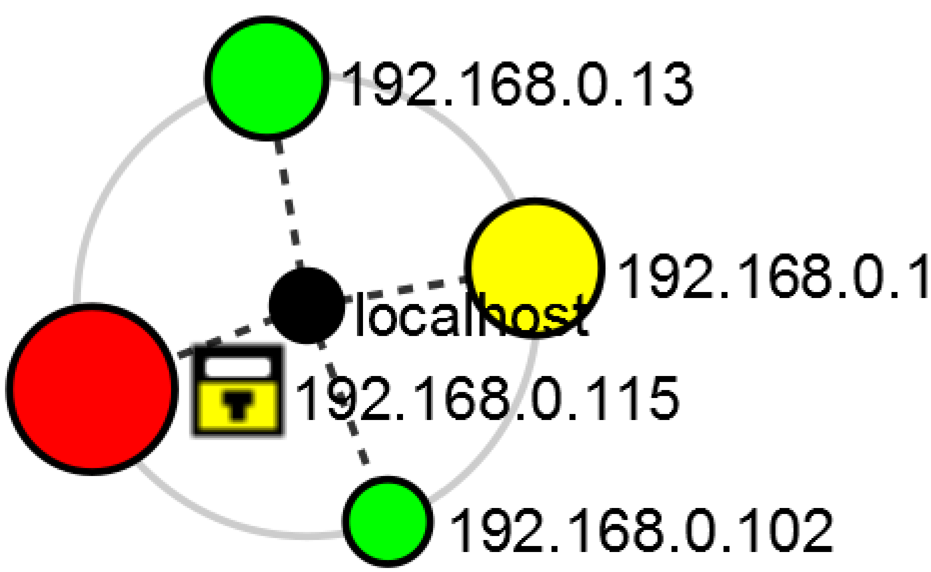

Figure 2 Nmap network Topology Detected over network Scan

192.168.0.1

Host is up with low latency (0.0100s).

Open ports:

22/tcp: SSH

53/tcp: Domain

80/tcp: HTTP

1900/tcp: UPnP

MAC Address: D8:47:32:04:EA:C6 (TP-Link Technologies)

192.168.0.13

Host is up with low latency (0.010s).

Open ports:

22/tcp: SSH

80/tcp: HTTP

MAC Address: B0:4E:26:7D:15:7E (TP-Link Technologies)

192.168.0.102

Host is up with low latency (0.011s).

All 100 scanned ports are in ignored states.

MAC Address: 42:5C:A9:A0:B5:1F (Unknown)

192.168.0.115

Host is up with extremely low latency (0.000020s).

Open ports:

135/tcp: MSRPC

139/tcp: NetBIOS-SSN

445/tcp: Microsoft-DS

1433/tcp: MS-SQL-S

The Nmap scan results provide insightful details about the network hosts and the services they provide. Across the scanned IP addresses, several notable findings emerged. First, at 192.168.0.1, the scan detected an active host with minimal latency, revealing open ports for SSH, Domain, HTTP, and UPnP services, along with the MAC address associated with TP-Link technologies. Similarly, 192.168.0.13 showed a response with open ports for SSH and HTTP services, also associated with TP-Link technologies via its MAC address. However, at 192.168.0.102, despite the host responding immediately, all scanned ports were in the Ignore state, indicating potential security configurations or firewall restrictions. Finally, 192.168.0.115 showed a fast response and revealed open ports for MSRPC, NetBIOS-SSN, Microsoft-DS, and MS-SQL-S services, highlighting a variety of network functions. Overall, the Nmap scan provided basic insights into the network topology, helping administrators assess vulnerabilities, improve security configurations, and strengthen network defenses against potential threats.

Analysis of packet transmission using Wireshark:

- Packet transfer analysis helped identify suspicious activities and potential threats within the network. The results showed how Wireshark can be used to detect and combat threats in real-time.

In Figure 3 of the Wireshark results a series of TCP acknowledgments (ACKs) is captured from the source IP address 192.168.0.115 to the destination IP address 104.18.103.100, through port 443. The sequential acknowledgments indicate that the sender received the data packets successfully. Each packet is 54 bytes in size suggesting small data transfers took place. The consistent pattern of acknowledgments with increasing acknowledgment numbers (Ack) and window sizes (Win) suggests communication between the source and destination hosts. The timestamps show an exchange of packets within a period underscoring the efficiency of the data transfer process. In summary insights from Wireshark results shed light on network traffic dynamics and communication trends, between the source and destination hosts during a timeframe.

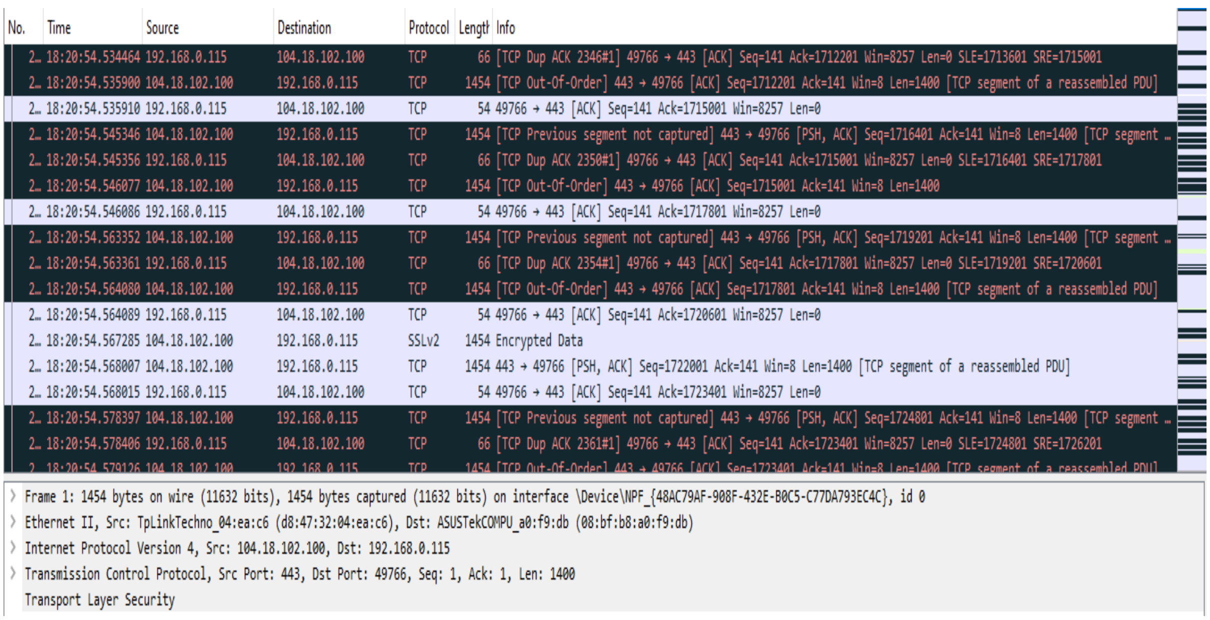

Figure *3* Discover Transmitted Packets Over the Network Using Wireshark

Summary of the results

The results obtained from the NetLogo simulation, Nmap scanning, and Wireshark analysis offer comprehensive insights into different aspects of network behavior, penetration testing, and packet transmission dynamics.

NetLogo Simulation Results:

The simulation orchestrates interactions between hackers and defenders within a simulated environment.
Global variables define the initial conditions, including the number of hackers and defenders.
The setup procedure initializes the simulation environment, creating and distributing turtles randomly.
The go procedure governs the simulation progression over time, invoking sub-procedures for movement and penetration checks.
Movement procedures dictate random movement behaviors for turtles.
Penetration check procedures assess potential attacks and simulate hacker-defender interactions.
Dynamic adjustment procedures allow for real-time changes to hacker and defender counts, facilitating scenario exploration.
Nmap Scanning Results:
Detailed data, on network hosts and the services they offer was revealed. The analysis also noted the responsiveness and open ports, along, with MAC addresses. Key discoveries include hosts providing services possibly restricted ports and overlooked ports suggesting security setups.

Wireshark Analysis Results:
Captured TCP acknowledgments between specific source and destination IPs over port 443.
Sequential acknowledgments with consistent packet lengths indicate ongoing data exchanges.
Timestamps reveal rapid packet exchange within a short timeframe, suggesting efficient communication.
In summary, the NetLogo simulation helps us understand how hackers and defenders interact while Nmap scanning uncovers network structure and service specifics. Wireshark analysis illuminates the dynamics of transmission. When combined these findings give us an understanding of network behavior assisting in evaluating vulnerabilities optimizing security and developing defense tactics.

Conclusion and Recommendations:

This paper delves into the intricacies of network security by taking an approach that leverages tools, like NetLogo for simulating networks, Nmap for vulnerability scanning and Wireshark for analyzing packets. The main goal was to grasp the complexities of cyber threats and devise strategies to bolster cybersecurity in networks. This study offers a framework for scrutinizing and boosting network security through penetration testing and network analysis tools. The insights gained offer guidance for organizations looking to safeguard their data and systems against evolving cyber threats. By implementing these recommendations organizations can strengthen their defense mechanisms. Ensure the safety of their networks, in todays landscape.

Based on the findings, the following recommendations can be made to enhance cybersecurity in enterprise networks:

1. Adoption of advanced penetration testing tools: organizations are encouraged to use penetration testing tools, like NetLogo, Nmap, and Wireshark for analyzing networks and identifying vulnerabilities.

2. Employee cybersecurity training: training employees on cybersecurity best practices and how to use advanced tools can reduce the risk of cyberattacks.

3. Develop advanced defense strategies: organizations must develop and update their defense strategies regularly to keep pace with growing and evolving cyber threats.

4. Conduct periodic security reviews: conducting periodic security reviews of networks and infrastructure can help uncover and address security vulnerabilities before they are exploited.

Acknowledgements:
We are very pleased to present this work on improving penetration testing techniques to improve cybersecurity, and we would like to express our deep gratitude to those who offered their valuable time and guidance in my time of need. It is a great honor to do this work in the esteemed Department of Computer Science, College of Computer Science and Mathematics, Tikrit University, Iraq.

References

[1] R. Shandler and M. A. Gomez, “The hidden threat of cyber-attacks–undermining public confidence in government,” Journal of Information Technology and Politics, vol. 20, no. 4, pp. 359–374, 2023, doi: 10.1080/19331681.2022.2112796.

[2] U. Inayat, M. F. Zia, S. Mahmood, H. M. Khalid, and M. Benbouzid, “Learning-Based Methods for Cyber Attacks Detection in IoT Systems: Methods, Analysis, and Future Prospects,” May 01, 2022, MDPI. doi: 10.3390/electronics11091502.

[3] B. Huang, Y. Li, F. Zhan, Q. Sun, and H. Zhang, “A Distributed Robust Economic Dispatch Strategy for Integrated Energy System Considering Cyber-Attacks,” IEEE Trans Industr Inform, vol. 18, no. 2, pp. 880–890, Feb. 2022, doi: 10.1109/TII.2021.3077509.

[4] Ö. Aslan, S. S. Aktuğ, M. Ozkan-Okay, A. A. Yilmaz, and E. Akin, “A Comprehensive Review of Cyber Security Vulnerabilities, Threats, Attacks, and Solutions,” Mar. 01, 2023, MDPI. doi: 10.3390/electronics12061333.

[5] W. Duo, M. Zhou, and A. Abusorrah, “A Survey of Cyber Attacks on Cyber Physical Systems: Recent Advances and Challenges,” IEEE/CAA Journal of Automatica Sinica, vol. 9, no. 5, pp. 784–800, May 2022, doi: 10.1109/JAS.2022.105548.

[6] A. Kuzior, I. Tiutiunyk, A. Zielińska, and R. Kelemen, “Cybersecurity and cybercrime: Current trends and threats,” JOURNAL OF INTERNATIONAL STUDIES, vol. 17, no. 2, pp. 220–239, Jun. 2024, doi: 10.14254/2071-8330.2024/17-2/12.

[7] S. Temara, “Article no.AJARR.112469 Review Article Temara,” Asian Journal of Advanced Research and Reports, vol. 18, no. 3, pp. 1–16, 2024, doi: 10.9734/ajarr/2024/v18i3610ï.

[8] C. Bain and U. Wilensky, “Sorting Out Algorithms: What Makes One Better than Another?,” in Proceedings of the 50th ACM Technical Symposium on Computer Science Education, New York, NY, USA: ACM, Feb. 2019, pp. 1278–1278. doi: 10.1145/3287324.3293856.

[9] M. Mirjalili, A. Nowroozi, and M. Alidoosti, “A survey on web penetration test.” [Online]. Available: https://www.researchgate.net/publication/270523617

[10] Y. Zhang, J. Wu, D. Wang, and S. zhang, “Research and application of penetration testing method in industrial control system,” SPIE-Intl Soc Optical Eng, Dec. 2021, p. 43. doi: 10.1117/12.2624840.

[11] D. Saravanan and D. Stalin David, “Portable Appliance Penetration Testing and Susceptibility Assessment,” Artech Journal of Effective Research in Engineering and Technology (AJERET), vol. 2, pp. 7–12, 2021, [Online]. Available: http://www.csoonline.com/article

[12] H. Yunita et al., “Spatially Distribution of Soil Ultimate Bearing Capacity at Singkil-Aceh Based on a Static Cone Penetration Test,” Aceh International Journal of Science and Technology, vol. 11, no. 1, pp. 1–11, Apr. 2022, doi: 10.13170/aijst.11.1.23287.

[13] E. A. Altulaihan, A. Alismail, and M. Frikha, “A Survey on Web Application Penetration Testing,” Mar. 01, 2023, MDPI. doi: 10.3390/electronics12051229.

[14] L. J. Valencia, “Artificial Intelligence as the New Hacker: Developing Agents for Offensive Security,” May 2024, [Online]. Available: http://arxiv.org/abs/2406.07561

[15] E. Sulis and M. Tambuscio, “Simulation of misinformation spreading processes in social networks: an application with NetLogo.” [Online]. Available: https://el.media.mit.edu/logo-foundation/

[16] S. Stošović, N. Vukotić, D. Stefanović, and N. Milutinović, “Automation of Nmap Scanning of Information Systems,” in 2024 23rd International Symposium INFOTEH-JAHORINA (INFOTEH), IEEE, Mar. 2024, pp. 1–5. doi: 10.1109/INFOTEH60418.2024.10496014.

[17] D. Bayu Rendro and W. Nugroho Aji, “ANALISIS MONITORING SISTEM KEAMANAN JARINGAN KOMPUTER MENGGUNAKAN SOFTWARE NMAP (STUDI KASUS DI SMK NEGERI 1 KOTA SERANG),” vol. 7, no. 2, 2020.

[18] G. Jain and Anubha, “Application of SNORT and Wireshark in Network Traffic Analysis,” IOP Conf Ser Mater Sci Eng, vol. 1119, no. 1, p. 012007, Mar. 2021, doi: 10.1088/1757-899x/1119/1/012007.

[19] R. Afzal and R. K. Murugesan, “Implementation of a Malicious Traffic Filter Using Snort and Wireshark as a Proof of Concept to Enhance Mobile Network Security,” Journal of Telecommunications and Information Technology, vol. 2022, no. 1, pp. 64–71, 2022, doi: 10.26636/jtit.2022.155821.

[20] N. Alsharabi, M. Alqunun, and B. A. H. Murshed, “Detecting Unusual Activities in Local Network Using Snort and Wireshark Tools,” Journal of Advances in Information Technology, vol. 14, no. 4, pp. 616–624, 2023, doi: 10.12720/jait.14.4.616-624.

The Zagreb index of the idempotent divisor graph of commutative ring

Luma Ahmed Khaleel

l.a.khaleel81@uomosul.edu.iq

Department of Mathematics, College of Education for Pure Science, University of Mosul, Mosul, Iraq

The Zagreb index of the idempotent divisor graph of commutative ring

Luma Ahmed Khaleel

l.a.khaleel81@uomosul.edu.iq

Department of Mathematics, College of Education for Pure Science, University of Mosul, Mosul, Iraq

ABSTRACT:

The idempotent divisor graph of a commutative ring $\mathcal{R}$ is a graph with vertices set in $\mathcal{R}$ * = $\mathcal{R}$ -{0}, and two distinct vertices d_1 ,d_2 are adjacent if and only if $d_1 d_2$ = e. For some non-unit idempotent element $e^2 = e \in \mathcal{R}$, it is denoted by Π ($\mathcal{R}$) . In this paper, we find some basic properties of this graph when a ring $\mathcal{R}$ is direct product of field order 2 and local ring of nilpotency 2. As well as we fined The Zagreb index of this graph.

Key word: idempotent divisor graph, zero divisor graph, direct product, Zagreb index of graph.

1. Introduction

We assume that R is finitely commutative ring with identity $1 \neq 0$, and Z($\mathcal{R}$) the set of nonzero zero- divisors of $\mathcal{R}$. We denote U($\mathcal{R}$) (I($\mathcal{R}$) respectively) the sets of every unit elements (idempotent elements respectively) of the ring $\mathcal{R}$ respectively. We refer as to |S| a cardinality of a set S and F_s to a field of order s, where s is a power of prime number p. In [14] 2022 the authors H. Q. Mohammad and N. H. Shuker presented a new definition relating the theories of rings and graphs, which is called idempotent divisor graph and is denoted by$\Pi(\mathcal{R})$, and its vertices are lies in $\mathcal{R}^* = \mathcal{R}\backslash\{0\}$ and two different vertices d_1, d_2 adjacent if and only if $d_1 d_2 = e$, where e is an idempotent element that is not equal to 1. This graph is a generalized of the made by authors Anderson and Livingston in [1] 1999 denoted by $\Gamma(\mathcal{R})$ and its vertices are in $Z(\mathcal{R})^* = Z(\mathcal{R})\backslash\{0\}$and the two different vertices d_1, d_2 adjacent if and only if $d_1 d_2 = 0$. The authors in [1,14] have shown the relationship between the two graphs, and the graph $\Pi(R)$ is connected withare There . $diam(\Pi(R) \leq 3$ many authors study in this like see for example [11,12, 15,16] and [17]. The author of the source [2] also studied a special case of this graph, which is when the ring R is the direct product of two fields F and F'. In a graph theory, we review some concepts from basic graph theory. "Let G be a (undirected) graph. Recall that G is connected if there is a path between any two distinct vertices of G. The graph G is complete if any two distinct vertices are adjacent. The complete graph with n vertices is denoted by K_r. A path in a graph is a succession of adjacent edges, with no repeated edges, that joins two vertices. A path on vertices P_n, is the simple graph consisting of path. For two vertices d_1 and d_2 in G, $d(d_1,d_2)$ denotes the length of the shortest path from $d_1$to d_2. We then define the diameter of a graph, denoted by $diam(G) = sup\{d(d_1,d_2) : d_1$and d_2 vertices of G}. Let G be a connected graph and $d \in V(G)$, the eccentricity $e(d)$ of a vertex d in graph G is the distance from d to a vertex farthest from d', that is $e(d) = max\{ d' \in V(G) : d(d,d')\}$. The radius of G denoted by $rad(G)$ that is $rad(G) = min\{ e(d): d \in V(G)\}$ and the center of G, $Cent(G) = \{d \in V(G) : e(d) = rad(G)\}$. A subgraph H of G is an induced subgraph of G if two vertices of H are adjacent in H if and only if they are adjacent in G. The chromatic number of G is the minimum number of colors needed to color the vertices of G so that no two adjacent vertices share the same color, and is denoted by χ(G). A complete subgraph K_r of a graph G is called a clique, and ω(G) is the clique number of G, which is the greatest integer r≥1 such that $K_r \subseteq G$. Let G_1 and G_2 are two graphs, then $G_1 \cup G_2$ is graph with V($G_1 \cup G_2$) = V(G_1) ∪ V(G_2) and E($G_1 \cup G_2$) = E(G_2) ∪ E(G_2), and $G_1 + G_2$ is a graph with V($G_1 \cup G_2$) = V(G_1) ∪ V(G_2) and E($G_1 + G_2$) = E(G_1) ∪ E(G_2) ∪{{u,v}: u ∈ V(G_1), v ∈ V(G_2)}" see for example [4,18] and [9].

In a ring theory, " For a ring $\mathcal{R}$, a proper ideal M is called maximal, if whenever K is an ideal of R satisfied M⊂K⊆R, then K=$\mathcal{R}$, if $\mathcal{R}$ has one maximal ideal, then is called local. If $\mathcal{R}$ finite non-local, then $\mathcal{R}$ is a direct product of the local rings. A non-zero element d of a ring $\mathcal{R}$ is called nilpotent if $d^i = 0$ for some positive integer i. The smallest integer i > 0 such that $d^i = 0$ but $d^{i-1} \neq 0$ is called the nilpotency index (or index of nilpotency) of the d. an element e in a ring $\mathcal{R}$ is said to be idempotent if $e=e^2$". For more details see [3,5] and [6].

This paper consists of two items dealing in the second item study idempotent divisor graph when a ring R direct product of local ring and field order 2 and provide some properties of this graph such as order and size in addition to that we find clique number and center for this graph. Finally, we find the Zagreb index of this graph using the results obtained in the second item

2. Zagreb index of the idempotent divisor graph .

Initially, we will outline the general classification of graph $\Pi(F_2\times\mathcal{R}')$ by identifying adjacencies of this graph. $\mathcal{R}'$ is a finite local commutative ring with index of nilpotency 2 and F is a field. Specially, F_2 is a field with two elements.

Theorem 2.1.

Let F_2 be a field order 2 and $\mathcal{R}'$ local ring with maximal ideal M satisfied $M^2=(0)$. Then $\Pi(F_2\times\mathcal{R}')\cong K_1+(K_{2|Z(\mathcal{R}')^*|})\cup |N_1|\, K_2\cup \frac{1}{2}|N_2|\, P_4)$ where $N_1=\{c\in U(\mathcal{R}'): c=c^{-1}|$ and

$N_2=\{c\in U(\mathcal{R}'): c\neq c^{1}\}$.

Proof.

Let $(a_1,d_1)\in F_2\times\mathcal{R}'-\{(0,0)\}$. To find adjacent vertices in $\Pi(F_2\times\mathcal{R}')$. A first step a vertex $(1,0).(a_1,d_1)=(a_1,0)$ is an idempotent element not equal an identity. A second step we discuss when $d_1\in Z(\mathcal{R}')^*$ and $a_1\in F_2=\{0,1\}$. Now, since $M^2=0$ and $Z(\mathcal{R}')=M$, then $d_1.\, d_2=0$ for all $d_1, d_2\in Z(\mathcal{R}')^*$. So, if $d_2\in Z(\mathcal{R}')^*$, then $(1, d_1)$ adjacent with $(0,d_2)$, $(1, d_2)$, and $(1,0)$. Similarly, $(0, d_1)$ adjacent with $(0, d_2)$, $(1, d_2)$ and $(1,0)$. So that degree $(a_1, d_1) = 2|Z(\mathcal{R}')^*|+1$; $a_1\in F_2$, $d_1\in Z(\mathcal{R}')^*$. A final step we discuss when $c\in U(\mathcal{R}')$ and $a_1\in F_2=\{0,1\}$. We see that there are two cases:

Case A:

If $c=c^{-1}$, then $(1, c)$ adjacent with only two vertices $(0, c)$ and $(1,0)$. Similarly $(0, c)$ adjacent with only two vertices $(1, c)$ and $(1,0)$. So that there are $|N_1|$ sub graphs induced by $N_1=\{(1,c),(0,c):c\in U(\mathcal{R}')$ and $c=c^{-1}\}$.

Case B:

If $c \neq c^{-1}$, then (1, c) adjacent with only two vertices $(0, c^{-1})$ and (1,0). So that degree (1, c) = 2. As well as, (0, c) adjacent with only three vertices $(1, c^{-1})$, $(0, c^{-1})$ and (1,0). So that there are $\frac{1}{2}N_2$ sub graphs induced by $N_2=\{(1,c),(1,c^{-1}),(0,c),(0,c^{-1}): c \in U(\mathcal{R}')$ and $c \neq c^{-1}\}$.

From the above adjacency steps, we conclude that

$\Pi(F_2 \times \mathcal{R}') \cong K_1+(K_{2|Z(\mathcal{R}')^*|}) \cup |N_1|\ K_2 \cup \frac{1}{2}|N_2|\ P_4)$.

Corollary 2.2.

Let $\mathcal{R} \cong F_2 \times \mathcal{R}'$ such that $\mathcal{R}'$ is local ring with $M^2=0$, then $diam(\Pi\ (F_2 \times \mathcal{R}') = 2$ and $cent(\mathcal{R}) = \{(1,0)\}$.

Proof.

Directly by fact (1,0) the only adjacent with every other vertex.

Proposition 2.3.

Let $\mathcal{R} \cong F_2 \times \mathcal{R}'$ such that $\mathcal{R}'$ is local ring with $M^2=(0)$**.** Then $\chi(\mathcal{R})=\omega(\mathcal{R}) = |Z(\mathcal{R}')^*|+1$.

Proof.

Since $V(\mathcal{R}) = \cup S_i$ for $1 \leq i \leq 4$, where $S_1=\{(1,0)\}$, $S_2=\{(1,1), (0,-1), (0,1), (1,-1)\}$, $S_3=\{(1,c), (0,c) : c \in U(\mathcal{R}')\}$, $S_4=\{(1,d),(0,d) : d \in Z(\mathcal{R}')^*\}$**.** The element in set S_1 adjacent to every element in S_2, S_3 and S_4, and we see that a subset S_4 is a complete sub graph of $\Pi(\mathcal{R})$. As well as any element in S_2 and S_3 non adjacent in any element in S_4. So, a graph $\Pi(\mathcal{R})$ have a minimal coloring $S=S_1 \cup S_4$ and complete sub graph H induced by S. Therefore, $\chi(\mathcal{R}) =\omega(\mathcal{R}) = |S|=|S_4|+1$.

Theorem 2.4.

Let $\mathcal{R} \cong F_2 \times \mathcal{R}'$ such that $\mathcal{R}'$ is a local ring, then

$$deg(v) = \begin{cases} 2r-2 & : \text{if} \quad v \in \{(1,0)\} : r = |\mathcal{R}'|, \\ 2|Z(\mathcal{R}')^*|+1 : & \text{if} \quad v \in \{(1,d_1)\},\{(0,d_1)\} : d_1 \in Z(\mathcal{R}')^*, \\ 2 & : \text{if} \quad v \in \{(0,d_1)\}: d_1 \in U(\mathcal{R}'), d_1^2 = 1, \\ 3 & : \text{if} \quad v \in \{(0,d_1)\}: d_1 \in U(\mathcal{R}'), d_1^2 \neq 1 \\ 2 & : \text{if} \quad v \in \{(1,d_1)\}, d_1 \in U(\mathcal{R}'). \end{cases}$$

Proof.

Since (1,0) be adjacent with every other vertex then deg(1,0)=2r-2, where $r=|\mathcal{R}|$. Also, for each $a=(a_1,d_1) \in \mathcal{R}\backslash\{0\}$, where $a_1=0$ or 1 and $d_1 \in \mathcal{R}'=U(\mathcal{R}') \cup Z(\mathcal{R}')^*$. If $d_1 \in Z(\mathcal{R}')^*$, then $(1, d_1)$ and $(0, d_1)$ adjacent with vertices $(1,0)$,$(0, d_1)$ and $(0, d_2)$,where $d_1 \in Z(\mathcal{R}')^*$. Therefore $deg(1,d_1)= deg(0,d_1)=2|Z(\mathcal{R}')^*|+1$. If $d_1 \in U(\mathcal{R}')$, then$(1,d_1)$ adjacent with $(1,0)$,$(0,d_1^{-1})$.as well as $(0, d_1)$ adjacent with $(1,0)$, $(1, d_1^{-1})$, $(0, d_1^{-1})$. So $deg(1,d_1)=2$ and $deg(0,d_1)=2$ if $d_1^2=1$ and $deg(0,d_1)=3$ if $d_1^2 \neq 1$

Theorem 2.5.

The order of $\Pi(F_2 \times \mathcal{R}') = 2\mathcal{R}'-1$ and the size is $m(\Pi(F_2 \times \mathcal{R}')) = \frac{1}{2}(2r-2 +(2|Z(\mathcal{R}')^*|+1)|Z(\mathcal{R}')^*| +2|N_1|+3|N_2|+2(|N_1|+|N_2|))$, where $N_1=\{c \in U(\mathcal{R}'): c=c^{-1}\}$ and $N_2=\{c \in U(\mathcal{R}'): c \neq c^1\}$.

Proof.

Clearly the order of $\Pi(F_2 \times \mathcal{R}') =|F_2 \times \mathcal{R}'|=2\mathcal{R}'-1$.

Now, to find the size of a graph $\Pi(F_2 \times \mathcal{R}')$. Since $2m(\Pi(F_2 \times \mathcal{R}'))=\sum_{v \in \pi(F_2 \times \acute{R})} \deg(v)$, then

$$2m\Pi(F2 \times \mathcal{R}') = deg(1,0) + \sum_{v \in \{(1,d),(0,d):d \in Z(\mathcal{R})^*\}} \deg(v) + \sum_{v \in \{(0,c),c \in U(\mathcal{R}):c^2=1\}} \deg(v)$$
$$+ \sum_{v \in \{(0,c),c \in U(\acute{\mathcal{R}}):c^2 \neq 1\}} \deg(v) + \sum_{v \in \{(1,c),c \in U(\acute{\mathcal{R}})\}} \deg(v)$$

So, by theorem 2.4 we have

$2m\Pi(F_2 \times \mathcal{R}')=2r-2 +(2|Z(\mathcal{R}')^*|+1)|Z(\mathcal{R}')^*| + 2|N_1|+3|N_2|+2(|N_1|+|N_2|)$, where $N_1=\{c \in U(\mathcal{R}'): c=c^{-1}\}$ and $N_2=\{c \in U(\mathcal{R}'): c \neq c^1\}$. Hence $m\Pi(F2 \times \mathcal{R}') = \frac{1}{2}(2r-2 +(2|Z(\mathcal{R}')^*|+1)|Z(\mathcal{R}')^*| +2|N_1|+3|N_2|+2(|N_1|+|N_2|))$

Example: Let $\mathcal{R} \cong Z_2 \times Z_9$, then a graph $\Pi(\mathcal{R})$ presented in figure 1:

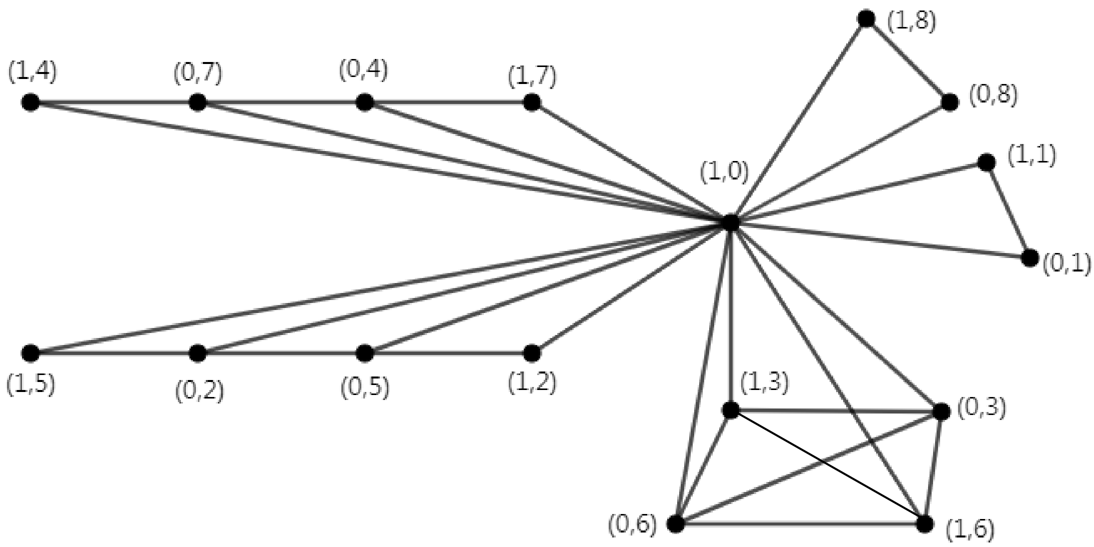

Figure 1: $\Pi(Z_2 \times Z_9)$

We note that $Z(Z_9)^* = \{3,6\}$ and $U(Z_9) = \{1,2,4,5,7,8\} = N_1 \cup N_2$, where $N_1 = \{1,8\}$ and $N_2 = \{2,4,5,7\}$.

Therefore $\Pi(Z_2 \times Z_9) = K_1 + (K_4 \cup 2K_2 \cup 2P_4)$.

Recall that "The Zagreb of a graph indices of the graph Π ($F_2 \times \mathcal{R}'$) , denoted by Z_1 (Π ($F_2 \times \mathcal{R}'$)) and defined byZ_1 (Π ($F_2 \times \mathcal{R}'$)) = $\sum_{v \in \pi(F_2 \times \acute{R})} (\deg(u))^2$"[8]. There are many authors study in this like [7,10] and [13]. Finally, we present find the Zagreb of a graph index of the graph $\Pi(F_2 \times \mathcal{R}')$, where F_2={0,1} is a field order 2 and $\mathcal{R}'$ is a local ring with nilpotency 2.

Theorem2.6.

The Zagreb of a graph index of the graph Π ($F_2 \times \mathcal{R}'$) is given by

Zag (Π ($F_2 \times \mathcal{R}'$))

$= 4(r^2 - r + 1) + 4[|Z(\mathcal{R}')^*|^4 + |Z(\mathcal{R}')^*|^3] + |Z(\mathcal{R}')^*|^2 + 8|N_1|^2 + 13|N_2|^2 + 8|N_1|.|N_2|$

Proof.

The Zagreb of a graph index of the graph Π ($F_2 \times \mathcal{R}'$)is

Zag (Π ($F_2 \times \mathcal{R}'$))= $\sum_{v \in \pi(F_2 \times \acute{R})} (\deg(v))^2$

$= \deg(1,0) + \sum_{v \in \{(1,d),(0,d)} (\deg(v))^2 + \sum_{v \in \{(0,c), c \in U(\acute{R}); C^2 = 1\}} (\deg(v))^2$

$+ \sum_{v \in \{(0,c), c \in U(\acute{R}); C^2 \neq 1\}} (\deg(v))^2 + \sum_{v \in \{(1,c), c \in U(\acute{R})\}} (\deg(v))^2$

Since

$=(2r-2)^2 + ((2|Z(\mathcal{R}')^*| + 1)\,|Z(\mathcal{R}')^*|)^2 + (2|N_1|)^2 + (3|N_2|)^2 + (2(|N_1|+|N_2|))^2$

$= 4(r^2-r+1) + [2|Z(\mathcal{R}')^*|^2 + |Z(\mathcal{R}')^*|]^2 + 4|N_1|^2 + 9|N_2|^2 + 4(|N_1|+|N_2|)^2$

$=4(r^2-r+1) + 4[|Z(\mathcal{R}')^*|^4 + |Z(\mathcal{R}')^*|^3] + |Z(\mathcal{R}')^*|^2 + 8|N_1|^2 + 13|N_2|^2 + 8|N_1|.|N_2|$

Example 3.2 : In graph $\pi(F_2 \times Z_9)$, then The Zagreb of a graph index is

Zag $(\pi(F_2 \times Z_9))$**=** $\sum_{v \in \pi(F_2 \times Z_9)} (\deg(v))^2 = (\deg(1,0))^2$

$+(\deg(1,2))^2 + (\deg(1,4))^2 + (\deg(1,5))^2 + (\deg(1,7))^2 + (\deg(0,2))^2$

$+(\deg(0,4))^2 + (\deg(0,5))^2 + (\deg(0,7))^2 + (\deg(0,1))^2 + (\deg(0,8))^2$

$+(\deg(1,1))^2 + (\deg(1,8))^2 + (\deg(1,3))^2 + (\deg(1,6))^2 + (\deg(0,3))^2$

$+(\deg(0,6))^2 = 374.$

References

1. D. F. Anderson and P. S. Livingston, The zero-divisor graph of a commutative ring, Journal of Algebra, 1999.
2. M.N.Authman Alghabsha , Idempotent Divisor Graph of Commutative Rings, Doctor Thesis, College of Computer Science and Mathematics, The University of Mosul, Iraq, 2022.
3. G. Bini, F. Flamini, Finite commutative rings and their applications. Vol. 680. Springer Science & Business Media, 2002.
4. G. Chartrand and L. Lesniak. Graphs & digraph , 3rded, Wadsworth and Brooks / Cole, California , 1986.
5. D.S. Dummit and R.M. Foote . Abstract Algebra. Wiley ,2003.
6. J. B. Fraleigh. A first course in abstract algebra. Pearson Education India, 2003.
7. I.Gutman , K.C.Das . The first Zagreb index 30 years after. MATCH Commun. Math. Comput. Chem., 50, 83–92 , 2004.

8. I.Gutman , N. Trinajstić, Graph theory and molecular orbitals. Total π-electron energy of alternant hydrocarbons, Chem. Phys. Lett., 17 535–538, 1972.
9. J.L.Gross and J.Yellen, Handbook of Graph Theory; CRC Press: Boca Raton, FL, USA, 2004.
10. I.Gutman,; E. Milovanovi´c,; I. Milovanovi´c, Beyond the Zagreb indices. AKCE Int. J. Graphs Comb. 17, 74–85 , 2018.
11. L. A. Khaleel , H. Q. Mohammad, N. H. Shuker ,Tripotent Divisor Graph of a Commutative Ring , International Journal of Mathematics and Mathematical Sciences Vol. 2024, Article ID 1954058, 9 pages,2024.
12. H. Q. Mohammad, Sh. H. Ibrahem, and L. A. Khaleel , The metric chromatic number of zero divisor graph of a ring Zn, International Journal of Mathematics and Mathematical Sciences ,vol. 2022, Article ID 9069827, 4 pages, 2022.
13. N. A.Mazlan , H. I. Mat Hassim, N. H.Sarmin and S. M. Salih Khasraw. The first Zagreb index of zero-divisor type graph for some rings of integers modulo n. Proc. Sci. Math., 29-32 ,2022.
14. H. Q. Mohammad, N. H. Shuker, Idempotent divisor graph of commutative ring. Iraqi journal of science ,645-651 , 2022.
15. Mukhtar, and Aamir, et al. Computing the size of zero divisor graphs. Journal of Information and Optimization Sciences 41.4, 855-864, 2020.
16. C. J.Rayer, and R. S. Jeyaraj . Applications on topological indices of zero-divisor graph associated with commutative rings. Symmetry, 15(2), 335, 2023.
17. P. Singh & V. K. Bhat , Zero-divisor graphs of finite commutative rings: A survey. Surveys in Mathematics and its Applications, 15(14), 371–397. 2020
18. D. B. West, Introduction to Graph Theory(2nd Edn), Prentice Hall, Upper Saddle River ,2001.

دراسة عدد من العوامل المؤثرة على كفاءة ازالة صبغة الليشمانيا من محاليلها المائية بطريقة التلبيد الكهربائي باستخدام اقطاب الستانلس استيل

يوسف صباح رضوان[1] , احمد سعيد عثمان[2]

Ys230022pep@st.tu.edu.iq dra.dabbagh@tu.edu.iq

قسم الكيمياء, كلية التربية للعلوم الصرفة, جامعة تكريت, تكريت, العراق

دراسة عدد من العوامل المؤثرة على كفاءة ازالة صبغة الليشمانيا من محاليلها المائية بطريقة التلبيد الكهربائي باستخدام اقطاب الستانلس استيل

[1]يوسف صباح رضوان , [2]احمد سعيد عثمان

Ys230022pep@st.tu.edu.iq dra.dabbagh@tu.edu.iq

قسم الكيمياء, كلية التربية للعلوم الصرفة, جامعة تكريت, تكريت, العراق

الخلاصة (Abstract)

اشتمل البحث على دراسة لعدد من العوامل المؤثرة على عملية التلبيد الكهربائي مثل(تركيز الصبغة، تركيز الألكتروليت ونوع القطب المستخدم في العملية . تم تطبيق البيانات باستخدام خلية زجاجية مصنوعة بالابعاد الطول(10cm) العرض (8cm) الارتفاع (6cm) بسعة 300ml مليلتر بإستخدام قطب الستانلس ستيل(SS316) كل واحد منها بأبعاد الطول(8) العرض (7cm) سم السمك (0.1cm) ربطت بمسافة بين الاقطاب (4cm) وتوصيلها إلى مصدر طاقة كهربائي وبجهود مختلفة (5,10,15,20,25V) و بمدى من التراكيز (100,200,300,400ppm) للصبغة المذكورة آنفاً وبإستخدام الملح (Na2SO4) كالكتر وليت وبتراكيز (50,100,150ppm) عند درجة حرارة المختبر. تشير النسبة المئوية للإزالة (R%) على أنها تزداد مع زيادة كل من الزمن ونقصان تركبز الالكتروليت ونقصان تركيز الصبغة عند استخدام قطب الستانلس ستيل(SS316) . اتضح من الدراسة ان افضل نسبة إزالة تحققت عند تركيز (100ppm) عند قطب الستانلس ستيل حققت بنسبة (88%) و بتركيز الكتروليت (50ppmm) اشارت النتائج ان النسبة المئوية للإزالة للصبغة المدروسة تزداد وحسب الترتيب التالي: تمت دراسة حركية الإزالة للصبغة وبتركيز (200ppm) مع وجود الالكتروليت ومن خلال تطبيق معادلة المرتبة الأولى حيث اعطت قوة علاقة جيدة جداً دليل على سلوك العملية المرتبة الأولى الوهمية الكاذبة وتم حساب قيم ثابت السرعة k.

ومن ثم تم حساب قيم (△H) و(△G)و(△S) ومن خلال قيمة (△H) السالبة دلالة على ان التفاعل باعث للحرارة, وقيمة (△G) الموجبة الدلالة على ان العملية تلقائية ومن خلال قيمة (△S) الموجبة دلالة على وجود حالة نهائية اكثر من عشوائية وذلك بسبب وجود اكثر من طور في المحلول.

الكلمات المفتاحية: التخثير الكهربائي, قطب الستانلس ستيل, صبغة ليشمان.

المقدمة:

Introduction :

يعد التلوث من اهم مشاكل العصر التي تواجه العالم لذا يتطلب ايجاد طرق للتخلص من التلوث(1). حيث ادى التقدم في الصناعة احداث اضرار بيئية نتيجة طرح المخلفات السامة من المصانع في مياه الانهار, تعد الاصباغ احدى الاسباب الرئيسية لتلوث المياه. يعتبر التخثير الكهربائي تقنية كهروكيميائية حيث يتاكل قطب الالمنيوم(الانود) لاطلاق مود التخثر النشطة في المحلول.(2)

إلى جانب الاستخدام الواسع النطاق للأصباغ الاصطناعية في صناعات النسيج والأغذية والجلود والورق، فإنها تستخدم أيضًا بكميات أقل في المختبرات الصيدلانية والسريرية. تُستخدم صبغة الليشمان على نطاق واسع في مختبرات أمراض الدم التشخيصية(3). إن فائض البقع التي يتم تصريفها في مياه الصرف الصحي يسبب تلوث المياه.

الأصباغ يمكن أن يكون لها تأثيرات خطيرة حادة على الأنظمة الحية اعتمادًا على وقت التعرض وتركيزات الصبغة [4]

يتم فقدان حوالي 110,000 طن او اكثر من 100,000 نوع من الاصباغ المتاحة تجاريا اثناء عملية الصباغة سنويا على شكل نفايات سائلة.[5] معظم هذه الصبغة مسرطنة ومطفرة وسامة للكائنات المائية.[6]

يعد التلوث إحدى المشكلات التي يواجهها الإنسان والبيئة، خاصة بسبب التقدم التكنولوجي الذي يأتي مع الحياة. يتخذ التلوث في الوقت الحاضر أشكالًا عديدة، بما في ذلك تلوث الهواء والماء والتربة الناجم عن بعض الملوثات. إن المواد الكيميائية العضوية وغير العضوية الضارة، وكذلك زيادة أو نقصان نسب مركبات أساسية معينة في البيئة مقارنة بالنسب الطبيعية، تحدث بسبب التدخلات البشرية أو الأحداث الطبيعية[7] بسبب حاجة الإنسان الملحة إلى الماء، وبقاءه مرتبط ببقاء الماء ونقائه. تعتبر ملوثات المياه من أهم وأخطر الملوثات البيئية. ورغم ذلك لم تتحسن معاملتها وذلك بسبب زيادة النشاط السكاني والزراعي والصناعي وخاصة في المناطق القريبة من مصادر هذه المياه مما أدى إلى انخفاض خصائصها نتيجة زيادة تركيز العديد من الملوثات في هذه المياه. الطبيعية والكيميائية[8].

يهتم العديد من الباحثين ومنظمات حماية البيئة بمشكلة تنقية المياه. لقد تم اكتشاف أن معظم ما يلوث المياه هي المواد الكيميائية المستخدمة في الصناعات المختلفة، وخاصة الأصباغ، والمواد الكيميائية الناتجة عن تحلل الأصباغ المستخدمة في الصناعات النسيجية، حيث تعتبر الأصباغ من أكبر وأهم المركبات العضوية المستخدمة في الصناعات الكيميائية في العالم[9].

تعتبر الأصباغ من العناصر العضوية الملوثة لمصادر المياه بسبب أهميتها و انتشارها في الصناعات المائية المتنوعة، حيث تستخدم في صناعات النسيج والطباعة، كمضافات في الصناعات النفطية، وفي العديد من التخصصات الأخرى. ويتم تصنيع حوالي (5 × 107 طن) من هذه الأصباغ سنوياً. يتم استخدامه في جميع أنحاء العالم، ويتم استخدام العديد من المواد الكيميائية المختلفة في تركيبه؛ السلوك البيني غير معروف. وهي كبيرة الحجم، ويفقد حوالي 10-15% من هذه الأصباغ على شكل فضلات في الماء بسبب الصناعات المختلفة التي يتم إلقاؤها في مصادر المياه أو التربة، مما يسبب مشاكل كبيرة للكائنات الحية. وتزايد الاهتمام بإزالتها بعد أن أدرك أن الكثير منها.فالمواد الأولية المستخدمة في تحضير هذه الأصباغ هي في الأصل من العوامل المسببة للأمراض السرطانية؛ ونتيجة لذلك، فمن المستحسن إزالة هذه المركبات من الماء قبل إطلاقها في البيئة، ليس فقط لأسباب جمالية ولكن أيضًا بسبب سميتها وتأثيراتها طويلة المدى على الإنسان والنظام البيئي.[10,11]

وقد أجريت العديد من الدراسات في السنوات الأخيرة، وتم تطوير طرق وتقنيات فيزيائية وكيميائية وبيولوجية مختلفة لتقليل تلوث المياه وإزالة هذه الأصباغ. وتشمل هذه التقنيات الترسيب، والامتزاز، وفصل الغشاء، والأكسدة الكيميائية، والتبادل الأيوني، والمعالجة الهوائية واللاهوائية[12]

ويعتبر الامتزاز من أهم هذه التقنيات بسبب كفاءته العالية في هذا المجال، وبساطة العملية المستخدمة لهذا الغرض مقارنة بالطرق الأخرى، وتكلفته الاقتصادية المنخفضة رغم وجود بعض المواد الماصة باهظة الثمن. تحول العديد من الباحثين مؤخرًا إلى تطوير مواد ماصة جديدة باستخدام هذه التقنية. بعض المواد ذات أصل طبيعي، ولا يوجد تقريبًا أي صناعة اليوم لا تحتوي على مرافق لمعالجة نفايات الحياة[13].

أظهرت العديد من الدراسات أن تقنية النانو هي وسيلة فعالة لمعالجة مياه الصرف الصحي من خلال الامتزاز والتحلل. ومن أهم هذه التقنيات هي امتزاز معادن التكافؤ النانوية وعمليات الأكسدة المتقدمة (AOPs) وغيرها من

العمليات الفعالة في إزالة الملوثات العضوية وغير العضوية من خلال عملية التحلل والامتزاز بطريقة فعالة ومفيدة. بطريقة سريعة[14,15].

(Dwane,2018) وجماعته قاموا باستخدام تقنية التخثير الكهربائي في إزالة صبغة المثلين الزرقاء من مياه الصرف الصناعي .حيث تم الحصول على نسبة إزالة (97%) وذلك عند ظروف التشغيل الأتية الجهد المسلط هو (3.1V) ., كثافة التيار هي ($347mA/cm^2$) وزمن التخثيرهو (2.5min) والمسافة بين الأقطاب هي (2cm) وبذلك تدل النتائج على إمكانية استخدام التخثيرالكهربائي في إزالة الصبغات من مياه الصرف الصناعي على نطاق واسع .[16]

(M.Ravi Kumar & Bedewi Bilal 2018) قاموا بازالة صبغة Congo Red من مياه الصرف الصحى بطريقة الامتزاز باستخدام مواد ماصة منخفضة التكلفة ؛ وصديقة للبيئة حيث تمت دراسة عدد من المتغيرات على عملية الازالة وهي (الزمن: الدالة الحامضية؛ التركيزالابتدائي للصبغة؛ كمية المادة المازه, درجة الحرارة) وتم الحصول على نسبة إزالة عالية وهي 99.70% حيث كانت الظروف المثلى للحصول على هذه الازالة هي (درجة الحرارة 298K, PH=2-12, التركيز هو 100-300MG/L, كمية المادة المازة هي 0.1mg) وأشارت النتائج الى ان نموذج فريندلخ هو الأنسب لتلائم بيانات التوازن [17].

(Zainap Abdul Razaq 2018) قامت بدراسة لإزالة صبغتين حامضيتين من المياه النسيجية الملونة وهي الصبغة الحامضية الحمراء والصبغة الحامضية الزرقاء باستخدام عملية الأمتزاز في المعالجة, وتم استخدام ماده مازه معدومة الكلفة وهي بقايا مخلفات صناعة السمنت أي الغبار المتساقط من صناعة السمنت والطابوق والذي يعتبر من مخلفات الصناعة والتي لابد من التخلص منها, وتمت دراسة بعض المتغيرات وهي (تأثير الدالة الحامضية, التركيز, وقت التلامس, كمية المادة المازة) فوجد ان الظروف المثلى لهذه العملية هي (PH=2.5 للصبغة الحامضية الحمراء و (PH=6.5) للصبغة الحامضية الزرقاء, كمية المادة المازة للصبغتين هي (0.2g), الزمن للصبغتين (40min), التركيز للصبغتين هو(50mg/L), وكانت كفاءة الازالة هي(97%) للصبغة الحامضية الحمراء و(91%) للصبغة الحامضية الزرقاء.[18]

(Shrooq Mahdi Al-Bayyati 2020) تم استخدام طريقة التخثير الكهرباتي في إزالة صبغة (Orang12) من المحلول الماني باستعمال قطبين من الالمنيوم النقي بخلية تحليل حجمها (500ml) وتم اخذ ثلاثة تراكيز للصبغة هي (50,100,150ppm) وبدرجات حراره مختلفة هي ($20,25,30,35C^o$)وبفولتيات مختلفة هي(10,20,30V) والدالة الحامضية (5,7,9)وكانت المساحة السطحية للقطب هي($24cm^2$)والمسافة بين القطبين هي(1.2cm) وكانت نسبة الازالة هي(99.64%) وكانت الظروف المثلى لعملية الازالة هي التركيز(50ppm) ودرجة الحرارة هي ($35C^o$)»وبفولتيه (30v) و (PH=5) والمسافة بين القطبين (1cm). [19]

(Ihsan Habib Dakhil and Ahmed Hassan Ali 2020) قاموا بدراسة إزالة صبغة المثلين الزرقاء (Methylene Blue) من مياه الصرف الصناعي بطريقة الامتزاز باستخدام الكاربون المنشط المحضر من المخلفات الزراعية ؛ وتمت دراسة بعض المتغيرات المؤثرة على عملية الامتزاز و هي (الدالة الحامضية -PH=2 10, الزمن من 10-150min, التركيز الاولي للصبغة من 100-1000mg/l, كمية الكاربون المنشط كانت من 0.1-1g/100ml حيث كانت الظروف المثلى للحصول على افضل نسبة إزالة هي (الزمن 120min, PH=7, التركيز100mg/l, وزن الكاربون المنشط المضاف هو0.7g/100ml وتم الحصول على نسبة ازالة عالية جدا وهو 98.19%.[20]

وفي سنة 2020 قاموا Ahmed وجماعته بدراسة العوامل المؤثرة على عملية التلبيد الكهربائي لإزالة صبغة (supra green), و (blue-2) من محاليلها المائية كملوث باستخدام خلية الكتروليتية واقطاب من الالمنيوم النقي والستانلس ستيل (SS18) وبجهد مسلط 30V وبمدى من التراكيز (50,100,150,200ppm) واستخدام كبريتات الصوديوم كالكتروليت وبتركيزppm(50,100,150) حيث اتضح من الدراسة افضل نسبة ازالة تحققت عند تركيز200ppm عند قطب الالمنيوم وبنسبة ازالة 86.6% للصبغة Blue-2 وبنسبة 58% لصبغة supra green وبتركيز 150ppm للالكتروليت وتم حساب حركية الازالة للصبغات وكانت من المرتبة الاولى الوهمية الكاذبة [21].

(Ahmed Saeed Othman and Roaa Khalid, Attala.B.Dakhil 2021) تم استخدام طريقة التخثير الكهربائي في إزالة صبغة ((Yellow No10) وصبغة(Orange1) من المحلول المائي باستخدام اقطاب من الالمنيوم النقي واقطاب من (SS304)اخذ تراكيز مختلفة من الصبغة وهي(50,100,150ppm) وكذلك بفولتيات (5,10,15,20,25) واستخدامNaCl كمحلول الكتر وليتي بتركيز (50ppm) وزمن(100min).ان افضل النتائج وافضل إزالة في الصبغتين باستخدام اقطاب الالمنيوم كانت (95.24% Yellow No 10) و(Orang1 91.69%) بإضافة محلول الكتروليتى. اما افضل نسبة بدون محلول الكتر وليتي هى 97.31% Yellow No 10 () و (Orang193.77%).[22]

(Teshal Adane & Sintayehu.M.H.& Esayas Alemayehu 2022)قاموا بإزالة صبغة (Reactive Red 198, من محلولها المائي بطريقة الامتزاز باستخدام البنتونيت المنشط الممزوج مع مادة خاصة لقصب السكر كماده مازة تمت دراسة عدد من العوامل المؤثرة على الامتزاز مثل (الدالة الحامضية PH, تركيز الصبغة الاولي ؛ كمية المادة المازه؛ الزمن) حيث كانت الظروف المثلى للحصول على افضل إزالة هي (PH=2) تركيز العينة15mg/l, كمية المادة المازة3.7g/l , الزمن150min). تم الحصول على افضل نسبة إزالةوهي 97%. كذلك تم التحقق من كفاءة المادة الماصة من اجل تحديد حركيات الامتصاص, حيث تم سلوك التفاعل من المرتبة الثانية الوهمية الكاذبة. تم استخدام نماذج امتصاص مختلفة فلوحظ ان امتزاز صبغة (RR198) تم تمثيلة جيدا بواسطة ايزوثيرم لانكماير .[23]

2-الجزء العملي

1-2الاجهزة والمواد

1. ميزان الكتروني حساس
2. جهاز الرج والتحريك Hot plate
3. جهاز مطيافية الاشعة المرئية وفوق البنفسجية UV.Vissible spectro
4. جهاز قياس الجهد
5. خلية القياس من الزجاج
6. زجاجيات عامة
7. ماء مقطر
8. محلول الكتروليتي كبريتات الصوديوم
9. صبغة ليشمان :

هي صبغة متعادلة زرقاء اللون , وهي تتكون من الايوسين صبغة حمراء حامضية وصبغة المثيلين الزرقاء القاعدية.

اسم الصبغة: Leishman

الاسم العلمي: Leishmania

الصيغة التركيبية:

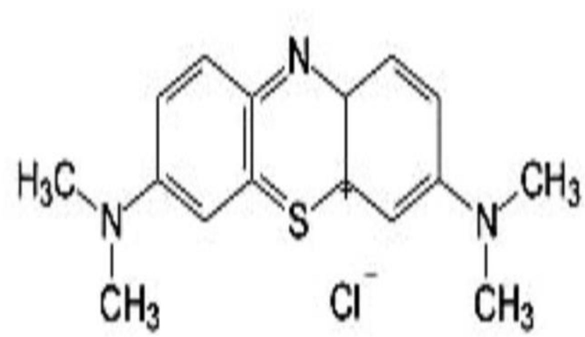

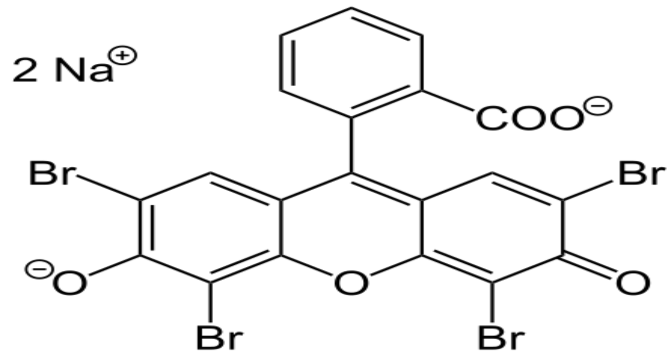

الصيغة الجزيئية: $C_{27}H_{27}ClN_2O_3S$
الوزن الجزيئي: 854.03g/mole

الطول الموجي :644nm

2- 2طريقة العمل

1- تحضير المحلول القياسي:

تم تحضير محلول قياسي للصبغة بتراكيز(100ppm) باذابة (1g) من الصبغة في (1000ml) من الماء المقطر وحضرت منه تراكيز مختلفة من الصبغة على التوالي (100ppm,200ppm,300ppm,400ppm). وبنفس الطريقة كذلك تم تحضير المحلول الالكتروليتي (Na_2SO_4)حيث تم اذابة (1g) من الملح في (1000ml) من الماء المقطر وباستعمال قانون التخفيف ($M_1V_1=M_2V_2$) تم تحضير تراكيز مختلفة من الملح على التوالي (50ppm,100ppm,150ppm) .

2-تحضير الخلية الكهربائية :

باستعمال خلية تحليل كهربائية مصنوعة من الزجاج ابعادها (الطول 10cm , وعرضها 8cm , وارتفاعها 6cm) وبسعة (300ml) وباستعمال اقطاب الالمنيوم ابعادها (الطول 8cm , وعرضه 7cm ,وبسمك 0.1cm) والمسافة بين الأقطاب (4cm), وكما موضح بالشكل(a-b)

الشكل(a)

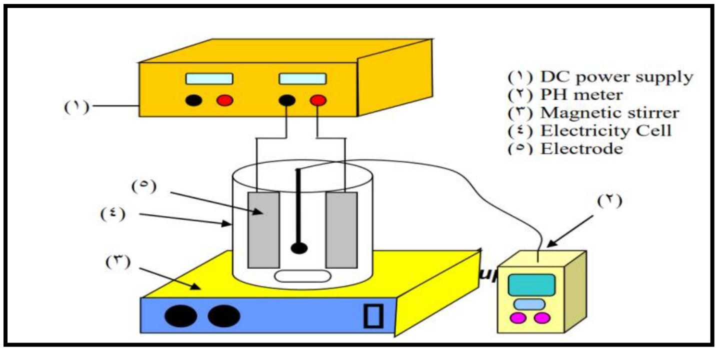

الشكل(b)

3- النتائج والمناقشة :

تم دراسة بعض المتغيرات التي تؤثر على نسبة الازالة .

1-3 تأثير التركيز الابتدائي للصبغة :

استخدمت اربعة تراكيز للصبغة وهي (100ppm,200ppm,300ppm,400ppm) وتم قياس التركيز المتبقي من خلال قياس الامتصاص المتبقي مع الزمن ولمدة(100min) ولكل تركيز ولمسافة (4cm) واستخدم تركيز من الالكتروليت (50ppm) عند دالة حامضية (6.9) وبطول موجي (544nm) ثم نحسب النسبة المئوية للإزالة.كما في الجداول والاشكال(1-5)

الجدول (1) قيم الامتصاص والنسبة المئوية للإزالة لصبغة Leishman بفولتية ثابتة (5volt) وبتراكيز مختلفة باستخدام قطبين من (الستانلس ستيلSS316) وبدرجة حرارة (298K).

5V								
Time(min)	100ppm		200ppm		300ppm		400ppm	
0	Abs.0.272	%R	Abs=0.507	%R	Abs.0.706	%R	Abs.0.912	%R
10	0.216	21	0.409	19	0.588	17	0.777	15
20	0.209	23	0.398	21	0.562	20	0.759	17
30	0.199	27	0.387	24	0.551	22	0.741	19
40	0.191	30	0.366	28	0.533	25	0.714	22
50	0.184	32	0.351	31	0.511	28	0.678	26
60	0.176	35	0.339	33	0.488	31	0.651	29
70	0.171	37	0.326	36	0.467	34	0.622	32
80	0.161	41	0.311	39	0.441	37	0.596	35
90	0.152	44	0.296	42	0.426	40	0.568	38
100	0.144	47	0.286	44	0.411	42	0.546	40

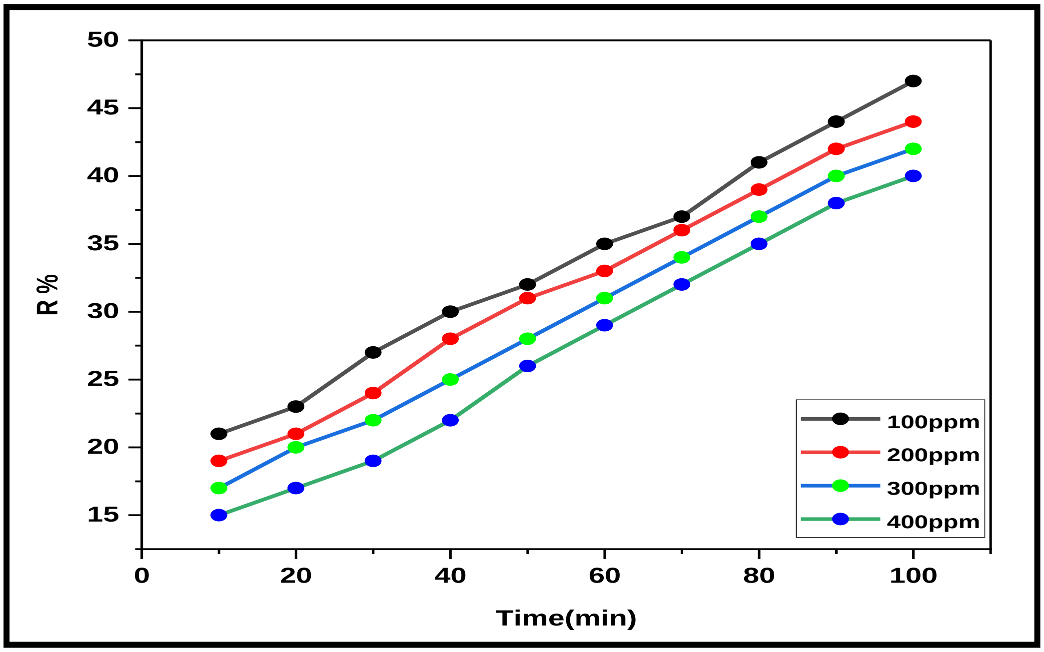

الشكل(1) الشكل (3-9) كفاءة الإزالة لصبغة Leishman بفولتية ثابتة (5volt) وبتراكيز مختلفة.

الجدول (2) قيم الامتصاص والنسبة المئوية للإزالة لصبغة Leishman بفولتية ثابتة (10volt) وبتراكيز مختلفة باستخدام قطبين من (الستانلس ستيلSS316) وبدرجة حرارة (298K).

10V								
Time(min)	100ppm		200ppm		300ppm		400ppm	
0	0.274	%R	Abs=0.509	%R	Abs.0.711	%R	Abs.0.913	%R
10	0.188	31	0.362	29	0.522	27	0.698	24
20	0.181	34	0.344	32	0.501	30	0.677	26
30	0.172	37	0.329	35	0.495	32	0.651	29
40	0.165	40	0.314	38	0.472	34	0.632	31
50	0.154	44	0.301	41	0.451	37	0.601	34
60	0.148	46	0.291	43	0.429	40	0.569	38
70	0.141	49	0.271	47	0.401	44	0.542	41
80	0.133	51	0.252	50	0.372	48	0.501	45
90	0.126	54	0.238	53	0.348	51	0.468	49
100	0.116	58	0.224	56	0.327	54	0.448	51

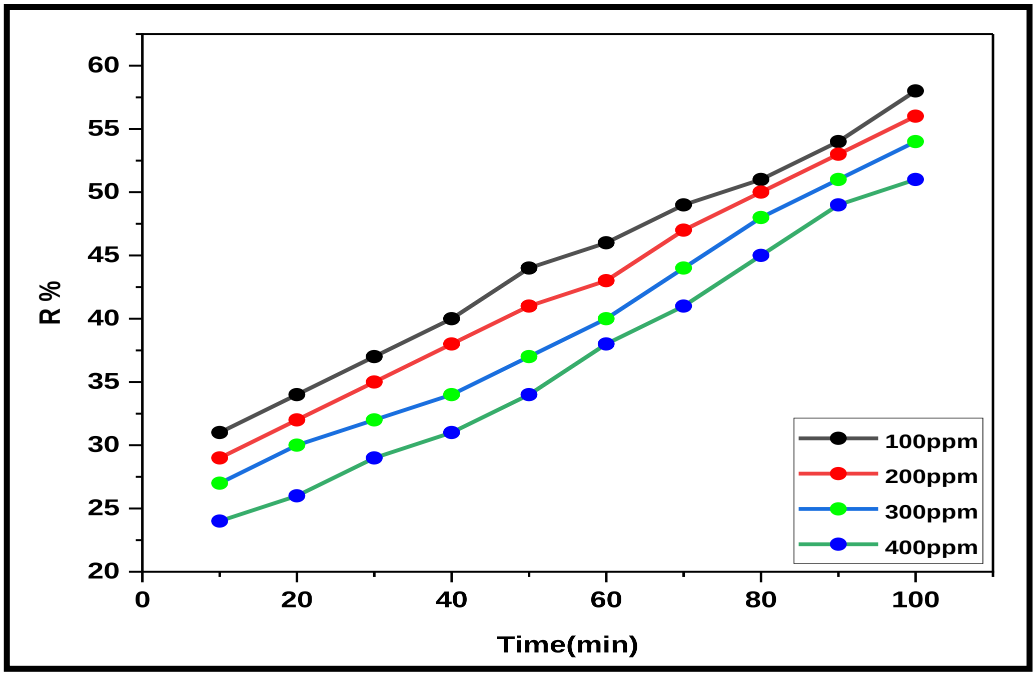

الشكل (10-3) كفاءة الإزالة لصبغة Leishman بفولتية ثابتة (10volt) وبتراكيز مختلفة.

الجدول (3) قيم الامتصاص والنسبة المئوية للإزالة لصبغة Leishman بفولتية ثابتة (15volt) وبتراكيز مختلفة باستخدام قطبين من (الستانلس ستيلSS316) وبدرجة حرارة (298K).

15V								
Time(min)	100ppm		200ppm		300ppm		400ppm	
0	0.279	%R	Abs=0.504	%R	Abs.0.709	%R	Abs.0.915	%R
10	0.171	39	0.316	37	0.467	34	0.628	31
20	0.162	42	0.302	40	0.442	38	0.608	34
30	0.151	46	0.288	43	0.421	41	0.571	38
40	0.142	49	0.271	46	0.398	44	0.544	41
50	0.138	51	0.258	49	0.378	47	0.508	44
60	0.128	54	0.242	52	0.359	50	0.479	48
70	0.116	58	0.228	55	0.336	53	0.448	51
80	0.108	61	0.208	59	0.305	57	0.414	55
90	0.095	66	0.183	64	0.278	61	0.384	58
100	0.068	69	0.172	66	0.257	64	0.362	60

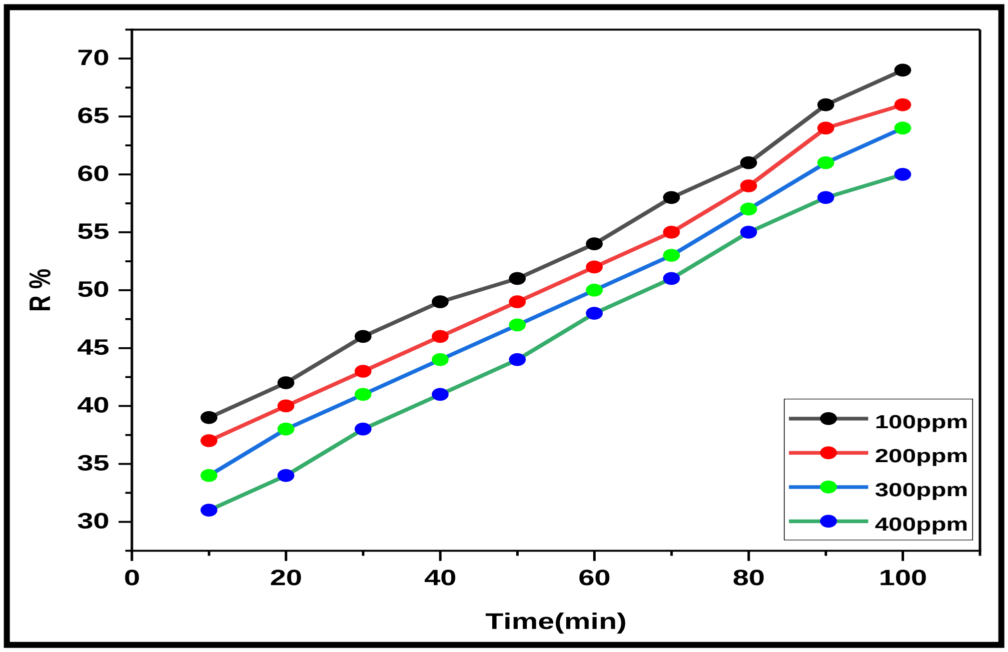

الشكل (3-11) كفاءة الإزالة لصبغة Leishman بفولتية ثابتة (15volt) وبتراكيز مختلفة .

الجدول (3-11) قيم الامتصاص والنسبة المئوية للإزالة لصبغة Leishman بفولتية ثابتة (20volt) وبتراكيز مختلفة باستخدام قطبين من (الستانلس ستيلSS316) وبدرجة حرارة (298K).

20V								
Time(min)	100ppm		200ppm		300ppm		400ppm	
0	0.277	%R	Abs=0.502	%R	Abs.0.714	%R	Abs.0.917	%R
10	0.144	48	0.272	46	0.401	44	0.536	42
20	0.136	51	0.261	48	0.388	46	0.507	45
30	0.128	54	0.241	52	0.359	50	0.478	48
40	0.116	58	0.228	55	0.338	53	0.452	51
50	0.108	61	0.207	59	0.309	57	0.426	54
60	0.101	64	0.196	61	0.287	60	0.394	57
70	0.091	67	0.174	65	0.266	63	0.358	61
80	0.083	70	0.158	69	0.238	67	0.334	64
90	0.069	75	0.142	72	0.208	71	0.296	68
100	0.062	78	0.122	76	0.187	74	0.265	71

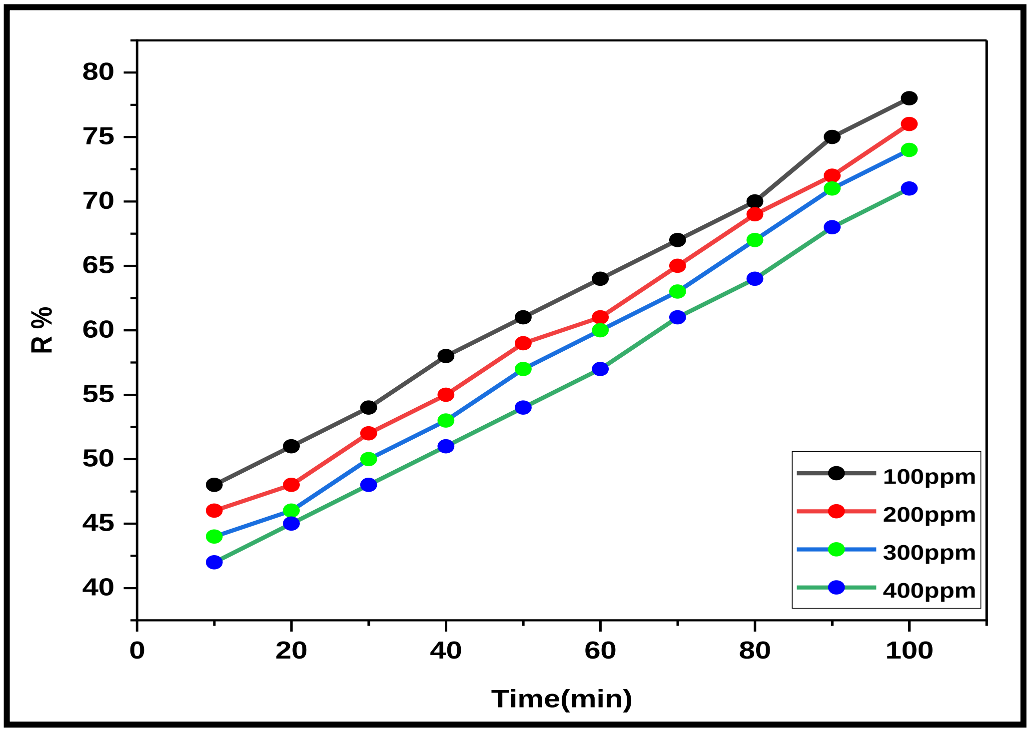

الشكل (3-12) كفاءة الإزالة لصبغة Leishman بفولتية ثابتة (20volt) وبتراكيز مختلفة .

الجدول (3-12) قيم الامتصاص والنسبة المئوية للإزالة لصبغةLeishman بفولتية ثابتة (25volt) وبتراكيز مختلفة باستخدام قطبين من (الستانلس ستيلSS316) وبدرجة حرارة (298K).

25V								
Time(min)	100ppm		200ppm		300ppm		400ppm	
0	0.288	%R	Abs=0.506	%R	Abs.0.716	%R	Abs.0.908	%R
10	0.122	58	0.228	55	0.336	53	0.455	50
20	0.112	61	0.207	59	0.311	57	0.431	53
30	0.104	64	0.192	62	0.288	60	0.392	57
40	0.092	68	0.174	66	0.257	64	0.358	61
50	0.084	71	0.158	69	0.235	67	0.328	64
60	0.076	74	0.142	72	0.211	71	0.291	68
70	0.066	77	0.129	75	0.186	74	0.258	72
80	0.056	81	0.108	79	0.167	77	0.231	75
90	0.046	84	0.093	82	0.144	80	0.209	78
100	0.035	88	0.072	86	0.123	83	0.174	81

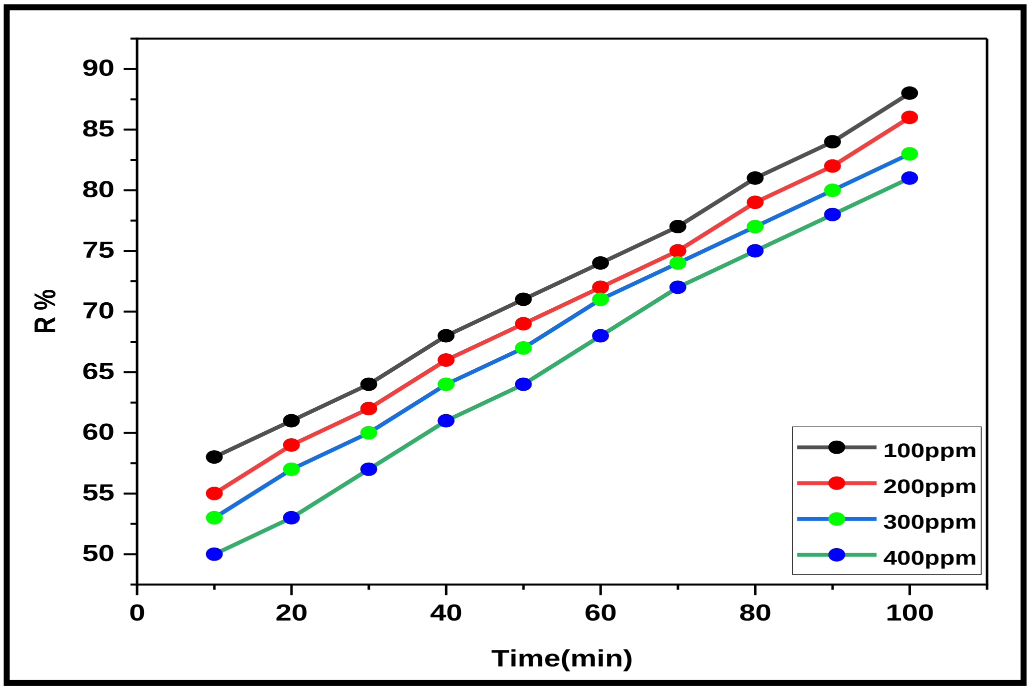

الشكل (3-13) كفاءة الإزالة لصبغة Leishman بفولتية ثابتة (25volt) وبتراكيز مختلفة

3-2- تأثير الفولتية:

تعتبر الفولتية من العوامل المؤثرة على كفاءة الازالة لصبغة Leishman اذ تمت دراسة كفاءة الازالة باستخدام خمسة انواع من الفولتيات على التوالي وهي (5v,10v,15v,20v,25 v) عند تركيز(200ppm) من الصبغة, و تركيز الالكتروليت (50ppm) عند دالة حامضية (6.9) وبمسافة(4cm) وبزمن لغاية (100min) وبدرجة حرارة (298K), عند طول موجي (544nm) وباستعمال قطبين من الالمنيوم النقي.وكما في الجدول(6)

الجدول (3-13) قيم الامتصاص والنسبة المئوية للإزالة لصبغة Leishman بتركيز ثابت (25ppm)وبفولتيات مختلفة لقطبين من (الستانلس ستيل(SS316) وبدرجة حراة (298K).

Time(min)	5V		10V		15V		20V		25V	
0	Abs.0.507	%R	Abs=0.509	%R	Abs.0.504	%R	Abs.0.502	%R	Abs.0.506	
10	0.409	19	0.362	29	0.316	37	0.272	46	0.228	55
20	0.398	21	0.344	32	0.302	40	0.261	48	0.207	59
30	0.387	24	0.329	35	0.288	43	0.241	52	0.192	62
40	0.366	28	0.314	38	0.271	46	0.228	55	0.174	66
50	0.351	31	0.301	41	0.258	49	0.207	59	0.158	69
60	0.339	33	0.291	43	0.242	52	0.196	61	0.142	72
70	0.326	36	0.271	47	0.228	55	0.174	65	0.129	75
80	0.311	39	0.252	50	0.208	59	0.158	69	0.108	79
90	0.296	42	0.238	53	0.183	64	0.142	72	0.093	82
100	0.286	44	0.224	56	0.172	66	0.122	76	0.072	86

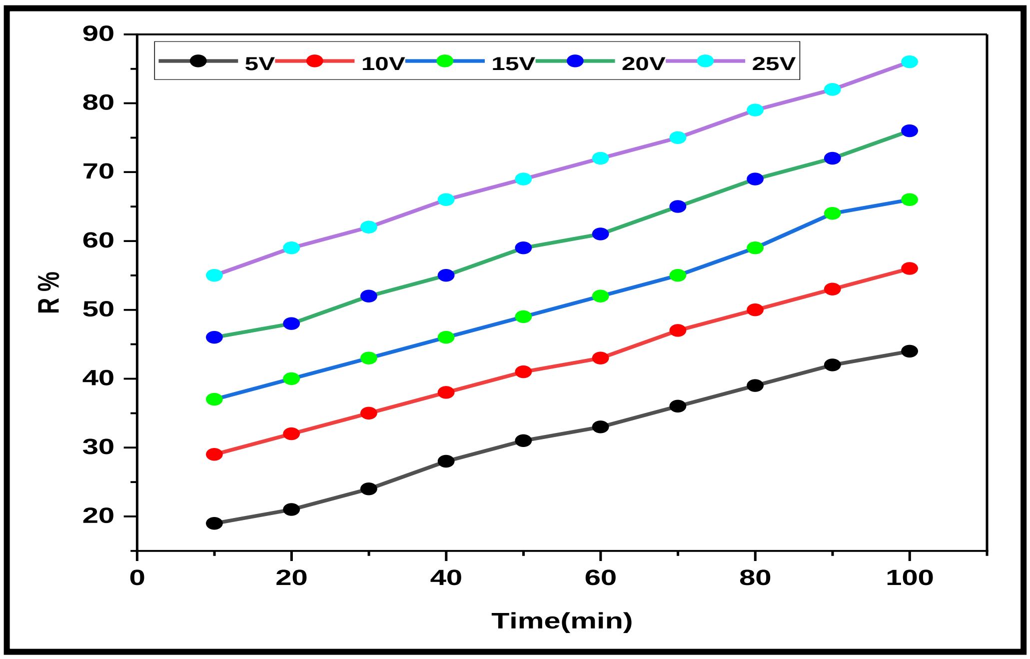

الشكل (3-14) كفاءة الإزالة لصبغة Leishman بتركيز ثابت (25ppm) وبفولتيات مختلفة.

نلاحظ من خلال الشكل (3-14) زيادة الفولتية ادت الى زيادة كفاءة الازالة.

3تأثير الألكتروليت :
بعد اضافة المحلول الالكتروليتي من العوامل المؤثرة على كفاءة الازالة لصبغة Leishman اذ تم استخدام ملح (Na_2SO_4) وبتراكيز مختلفة من الالكتروليت هي (50ppm,100ppm,150ppm) مع تركيز ثابت من الصبغة (200ppm) وبدالة حامضية(6.9) وبمسافة ثابتة (4cm) عند طول موجي (544nm) ولفترة زمنية (100min) وبدرجة حرارة (298K).
وكما في الشكل والجدول(7).

الجدول (3-14) قيم الامتصاص والنسبة المئوية للإزالة لصبغة Lieshman بفولتية ثابتة (25volt) وبتركيز(200ppm) ثابت من الصبغة باستخدام قطبين من الستانلس ستيل(SS316) وبدرجة حرارة (293K) عند إضافة محلول إلكتروليتي بتراكيز (50,100,150 ppm) مختلفة.

Time(mine)	50ppm	R%	100ppm	R%	150ppm	R%
0	Abs.0.506		0.509		Abs.0.511	
10	0.228	55	0.239	53	0.261	49
20	0.207	59	0.226	56	0.245	52
30	0.192	62	0.208	59	0.225	56
40	0.174	66	0.186	63	0.204	60
50	0.158	69	0.171	66	0.191	63
60	0.142	72	0.152	70	0.169	67
70	0.129	75	0.136	73	0.148	71
80	0.108	79	0.119	77	0.132	74
90	0.093	82	0.103	80	0.113	78
100	0.072	86	0.087	83	0.096	81

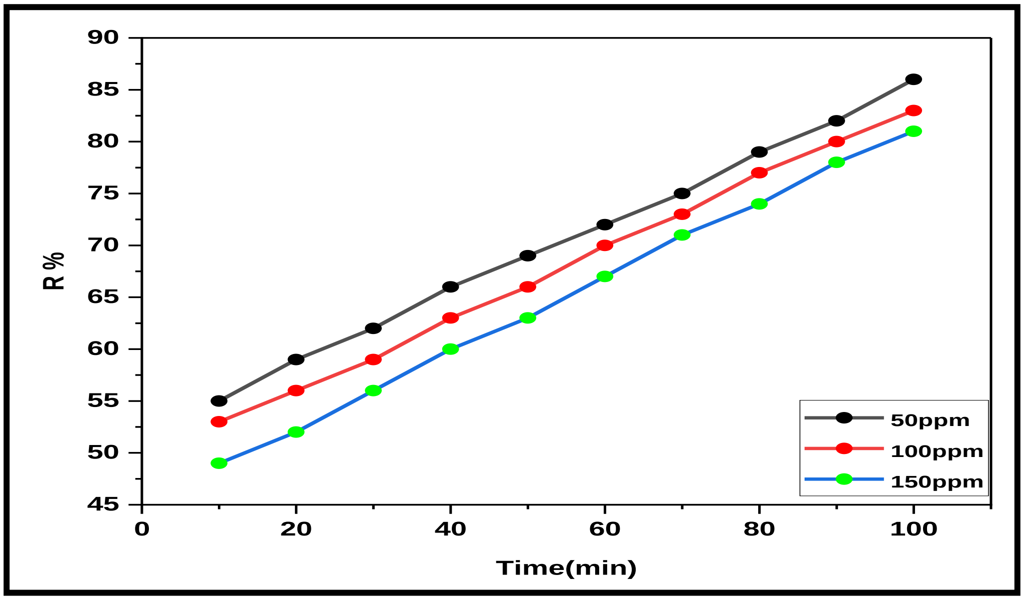

الشكل (7) كفاءة الإزالة لصبغة Leishman بتركيز ثابت (200ppm) بفولتية ثابتة (25volt) عند إضافة محلول إلكتروليتي بتراكيز مختلفة (50,100,150 ppm).

نلاحظ من خلال الشكل(3-15) تقل كفاءة الازالة مع زيادة تركيز الالكتروليت.

دراسة الحركية للصبغة Kinetic Studies Of The Pesticides [25,24]

تمت دراسة حركية إزالة المبيدات بعملية التخثير الكهربائي (Electrocoagulation) من خلال معادلة المرتبة الأولى :-

$$\text{Ln } a/a\text{-}x = K \cdot t \;\ldots\ldots\ldots\ldots\ldots\ldots(1\text{-}3)$$

وذلك من خلال رسم علاقة بيانية بين (Ln a/a-x) مع الزمن للاصباغ بتركيز (200ppm) وبفولتية (25 volt) للصبغة المدروسة ومع الكتروليت بتركيز(200ppm) لأقطاب والستانلس ستيل SS316 . حيث أعطت قوة علاقة جيدة دلالة على سلوك العملية بالمرتبة الأولى الوهمية الكاذبة وكذلك تم حساب ثابت معدل سرعة التفاعل (K) كما في الاشكال ا

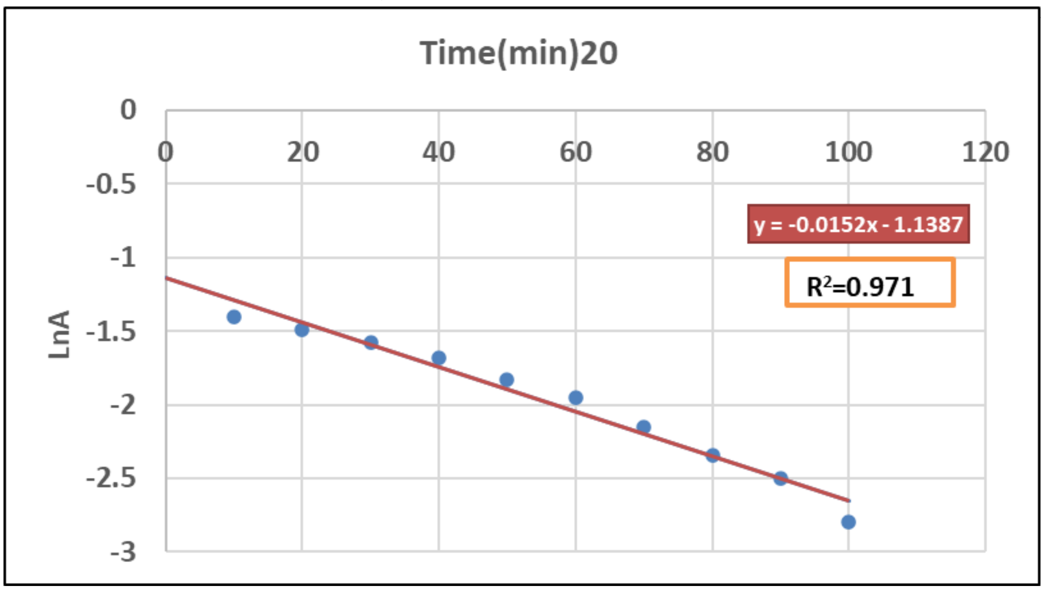

الشكل (8) حركية صبغة Leishman بتركيزثابت (200PPm) وبفولتية ثابتة (25 volt) وبمسافة(4cm) مع الكتروليت بتركيز(50ppm) باستخدام قطبين الستانلس ستيل وبدرجة حرارة(20C°).

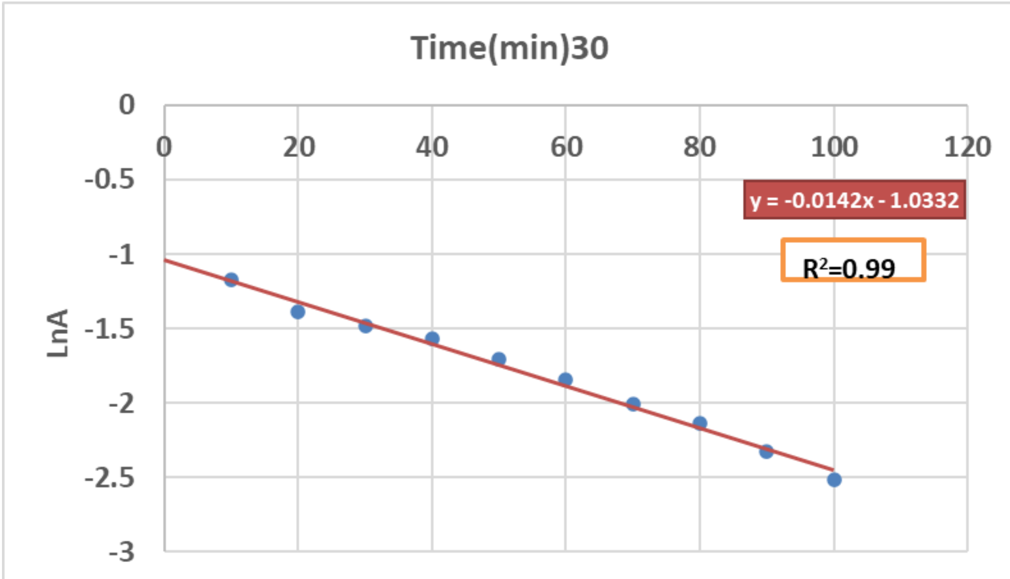

الشكل (9) حركية صبغة Leishman بتركيزثابت (200PPm) وبفولتية ثابتة (25 volt) وبمسافة(4cm) مع الكترووليت بتركيز(50ppm) باستخدام قطبين الستانلس ستيل وبدرجة حرارة(30C°).

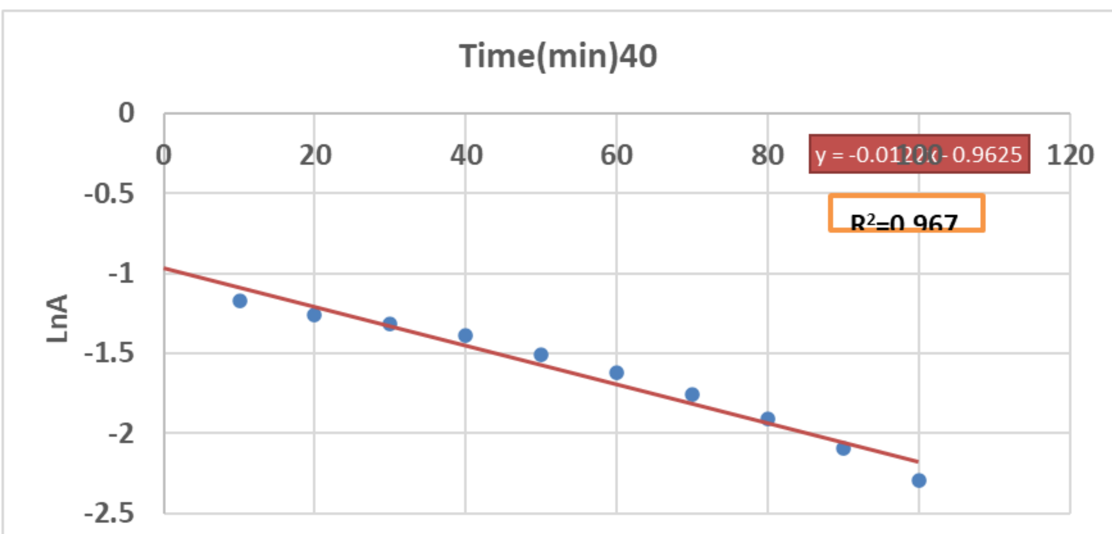

الشكل (10) حركية صبغة Leishman بتركيزثابت (200PPm) وبفولتية ثابتة (25 volt) وبمسافة(4cm) مع الكترووليت بتركيز(50ppm) باستخدام قطبين الستانلس ستيل وبدرجة حرارة(40C°).

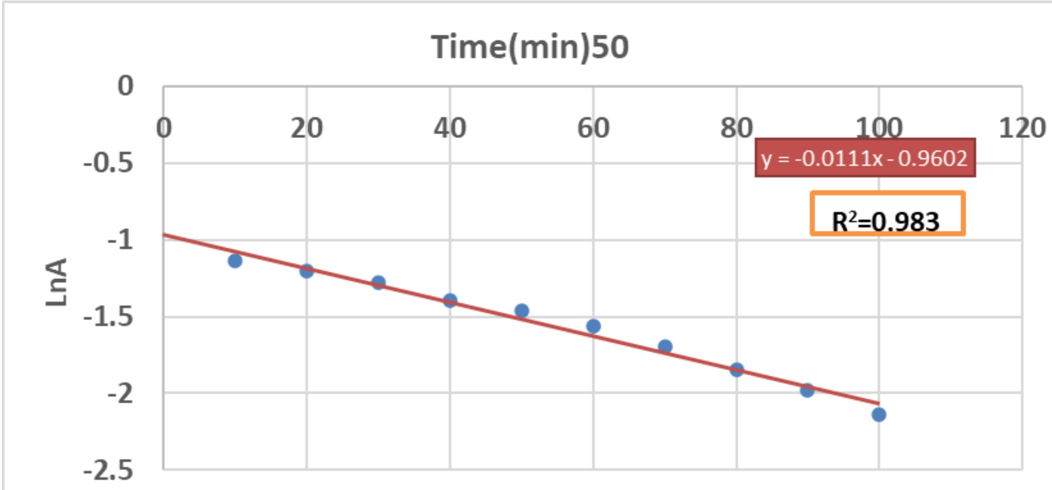

الشكل (11) حركية صبغة Leishman بتركيز ثابت (200PPm) وبفولتية ثابتة (25 volt) وبمسافة(4cm) مع الكتروليت بتركيز(50ppm) باستخدام قطبين الستانلس ستيل وبدرجة حرارة(50C°).

5 ميكانيكية التخثير الكهربائي لقطب الستانلس ستيل: [26,27,28]

تعتمد هذه التقنية على تحلل القطب الموجب لتكوين ايونات مختارة عند تطبيق تيار كهربائي. تتحلل الايونات لتكوين هيدروكسيدات ونواتج التحلل الاخرى لأيونات المعادن. في اقطاب الالمنيوم, يحتوي الالمنيوم على الميكانيكية التالية:

Anode $4Fe_{(s)} \rightarrow 4Fe^{+2}_{(aq)} + 8e^-$ (1)

$$4Fe^{+2}_{(aq)} + 10H_2O_{(l)} + O_{2(g)} \rightarrow 4Fe(OH)_{3(s)} + 8H^+_{(aq)} \quad (2)$$

Cathode $8H^+_{(aq)} + 8e^- \rightarrow 4H_{2(g)}$ (3)

Overall $4Fe_{(s)} + 10H2O_{(l)} + O_{2(g)} \rightarrow 4Fe(OH)_{3(s)} + 4H_{2(g)}$ (4)

<u>Mechanism2 :</u>

Anode: $Fe_{(s)} \rightarrow Fe^{+2}_{(aq)} + 2e^-$ (5)

$Fe^{+2}_{(aq)} + 2OH^-_{(aq)} \rightarrow Fe(OH)_{2(s)}$ (6)

Cathode: $2H_2O_{(l)} + 2e^- \rightarrow H_{2(g)} + 2OH^-_{(aq)}$ (7)

Overall: $Fe_{(s)} + 2H_2O_{(l)} \rightarrow Fe(OH)_{2(s)} + H_{2(g)}$ (8)

ولذلك, ونتيجة للتحلل المائي تتفكك جزيئات الماء الى ايونات الهيدروجين والهيدروكسيد, يكون القطب الموجب(الانود) اقرب الى الحمض(ايونات الهيدروكسيد) لإنتاج غاز الاوكسجين, بينما القطب السالب(الكاثود) يكون اقرب الى القاعدة(ايونات الهيدروجين) وينتج غاز الهيدروجين كما في المعادلة رقم(7) اعلاه

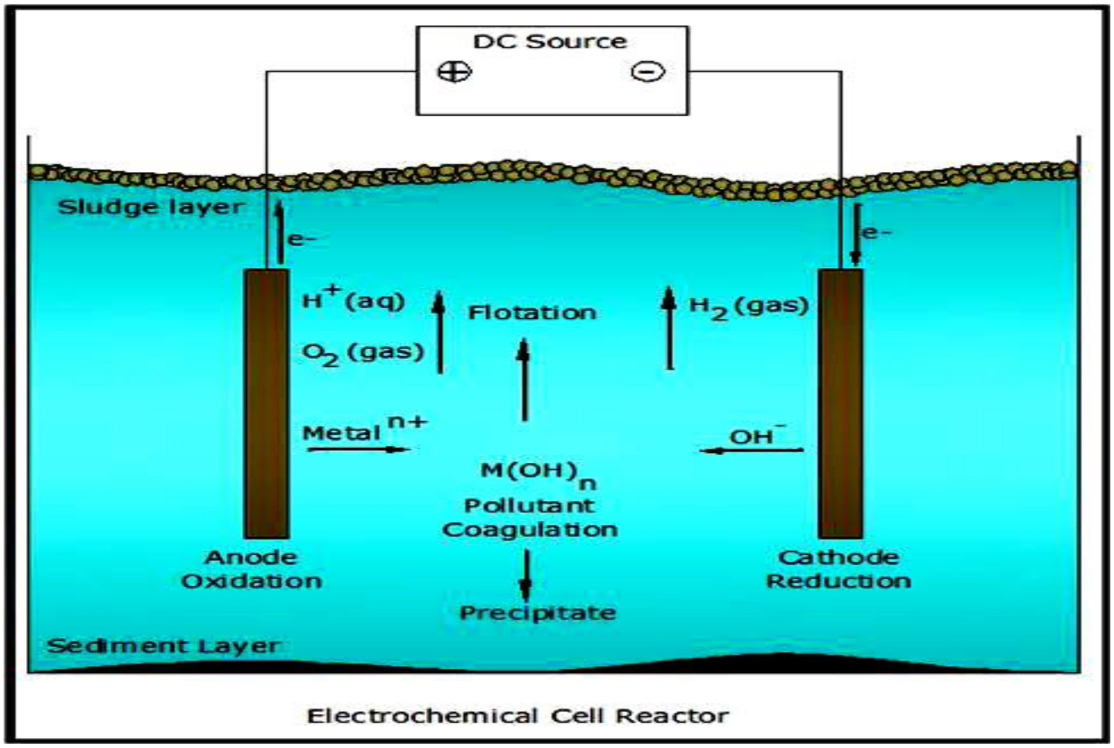

الشكل (12) يوضح التفاعلات الكهروكيميائية لقطبين في خلية التخثير الكهربائي.

-5- حساب الدوال الثرموداينمكية[29,30] Determination of the thermodynamic function:

تعطي الدوال الثرموداينمكية تفسيرا مميزا عند دراسة عملية التلبيد لصبغة الليشمانيا وتعد من المتغيرات المهمة التي توضح طبيعة النظام ونوع القوى المسيطرة عليه, فضلا على انها تعطي فكرة نوع التداخلات الجزيئية التي يمكن ان تحدث خلال عملية التلبيد والتي لها دور كبير في تحديد كفاءته, وبالاعتماد على التغير الحاصل لإزالة الصبغة عند زمن 100 دقيقة كقيمة لثابت الاتزان لتركيز صبغة ppm200 من خلال دراسة تاثير درجة الحرارة على قيم ثابت الاتزان .

تم حساب الانثالبي($\triangle H$)من خلال الرسوم البيانية في الاشكال (28)

ومن ثم حساب قيم ($\triangle G$) و ($\triangle S$) من خلال العلاقتين (3-3,4-3)

$\triangle G^o = -RTLnK_{eq}$ ------------------------(3-3)

$\triangle G^o = \triangle H - T\triangle S$ --------------------------(4-3)

قطب الستانلس ستيل(SS316)

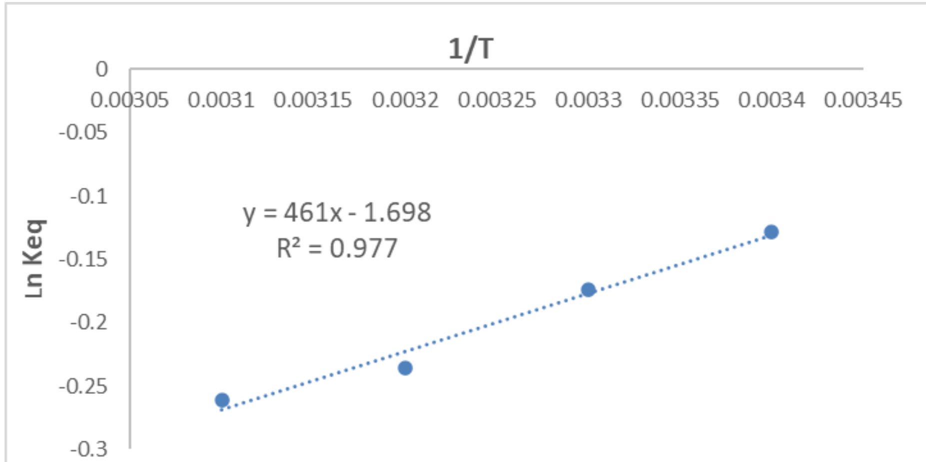

الشكل(13)علاقة لوغارتم ثابت الاتزان مع مقلوب درجة الحرارة لصبغة Lieshman بتركيزثابت (200PPm) وبفولتية ثابتة (25 volt) وبمسافة(4cm) مع الكتروليت بتركيز(50ppm) باستخدام قطبين الستانلس ستيل وبدرجات حرارية مختلفة ($20,30,40,50C^O$) وبفولتية ثابتة (25 volt) وبمسافة(4cm) مع الكتروليت بتركيز(50ppm) باستخدام قطبين الستانلس ستيل وبدرجات حرارية مختلفة (293,303,313,323K).

جدول(8) يوضح حساب قيم الانتروبي والطاقة الحرة لقطب الستانلس ستيل

التغير في الطاقة الحرة KJ/mol (△G)	التغير في الانتروبي (△S)KJ/mol.K
0.311	0.014
0.438	0.014
0.614	0.014
0.701	0.014

من خلال قيم الانثالبي السالبة تعطي دليل على كون عملية التلبيد باعثة للحرارة وقيم الطاقة الحرة الموجبة تدل على ان العلمية تلقائية بالاتجاه العكسي وقيم التغير بالانتروبي الموجبة تدل على وجود حالة نهائية اكثر عشوائية بسبب وجود اكثر من طور في المحلول طور بالحالة الصلبة مترسب أحيانا او يطفو فوق سطح المحلول.

الاستنتاجات:-

1-تتأثر نسبة الازالة بتركيز الصبغة اي انه تقل نسبة الازالة بزيادة التركيز للصبغة والعكس.

2-من خلال دراستنا بالظروف التجريبية المستخدمة ان افضل نسية ازالة لصبغة ليشمان عند تركيز (100ppm) وباستخدام قطب الستانلس ستيل وبجهد(25v) وبسرعة رج (60rpm) وبمسافة بين الاقطاب (4cm) وباستخدام محلول الكتروليتي كبريتات الصوديوم بتركيز(50ppm) حيث بلغت نسبة الازالة (88%), حيث بلغت اقل نسبة ازالة عند (5v) وبتركيز (400ppm) حيث قدرت النسبة 40%.

3-ان نسبة الازالة تتأثر بتركيز الالكتروليت حيث تقل نسبة الازالة بزيادة الالكتروليت وباستخدام قطب الستانلس ستيل, حيث بلغت اقل نسبة ازالة عند تركيز (150ppm) من الالكتروليت 81% واعلى نسبة ازالة عند تركيز (50ppm) من الالكتروليت 86% .

4- من خلال دراسة الحركية للصبغة وقيمة معامل الارتباط (R) العالية دلالة على سلوك العملية (المرتبة الأولى الوهمية الكاذبة).

المصادر: References
:

1- N. N.N,Marei,N.N,Vitale,G.and Arar.L.A(2015)'Adsorptiva removal of Dyes from synthetic and real textile wastewater using magnetic iron oxid nanoparticles: Thermodynamic and mechanistic incights Canadian Journal of chemical Engineering.93(11)pp:1965-1974.
2- Can . p.Carmona,M. Lobato,J.Martinez,F. & Rodrigo, M.A.'Electro dissolution of aluminum electrodes in electrocoagulation process Industrial Engineering Chemical research.vol.44.(2005)4178-4185.
3- KA. Fasakin, G.RA. Okogun, C.T. Omisakin, A.A. Adeyemi, AJ. Esan, Modified Leishman stain: the mystery unfolds, Br. J. Med. Med. Res. 4 (27) (2014) 4591-4006.
4- BH. Hameed, Equilibrium and kinetic studies of methyl violet sorption by agricultural waste, J. Hazard. Mater. 154 (2008) 204-212.
5- R. Y.;yamini, Y.; Faraji, M. and Nourmohammadian(2016)" Modified magnetite nanoparticles with cetyltrimethy lammonium bromide as superior adsorbent for rapid removal of the dis perse dye from wastewater of textile companies'nano.Chem .Res.J,1(1):49-56.
6- F. A.P.;Eder,C.L.;Silvio,L.P; and dias,A.M(2008)'Methelen blue biosorption from aqueous solution by yellow passion fruit waste'Hazardous materials J,150,703-712.

7- A. Siddiqua, J. N. Hahladakis, and W. A. K. A. Al-Attiya, "An overview of the environmental pollution and health effects associated with waste landfilling and open dumping," Environmental Science and Pollution Research, vol. 29, no. 39, pp. 58514-58536, 2022.
8- C. G. Daughton, "Non-regulated water contaminants: emerging research," Environ Impact Assess Rev, vol. 24, no. 7-8, pp. 711-732, 2004.
9- B. S. Rathi, P. S. Kumar, and D.-V. N. Vo, "Critical review on hazardous pollutants in water environment: Occurrence, monitoring, fate, removal technologies and risk assessment," Science of The Total Environment, vol. 797, p. 149134, 2021.
10- A. A., Mohd-Setapar, S. H., Chuong, C. S., Khatoon, A., Wani, W. A., Kumar, R., & Rafatullah, M., "Review on various types of pollution problem in textile dyeing & printing industries of Bangladesh and recommandation for mitigation," Journal of Textile Engineering & Fashion Technology, vol. 5, no. 4, pp. 220-226, 2019.
11- P. Kalivel, "Treatment of Textile Dyeing Waste Water Using TiO2/Zn Electrode by Spray Pyrolysis in Electrocoagulation Process," in Dyes and Pigments-Novel Applications and Waste Treatment, DOI: 10.5772/intechopen.95325, 2021.
12- A. A., Mohd-Setapar, S. H., Chuong, C. S., Khatoon, A., Wani, W. A., Kumar, R., & Rafatullah, M., "Recent advances In new generation dye removal technologies: novel search for approaches to reprocess wastewater," RSC Adv, vol. 5, no. 39, pp. 30801-30818, 2015.
13- A. Samadi-Maybodi, H. Ghezel-Sofla, and P. BiParva, "Co/Ni/Al-LTH layered triple hydroxides with zeolitic imidazolate frameworks (ZIF-8) as high efficient Removal of diazinon from aqueous solution," J Inorg Organomet Polym Mater, vol. 33, no. 1, pp. 10-29, 2023.
14- B. D. Deshpande, P. S. Agrawal, M. K. N. Yenkie, and S. J. Dhoble, "Prospective of nanotechnology in degradation of waste water: A new challenges," Nano-Structures & Nano-Objects, vol. 22, p. 100442, 2020.
15- A. S. Mahmoud, R. S. Farag, M. M. Elshfai, L. A. Mohamed, and S. M. Ragheb, "Nano zero-valent aluminum (nZVAI) preparation, characterization, and application for the removal of soluble organic matter with artificial intelligence, isotherm study, and kinetic analysis," AIr, Soil and Water Research, vol. 12: 1 13, no. DOI:10.1178622119878707, p. 1178622119878707, 2019.

16- Du.,xiaoxue, etc. Al."Application of Modified Electrocoagulatio for Efficient color Removal from synthetic Methylene Blu wastewater." Int.J. Electrochem.Sci13(2018):5575-5588.

17- M.RaviKumar & BedewiBilal . " Removal Of Congo Red Dye FromWastewater Using Adsorption." International Journal Engineering and Techniques , V-4, I-1 , (2018).

18- Zain. Abdul Razaq ." Testing the Ability of using Cement Kilns WasteFor Removing acid Dyes Wastewater by Adsorption Methode" Environmental Enginering Dept.Al-Mustansirah University-Baghadad-Iraq (2018).

19- Sh. Mahdi AL-Bayati , Attalh B, Dekhyl,,Waleed.M. Sheet Alabdraba using and styding the Efficiency of Electrochemical coagulation In Removing Acid Orange 12 Dye from wastewater,,MSC.thesis university Of Tikrit (2020).

20- Ihs .H.Dakhil and Ahmed .H.Ali " Adsorption of Methylene blue dyeFrom industrial wastewater using activated carbon prepared from agriculture Wastes" Dept-Chemical Enginering- Al-Muthana University —Iraq (2020).

21- A. Saeed Othman and Ahmed Aljebory " Removing of some Medical Pigment of Waste Water by Electrocoagulation".M.S.C University Of Tikrit Department of Chemistry. (2020).

22- A .S. Othman and Roaa Khaled ,,Atallah.B.Dakhil." Study Of TheFactors affecting the Electrocoagulation Efficiency Of dyes(Yellow No10,,Orangel) From their aqueous Solution"MSC thesis University Of Tikrit (2021).

23- T.Adane &Sintayehu .M.H & Esayas . A."Acid activated bentonite blendedWith Sugracane bagasse ash low cost adsorbents for removal of reactive red 198Dyes ". Dept-Chemical Engineering ~Addis Ababa University.(2022).

24- Vik. K.Sangal ; I-Mishra & J.P. Kushwahai." Electrocoagulation Of Soluble Oil Wastewater : Parametric and Kinetic Study ." Sepration Science and Technology .48 ; 1-131 .(2013).

25- M. Kostic. Analysis of Enthalpy Approximation for Compressed Liguid Water, IMECE 2004, ASME Proceedings ASME, New York, 2004.

26- Abd. Alghamdi &BadiaaGhemaout "electrocoagulation process:Amechanistic Review at the down of its Modeling" Journal of environment(science and allied research V.2;1SSue1,2019).

27- D.Ghernaout , M.W.Naceur & A.Khelifa "Study On Meachanism of Electrocoagulation With Iron electrodes in idealized Condition and Electrocoagulation of humic acid Solution In batch Using Aluminium electrodesDesalination and Water Treatment" 8,pp:91-99 (2009).

28- N. J. Mahri M; and Bazarafishan "Application of Electrocoagulation Process in Removal of Zinc and copper from aqueous solution by Aluminum Electrodes" international Journal of Enviriron Metal Research Vol-4- No 201-208(2010).

29- Y.A. Cengel and. M. Cimbala, Fluid Mechanics Fundamentals and Applications. New York: McGraw Hill, 2006.

30- H.Liepmann and A . Roshko . Element of Gas Dynamics Dover Publications, Mineola, NY, 2001.

Finding Ideal Points in PG(3,2), PG(3,3)

Hajir Hayder Abdullah[2]*, Sahbaa Abd alstar Younus[2], Wafa Younus Yahya[3]

[1]*Department of mathematics, College of Education for pure Science, University of Al-Hamdaniya, Nineveh, Iraq*

[2]*Department of mathematics, College of Education for pure Science, University of Al-Hamdaniya, Nineveh, Iraq* [3]*Department of mathematics, College of Education for pure Science, University of Al-Hamdaniya, Nineveh, Iraq*

* hajarhayder@uohamdaniya.edu.iq

Finding Ideal Points in PG(3,2), PG(3,3)

Hajir Hayder Abdullah[3]*, Sahbaa Abd alstar Younus[2], Wafa Younus Yahya[3]

[1]Department of mathematics, College of Education for pure Science, University of Al-Hamdaniya, Nineveh, Iraq

[2]Department of mathematics, College of Education for pure Science, University of Al-Hamdaniya, Nineveh, Iraq [3]Department of mathematics, College of Education for pure Science, University of Al-Hamdaniya, Nineveh, Iraq

Abstract

The mean goal of this research is to find ideal points, that is those points that appear continuously even after changing the point formula (x, y, z, w) and rearranging it in another way, and finding the distance between it and the original point .d(e) the divergent point e^n the point with a weight equal n, o(e) order of point, e^* the point generated by the element e .d the distance generated between the point.

Keywords: Projective plane, Projective space, Coding theory, Incidence matrix.

ايجاد النقاط المثالية في PG(3,2), PG(3,3)

هاجر حيدر عبدالله[1]*, صهباء عبد الستار يونس[2], وفاء يونس يحيى[3]

[1]قسم الرياضيات، كلية التربية للعلوم الصرفة، جامعة الحمدانية، نينوى، العراق

[2]قسم الرياضيات، كلية التربية للعلوم الصرفة، جامعة الحمدانية، نينوى، العراق

[3]قسم الرياضيات، كلية التربية للعلوم الصرفة، جامعة الحمدانية، نينوى، العراق

الخلاصة

الهدف الرئيسي لهذا البحث هو ايجاد النقاط المثالية اي تلك النقاط التي تظهر باستمرار حتى بعد تغيير صيغة النقطة (x ,y ,z ,w) واعادة ترتيبها بشكل اخر وايجاد المسافة بينها وبين النقطة الاصلية . d(e) النقطة المتباعدة, e^n النقطة الي وزنها n , o(e) رتبة العنصر, e^* النقاط المتولدة من النقطة الاصلية.

* hajarhayder@uohamdaniya.edu.iq

1. Introduction

In this research, the points of field 2 and field 3 were presented so that the elements of field 2 are {0,1}, and the elements of field 3 are {0,1,2} [10][13]. In addition to that, field 2 contains 15 points and field 3 contains 40 points, which are in the form (x, y, z, w). The general form of the point (x, x, z, w) was converted to (x^2, z, w), meaning that the x is repeated twice, and this point was converted into the form of a matrix whose elements are 0 and 1, meaning that the number in the form x^2 presents in two lines within the matrix whose weight is x regardless of the line's and column's number, that is, there are two lines whose weight is x [14][2]. Many matrices could be generated based on the place value of a certain number which showed that the matrices contains points belong to the fields 2 and 3 after converting the point formula, we called these points "The ideal points" or "The basic points" in the fields 2 and 3 because they appear constantly and always be repeated even after the general shape of the point gets changed, and according to that, we rearranged the field elements based on the sequence of the ideal points as well as finding the distance between the ideal points in addition to the distance between the original point and generated points [3][8].

2- Convert the points formula in field 2

Theorem 2.1 [8]: Every field (f) in the projective space contains exactly f^3+f^2+f+1 points. Meaning that the number of points in field 2 is 15

Theorem 2.2 [10]: Every line in the projective space contains exactly f^2+f+1 points.

Theorem 2.3 [7]**:** A f- ary (n , M ,2e +1)-code c satisfies

$$M \{\binom{n}{0}+\binom{n}{1}(f-1)+\ldots+\binom{n}{e}(f-1)^e\}\leq f^n$$

Corollary 2.4 [7] : f- ary (n , M ,2e +1)-code c is perfect if and only if equality holds in theorem 2.3

The following points represent the field 2 points and its dimension, which can be obtained from a certain matrix based on a certain equation:

e_1=[1,0,0,0]=[1,0^3] , e_2=[0,1,0,0]=[1,0^3] , e_3=[0,0,1,0]=[1,0^3] ,e_4=[0,0,0,1]=[0^3,1] , e_5=[1,1,0,0]=[1^2,0^2] ,e_6=[0,1,1,0]=[1^2,0^2] ,e_7=[0,0,1,1]=[1^2,0^2] ,e_8=[1,1,0,1]=[1^3,0] ,e_9=[1,0,1,0]=[1^2,0^2], e_{10}=[0,1,0,1]=[1^2,0^2] ,e_{11}=[1,1,1,0]=[1^3,0] ,e_{12}=[0,1,1,1]=[0,1^3] ,e_{13}=[1,1,1,1]=[1^4] ,e_{14}=[1,0,1,1]=[1^3,0] ,e_{15}=[1,0,0,1]=[1^2,0^2]

We should remember that e_i such that i =1,2,3,…..,15 has been previously obtained, and when multiplying the point [1,0,0,0] by the original matrix, we obtain the rest of the points.

Now, we explain the matrices that can be generated from e_i, that is, the maximum number of matrices. We start with the point e_1

$$\begin{bmatrix}1&0&0&0\\0&0&0&0\\0&0&0&0\\0&0&0&0\end{bmatrix},\begin{bmatrix}0&1&0&0\\0&0&0&0\\0&0&0&0\\0&0&0&0\end{bmatrix},\begin{bmatrix}0&0&1&0\\0&0&0&0\\0&0&0&0\\0&0&0&0\end{bmatrix},\begin{bmatrix}0&0&0&1\\0&0&0&0\\0&0&0&0\\0&0&0&0\end{bmatrix},\begin{bmatrix}0&0&0&0\\1&0&0&0\\0&0&0&0\\0&0&0&0\end{bmatrix},\begin{bmatrix}0&0&0&0\\0&1&0&0\\0&0&0&0\\0&0&0&0\end{bmatrix}$$

$$,\begin{bmatrix}0&0&0&0\\0&0&1&0\\0&0&0&0\\0&0&0&0\end{bmatrix},\begin{bmatrix}0&0&0&0\\0&0&0&1\\0&0&0&0\\0&0&0&0\end{bmatrix},\begin{bmatrix}0&0&0&0\\0&0&0&0\\1&0&0&0\\0&0&0&0\end{bmatrix},\begin{bmatrix}0&0&0&0\\0&0&0&0\\0&1&0&0\\0&0&0&0\end{bmatrix},\begin{bmatrix}0&0&0&0\\0&0&0&0\\0&0&1&0\\0&0&0&0\end{bmatrix},\begin{bmatrix}0&0&0&0\\0&0&0&0\\0&0&0&1\\0&0&0&0\end{bmatrix}$$

$$,\begin{bmatrix}0&0&0&0\\0&0&0&0\\0&0&0&0\\1&0&0&0\end{bmatrix},\begin{bmatrix}0&0&0&0\\0&0&0&0\\0&0&0&0\\0&1&0&0\end{bmatrix},\begin{bmatrix}0&0&0&0\\0&0&0&0\\0&0&0&0\\0&0&1&0\end{bmatrix},\begin{bmatrix}0&0&0&0\\0&0&0&0\\0&0&0&0\\0&0&0&1\end{bmatrix}$$

We obtained sixteen matrices from $e_1$while changing the location of number 1. We notice that the sixteen matrices contain the points 1, 2, 3 and 4 only and no matter how frequent the location of number 1 gets changed, we always obtain these four points only. Based on that, we can say that each point is converted and as the same formula of the first point regardless of the location of number 1generated four points , which is in the form [1,0^3] generates four different points, and from here we say that each point from field 2, which is in the form of the first point, generates four different points.

O($e_4$4= e_4^*),e_3^*,e_2^*, e_1^*)=(e_1 ,e_2 ,e_3 ,

Let's move on the point e_5=[1,1,0,0]=[1^2,0^2]

$$\begin{bmatrix}1&0&0&0\\1&0&0&0\\0&0&0&0\\0&0&0&0\end{bmatrix},\begin{bmatrix}0&1&0&0\\0&1&0&0\\0&0&0&0\\0&0&0&0\end{bmatrix},\begin{bmatrix}0&0&1&0\\0&0&1&0\\0&0&0&0\\0&0&0&0\end{bmatrix},\begin{bmatrix}0&0&0&1\\0&0&0&1\\0&0&0&0\\0&0&0&0\end{bmatrix},\begin{bmatrix}1&0&0&0\\1&0&0&0\\0&0&0&0\\0&0&0&0\end{bmatrix},\begin{bmatrix}1&0&0&0\\0&1&0&0\\0&0&0&0\\0&0&0&0\end{bmatrix}$$

$$,\begin{bmatrix}1&0&0&0\\0&0&1&0\\0&0&0&0\\0&0&0&0\end{bmatrix},\begin{bmatrix}1&0&0&0\\0&0&0&1\\0&0&0&0\\0&0&0&0\end{bmatrix},\begin{bmatrix}1&0&0&0\\0&0&0&0\\1&0&0&0\\0&0&0&0\end{bmatrix},\begin{bmatrix}1&0&0&0\\0&0&0&0\\0&1&0&0\\0&0&0&0\end{bmatrix},\begin{bmatrix}1&0&0&0\\0&0&0&0\\0&0&1&0\\0&0&0&0\end{bmatrix},\begin{bmatrix}1&0&0&0\\0&0&0&0\\0&0&0&1\\0&0&0&0\end{bmatrix}$$

$$,\begin{bmatrix}1&0&0&0\\0&0&0&0\\0&0&0&0\\1&0&0&0\end{bmatrix},\begin{bmatrix}1&0&0&0\\0&0&0&0\\0&0&0&0\\0&1&0&0\end{bmatrix},\begin{bmatrix}1&0&0&0\\0&0&0&0\\0&0&0&0\\0&0&1&0\end{bmatrix},\begin{bmatrix}1&0&0&0\\0&0&0&0\\0&0&0&0\\0&0&0&1\end{bmatrix}.$$

These matrices are not the maximum or all matrices that can be generated from the fifth point, but it is showed that no matter how the location of the number 1 changes, the points 1, 2, 3 and 4 will appear. So, the fifth point, that is in the form of e_5=[1,1,0,0] =[1^2,0^2] generates the first four points and each point, that is in the form of the fifth point, generates these points only.

O(e_5 ,= 4e_4^*),e_3^*,e_2^*, e_1^*)=(e_{15} , e_9 , e_{10} ,e_7 ,e_6

O(e_8= 4e_4^*),e_3^*,e_2^*, e_1^*=(e_{12}, e_{13}) ,e_{14} ,e_{11} ,

Then, the elements generated from all points of field 2 are (e_1^*, e_2^*, e_3^*, e_4^*) which are basic and always exist.

Now, you will publish the table in which we will show the distance between the main original points and the generated elements

Table 2-1: Ideal points in PG(3,2)

Points	The code	Points generated from e_i (Ideal points in `projective space of order 2)	Number of matrices generated from e_i	Distance between e_i and e_i^*
e_1	e_1^4	e_1^* , e_2^*,e_3^*,e_4^*	16	Not found ,2,2,2
e_2	e_2^4	e_1^* , e_2^*,e_3^*,e_4^*	16	2,not found ,2,2
e_3	e_3^4	e_1^* , e_2^*,e_3^*,e_4^*	16	2,2,not found,2
e_4	e_4^4	e_1^* , e_2^*,e_3^*,e_4^*	16	2,2,2,not found
e_5	e_5^4	e_1^* , e_2^*,e_3^*,e_4^*	96	1,1,3,3
e_6	e_6^4	e_1^* , e_2^*,e_3^*,e_4^*	96	3,1,1,3

e_7	e_7^4	e_1^* , e_2^*,e_3^*,e_4^*	96	3,3,1,1
e_8	e_8^4	e_1^* , e_2^*,e_3^*,e_4^*	256	2,2,4,2
e_9	e_9^4	e_1^* , e_2^*,e_3^*,e_4^*	96	1,3,1,3
e_{10}	e_{10}^4	e_1^* , e_2^*,e_3^*,e_4^*	96	3,1,3,1
e_{11}	e_{11}^4	e_1^* , e_2^*,e_3^*,e_4^*	256	2,2,3,4
e_{12}	e_{12}^4	e_1^* , e_2^*,e_3^*,e_4^*	256	4,2,2,2
e_{13}	e_{13}^4	e_1^* , e_2^*,e_3^*,e_4^*	256	3,3,3,3
e_{14}	e_{14}^4	e_1^* , e_2^*,e_3^*,e_4^*	256	2,4,2,1
e_{15}	e_{15}^4	e_1^* , e_2^*,e_3^*,e_4^*	96	1,3,3,1

3- Convert the points formula in field 3

e_1=[1,0,0,0]=[1,0^3], e_2=[0,1,0,0]=[1,0^3] , e_3=[1,1,0,0]=[1^2,0^2] , e_4=[2,1,0,0]=[2^1,1^1,0^2] , e_5=[0,1,1,0]=[1^2,0^2] ,e_6=[1,1,1,0]=[1^3,0] ,e_7=[2,1,1,0]=[2^1,1^2,0] ,e_8=[0,2,1,0]=[2^1,1^1,0^2], e_9=[0,0,1,0]=[0^3,1] ,e_{10}=[1,0,1,0]=[1^2,0^2] , e_{11}=[2,0,1,0]=[2^1,1^1,0^2], e_{12}=[1,2,1,0]=[2^1,1^2,0] , e_{13}=[2,2,1,0]=[2^2,1,0] , e_{14}=[0,0,0,1]=[0^3,1], e_{15}=[1,0,0,1]=[1^2,0^2] , e_{16}=[2,0,0,1]=[2,1,0^2] ,e_{17}=[0,1,0,1]=[1^2,0^2] , e_{18}=[1,1,0,1]=[1^3,0], e_{19}=[2,1,0,1]=[2^1,1^2,0^2] , e_{20}=[0,2,0,1]=[2^1,1,0^2], e_{21}=[1,2,0,1]=[1^2,0,2], e_{22}=[2,2,0,1]=[2^2,0,1], e_{23}=[0,0,1,1]=[1^3,0^2] , e_{24}=[1,0,1,1]=[1^3,0] , e_{25}=[2,0,1,1]=[2,0,1^2], e_{26}=[0,1,1,1]=[1^3,0] , e_{27}=[1,1,1,1]=[1^4] , e_{28}=[2,1,1,1]=[2^1,1^3] , e_{29}=[0,2,1,1]=[1^2,0^1, 2^1], e_{30}=[1,2,1,1]=[1^3,2^1], e_{31}=[2,2,1,1]=[1^2,2^2] , e_{32}=[0,0,2,1]=[0^2,1^1 ,2^1] ,e_{33}=[1,0,2,1]=[0^1,1^2, 2^1], e_{34}=[2,0,2,1]=[0^1,1^2, 2^2] , e_{35}=[0,1,2,1]=[1^2,0^1,2^1] , e_{36}=[1,1,2,1]=[1^3,2^1],

e_{37}=[2,1,2,1]=[2^2,1^2] , e_{38}=[0,2,2,1]=[1^2,0^1,2^2] , e_{39}=[1,2,2,1]=[1^1,2^2], e_{40}=[2,2,2,1]=[1^1,2^3]

Table 3-1:Ideal points in PG(3,3)

Points	The code	Points generated from e_i	Distance between e_i and e_i^*
e_1	e_1^4	e_1^* , e_2^*,e_9^*,e_{14}^*	Not found , 2,2,2
e_2	e_2^4	e_1^* , e_2^*,e_9^*, e_{14}^*	2,not found ,2,2
e_3	e_3^4	e_1^* , e_2^*,e_9^*,e_{14}^*	1,1,3,3
e_4	e_4^9	e_1^* , e_2^*,e_3^*,e_9^* e_{23}^*,e_{17}^*,e_{15}^*,e_{10}^*, e_{14}^*,	2,1,1,3,3,3,3,2,4
e_5	e_5^4	e_1^* , e_2^*,e_9^*,e_{14}^*	3,1,1,3
e_6	e_6^4	e_1^* , e_2^*,e_9^*,e_{14}^*	2,2,2,4
e_7	e_7^9	e_1^* , e_2^*,e_3^*,e_9^* e_{23}^*,e_{17}^*,e_{15}^*,e_{10}^*, e_{14}^*,	3,2,2,2,4,2,4,3,3
e_8	e_8^9	e_1^* , e_2^*,e_3^*,e_9^* e_{23}^*,e_{17}^*,e_{15}^*,e_{10}^*, e_{14}^*,	3,2,3,1,3,2,4,3,2
e_9	e_9^4	e_1^* , e_2^*,e_9^*,e_{14}^*	2,2,not found ,2
e_{10}	e_{10}^4	e_1^* , e_2^*,e_9^*,e_{14}^*	1,3,1,3
e_{11}	e_{11}^9	e_1^* , e_2^*,e_3^*,e_9^* e_{23}^*,e_{17}^*,e_{15}^*,e_{10}^*, e_{14}^*,	2,3,3,1,3,1,3,4,2

e_{12}	e_{12}^{9}	e_1^* , e_2^*,e_3^*,e_9^* e_{23}^*,e_{17}^*,e_{15}^*,e_{10}^*, e_{14}^*,	2,3,2,2,4,1,3,4,3
e_{13}	e_{13}^{9}	e_1^* , e_2^*,e_3^*,e_9^* e_{23}^*,e_{17}^*,e_{15}^*,e_{10}^*, e_{14}^*,	3,3,3,2,4,2,4,4,3
e_{14}	e_{14}^{4}	e_1^* , e_2^*,e_9^*,e_{14}^*	2,2,2,not found
e_{15}	e_{15}^{4}	e_1^* , e_2^*,e_9^*,e_{14}^*	1,3,3,1
e_{16}	e_{16}^{9}	e_1^* , e_2^*,e_3^*,e_9^* e_{23}^*,e_{17}^*,e_{15}^*,e_{10}^*, e_{14}^*,	2,3,3,3,1,3,1,2,2
e_{17}	e_{17}^{4}	e_1^* , e_2^*,e_9^*,e_{14}^*	3,1,3,1
e_{18}	e_{18}^{4}	e_1^* , e_2^*,e_9^*,e_{14}^*	2,2,4,2
e_{19}	e_{19}^{9}	e_1^* , e_2^*,e_3^*,e_9^* e_{23}^*,e_{17}^*,e_{15}^*,e_{10}^*, e_{14}^*,	3,2,2,4,2,4,2,1,3
e_{20}	e_{20}^{9}	e_1^* , e_2^*,e_3^*,e_9^* e_{23}^*,e_{17}^*,e_{15}^*,e_{10}^*, e_{14}^*,	3,2,3,3,1,4,2,1,2
e_{21}	e_{21}^{9}	e_1^* , e_2^*,e_3^*,e_9^* e_{23}^*,e_{17}^*,e_{15}^*,e_{10}^*, e_{14}^*,	2,3,2,4,2,3,1,2,3
e_{22}	e_{22}^{9}	e_1^* , e_2^*,e_3^*,e_9^* e_{23}^*,e_{17}^*,e_{15}^*,e_{10}^*, e_{14}^*,	3,3,3,4,2,4,2,2,3
e_{23}	e_{23}^{4}	e_1^* , e_2^*,e_9^*,e_{14}^*	3,1,1,1
e_{24}	e_{24}^{9}	e_1^* , e_2^*,e_3^*,e_9^* e_{23}^*,e_{17}^*,e_{15}^*,e_{10}^*, e_{14}^*,	2,4,3,2,2,1,1,3,1
e_{25}	e_{25}^{9}	e_1^* , e_2^*,e_3^*,e_9^* e_{23}^*,e_{17}^*,e_{15}^*,e_{10}^*, e_{14}^*,	3,4,4,2,2,2,2,3,1
e_{26}	e_{26}^{4}	e_1^* , e_2^*,e_9^*,e_{14}^*	4,2,2,2

e_{27}	e_{27}^{4}	e_1^* , e_2^*,e_9^*,e_{14}^*	3,3,3,3
e_{28}	e_{28}^{9}	e_1^* , e_2^*,e_3^*,e_9^* e_{23}^*,e_{17}^*,e_{15}^*,e_{10}^*, e_{14}^*,	4,3,3,3,3,3,3,2,2
e_{29}	e_{29}^{9}	e_1^* , e_2^*,e_3^*,e_9^* e_{23}^*,e_{17}^*,e_{15}^*,e_{10}^*, e_{14}^*,	4,3,4,2,2,3,3,2,1
e_{30}	e_{30}^{9}	e_1^* , e_2^*,e_3^*,e_9^* e_{23}^*,e_{17}^*,e_{15}^*,e_{10}^*, e_{14}^*,	3,4,3,3,3,2,2,3,2
e_{31}	e_{31}^{9}	e_1^* , e_2^*,e_3^*,e_9^* e_{23}^*,e_{17}^*,e_{15}^*,e_{10}^*, e_{14}^*,	4,4,4,3,3,3,3,3,2
e_{32}	e_{32}^{9}	e_1^* , e_2^*,e_3^*,e_9^* e_{23}^*,e_{17}^*,e_{15}^*,e_{10}^*, e_{14}^*,	3,3,4,2,1,3,2,2,1
e_{33}	e_{33}^{9}	e_1^* , e_2^*,e_3^*,e_9^* e_{23}^*,e_{17}^*,e_{15}^*,e_{10}^*, e_{14}^*,	2,4,3,3,2,2,1,3,2
e_{34}	e_{34}^{9}	e_1^* , e_2^*,e_3^*,e_9^* e_{23}^*,e_{17}^*,e_{15}^*,e_{10}^*, e_{14}^*,	3,4,4,3,2,3,2,3,2
e_{35}	e_{35}^{9}	e_1^* , e_2^*,e_3^*,e_9^* e_{23}^*,e_{17}^*,e_{15}^*,e_{10}^*, e_{14}^*,	4,2,3,3,2,4,3,1,2
e_{36}	e_{36}^{9}	e_1^* , e_2^*,e_3^*,e_9^* e_{23}^*,e_{17}^*,e_{15}^*,e_{10}^*, e_{14}^*,	3,3,2,4,3,3,2,2,3
e_{37}	e_{37}^{9}	e_1^* , e_2^*,e_3^*,e_9^* e_{23}^*,e_{17}^*,e_{15}^*,e_{10}^*, e_{14}^*,	4,3,3,4,3,4,3,2,3
e_{38}	e_{38}^{9}	e_1^* , e_2^*,e_3^*,e_9^* e_{23}^*,e_{17}^*,e_{15}^*,e_{10}^*, e_{14}^*,	4,3,4,3,2,4,3,2,2
e_{39}	e_{39}^{9}	e_1^* , e_2^*,e_3^*,e_9^* e_{23}^*,e_{17}^*,e_{15}^*,e_{10}^*, e_{14}^*,	3,4,3,4,3,3,2,3,3
e_{40}	e_{40}^{9}	e_1^* , e_2^*,e_3^*,e_9^* e_{23}^*,e_{17}^*,e_{15}^*,e_{10}^*, e_{14}^*,	4,4,4,4,3,4,3,3,3

First set

O(e_1 ,e_2 ,e_3 ,e_5 ,e_6 ,e_9 ,e_{10} ,e_{14} e_{15} ,e_{17} e_{18} ,e_{23} ,e_{26})e_{27} = 4 = (e_1^* , e_2^*,e_9^*,e_{14}^*)

Second set

O(e_8 ,e_{11} ,e_{12} e_{16} ,e_{19} ,e_{20} ,e_{21} ,e_{24} ,e_{25}, e_{28} ,e_{29} ,e_{30} , e_{31} ,e_{32} ,e_{33} e_{34} , e_4, e_{13}, e_7, e_{22}, e_{35} , e_{36}, e_{37} ,e_{38} ,e_{39} e_{40})= 9 = (e_1^* , e_2^*,e_3^*,e_9^*)e_{23}^*,e_{17}^*,e_{15}^*,e_{10}^*, e_{14}^*,

From the second group, we notice that the most frequent points are nine points, and based on that, we can say that e_1^*, e_2^*, e_3^*, e_9^*,e_{14}^*, e_{10}^*, e_{15}^*, e_{17}^*, e_{23}^* are ideal basic points in the field 3 in the projective space.

These results were reached by placing number 1 and making it represent the weight of the matrix, but by placing number 2 or 1 and 2 in the matrix, the results were completely different. An example of this is

$$\begin{bmatrix}2&0&0&0\\2&0&0&0\\0&0&0&0\\0&0&0&0\end{bmatrix}$$

$$,\begin{bmatrix}0&0&0&2\\2&0&0&0\\0&0&0&0\\0&0&0&0\end{bmatrix},\begin{bmatrix}0&2&0&0\\1&0&0&0\\0&0&0&0\\0&0&0&0\end{bmatrix}\begin{bmatrix}0&0&1&0\\2&0&0&0\\0&0&0&0\\0&0&0&0\end{bmatrix},\begin{bmatrix}1&0&0&0\\0&0&2&0\\0&0&0&0\\0&0&0&0\end{bmatrix},\begin{bmatrix}1&0&0&0\\0&2&0&0\\0&0&0&0\\0&0&0&0\end{bmatrix},$$

$$\begin{bmatrix}0&0&0&2\\0&0&0&2\\0&0&0&0\\0&0&0&0\end{bmatrix},\begin{bmatrix}0&2&0&0\\0&1&0&0\\0&0&0&0\\0&0&0&0\end{bmatrix}\begin{bmatrix}0&0&1&0\\0&0&2&0\\0&0&0&0\\0&0&0&0\end{bmatrix}$$

All points generated in the matrices above belong to the permutations of field 3, so we call these points the divergent points.

Set d(e) ={(2,0,0,0) , (0,2,0,0) , (0, 0, 0,2) ,…)

We will find the generated code based on the ideal points in field 2

If any ideal point does not lie on a straight line, then it is called a straight line

Δ_0^*

If one ideal point lies on a straight line, then it is called a straight line

Δ_1^*

If two ideal points lie on a straight line, then it is called a straight line

Δ_2^*

If three ideal points lie on a straight line, then it is called a straight line

Δ_3^*

If the ideal points lie on a straight line, then it is called a straight line

Δ_*^* Completely perfect

Note: If the rectum filter is 1 and if the non-rectal filter is 0

Table 3-2 : Lines in PG(3,2)

t_1	t_2	t_3	t_4	t_5	t_6	t_7	t_8	t_9	t_{10}	t_{11}	t_{12}	t_{13}	t_{14}	t_{15}
2	1	1	1	3	1	1	3	2	1	4	1	5	2	2
3	3	2	2	4	4	2	5	4	3	5	6	6	7	3
4	4	4	3	5	6	5	10	9	8	6	7	7	8	6
6	7	5	5	7	11	7	11	10	9	8	8	9	9	8
7	9	8	6	8	12	12	12	11	10	9	10	10	11	13
10	14	10	9	11	13	13	14	13	12	12	11	13	12	14
12	15	15	11	13	15	14	15	14	13	14	14	15	15	15

Table 3-3 : Lines in PG(3,3)

t_1	t_2	t_3	t_4	.	.	.	t_{37}	t_{38}	π_{39}	t_{40}
2	1	4	3	.	.	.	3	1	3	4
5	9	7	6	.	.	.	5	8	7	6
8	10	9	9	.	.	.	11	12	8	8
9	11	12	13	.	.	.	12	13	10	11
14	14	14	14	.	.	.	15	17	16	15
17	15	19	18	.	.	.	19	18	17	17
20	16	21	22	.	.	.	20	19	21	22
23	23	23	23	.	.	.	23	23	23	23

26	24	28	27	.	.	.	27	24	27	28
29	25	30	31	.	.	.	31	25	31	30
32	32	32	32	.	.	.	34	38	33	34
35	33	37	36	.	.	.	35	39	37	36
38	34	39	40	.	.	.	39	40	38	38

Table 3-4 :The code generated in field 2

	e_1^*	e_2^*	e_3^*	e_4^*	Type of Δ_i	Distance between ideal points in the line PG(3,2)
Δ_1	0	1	1	1	Δ_3^*	2,2,2,1,3,3,3,2,1,3,2,4,3,2,1
Δ_2	1	0	1	1	Δ_3^*	2,2,1,1,3,2,3,1,2,2,3,4,3
Δ_3	1	1	0	1	Δ_2^*	2,3,1,1,4,1,3,2,2,3,2,3
Δ_4	1	1	1	0	Δ_3^*	3,3,1,2,2,1,3,2,3,2,1
Δ_5	0	0	1	1	Δ_2^*	2,4,1,2,2,1,3,2,3,2
Δ_6	1	0	0	1	Δ_2^*	2,3,2,2,1,1 ,2,3,4
Δ_7	1	1	0	0	Δ_2^*	3,2,2,3,1,2,1,2
Δ_8	0	0	1	0	Δ_1^*	3,1,2,2,1,2,1
Δ_9	0	1	0	1	Δ_2^*	4,1,3,2,1,2
Δ_{10}	1	0	1	0	Δ_2^*	3,1,2,3,2
Δ_{11}	0	0	0	1	Δ_1^*	2,1,2,3
Δ_{12}	1	0	0	0	Δ_1^*	1,2,3
Δ_{13}	0	0	0	0	Δ_0^*	1,2
Δ_{14}	0	1	0	0	Δ_1^*	1
Δ_{15}	0	1	1	0	Δ_2^*	Not Found

Table 3-5 : The code generated in field 3

	e_1^*	e_2^*	e_3^*	e_9^*	e_{10}^*	e_{14}^*	e_{15}^*	e_{17}^*	e_{23}^*	Type of Δ_i	Distance between ideal points in the line PG(3,3)

Δ_1	0	1	0	1	0	1	0	1	0	Δ_4^*	8
Δ_2	1	0	0	1	1	1	1	0	1	Δ_6^*	3
Δ_3	0	0	0	1	0	1	0	0	1	Δ_3^*	4
Δ_4	0	0	1	1	0	1	0	0	1	Δ_4^*	5
Δ_5	1	0	0	0	0	1	1	0	0	Δ_3^*	3
Δ_6	0	0	0	0	0	1	0	0	0	Δ_1^*	2
Δ_7	0	0	1	0	1	1	0	0	0	Δ_3^*	4
Δ_8	1	0	0	0	0	1	1	0	0	Δ_3^*	3
Δ_9	1	1	1	0	0	1	1	1	0	Δ_6^*	3
Δ_{10}	0	1	0	0	0	1	0	1	0	Δ_3^*	5
Δ_{11}	0	1	0	0	1	1	0	0	0	Δ_3^*	4
Δ_{12}	0	0	1	0	0	1	0	0	0	Δ_2^*	4
Δ_{13}	0	0	0	0	1	1	0	0	0	Δ_2^*	2
Δ_{14}	1	1	1	1	1	0	0	0	0	Δ_4^*	1
Δ_{15}	0	1	0	1	0	0	0	0	0	Δ_2^*	4
Δ_{16}	0	1	0	1	0	0	1	0	0	Δ_3^*	6
Δ_{17}	1	0	0	1	1	0	0	0	0	Δ_3^*	3
Δ_{18}	0	0	0	1	0	0	0	0	0	Δ_1^*	2
Δ_{19}	0	0	1	1	0	0	1	0	0	Δ_3^*	4
Δ_{20}	1	0	0	1	1	0	0	1	0	Δ_4^*	4
Δ_{21}	0	0	0	1	0	0	0	1	0	Δ_3^*	4
Δ_{22}	0	0	0	1	0	0	0	1	0	Δ_2^*	4
Δ_{23}	1	1	1	0	0	0	0	0	0	Δ_3^*	1
Δ_{24}	0	1	0	0	0	0	0	0	0	Δ_1^*	2
Δ_{25}	0	1	0	0	1	0	1	0	0	Δ_3^*	6
Δ_{26}	1	0	0	0	0	0	0	0	0	Δ_1^*	1
Δ_{27}	0	0	0	0	0	0	0	0	0	Δ_0^*	Not found
Δ_{28}	0	0	1	0	1	0	0	0	0	Δ_2^*	4
Δ_{29}	1	0	0	0	0	0	0	1	0	Δ_2^*	3
Δ_{30}	0	0	1	0	0	0	0	1	0	Δ_2^*	4
Δ_{31}	0	0	0	0	1	0	1	1	0	Δ_3^*	4
Δ_{32}	1	1	1	0	0	0	0	0	1	Δ_4^*	2
Δ_{33}	0	1	0	0	1	0	0	0	1	Δ_3^*	5

Δ_{34}	0	1	0	0	0	0	1	0	1	Δ_3^*	5
Δ_{35}	1	0	0	0	0	0	0	0	1	Δ_2^*	2
Δ_{36}	0	0	0	0	1	0	0	0	1	Δ_2^*	3
Δ_{37}	0	0	1	0	0	0	1	0	1	Δ_3^*	5
Δ_{38}	1	0	0	0	0	0	0	1	1	Δ_3^*	2
Δ_{39}	0	0	1	0	1	0	0	1	1	Δ_4^*	5
Δ_{40}	0	0	0	0	0	0	1	1	1	Δ_3^*	1

Results:

We note that the minimum distance generated by the above code is 1 and the largest distance generated is 8

Ideal points in field 2 are : e_1^* , e_2^*,e_3^*,e_4^*

Ideal points in field 3 are : e_1^* , e_2^*,e_3^*,e_9^* e_{23}^*,e_{17}^*,e_{15}^*,e_{10}^*, e_{14}^*,

There is no perfect straight line, but straight line 27 we call it a trivial straight line because it does not contain any ideal point

Through the theorem, we test the ideality of the code generated from ideal point

$M\ \{\binom{n}{0}+\binom{n}{1}(f\text{-}1)+\ldots\ldots\ldots\ldots\ldots\ldots+\binom{n}{e}(f-1)^e\}\leq f^n$

$3^{36}\{\binom{40}{0}\}\leq 3^{40}$

[40 ,4,1]-code is not perfect

The valuse of the distance between the ideal points of the lines in field 2 are :1,2,3,4

The valuse of the distance between the ideal points of the lines in field 3are :1,2,3,4,5 ,6,8

Table 3-6 :Some Values of the distance between orginal points and ideal points in field 3, 2

1,3,3,1	1,1,3,3
2,3,3,3,1,3,1,2,2	3,1,1,3

3,1,3,1	3,3,1,1
2,2,4,2	2,2,4,2
3,2,2,4,2,4,2,1,3	1,3,1,3
3,2,3,3,1,4,2,1,2	3,1,3,1
2,3,2,4,2,3,1,2,3	2,2,3,4
3,3,3,4,2,4,2,2,3	4,2,2,2
3,1,1,1	3,3,3,3
2,4,3,2,2,1,1,3,1	2,4,2,1
3,4,4,2,2,2,2,3,1	1,3,3,1
4,2,2,2	
3,3,3,3	
4,3,3,3,3,3,3,2,2	
4,3,4,2,2,3,3,2,1	
3,4,3,3,3,2,2,3,2	
4,4,4,3,3,3,3,3,2	

3,3,4,2,1,3,2,2,1	
2,4,3,3,2,2,1,3,2	
3,4,4,3,2,3,2,3,2	
4,2,3,3,2,4,3,1,2	
3,3,2,4,3,3,2,2,3	
4,3,3,4,3,4,3,2,3	
4,3,4,3,2,4,3,2,2	
3,4,3,4,3,3,2,3,3	
4,4,4,4,3,4,3,3,3	

Reference

[1] A. A. Younis and N. Y. K. Yahya, "The construction (k + 1; n)-arcs and (k + 2; n)-arcs from incomplete (k; n)-arc in P G(3, q)", Palestine Journal of Mathematics, 12(Special Issue I), pp. 107–129, 2023.

[2] A. M. Khalaf and N. Y. K. Yahya, "New Examples in Coding Theory for Construction Optimal Linear Codes Related With Weight Distribution", AIP Conference Proceedings, 2845(1), 050043, 2023. DOI: https://dio.org/10.1063/5.0170590.

[3] A. S. AL-Mukhtar, "Complete Arcs and Surfaces in three-Dimensional Projective Space over Galois Field", Thesis University of Technology, Iraq, 2008.

[4] E. B. Al-Zangana & N. Y. K. Yahya, "Subgroups and Orbits by Companion Matrix in Three-Dimensional projective space", Baghdad science Journal, 2022. Doi: https://dio.org/10.21123/bsj.2022.19.4.0805.

[5] E. B. Al-Zangana, S. A. Joudah, "Action of Groups on the Projective Plane over the Field GF(41)", IOP Conf. Series: Journal of Physics: Conf. Series 1003, 2018. DOI: https://doi.org/10.1088/1742-6596/1003/1/012059.

[6] E. B. Al-Zangana,"Certain Types of Linear Codes over the Finite Field of Order Twenty-Five" Iraqi Journal of Science, Vol.62, No.11, pp:40194031, 2021. DOI: https://doi.org/10.24996/ijs.2021.62.11.22.

[7] F. N. Abdullah and N. Y. K. Yahya, "Bounds on Minimum Distance for Linear Codes Over GF(q)", Italian Journal of pure and Applied Mathematics, n.45.p.894-903, lSSN2239-0227, 2021.

[8] H. H. Abdullah, "New Applications of Coding Theory in The Projective Space of Order Three", Proceeding of 3rd International Conference of Mathematics and its Applications, TICMA2022, 2022. https://conferences.su.edu.krd/su/ticma2022. DOI: https://doi.org/10.31972/ticma2022.

[9] H. M. Khalaf and N. Y. K. Yahya, "A Geometric Construction of (K, r)-cap in PG(3, q) for q prime, 2 ≤q ≤997", Journal of Physics: Conference Series, 2322(1), 012043, 2022. DOI: https://dio.org/10.1088/1742-6596/2322/1/012043.

[10] H. M. Khalaf, "A New Geometric Method for Constructing Complete (k , n)-Arcs in PG(3,11)", AIP Conference Proceedings 2394, 070019, 2022. DOI: https://doi.org/10.1063/5.0121056.

[11] J. S. Radhi and E. B. Al-Zangana, "Complete (k,r)-Caps From Orbits In PG(3,11)", Iraqi Journal of Science, Vol.64, No.1, pp:347-353, 2023. DOI: https://doi.org/10.24996/ijs.2023.64.1.32.

[12] N. A. M. Al-Seraji, A. Bakheet and Z. S. Jafar, "Study of orbits on the finite projective plane", Journal of Interdisciplinary Mathematics, 2020. DOI: https://doi.org/10.1080/09720502.2020.1747195.

[13] N. Y. K. Yahya and E. B. Al-Zangana, "The Non-existence of [1864, 3, 1828]53 Linear Code by Combinatorial Technique", International Journal of Mathematics and Computer Science, 16(4), 1575–1581, 2021.

[14] N. Y. K. Yahya, "Applications Geometry of Space in PG(3, p)", Journal of Interdisciplinary Mathematics, 2021. DOI: https://dio.org/10.1080/09720502.2021.1885818.

On Some Mappings in Intuitionistic Topological Spaces

[1]Saleh,B.H

[2]Yassen, S.R

[3]Amina, K. H

[1,2]Department of Mathematics, College of Education for Pure Sciences,

Tikrit University, Tikrit, Iraq

[3]Materials Department, College of Engineering, Mustansiriyah University, Baghdad, Iraq.

[2]samer2017@tu.edu.iq

[3]Amina.kass@uomustansiriyah.edu.iq

On Some Mappings in Intuitionistic Topological Spaces

[1]Saleh,B.H

[2]Yassen, S.R

[3]Amina, K. H

[1,2]Department of Mathematics, College of Education for Pure Sciences, Tikrit University, Tikrit, Iraq

[3]Materials Department, College of Engineering, Mustansiriyah University, Baghdad, Iraq.

[2]samer2017@tu.edu.iq

[3]Amina.kass@uomustansiriyah.edu.iq

Abstract

This work presents new types of some generalized weak continuous, closed and open mappings like intuitionistic $Ig\alpha A*-$continuous$(resp., Ig\alpha A*$ closed map, $Ig\alpha A*$ open map$)$, $Ig\beta A*-$continuous $(resp., Ig\beta A*$ closed map, $Ig\beta A*$ open map$)$, $IgPA*-$continuous $(resp., IgPA*$ closed map, $IgPA*$ open map$)$, $IgSA*-$continuous

$(resp., IgSA*$ closed map, $IgSA*$ open map$)$ and $LIg-$ continuous $(resp., LIg-$ closed map, $LIg-$ open map$)$. Moreover, we introduced new types of some generalized weak irresolute mappings, Like intuitionistic $Ig\alpha A*-$irresolute, $Ig\beta A*-$irresolute, $IgPA*-$irresolute, $IgSA*-$irresolute$-$, $LIg-$ irresolutewith studying some properties related them. Also, we studying some relationships among these concepts. Finally, relationships among generalized weak continuous mappings and generalized weak continuous mappings are studied.

Keywords: Weak shapes, irresolute function, strong function, perfectly function.

Introduction

The area for intuitionistic topological areas has progressed through a series of significant contributions by diverse academics. Zadeh's (1965) groundbreaking study on fuzzy sets laid the foundation for this subject. In 1983, Atanassov proposed the idea of fuzzy sets that were intuitionistic, which added another degree of complication to the idea. In 1996, Çoker presented intuitionistic sets as well as points, providing up new paths for investigation. In 1997, Çoker established intuitionistic fuzzy topological areas, and later, in 2000, he expanded on this structure to include intuitionistic topological spaces. In 2001, Bayhan and Çoker introduced the $T1$ and $T2$ separating criteria for intuitionistic topological spaces. Further expanding the theoretical terrain. Yaseen and Mohammad (2012) introduced Regular as well as Weak Regularly intuitionistic topological areas, whereas Jassim (2013) established entirely normal and weakly normal intuitionistic topological areas. Yaseen (2022) generalized some weak forms of irresolute mappings in intuitionistic topological spaces. Selvanayaki and Ilango (2015) established IGPR continuity and compactness in intuitionistic topological spaces, also H Jassim et al. (2015) introduced concept of generalized sets and mappings in intuitionistic topological spaces whereas Selvanayaki & Ilango (2016) investigated homeomorphism in these areas. Ilango & Albinaa (2016) and Kim et al. (2017) investigated intuitionistic closure in intuitionistic topological spaces, Prova & Hossain (2020) proposed intuitive fuzzy-based regularity, while Chae *et al.* (2020) used interval-valued intuitionistic sets in topological applications. Islam et al. (2021) contributed by developing notations for intuitionistic fuzzy r-regular areas and Isewid *et al.* (2021) introduced some properties of regular and normal space on topological graph space. Haque, Akhter, and Murshed (2022) presented intuitionistic subspace topology and explored its features. Previous research has not focused on the qualities of intuitionistic regular sub spaces. Also, Isewid and Yaseen (2022) were provided the notion of a function poorly open to intuition raster spaces and we get some new descriptions of the opening up of theweak functions among the intuitive point areas.

This paper fills a gap by using the structure of extended sets as well as maps in intuitionistic topological spaces. Jassim et al. (2015) provides a revolutionary discovery. This insight expands our comprehension of intuitionistic topological spaces and investigates some properties related them and adds a new level to the area's debate.

2. Basic Concepts

In this part we give some concepts which are needed in our work.

Definition 2.1 (Çoker, 1996): Assume the two sub sets B_T with B_F for a set that is not empty X where $B_T \cap B_F = \emptyset$. If $B = (B_T, B_F)$, then B is known as an intuitionistic set (IS) of X. Here, B_T represents a set of members, while B_F is considered the sets of nonmembers of B.

In actuality, B_T represents a subset from X accepting or allowing of a specific opinion, view, proposal, or strategy, while B_F is a subset for X rejecting or against a similar opinion, viewpoint, suggestion, or strategy, respectively. Assume $\emptyset_I = (\emptyset, X)$ as well as $X_I = (X, \emptyset)$, wherein $\emptyset I$ represents the intuitionistic empty subset and X_I represents the intuitionistic entire set of X. In overall, $B_T \cup B_F$ does not equal X and $IS(X)$ denotes the set of every one of the ISs of X.

Definition 2.2 (Çoker, 1996): Assume an $IS\ B$ associated with a non-empty set X, with $\xi \in X$.
(i) $\xi_I = (\{\xi\}, \{\xi\}^c)$ corresponds to an intuitionistic point (IP), while $\xi_{IV} = (\emptyset, \{\xi\}^c)$ is a dis appearing point of X.
(ii) For $\xi \in B_T$, so $\xi_I \in B$; while $\xi \notin B_F$, so $\xi_{IV} \in B$.IP (X) refers to are all intuitionistic points and vanishing points in X.

Definition 2.3. (Coker, 2000). If $B = (B_T, B_F)$ represents an intuitionistic collection in Y, subsequently the prior image of B according to h, represented by $h^{-1}(B)$, represents the intuitionistic subset in X that is determined by
$h^{-1}(B) = \langle h^{-1}(B_T), h^{-1}(B_F)\rangle$
$M = (h(\mathrm{M}_T), h(\mathrm{M}_F))$ represents an intuitionistic set corresponding to X. The image of M underneath h, indicated by $h(M)$, is the intuitionistic subset in Y that is determined by $h(M) = (h(\mathrm{M}_T), h-(\mathrm{M}_F))$ where $h-(\mathrm{M}_F) = Y - (h(X - \mathrm{M}_F))$.

Definition 2.4. (Bayhan and Çoker, 2001)
Suppose M and N represent two intuitionistic collections on X and Y, respectively. The products intuitionistic sets of M and N on $X \times Y$ is defined as $\times V = \langle \mathrm{M}_T \times \mathrm{N}_T, (\mathrm{M}_T{}^c \times \mathrm{N}_T{}^c)\rangle$, where $M = (M_T, M_F)$, and $N = (N_T, N_F)$. If (X, τ) and (Y, φ) are ITS, subsequently the product of the topologies $\tau \times \varphi$ on $X \times Y$ represents the intuitionistic topologies provided by the basis $B = \{M \times N : M \in \tau, N \in \varphi\}$.

Definition: 2.5 (Jassim *et al.*, 2015) Take (X, T) have an ITS, and allow $M = (M_T, M_F)$ have an IS in X, subsequently M will be considered to be:
Intuitionistic generalized pre-regular closed sets ($Igpr$-closed) are those where $pcl\ (A) \subseteq U$ whenever $M \subseteq U$ as well as U is intuitionistic open in X.
Intuitionistic semi weakly generalized pre-regular closed sets ($Isgr$-closed) are those where $clint(A) \subseteq U$ whenever $M \subseteq U$ as well as U is intuitionistic semi open in X.

3. Some Generalized continuous Mappings in ITS

In this part, we introduce a new generalized continuous mapping in ITS such as;
$Ig\beta A * C$- continuous, $IgPA * C$- continuous, $IgSA * C$ – continuous, $Ig\alpha A * C$ – continuous and $LIgC$ – continuous with studying relationship among them and some properties related them. we start with the following definition:

Definition 3.1. Assume that (X, I_τ) and (Y, I_σ) are two ITSs and h represents a mapping from (X, I_τ) into (Y, I_σ). Then a mapping $h:\ (X, I_\tau) \to (Y, I_\sigma)$ considers below:

$Ig\beta A*$ -continuous if $h^{-1}(M)$ is $Ig\beta A * C$ -set in X for every $Ig\beta A * C$ - set M in Y.
$IgPA*$ -continuous if $h^{-1}(M)$ is $Ig\beta A * C$ -set in X for every $IgPA * C$ - set M in Y.
$IgSA*$ -continuous if $h^{-1}(M)$ is $Ig\beta A * C$-set in X for every intuitionistic $IgSA * C$ - set M in Y.
$Ig\alpha A*$-continuous if $h^{-1}(M)$ is $Ig\alpha A * C$-set in X for every intuitionistic $Ig\alpha A * C$- set M in Y.
LIg -continuous if $h^{-1}(M)$ is $LIgC$-set in X for every $LIgC$ - set M in Y.

Theorem 3.2. Suppose that $h:\ (X, I_\tau) \to (Y, I_\sigma)$ be a mapping. Then the below are holds:
If h is LIg -continuous, then, h is $Ig\alpha A*$-continuous map.
If h is $Ig\alpha A*$ -continuous then, h is $IgSA*$-continuous map.
If h is $Ig\alpha A*$ -continuous then, h is $IgPA*$-continuous map.
If h is $IgSA*$ -continuous then, h is $Ig\beta A*$-continuous map.
If h is $IgPA*$ -continuous then, h is $Ig\beta A*$-continuous map.

Proof:
Considering that $h:\ (X, I_\tau) \to (Y, I_\sigma)$ be a mapping and M is $LIgC$-set in Y. Then, $int(\mathrm{M}) \subseteq \mathrm{U}$ whenever $\mathrm{M} \subseteq \mathrm{U}$, U is IOS and M is $IA*$ such that $\mathrm{M} = \mathcal{M} \cup \aleph$, where $\mathcal{M}$ is IOS and $\aleph$ is ICS. Since, M is $LIgC$ – set, there exists an $Ig\alpha A * C$-set in Y, because every $LIgC$-set is $Ig\alpha A * C$-set. Now, since h is $LIgC$ -continuous as a result, $h^{-1}(M)$ is $LIgC$-set in $X$by assumption. Consequently, $h^{-1}(M)$ is an $Ig\alpha A * C$-set in X. Therefore, h is $Ig\alpha A*$-continuous map.
Considering that $h:\ (X, I_\tau) \to (Y, I_\sigma)$ be a mapping and M is $Ig\alpha A * C$-set in Y.Thus, $int_\alpha(cl_\alpha(int_\alpha(\mathrm{M}))) \subseteq \mathrm{U}$ whenever $\mathrm{M} \subseteq \mathrm{U}$, U is IαOS, and M is $I\alpha A*$ such that $\mathrm{M} = \mathcal{M} \cup \aleph$, where $\mathcal{M}$ is IαOS and $\aleph$ is IαCS. Since, M is $Ig\alpha A * C$ set, there exists an $Ig\alpha A * C$-set in Y, because every $Ig\alpha A * C$ -set is $Ig\alpha A * C$-set. Since h is $Ig\alpha A*$-continuous as a result, $h^{-1}(M)$ is $Ig\alpha A * C$ -set in X by assumption. Consequently, $h^{-1}(M)$ is an $IgSA * C$-set in X. Therefore, h is $IgSA*$-continuous map.
Considering that $h:\ (X, I_\tau) \to (Y, I_\sigma)$ be a mapping and M is $Ig\alpha A * C$-set in Y.Hence, $int_\alpha(cl_\alpha(int_\alpha(\mathrm{M}))) \subseteq \mathrm{U}$ whenever $\mathrm{M} \subseteq \mathrm{U}$, U is IαOS, and M is $I\alpha A*$ such that $\mathrm{M} = \mathcal{M} \cup \aleph$, where $\mathcal{M}$ is IαOS and $\aleph$ is IαCS. Since, M is $Ig\alpha A * C$ set, there exists an $Ig\alpha A * C$-set in Y, because every $Ig\alpha A * C$ -set is $IgPA * C$-set. Since h is $Ig\alpha A*$-continuous as a result, $h^{-1}(M)$ is $Ig\alpha A * C$ -set in X by assumption. Consequently, $h^{-1}(M)$ is an $IgPA * C$-set in X. Therefore, h is $IgPA*$-continuous map.

Considering that $h: (X, I_\tau) \to (Y, I_\sigma)$ be a mapping and M is $IgSA * C$-set in Y.Thus, $cl_S(int_S(M)) \subseteq U$ whenever $M \subseteq U$, U is ISOS and M is $ISA *$ such that $M = \mathcal{M} \cup \aleph$, where $\mathcal{M}$ is ISOS and $\aleph$ is ISCS. Since, M is $IgSA * C$ set, there exists an $Ig\beta A * C$-set in Y, because every $IgSA * C$ -set is $Ig\beta A * C$-set. Since h is $IgSA *$-continuous as a result, $h^{-1}(M)$ is $IgSA * C$-set in X by assumption. Consequently, $h^{-1}(M)$ is an $Ig\beta A * C$-set in X. Therefore, h is $Ig\beta A *$-continuous map.

Considering that $h: (X, I_\tau) \to (Y, I_\sigma)$ be a mapping and M is $IgPA * C$-set in Y.Thus $int_P(cl_P(M)) \subseteq U$ whenever $M \subseteq U$, U is IPOS and M is $IPA *$ such that $M = \mathcal{M} \cup \aleph$, where $\mathcal{M}$ is IPOS and $\aleph$ is IPCS. Since, M is $IgPA * C$ set, there exists an $Ig\beta A * C$-set in Y, because every $IgPA * C$ -set is $Ig\beta A * C$-set. Since h is $IgPA *$-continuous as a result, $h^{-1}(M)$ is $IgPA * C$-set in X by assumption. Consequently, $h^{-1}(M)$ is an $Ig\beta A * C$-set in X. Therefore, h is $Ig\beta A *$-continuous map.

Remark 3.3. The converse of Theorem 3.2. is not true, As seen in the following examples.

Example 3.4. Assume $X = \{\xi, \lambda, \kappa\}$ with topology $I_\tau = \{\widetilde{X}, \widetilde{\emptyset}, M, N\}$, where $M = \langle\{\xi\}, \{\lambda\}\rangle$, $N = \langle\{\xi, \kappa\}, \{\lambda\}\rangle$, and $Y = \{15,17,19\}$ with topology $I_\sigma = \{\widetilde{X}, \widetilde{\emptyset}, P, W\}$ where $P = \langle\{19\}, \emptyset\rangle, W = \langle\emptyset, \emptyset\rangle$ and $h: (X, I_\tau) \to (Y, I_\sigma)$ be a mapping defined by $h(\xi) = 15$, $h(\lambda) = 19$, $h(\kappa) = 17$. Then, the following are fulfilled:

h is $IgPA *$-continuous but, h is not $Ig\alpha A *$-continuous, because for $D = \langle\{15,17\}, \emptyset\rangle$ is $IgPA * C$-set in Y, $h^{-1}(D) = \langle\{\xi, \kappa\}, \emptyset\rangle \notin Ig\alpha A * C$.

h is $IgSA *$-continuous but, h is not $Ig\alpha A *$-continuous, because for $L = \langle\{15\}, \emptyset\rangle$ is $IgSA * C$-set in Y, $h^{-1}(L) = \langle\{\xi\}, \emptyset\rangle \notin Ig\alpha A * C$.

Example 3. 5. Assume $X = Y = \{\xi, \lambda, \kappa\}$ with topology $I_\tau = \{\widetilde{X}, \widetilde{\emptyset}, Q, R, K, W\}$, where $Q = \langle\emptyset, \{\xi\}\rangle$, $R = \langle\{\xi\}, \emptyset\rangle, W = \langle\{\kappa\}, \emptyset\rangle$, $K = \langle\{\xi, \kappa\}, \emptyset\rangle$ and $Y = \{15,17,19\}$ with topology $I_\sigma = \{\widetilde{X}, \widetilde{\emptyset}, P, L, J, V\}$ where $P = \langle\emptyset, \{15\}\rangle$, $L = \langle\emptyset, \emptyset\rangle, J = \langle\{19\}, \emptyset\rangle$, $V = \langle\{15, 19\}, \emptyset\rangle$ and $h: (X, I_\tau) \to (Y, I_\sigma)$

be a mapping defined by $h(\xi) = 15$, $h(\lambda) = 17$, $h(\kappa) = 19$. Then, the following are fulfilled:

h is $Ig\beta A *$-continuous but, h is not $IgPA *$-continuous, because for $E = \langle\{15, 19\}, \emptyset\rangle$ is $Ig\beta A * C$-set in Y, $h^{-1}(E) = \langle\{\xi, \kappa\}, \emptyset\rangle \notin IgPA * C$.

h is $Ig\beta A *$-continuous but, h is not $IgSA *$-continuous, because for $S = \langle\{17\}, \emptyset\rangle$ is $Ig\beta A * C$-set in Y, $h^{-1}(S) = \langle\{\lambda\}, \emptyset\rangle \notin IgSA * C$.

Example 3. 6. Assume $X = Y = \{\xi, \lambda\}$ with topology $I_\tau = \{\widetilde{X}, \widetilde{\emptyset}, Q, R, W\}$, where $Q = \langle\emptyset, \{\xi\}\rangle$, $R = \langle\{\xi\}, \emptyset\rangle, W = \langle\{\lambda\}, \emptyset\rangle$ and $Y = \{15,17,19\}$ with topology $I_\sigma =$

$\{\widetilde{X}, \widetilde{\emptyset}, P, J, K\}$ where $P = \langle \emptyset, \{15\} \rangle$, $J = \langle \emptyset, \emptyset \rangle$, $K = \langle \{19\}, \emptyset \rangle$ and $h : (X, I_\tau) \rightarrow (Y, I_\sigma)$ be a mapping defined by $h(\xi) = 15$, $h(\lambda) = 17$, $h(\kappa) = 19$. Then h is $Ig\alpha A*$-continuous but, h is not LIg-continuous, because for $T = \langle \{17\}, \emptyset \rangle$ is $Ig\alpha A * C$-set in Y, $h^{-1}(T) = \langle \{\lambda\}, \emptyset \rangle \notin LIgC$.

Proposition 3.7. Suppose a mapping $h : (X, I_\tau) \rightarrow (Y, I_\sigma)$ and for each subset $M \subseteq X$.Then, the below holds:

Whenever h is $Ig\alpha A * C$, thus $Ig\alpha A * \left(\mathrm{int}_\alpha\left(\mathrm{cl}_\alpha(\mathrm{int}_\alpha(\mathrm{h(M)}))\right)\right) \subset \mathrm{h}(Ig\alpha A * \mathrm{int}_\alpha\left(\mathrm{cl}_\alpha(\mathrm{int}_\alpha(\mathrm{M}))\right))$.

Whenever h is $IgSA * C$, thus $IgSA * \mathrm{int}_S(\mathrm{cl}_S(\mathrm{h(M)})) \subset \mathrm{h}(IgSA * \mathrm{int}_S(\mathrm{cl}_S(\mathrm{M})))$.

Whenever h is $IgPA * C$, thus $IgPA * \mathrm{int}_P(\mathrm{cl}_P(\mathrm{h(M)})) \subset \mathrm{h}(IgPA * \mathrm{int}_P(\mathrm{cl}_P(\mathrm{M})))$.

Whenever h is $Ig\alpha A * C$, thus $Ig\alpha A * \mathrm{cl}_\beta\left(\mathrm{int}_\beta(\mathrm{cl}_\beta(\mathrm{h(M)}))\right) \subset \mathrm{h}(Ig\alpha A * \mathrm{cl}_\beta\left(\mathrm{int}_\beta(\mathrm{cl}_\beta(\mathrm{h(M)}))\right))$.

Proof.

Assume that h is $Ig\alpha A * C$ and $\mathrm{M} \subset \mathrm{X}$. $\mathrm{cl}_\alpha(\mathrm{int}_\alpha(\mathrm{h(M)}))$ is $Ig\alpha A * C$ in X and so $\mathrm{h}(\mathrm{cl}_\alpha(\mathrm{int}_\alpha(\mathrm{M})))$ is $Ig\alpha A * C$ in (Y, I_σ). So, $\mathrm{h(M)} \subset \mathrm{h}(\mathrm{cl}_\alpha(\mathrm{int}_\alpha(\mathrm{M})))$,and hence $Ig\alpha A * (\mathrm{int}_\alpha(\mathrm{cl}_\alpha(\mathrm{int}_\alpha(\mathrm{h(M)})))) \subset Ig\alpha A * (\mathrm{int}_\alpha(\mathrm{cl}_\alpha(\mathrm{int}_\alpha(\mathrm{h}(\mathrm{cl}_\alpha(\mathrm{int}_\alpha(\mathrm{M}))))))) \rightarrow$ (i)

Since $h(\mathrm{cl}_\alpha(\mathrm{int}_\alpha(M)))$ is $Ig\alpha A * C$ in (Y, I_σ).Hence,

$Ig\alpha A * (\mathrm{int}_\alpha(\mathrm{cl}_\alpha(\mathrm{int}_\alpha(\mathrm{h}(\mathrm{cl}_\alpha(\mathrm{int}_\alpha(\mathrm{M}))))))) = \mathrm{h}(\mathrm{cl}_\alpha(\mathrm{int}_\alpha(\mathrm{M}))) \rightarrow$ (ii). Via (i) with (ii), we obtain for each subset $M \subseteq X$ $Ig\alpha A * \left(\mathrm{int}_\alpha\left(\mathrm{cl}_\alpha(\mathrm{int}_\alpha(\mathrm{h(M)}))\right)\right) \subset \mathrm{h}(Ig\alpha A * \mathrm{int}_\alpha\left(\mathrm{cl}_\alpha(\mathrm{int}_\alpha(\mathrm{M}))\right))$.

Assume that h is $IgSA * C$ and $\mathrm{M} \subset \mathrm{X}$. $\mathrm{int}_S(\mathrm{h(M)})$ is $IgSA * C$ in X and so $\mathrm{h}(\mathrm{int}_S(\mathrm{M}))$ is $IgSA * C$ in (Y, I_σ). So, $\mathrm{h(M)} \subset \mathrm{h}(\mathrm{int}_S(\mathrm{M}))$,

and hence $IgSA * \left(\mathrm{cl}_S(\mathrm{int}_S(\mathrm{h(M)}))\right) \subset IgSA * (\mathrm{cl}_S(\mathrm{int}_S(\mathrm{h}(\mathrm{cl}_S(\mathrm{int}_S(\mathrm{M})))))) \rightarrow$ (i)

Since $h(\mathrm{cl}_S(\mathrm{int}_S(M)))$ is $IgSA * C$ in (Y, I_σ).Hence,

$IgSA * (\mathrm{cl}_S(\mathrm{int}_S(\mathrm{h}(\mathrm{cl}_S(\mathrm{int}_S(\mathrm{M})))))) = \mathrm{h}(\mathrm{cl}_S(\mathrm{int}_S(\mathrm{M}))) \rightarrow$ (ii). Via (i) with (ii), we obtain for each subset $M \subseteq X$ $IgSA * IgSA * \mathrm{int}_S(\mathrm{cl}_S(\mathrm{h(M)})) \subset \mathrm{h}(IgSA * \mathrm{int}_S(\mathrm{cl}_S(\mathrm{M})))$.

Similarly, we can prove (3) and (4) as same way.

Theorem 3.8. Suppose that a two mapping $h : (X, I_\tau) \rightarrow (Y, I_\sigma)$ and $\varphi : (Y, I_\sigma) \rightarrow (Z, I_\rho)$ for each subset $M \subseteq X$.The below holds:

If both h and φ are LIg- continuous map then, $\varphi \circ \mathrm{h} : (X, I_\tau) \rightarrow (\mathrm{Z}, I_\rho)$ is LIg- continuous map.

If both h and φ are $Ig\alpha A*$- continuous map then, $\varphi \circ \mathrm{h} : (X, I_\tau) \rightarrow (\mathrm{Z}, I_\rho)$ is $Ig\alpha A*$-continuous map.

If both h and φ are $IgPA*$- continuous map then, $\varphi \circ \mathrm{h} : (X, I_\tau) \rightarrow (\mathrm{Z}, I_\rho)$ is $IgPA*$-continuous map.

If both h and φ are $IgSA*$- continuous map then, $\varphi \circ h: (X, I_\tau) \to (Z, I_\rho)$ is $IgSA*$-continuous map.
If both h and φ are $Ig\beta A*$- continuous map then, $\varphi \circ h: (X, I_\tau) \to (Z, I_\rho)$ is $Ig\beta A*$-continuous map.

Proof.

Assume K be $LIgC$ set in (X, I_τ). Because, h is an LIg- continuous map, h(K) is $LIgC$ set in (Y, γ).Thus, $\varphi(h(H))$ is $LIgC$ –set in (Z, I_ρ) because, φ is LIg continuous map, so $\varphi(h(H))$ is $LIgC$ –set in (Z, I_ρ). In other words, $\varphi \circ h(H) = \varphi(h(H))$ is $LIgC$ –set and therefore, $\varphi \circ h$ is $LIgC$- continuous map.

Assume K be $Ig\alpha A*C$ set in (X, I_τ). Because, h is an $Ig\alpha A*$- continuous map, h(K) is $Ig\alpha A*C$ set in (Y, γ).Thus, $\varphi(h(H))$ is $Ig\alpha A*C$ –set in (Z, I_ρ) because, φ is $Ig\alpha A*$ continuous map, so $\varphi(h(H))$ is $Ig\alpha A*C$ –set in (Z, I_ρ). In other words, $\varphi \circ h(H) = \varphi(h(H))$ is $Ig\alpha A*C$ –set and therefore, $\varphi \circ h$ is $Ig\alpha A*$- continuous map.

Similarly, we can prove (3), (4) and (5) as same way.

Theorem 3.9. if a map $h: (X, I_\tau) \to (Y, I_\sigma)$ is a bijective map. The arguments that follow are equivalent:

(i) h is $Ig\alpha A*O$.

(ii) h is $Ig\alpha A*C$.

(iii) $h^{-1}: (Y, I_\sigma) \to (X, I_\tau)$ is $Ig\alpha A*$continuous.

Proof: $(i) \Rightarrow$ (ii)

If F is an $Ig\alpha A*C$-set in (X, I_τ) then $X - F$ is $Ig\alpha A*O$ in (X, I_τ) . But h is $Ig\alpha A*O$, thus $h(X - F)$ is $Ig\alpha A*O$ in (Y, I_σ). Hence, $h(< F_1, F_2 >) =< h(F_1), Y - h(X - F_2) >$ is $Ig\alpha A*O$ in (Y, I_σ) and so $< Y - h(X - F_2), h(F_1) >=< h(F_2), h(F_1) >$ is $Ig\alpha A*C$ in (Y, I_σ). Because $Y - h(X - F_2) = h(F_2), < Y - h(X - F_2), h(F_1) >=$ $< h(F_2), h(F_1) >$ is $Ig\alpha A*C$ in (Y, I_σ) . Therefore,h^{-1} is $Ig\alpha A*C$.

(ii) ⇒ (iii)

Assume F be an $Ig\alpha A*C$ in (X, I_τ). Because h is bijective and $Ig\alpha A*C$, hence $h(F) = (h^{-1})^{-1}(F)$ is $Ig\alpha A*C$ in (Y, I_σ). Therefore h^{-1} is $Ig\alpha A*C$ -continuous.

(iii) ⇒ (i)

Assume F be an $Ig\alpha A*O$ in (X, I_τ). By assumption, $(h^{-1})^{-1}(F)$ is $Ig\alpha A*O$ in (Y, I_σ). Hence, $h(F)$ is $Ig\alpha A*O$ in (Y, I_σ). Thus, h is $Ig\alpha A*O$.

Theorem 3.10. if a map $h: (X, I_\tau) \to (Y, I_\sigma)$ is a bijective map. The arguments that follow are equivalent:

(i) h is $IgPA*O$.

(ii) h is $IgPA*C$.

(iii) $h^{-1}: (Y, I_\sigma) \to (X, I_\tau)$ is $IgPA*$continuous.

Proof: $(i) \Rightarrow$ (ii) If F is an $IgPA*C$-set in (X, I_τ) then $X - F$ is $IgPA*O$ in (X, I_τ) . But h is $IgPA*O$, thus $h(X - F)$ is $IgPA*O$ in (Y, I_σ). Hence,

$h(< F_1, F_2 >) =< h(F_1), Y - h(X - F_2) >$ is $IgPA * O$ in (Y, I_σ) and so
$< Y - h(X - F_2), h(F_1) >=< h(F_2), h(F_1) >$ is $IgPA * C$ in (Y, I_σ). Because
$Y - h(X - F_2) = h(F_2), < Y - h(X - F_2), h(F_1) >=$
$< h(F_2), h(F_1) >$ is $IgPA * C$ in (Y, I_σ) . Therefore,h^{-1} is $IgPA * C$.
(ii) ⇒ (iii) Assume F be an $IgPA * C$ in (X, I_τ). Because h is bijective and $IgPA * C$, hence $h(F) = (h^{-1})^{-1}(F)$ is $IgPA * C$ in (Y, I_σ). Therefore h^{-1} is $IgPA * C$ -continuous.
(iii) ⇒ (i) Assume F be an $IgPA * O$ in (X, I_τ). By assumption, $(h^{-1})^{-1}(F)$ is $IgPA * O$ in (Y, I_σ). Hence, $h(F)$ is $IgPA * O$ in (Y, I_σ). Thus, h is $IgPA * O$.

Theorem 3.11. if a map $h : (X, I_\tau) \rightarrow (Y, I_\sigma)$ is a bijective map. The arguments that follow are equivalent:
(i) h is $IgSA * O$.
(ii) h is $IgSA * C$.
(iii) $h^{-1}: (Y, I_\sigma) \rightarrow (X, I_\tau)$ is $IgSA *$continuous.
Proof: obvious.

Theorem 3.12. if a map $h : (X, I_\tau) \rightarrow (Y, I_\sigma)$ is a bijective map. The arguments that follow are equivalent:
(i) h is $Ig\beta A * O$.
(ii) h is $Ig\beta A * C$.
(iii) $h^{-1}: (Y, I_\sigma) \rightarrow (X, I_\tau)$ is $Ig\beta A *$continuous.
Proof: obvious.

Theorem 3.13. if a map $h : (X, I_\tau) \rightarrow (Y, I_\sigma)$ is a bijective map. The arguments that follow are equivalent:
(i) h is $LIgO$.
(ii) h is $LIgC$.
(iii) $h^{-1}: (Y, I_\sigma) \rightarrow (X, I_\tau)$ is LIg continuous.
Proof: obvious.

Definition 3.14. A map $h : (X, I_\tau) \rightarrow (Y, I_\sigma)$ consider to be:
LIg –closed map if the image h(M) is LIg-closed in (Y, I_σ) for each $LIgC -$ set M in(X, I_τ).
$Ig\alpha A *$ –closed map if the image h(M) is $Ig\alpha A *$-closed in (Y, I_σ) for each $Ig\alpha A * C -$ set M in(X, I_τ).
$IgPA *$ –closed map if the image h(M) is $IgPA *$-closed in (Y, I_σ) for each $IgPA * C -$ set M in(X, I_τ).
$IgSA *$ –closed map if the image h(M) is $IgSA *$-closed in (Y, I_σ) for each $IgSA * C -$ set M in(X, I_τ).
$Ig\beta A *$ –closed map if the image h(M) is $Ig\beta A *$-closed in (Y, I_σ) for each $Ig\beta A * C -$ set M in(X, I_τ).

Theorem 3.15. Suppose that a two mapping $h:\ (X, I_\tau)\ \rightarrow\ (Y, I_\sigma)$ and $\varphi: (Y, I_\sigma)\ \rightarrow (Z, I_\rho)$ for each subset $M \subseteq X$.Then the below holds:

If both h and φ are LIg- closed map then, $\varphi \circ \mathrm{h}: (X, I_\tau) \rightarrow (\mathrm{Z}, I_\rho)$ is LIg - closed map.

If both h and φ are $Ig\alpha A*$- closed map then, $\varphi \circ \mathrm{h}: (X, I_\tau) \rightarrow (\mathrm{Z}, I_\rho)$ is $Ig\alpha A*$- closed map.

If both h and φ are $IgPA*$- closed map then, $\varphi \circ \mathrm{h}: (X, I_\tau) \rightarrow (\mathrm{Z}, I_\rho)$ is $IgPA* -$closed map.

If both h and φ are $IgSA*$ - closed map then, $\varphi \circ \mathrm{h}: (X, I_\tau) \rightarrow (\mathrm{Z}, I_\rho)$ is $IgSA*$ - closed map.

If both h and φ are $Ig\beta A*$- closed map then, $\varphi \circ \mathrm{h}: (X, I_\tau) \rightarrow (\mathrm{Z}, I_\rho)$ is $Ig\beta A*$ - closed map.

Proof.

Assume K be an $LIgC -$ set in (X, I_τ) .Since h is LIg- closed map, h(K) is $LIgC -$ set in (Y, I_σ). Since φ is LIg- closed map, φ(h(K)) is $LIgC -$ set in (Z, I_ρ) .Thus, $\varphi \circ \mathrm{h}$ is LIg - closed map.

Assume K be an $Ig\alpha A * C -$ set in (X, I_τ) .Since h is $Ig\alpha A*$- closed map, h(K) is $Ig\alpha A * C -$ set in (Y, I_σ). Since φ is $Ig\alpha A*$- closed map, φ(h(K)) is $Ig\alpha A * C -$ set in (Z, I_ρ) .Thus, $\varphi \circ \mathrm{h}$ is $Ig\alpha A*$ - closed map.

Similarly, we can prove (3), (4) and (5) as same way.

Definition 3.16. A map $h:\ (X, I_\tau)\ \rightarrow\ (Y, I_\sigma)$ consider to be:

$LIg -$open map if the image h(M) is LIg-closed in (Y, I_σ) for each $LIgO -$ set M in(X, I_τ).

$Ig\alpha A* -$ open map if the image h(M) is $Ig\alpha A*$-closed in (Y, I_σ) for each $Ig\alpha A * O -$set M in(X, I_τ).

$IgPA* -$ open map if the image h(M) is $IgPA*$-closed in (Y, I_σ) for each $IgPA * O -$ set M in(X, I_τ).

$IgSA* -$ open map if the image h(M) is $IgSA*$-closed in (Y, I_σ) for each $IgSA * O -$ set M in(X, I_τ).

$Ig\beta A* -$ open map if the image h(M) is $Ig\beta A*$-closed in (Y, I_σ) for each $Ig\beta A * O -$ set M in(X, I_τ).

Theorem 3.17. Suppose that a two mapping $h:\ (X, I_\tau)\ \rightarrow\ (Y, I_\sigma)$ and $\varphi: (Y, I_\sigma)\ \rightarrow (Z, I_\rho)$ for each subset $M \subseteq X$.Then the below holds:

If both h and φ are LIg- closed map then, $\varphi \circ \mathrm{h}: (X, I_\tau) \rightarrow (\mathrm{Z}, I_\rho)$ is LIg - closed map.

If both h and φ are $Ig\alpha A*$- closed map then, $\varphi \circ \mathrm{h}: (X, I_\tau) \rightarrow (\mathrm{Z}, I_\rho)$ is $Ig\alpha A*$- closed map.

If both h and φ are $IgPA*$- closed map then, $\varphi \circ \mathrm{h}: (X, I_\tau) \rightarrow (\mathrm{Z}, I_\rho)$ is $IgPA* -$closed map.

If both h and φ are $IgSA*$ - closed map then, $\varphi \circ \mathrm{h}: (X, I_\tau) \rightarrow (\mathrm{Z}, I_\rho)$ is $IgSA*$ - closed map.

If both h and φ are $Ig\beta A*$- closed map then, $\varphi \circ \mathrm{h}: (X, I_\tau) \rightarrow (\mathrm{Z}, I_\rho)$ is $Ig\beta A*$ - closed map.

Proof.

Assume K be an $LIgO -$ set in (X, I_τ) .Since h is LIg- open map, h(K) is $LIgO -$ set in (Y, I_σ). Since φ is LIg- open map, φ(h(K)) is $LIgC -$ set in (Z, I_ρ) .Thus, $\varphi \circ \mathrm{h}$ is LIg - open map.

Similarly, we can prove (2), (3), (4) and (5) as same way.
Remark 3.18. The following figure shows the relationships among the concepts discussed in this part that have been created.

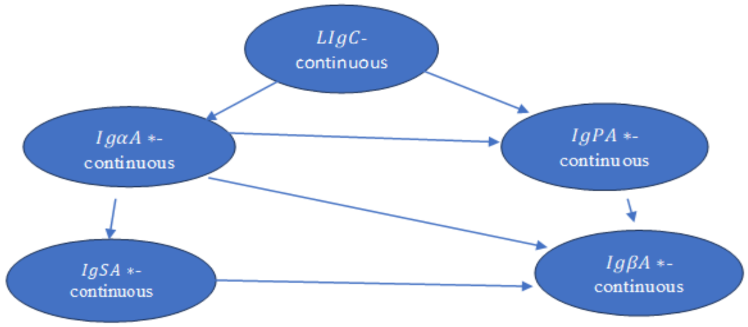

Fig 1. Showing the relationships among the continuous mappings that have been created

4. Some Generalized Irresolute Mappings in ITS

In this part, we began with the following definition:

Definition 4.1. Assume that (X, I_τ) and (Y, I_σ) are two ITSs and h represents a mapping from (X, I_τ) into (Y, I_σ). Then a mapping $h: (X, I_\tau) \to (Y, I_\sigma)$ considers below:
$Ig\beta A*$ -irresolute if $h^{-1}(M)$ is $Ig\beta A*O$ -set in X for every $Ig\beta A*O$ - set M in Y.
$IgPA*$ - irresolute if $h^{-1}(M)$ is $Ig\beta A*O$ -set in X for every $IgPA*O$ - set M in Y.
$IgSA*$ -irresolute if $h^{-1}(M)$ is $Ig\beta A*O$-set in X for every intuitionistic $IgSA*O$ - set M in Y.
$Ig\alpha A*$- irresolute if $h^{-1}(M)$ is $Ig\alpha A*O$-set in X for every intuitionistic $Ig\alpha A*O$- set M in Y.
LIg - irresolute if $h^{-1}(M)$ is $LIgO$-set in X for every $LIgO$ - set M in Y.

Theorem 4.2. *Suppose that $h: (X, I_\tau) \to (Y, I_\sigma)$ be a mapping.*
Then the below are holds:
If h is LIg - irresolute, then, h is $Ig\alpha A*$- irresolute map.
If h is $Ig\alpha A*$- irresolute then, h is $IgSA*$- irresolute map.
If h is $Ig\alpha A*$ -continuous then, h is $IgPA*$- irresolute map.
If h is $IgSA*$- irresolute then, h is $Ig\beta A*$- irresolute map.
If h is $IgPA*$- irresolute then, h is $Ig\beta A*$- irresolute map.

Proof:
Considering that $h: (X, I_\tau) \to (Y, I_\sigma)$ be a mapping and M is $LIgO$-set in Y. Then, $int(M) \subseteq U$ whenever $M \subseteq U$, U is IOS and M is $IA*$ such that $M = \mathcal{M} \cup \aleph$, where $\mathcal{M}$ is IOS and $\aleph$ is ICS. Since, M is $LIgO$ – set, so there exists an $Ig\alpha A*O$-set in Y, because every $LIgP$-set is $Ig\alpha A*O$-set. Now, since h is $LIgO$- irresolute

as a result, $h^{-1}(M)$ *is* $LIgO$*-set in* X*by assumption. Consequently,* $h^{-1}(M)$ *is an* $Ig\alpha A*O$*-set in* X*. Therefore, h is*

$Ig\alpha A*$*- irresolute map.*

Considering that $h:(X,I_\tau)\rightarrow(Y,I_\sigma)$ *be a mapping and* M *is* $Ig\alpha A*O$*-set in* Y*.Thus,* $int_\alpha(cl_\alpha(int_\alpha(M)))\subseteq U$ *whenever* $M\subseteq U$ *,* U *is IαOS, and* M *is* $I\alpha A*$ *such that* $M=\mathcal{M}\cup\aleph$*, where* $\mathcal{M}$ *is IαOS and* $\aleph$ *is IαOS. Since,* M *is* $Ig\alpha A*C$ *set, so there exists an* $IgSA*O$*-set in* Y*, because every* $Ig\alpha A*O$ *-set is* $IgSA*O$*-set. Since* h *is* $Ig\alpha A*$*- irresolute as a result,* $h^{-1}(M)$ *is*

$Ig\alpha A*O$ *-set in* X *by assumption. Consequently,* $h^{-1}(M)$ *is an* $IgSA*O$*-set in* X*.*

Therefore, h is $IgSA*$*- irresolute map.*

Considering that $h:(X,I_\tau)\rightarrow(Y,I_\sigma)$ *be a mapping and* M *is* $Ig\alpha A*O$*-set in* Y*.Hence,* $int_\alpha(cl_\alpha(int_\alpha(M)))\subseteq U$ *whenever* $M\subseteq U$ *,* U *is IαOS, and* M *is* $I\alpha A*O$ *such that* $M=\mathcal{M}\cup\aleph$*, where* $\mathcal{M}$ *is IαOS and* $\aleph$ *is IαCS. Since,* M *is* $Ig\alpha A*O$ *set, so there exists an* $Ig\alpha A*O$*-set in* Y*, because every* $Ig\alpha A*O$ *-set is* $IgPA*O$*-set. Since* h *is* $Ig\alpha A*$*- irresolute as a result,* $h^{-1}(M)$ *is* $Ig\alpha A*OC$ *-set in* X *by assumption. Consequently,* $h^{-1}(M)$ *is an* $IgPA*OC$*-set in* X*. Therefore, h is* $IgPA*$*- irresolute map.*

Considering that $h:(X,I_\tau)\rightarrow(Y,I_\sigma)$ *be a mapping and* M *is* $IgSA*O$*-set in* Y*.Thus,* $cl_S(int_S(M))\subseteq U$ *whenever* $M\subseteq U$*,* U *is ISOS and* M *is* $ISA*$ *such that* $M=\mathcal{M}\cup\aleph$*, where* $\mathcal{M}$ *is ISOS and* $\aleph$ *is ISCS. Since,* M *is* $IgSA*O$ *set, so there exists an* $Ig\beta A*O$*-set in* Y*, because every* $IgSA*O$ *-set is* $Ig\beta A*O$*-set. Since* h *is* $IgSA*$*- irresolute as a result,* $h^{-1}(M)$ *is* $IgSA*O$*-set in* X *by assumption. Consequently,* $h^{-1}(M)$ *is an* $Ig\beta A*O$*-set in* X*. Therefore, h is* $Ig\beta A*$*- irresolute map.*

Considering that $h:(X,I_\tau)\rightarrow(Y,I_\sigma)$ *be a mapping and* M *is* $IgPA*O$*-set in* Y*.Thus* $int_P(cl_P(M))\subseteq U$ *whenever* $M\subseteq U$*,* U *is IPOS and* M *is* $IPA*$ *such that* $M=\mathcal{M}\cup\aleph$*, where* $\mathcal{M}$ *is IPOS and* $\aleph$ *is IPCS. Since,* M *is* $IgPA*O$ *set, so there exists an* $Ig\beta A*O$*-set in* Y*, because every* $IgPA*O$ *-set is* $Ig\beta A*O$*-set. Since* h *is* $IgPA*$*- irresolute as a result,* $h^{-1}(M)$ *is* $IgPA*O$*-set in* X *by assumption. Consequently,* $h^{-1}(M)$ *is an* $Ig\beta A*O$*-set in* X*. Therefore, h is* $Ig\beta A*$*- irresolute map.*

Remark 4.3. The converse of Theorem 4.2. is not true, As seen in the following examples.

Example 4.4. Assume $X=\{\xi,\lambda,\kappa\}$ with topology $I_\tau=\{\widetilde{X},\widetilde{\emptyset},M,N,W\}$, where $M=\langle\{\xi\},\{\lambda\}\rangle$,$N=\langle\{\kappa\},\{\lambda\}\rangle$, $N=\langle\{\xi,\kappa\},\{\lambda\}\rangle$, and $Y=\{15,17\}$ with topology $I_\sigma=\{\widetilde{X},\widetilde{\emptyset},P,W,L\}$ where $P=\langle\{15\},\emptyset\rangle$, $W=\langle\emptyset,\emptyset\rangle$, $L=P=\langle\emptyset,\{17\}\rangle$, and $h:(X,I_\tau)\rightarrow(Y,I_\sigma)$ *be* a mapping

defined by $h(\xi) = 15$, $h(\lambda) = h(\kappa) = 17$. Then, the following are fulfilled:
h is $IgPA*$- irresolute but, h is not $Ig\alpha A*$- irresolute, because for $D = \langle\{17\}, \emptyset\rangle$ is $IgPA*O$-set in Y, $h^{-1}(D) = \langle\{\lambda, \kappa\}, \emptyset\rangle \notin Ig\alpha A*O$.
h is $IgSA*$- irresolute but, h is not $Ig\alpha A*$- irresolute, because for $E = \langle\{17\}, \emptyset\rangle$ is $IgSA*O$-set in Y, $h^{-1}(L) = \langle\{\lambda, \kappa\}, \emptyset\rangle \notin Ig\alpha A*O$.

Example 4.5. Assume $X = Y = \{\xi, \lambda, \kappa\}$ with topology $I_\tau = \{\widetilde{X}, \widetilde{\emptyset}, Q, R, K, W\}$, where $Q = \langle\emptyset, \emptyset\rangle$, $R = \langle\{\xi\}, \emptyset\rangle$, $W = \langle\{\kappa\}, \emptyset\rangle$, $K = \langle\{\lambda, \kappa\}, \emptyset\rangle$ and $Y = \{15,17,19\}$ with topology $I_\sigma = \{\widetilde{X}, \widetilde{\emptyset}, P, L, J, V\}$ where $P = \langle\emptyset, \{15\}\rangle$, $L = \langle\emptyset, \emptyset\rangle$, $J = \langle\{19\}, \emptyset\rangle$, $V = \langle\{15, 19\}, \emptyset\rangle$ and $h: (X, I_\tau) \to (Y, I_\sigma)$

be a mapping defined by $h(\xi) = 15 = h(\lambda)$, $h(\kappa) = 19$. Then, the following are fulfilled:
h is $Ig\beta A*$- irresolute but, h is not $IgPA*$- irresolute, because for $E = \langle\{15\}, \emptyset\rangle$ is $Ig\beta A*O$-set in Y, $h^{-1}(E) = \langle\{\xi, \lambda\}, \emptyset\rangle \notin IgPA*O$.
h is $Ig\beta A*$- irresolute but, h is not $IgSA*$- irresolute, because for $E = \langle\{15\}, \emptyset\rangle$ is $Ig\beta A*O$-set in Y, $h^{-1}(S) = \langle\{\xi, \lambda\}, \emptyset\rangle \notin IgSA*O$.

Recall Example 3.6. We see that h is $Ig\alpha A*$- irresolute but, h is not LIg- irresolute, because for $T = \langle\{15\}, \emptyset\rangle$ is $Ig\alpha A*O$-set in Y, $h^{-1}(T) = \langle\{\xi\}, \emptyset\rangle \notin LIgO$.

Theorem 4.6. Assume $h: (X, I_\tau) \to (Y, I_\sigma)$ be a mapping. Then the following fulfil:
If h is $Ig\alpha A*$- continuous and $Ig\alpha A*O$- then $h(M)$ is $Ig\alpha A*O(Y, I_\sigma)$, for every $M \in Ig\alpha A*(X, I_\tau)$.
If h is $IgPA*$- continuous and $IgPA*O$- then $h(M)$ is $IgPA*O(Y, I_\sigma)$, for every $M \in IgpA*(X, I_\tau)$.
If h is $IgSA*$- continuous and $IgSA*O$- then $h(M)$ is $IgSA*O(Y, I_\sigma)$, for every $M \in IgSA*(X, I_\tau)$.
If h is $Ig\beta A*$- continuous and $Ig\beta A*O$- then $h(M)$ is $Ig\beta A*O(Y, I_\sigma)$, for every $M \in Ig\beta A*(X, I_\tau)$.
If h is LIg- continuous and $LIgO$- then $h(M)$ is $LIgO(Y, I_\sigma)$, for every $M \in LIgO(X, I_\tau)$.

Proof:
Assume $M \in Ig\alpha A*(X, I_\tau)$.Thus $Q \in (X, I_\tau)$ such that $Q \subseteq M \subseteq Ig\alpha A*cl_\alpha(Q)$ and $h(Q) \subseteq h(M) \subseteq h(Ig\alpha A*cl_\alpha(Q))$. Because h is $Ig\alpha A*$- continuous and $h(\sigma) \in (Y, I_\sigma)$ and h is $Ig\alpha A*O$, hence, $h(Ig\alpha A*cl_\alpha(Q)) \subseteq Ig\alpha A*cl_\alpha(h(Q))$. Therefore, $h(M)$ is $Ig\alpha A*O(Y, I_\sigma)$.
Assume $M \in IgPA*(X, I_\tau)$.Thus $Q \in (X, I_\tau)$ such that $IgPA*int_P(Q) \subseteq Q \subseteq M$ and $h(IgPA*int_P(Q)) \subseteq h(Q) \subseteq h(M)$. Because h is $IgPA*$- continuous and $h(\sigma) \in (Y, I_\sigma)$ and h is $IgPA*O$, hence, $h(IgPA*int_P(Q)) \subseteq IgPA*int_P(h(Q))$. Therefore, $h(M)$ is $IgPA*O(Y, I_\sigma)$.

Similarly, we can prove (3), (4) and (5) as similar way.

Theorem 4.7. Assume $h: (X, I_\tau) \to (Y, I_\sigma)$ be a mapping. Then the following fulfil:

If h is $Ig\alpha A*$- continuous and $Ig\alpha A*O$- then h is $Ig\alpha A*$ - irresolute.
If h is $IgPA*$- continuous and $IgPA*O$- then h is $Ig\alpha P*$ - irresolute.
If h is $IgSA*$- continuous and $IgSA*O$- then h is $IgSA*$ - irresolute.
If h is $Ig\beta A*$- continuous and $Ig\beta A*O$- then h is $Ig\beta A*$ - irresolute.
If h is LIg- continuous and $LIgO$- then h is LIg - irresolute.

Proof:

Assume $M \in Ig\alpha A*(Y, I_\sigma)$, so there exist is IOS $Q \subseteq Y$ such that $Q \subseteq M \subseteq Ig\alpha A*cl_\alpha(Q)$. Thus, $h^{-1}(Ig\alpha A*cl_\alpha(Q)) = Ig\alpha A*cl_\alpha(h^{-1}(Q))$ and so $h^{-1}(Q) \subseteq h^{-1}(M) \subseteq h^{-1}(Ig\alpha A*cl_\alpha(Q)) = Ig\alpha A*cl_\alpha(h^{-1}(Q))$. Now because h is $Ig\beta A*$-continuous, then $h^{-1}(Q)$ is an $Ig\alpha A*O$-set. Therefore, $h^{-1}(M)$ is h is $Ig\alpha A*$ - irresolute.
Assume $M \in IgPA*(Y, I_\sigma)$, so there exist is IOS $Q \subseteq Y$ such that $IgPA*int_P(Q) \subseteq Q \subseteq M$. Thus, $h^{-1}(IgPA*int_P(Q)) = IgPA*int_P(h^{-1}(Q))$ and so $h^{-1}(IgPA*int_P(Q)) \subseteq h^{-1}(Q) \subseteq h^{-1}(M) = IgPA*int_P(h^{-1}(Q))$. Now because h is $Ig\beta A*$- continuous, then $h^{-1}(Q)$ is an $IgPA*O$-set. Therefore, $h^{-1}(M)$ is h is $IgPA*$ - irresolute.

Similarly, we can prove (3), (4) and (5) as similar way.

Theorem 4.8. Assume $h: (X, I_\tau) \to (Y, I_\sigma)$ be a mapping. Then the following fulfil:

h is $Ig\alpha A*$- irresolute iff $h^{-1}(M)$ is $Ig\alpha A*$-closed map for every $Ig\alpha A*C$ –set M of Y.
h is $IgPA*$- irresolute iff $h^{-1}(M)$ is $IgPA*$-closed map for every $IgPA*C$ –set M of Y.
h is $IgSA*$- irresolute iff $h^{-1}(M)$ is $IgSA*$-closed map for every $IgSA*C$ –set M of Y.
h is $Ig\beta A*$- irresolute iff $h^{-1}(M)$ is $Ig\beta A*$-closed map for every $Ig\beta A*C$ –set M of Y.
h is LIg- irresolute iff $h^{-1}(M)$ is LIg-closed map for every $LIgC$ –set M of Y.

Proof:

Necessary condition: Assume $h: (X, I_\tau) \to (Y, I_\sigma)$ is $Ig\alpha A*$- irresolute, thus for each $Ig\alpha A*O$- set W of Y, $h^{-1}(W)$ i is $Ig\alpha A*O(X, I_\tau)$. Now, if M is any $Ig\alpha A*C$ set of (Y, I_σ), hence, $Y - M$ is $Ig\alpha A*O$. So, $h^{-1}(Y - M)$ is $Ig\alpha A*O$, but $h^{-1}(Y - M) = X - h^{-1}(M)$ and therefore, $h^{-1}(M)$ is $Ig\alpha A*C$.
Sufficient condition: Assume $M \in (Y, I_\sigma)$ be an $IgPA*C$-set. Then $h^{-1}(M)$ is $Ig\alpha A*C$ – set in X by assumption. Now, if W is any $Ig\alpha A*O(Y, I_\sigma)$, thus $Y - W$ is $Ig\alpha A*C$. So that,

$h^{-1}(Y - N) = X - h^{-1}(N)$ is $Ig\alpha A * C$. Thus $h^{-1}(N)$ is $Ig\alpha A * O$. Therefore, h is $Ig\alpha A *$-irresolute.
Necessary condition: Assume $h : (X, I_\tau) \to (Y, I_\sigma)$ is $IgPA *$- irresolute, thus for each $IgPA * O$- set W of Y, $h^{-1}(W)$ i is $IgPA * O(X, I_\tau)$. Now, if M is any $IgPA * C$ set of (Y, I_σ), hence, $Y - M$ is $IgPA * O$. So, $h^{-1}(Y - M)$ is $IgPA * O$, but $h^{-1}(Y - M) = X - h^{-1}(M)$ and therefore, $h^{-1}(M)$ is $IgPA * C$.
Sufficient condition: Assume $M \in (Y, I_\sigma)$ be an $IgPA * C$-set. Then $h^{-1}(M)$ is $IgPA * C -$ set in X by assumption. Now, if W is any $IgPA * O(Y, I_\sigma)$, thus $Y - W$ is $IgPA * C$. So that, $h^{-1}(Y - N) = X - h^{-1}(N)$ is $IgPA * C$. Thus $h^{-1}(N)$ is $IgPA * O$. Therefore, h is $IgPA *$-irresolute.
Similarly, we can prove (3), (4) and (5) as similar way.

Theorem 4.9. Assume $h : (X, I_\tau) \to (Y, I_\sigma)$ be a mapping. Then the following fulfil:
If h is an $Ig\alpha A *$-irresolute then h is an $Ig\alpha A *$- continuous.
If h is an $IgPA *$-irresolute then h is an $IgPA *$- continuous.
If h is an $IgSA *$-irresolute then h is an $IgSA *$- continuous.
If h is an $Ig\beta A *$-irresolute then h is an $Ig\beta A *$- continuous.
If h is an LIg-irresolute then h is an LIg- continuous.
Proof.
Assume that M is an $Ig\alpha A * O(Y, I_\sigma)$. As every intuitionistic open set is $Ig\alpha A * O$,and so M is $Ig\alpha A * O(Y, I_\sigma)$. By hypothesis, h is $Ig\alpha A *$-irresolute. Thus, $h^{-1}(M)$ is $Ig\alpha A * O(X, I_\tau)$. Consequently, h is $Ig\alpha A *$- continuous.
Assume that M is an $IgPA * O(Y, I_\sigma)$. As every intuitionistic open set is $IgPA * O$, and so M is $IgPA * O(Y, I_\sigma)$. By hypothesis, h is $IgPA *$-irresolute. Thus, $h^{-1}(M)$ is $IgPA * O(X, I_\tau)$. Consequently, h is $IgPA *$- continuous.
Similarly, we can prove (3), (4) and (5) as similar way.

Remark 4.10. The converse of Theorem 4.9. is not true, As seen in the following examples.
Recall Examples 3.1.4. and 3.1.5. We see that the following:
h is $Ig\alpha A *$- continuous but not $Ig\alpha A *$- irresolute.
h is $Ig\alpha A *$- continuous but not $Ig\alpha A *$- irresolute.
h is $Ig\alpha A *$- continuous but not $Ig\alpha A *$- irresolute.
h is $Ig\alpha A *$- continuous but not $Ig\alpha A *$- irresolute.

Example 4.11. Let $X = \{\xi, \lambda\} = Y$, $I_\tau = \{\widetilde{X}, \widetilde{\emptyset}, \langle Q, \xi \rangle\}, I_\sigma = \{\widetilde{Y}, \widetilde{\emptyset}, \langle Q, \xi \rangle\}$ and define $h : (X, I_\tau) \to (Y, I_\sigma)$ by $h(\xi) = \xi, h(\lambda) = \lambda$ then h is an LIg- continuous but not an LIg-irresolute.

Theorem 4.12. Assume $h:\ (X,I_\tau)\ \rightarrow\ (Y,I_\sigma)$ and $\varphi:(Y,I_\sigma)\ \rightarrow(Z,I_\rho)$ are two mappings.
Then the following holds:
If h and φ be both $Ig\alpha A*$- irresolute then $\varphi\circ\ h:\ (X,I_\tau)\ \rightarrow\ (Z,I_\rho)$ is $Ig\alpha A*$- irresolute.
If h and φ be both $IgPA*$- irresolute then $\varphi\circ\ h:\ (X,I_\tau)\ \rightarrow\ (Z,I_\rho)$ is $IgPA*$- irresolute.
If h and φ be both $IgSA*$- irresolute then $\varphi\circ\ h:\ (X,I_\tau)\ \rightarrow\ (Z,I_\rho)$ is $IgSA*$- irresolute.
If h and φ be both $Ig\beta A*$- irresolute then $\varphi\circ\ h:\ (X,I_\tau)\ \rightarrow\ (Z,I_\rho)$ is $Ig\beta A*$- irresolute.
If h and φ be both LIg- irresolute then $\varphi\circ\ h:\ (X,I_\tau)\ \rightarrow\ (Z,I_\rho)$ is LIg- irresolute.
Proof:
Let $F\ \subseteq\ Z$ is an $Ig\alpha A*O$ then $\varphi^{-1}(F)$ is $Ig\alpha A*$- irresolute so $(h^{-1}(\varphi^{-1}(F)))$ is $Ig\alpha A*O$ because, h, φ are both $Ig\alpha A*$- irresolute. Hence, $(\varphi\circ\ h)^{-1}(F)\ =\ (h^{-1}(\varphi^{-1}(F)))$ is an $Ig\alpha A*O$. Therefore, $\varphi\circ\ h$ is $Ig\alpha A*$- irresolute.
Let $F\ \subseteq\ Z$ is an $IgPA*O$ then $\varphi^{-1}(F)$ is $IgPA*$- irresolute so $(h^{-1}(\varphi^{-1}(F)))$ is $IgPA*O$ because, h, φ are both $IgPA*$- irresolute. Hence, $(\varphi\circ\ h)^{-1}(F)\ =\ (h^{-1}(\varphi^{-1}(F)))$ is an $IgPA*O$. Therefore, $\varphi\circ\ h$ is $IgPA*$- irresolute.
Similarly, we can prove (3), (4) and (5) as similar way.

Theorem 4.13. Assume $h:\ (X,I_\tau)\ \rightarrow\ (Y,I_\sigma)$ and $\varphi:(Y,I_\sigma)\ \rightarrow(Z,I_\rho)$ are two mappings.
Then the following holds:
If h is an $Ig\alpha A*$- irresolute and φ is an $Ig\alpha A*$- continuous then $\varphi\circ\ h:\ (X,I_\tau)\ \rightarrow\ (Z,I_\rho)$ is $Ig\alpha A*$- continuous.
If h is an $IgPA*$- irresolute and φ is an $IgPA*$- continuous then $\varphi\circ\ h:\ (X,I_\tau)\ \rightarrow\ (Z,I_\rho)$ is $IgPA*$- continuous.
If h is an $IgSA*$- irresolute and φ is an $IgSA*$- continuous then $\varphi\circ\ h:\ (X,I_\tau)\ \rightarrow\ (Z,I_\rho)$ is $IgSA*$- continuous.
If h is an $Ig\beta A*$- irresolute and φ is an $Ig\beta A*$- continuous then $\varphi\circ\ h:\ (X,I_\tau)\ \rightarrow\ (Z,I_\rho)$ is $Ig\beta A*$- continuous.
If h is an LIg- irresolute and φ is an LIg- continuous then $\varphi\circ\ h:\ (X,I_\tau)\ \rightarrow\ (Z,I_\rho)$ is LIg-continuous.
Proof.
Assume M is $Ig\alpha A*C(Z,I_\rho)$, so, $\varphi^{-1}(M)$ is $Ig\alpha A*C(Y,I_\sigma)$. Consequently,
$h^{-1}(\varphi^{-1}(\bar{M}))\ =\ (\varphi\ \circ h)^{-1}(\bar{M})$ is $Ig\alpha A*O(X,I_\tau)$, because h is $Ig\alpha A*$-irresolute. Hence, $h^{-1}(\varphi^{-1}(M))=(\varphi\ \circ h)^{-1}(M)$ is $Ig\alpha A*C(X,I_\tau)$ Therefore, $\varphi\circ\ h$ is also an $Ig\alpha A*$-continuous.
Assume M is $IgPA*C(Z,I_\rho)$, so, $\varphi^{-1}(M)$ is $IgPA*C(Y,I_\sigma)$. Consequently,
$h^{-1}(\varphi^{-1}(\bar{M}))\ =\ (\varphi\ \circ h)^{-1}(\bar{M})$ is $IgPA*O(X,I_\tau)$, because h is $IgPA*$-irresolute. Hence,

$h^{-1}(\varphi^{-1}(M)) = (\varphi \circ h)^{-1}(M)$ is $IgPA * C(X, I_\tau)$ Therefore, $\varphi \circ h$ is also an $IgPA *$-continuous.

Similarly, we can prove (3), (4) and (5) as similar way.

5. Conclusion

The article you cited presents the idea of a generalized weak continuous, closed and open mappings in intuitionistic topological environments and analyzes numerous results associated with this new sets. It implies that the concepts and results provided in the work can be applied to different kinds of topological spaces, like ideal topological spaces and others.

References

Bayhan, S., & Çoker, D. (2001). On separation axioms in intuitionistic topological spaces. International Journal of Mathematics and Mathematical Sciences, 27, 621-630.

Chae, G. B., Kim, J., Lee, J. G., & Hur, K. (2020). Interval-valued intuitionistic sets and their application to topology. Annals of Fuzzy Mathematics and Informatics.

Coker, D. (1996). A note on intuitionistic sets and intuitionistic points. Turkish Journal of Mathematics, 20(3), 343-351.

Coker D, An introduction to intuitionistic topological spaces, Busefal, (2000),51-56.

H Jassim, T., R Yaseen, S., & S AbdualBaqi, L. (2015). Some generalized sets and mappings in intuitionistic topological spaces. Journal of AL-Qadisiyah for computer science and mathematics, 7(2), 80-96.

Ilango, G., & Albinaa, T. A. (2016). Properties of α-interior and α-closure in intuitionistic topological spaces. IOSR Journal of Mathematics (IOSR-JM), 12(6), 91-95.

Isewid, R. A., Aziz, N. I., Yaseen, S. R., & Qasem, M. R. (2021, May). Some Properties of Regular and Normal Space on Topological Graph Space. In Journal of Physics: Conference Series (Vol. 1879, No. 2, p. 022106). IOP Publishing.

Isewid, R. A., & Yaseen, S. R. (2022). Some results of weakly mapping in intuitionistic bi-topological spaces. International Journal of Nonlinear Analysis and Applications, 13(1), 3191-3195.

Islam, S., Hossain, S., & Mahbub, A. (2021). On intuitionistic fuzzy r-regular spaces. International Journal of Fuzzy Mathematical Archive, 19(2), 149-159.

Jassim, T. H. (2013). Completely normal and weak completely normal in intuitionistic topological spaces. International Journal of Scientific & Engineering Research, 4(10), 438– 442.

Kim, J. H., Lim, P. K., Lee, J. G., & Hur, K. (2017). Intuitionistic topological space. Annals of Fuzzy Mathematics and Informatics.

Prova, T. T., & Hossain, M. S. (2020). Intuitionistic fuzzy based regular and normal spaces. Notes on Intuitionistic Fuzzy Sets, 26(4), 53-63.

Selvanayaki, S., & Ilango, G. (2015). IGPR-continuity and compactness intuitionistic topological spaces. British Journal of Mathematics & Computer Science, 11(2), 1-8.

Selvanayaki, S., & Ilango, G. (2016). Homeomorphism on intuitionistic topological spaces. Ann. Fuzzy Math. Inform, 11(6), 957-966.

Yaseen, S. R., Aziz, N. I., & Aziz, S. I. (2018). Generalized Weak Forms of Irresolute Mappings in Intuitionistic Topological Spaces. Kirkuk Journal of Science, 13(4), 34-44.

Yaseen, Y. J., & Mohammad, R. A. (2012). Regular and weak regular in intuitionistic topological spaces. Journal of University of Anbar for Pure Science, 6(3).

Zadeh, L. A. (1965). Fuzzy sets, information and control. 8(3), 338–353. https://doi.org/https://doi.org/10.1 016/S0019-9958(65)90241-X

On S_*-I-open and pre^*-I-open Sets in Ideal Topological Spaces

[1,*]Ali Shaker Mahmoud

[2,*]Yassen, S.R

[1,2]Department of Mathematics, College of Education for Pure Sciences, Tikrit University, Tikrit, Iraq

[1,*]as230014pep@st.tu.edu.iq.

[2,*] samer2017@tu.edu.iq.

On S^*-I-open and pre^*-I-open Sets in Ideal Topological Spaces

[1,*]Ali Shaker Mahmoud

[2,*]Yassen, S.R

[1,2]Department of Mathematics, College of Education for Pure Sciences, Tikrit University, Tikrit, Iraq

[1,*]as230014pep@st.tu.edu.iq.

[2,*] samer2017@tu.edu.iq.

Abstract: In this study, we explore and delineate several characteristics of S^*-I-open sets, and pre^*-I-open sets within ideal topological spaces. Additionally, we establish connections between pre^*-I-open sets, and S^*-I-open sets in these spaces. Ultimately, we achieve a decomposition of continuity, enhancing the understanding of how these sets interact and contribute to the broader topological framework

Keywords: S^*-I-open sets, pre^*-I-open sets, pre^*-I-continuous, S^*-I-continuous.

1. Introduction

This paper introduced and investigates the properties of new class are S^*-I-open sets and pre^*-I-open sets within ideal topological spaces, the counterparts of which such as $semi^*$-I-open sets and others have been previously explored in references [1-4] respectively. We delve into the properties of these sets and explore the interrelationships among S^*-I-open sets, pre^*-I-open sets and some concepts in such spaces. In addition, we present and discuss various analyzes of continuous functions, expanding on the theoretical framework established by previous studies. This research not only deepens the understanding of these unique types of sets, but also enhances the discourse about their

M

role in the structural dynamics of ideal topological spaces.

An ideal I on a nonempty set X comprises a nonempty subset of subsets of X that meet specific criteria: if M is part of I and N is a subset of M, then N is also part of I; similarly, if both M and N belong to I, their union $M \cup N$ must also be in I [5]. This concept has been further applied in diverse fields as studied by Jankovic and Hamlett [6], Mukherjee and colleagues [7], Arenas et al. [8], Nasef and Mahmoud [9], among others. In the context of a topological space (X, τ) equipped with an ideal I, and considering $\wp(X)$ as the set of all subsets of X, a particular set operator $(.)^*: \wp(X) \to \wp(X)$, termed a local function [5], is defined for a subset M of X as follows: $M^*(I, \tau) = \{x \in X \mid \forall G \in \tau(x), G \cap M \notin I\}$, indicating the elements x in X for which every neighborhood G intersects M outside of I. In the context where $\tau(x)$ represents the set of all neighborhoods G in τ containing the point x, the combined set $M \cup M^*(I, \tau)$ is defined as the Kuratowski closure operator for the topology τ^*, known as the $*$-topology, which is more refined than τ. To avoid ambiguity, M^* is typically used to denote $M^*(I, \tau)$. Frequently, X^*derived from this definition, constitutes a proper subset of X. Within this framework, the terms "space" explicitly refers to a topological space (X, τ), absent any distinct separation properties. For any subset M of X, $Cl(M)$ and $Int(M)$ signify the closure and interior of M^* within (X, τ), respectively.

A topological space (X, τ) equipped with an ideal I is referred to as an ideal topological space, denoted by (X, τ, I). A subset M within an ideal space (X, τ) is termed R-I-open (respectively R-I-closed) if $M = Cl^*(Int(A))$(respectively $M = Int(Cl^*(M))$). A point $x \in X$ is identified as a δ-I-cluster point of M if $Int(Cl*(U)) \cap M \neq \emptyset$ for every open set U that contains x. The collection of all δ-I-cluster points of M is known as the δ-I-closure of M, denoted by $\delta Cl^I(M)$ [10]. The δ-I-interior of M is defined as the union of all R-I-open sets of X that are contained within M, and is denoted by $\delta Int^I(M)$. A set M is considered δ-I-closed if $\delta Cl^I(M) = M$. The δ-I-open sets generate a topology $\tau\delta^I$, which is coarser than τ. In the context of topological spaces with an associated ideal I, a subset U of an ideal topological space (X,τ,I) can be categorized as follows:

1. $\mathrm{Semi}^* - \mathrm{I}$ –open [2]: A set U is $\mathrm{Semi}^* - \mathrm{I}$ –open if $\mathrm{U} \subseteq \mathrm{Cl}(\delta\mathrm{Int}^{\mathrm{I}}(\mathrm{U}))$.
2. $\mathrm{Pre}^* - \mathrm{I}$ –open [1]: A set U is $\mathrm{Pre}^* - \mathrm{I}$ –open if $\mathrm{U} \subseteq \mathrm{Int}(\delta\mathrm{Cl}^{\mathrm{I}}(\mathrm{U}))$.
3. e-I-open [3]: A set U is e-I-open if $U \subseteq Cl(\delta\mathrm{Int}^{\mathrm{I}}(U)) \cup Int(\delta\mathrm{Cl}^{\mathrm{I}}(U))$.
4. βGj^* –set [11]: A set U is a βGj^* –set if $U = V \cap K$, where V is δ^I-open and K is e-I-closed.
5. Weakly δ^I-local closed [12]: A set U is weakly δ^I-local closed if $U = V \cap K$, where V is an open set and K is a δ^I-closed set in X.

2. Some properties of $\mathbf{S}^*$-I-open open sets and $\mathbf{pre}^*$-I-open sets in ideal topological spaces

Definition 2.1. Let (X,τ,I) be an ideal topological space and let W be a subset X then (X,τ,I) is considered to be:

1. $S^* - \mathrm{I}$ –open: if $\mathrm{W} \subseteq \mathrm{Cl}(\mathrm{Int}^{\mathrm{I}}(\delta\mathrm{Cl}^{\mathrm{I}}(\mathrm{W})))$.
2. $pre^* - I$ –open: if $\mathrm{W} \subseteq \mathrm{Int}(\mathrm{Cl}^{\mathrm{I}}(\delta\mathrm{Int}^{\mathrm{I}}(W))) \cup \mathrm{Cl}(\mathrm{Int}^{\mathrm{I}}(\delta\mathrm{Cl}^{\mathrm{I}}(W)))$.

Proposition 2.2. Let (X,τ,I) be an ideal topological space. A subset W is $weakly^*$ δ^I-locally closed if and only if $W = P \cap \delta\mathrm{Int}^{\mathrm{I}}(\delta\mathrm{Cl}^{\mathrm{I}}(\mathrm{W}))$, where P is an open set.

Proof: Assume W is $weakly^*$ δ^I-locally closed. Thus, $W = P \cap M$, where P is an open set and M is δ^I-closed. So, $W \subseteq M$ and $\delta\mathrm{Int}^{\mathrm{I}}\left(\delta\mathrm{Cl}^{\mathrm{I}}(W)\right) \subseteq \delta\mathrm{Int}^{\mathrm{I}}\left(\delta\mathrm{Cl}^{\mathrm{I}}(M)\right) = \delta\mathrm{Cl}^{\mathrm{I}}(W) \subseteq \delta\mathrm{Cl}^{\mathrm{I}}(M) = M$. Hence, $W \subseteq P \cap \delta\mathrm{Int}^{\mathrm{I}}\left(\delta\mathrm{Cl}^{\mathrm{I}}(W)\right)$. Therefore, $W = P \cap \delta\mathrm{Int}^{\mathrm{I}}(\delta\mathrm{Cl}^{\mathrm{I}}(\mathrm{W}))$.

Proposition 2.3. Let (X,τ,I) be a δ^I-extremally disconnected ideal space and $W \subseteq X$. the subsequent characteristics occur:

1. W is an open set.
2. W is S^* –I-open and$weakly^*$ δ^I-local closed.
3. W is pre^* –I-open and weakly δ^I-local closed.

Proof: (1) implies (2) and (3): The proof is straightforward. (3) implies (1): Assume W is an pre^*-I-open and weakly δ^I-local closed set in X. It follows that $Q \subseteq \mathrm{Int}\left((\mathrm{Cl}^{\mathrm{I}}(\delta\mathrm{Int}^{\mathrm{I}}(Q)))\right) \cup \mathrm{Cl}(\mathrm{Int}^{\mathrm{I}}(\delta\mathrm{Cl}^{\mathrm{I}}(Q)))$. Since W is a weakly δ^I-local closed set, by Proposition 3.2 there exists an open set P such that $W = P \cap \delta\mathrm{Int}^{\mathrm{I}}\left(\delta\mathrm{Cl}^{\mathrm{I}}(W)\right)$. Thus,

$$W \subseteq P \cap [\mathrm{Int}\left((\mathrm{Cl}^{\mathrm{I}}(\delta\mathrm{Int}^{\mathrm{I}}(W)))\right) \cup \mathrm{Cl}(\mathrm{Int}^{\mathrm{I}}(\delta\mathrm{Cl}^{\mathrm{I}}(W)))]$$
$$= (P \cap \mathrm{Int}\left((\mathrm{Cl}^{\mathrm{I}}(\delta\mathrm{Int}^{\mathrm{I}}(W)))\right)) \cup (P \cap \mathrm{Cl}(\mathrm{Int}^{\mathrm{I}}(\delta\mathrm{Cl}^{\mathrm{I}}(W))))$$
$$\subseteq Int(P \cap (\mathrm{Cl}^{\mathrm{I}}(\delta\mathrm{Int}^{\mathrm{I}}(W)))) = Int(W)$$

Hence, $W \subseteq Int(W)$ and so W is an open set in X.

Proposition 2.4. When the subset W of an ideal topological space is considered, the subsequent characteristics occur (X, τ, I):

1. If W is S^* –I-open set, then $S\delta\mathrm{Int}^{\mathrm{I}}(\delta\mathrm{Cl}^{\mathrm{I}}(W)) = \mathrm{Cl}(\delta\mathrm{Int}^{\mathrm{I}}(\delta\mathrm{Cl}^{\mathrm{I}}(W)))$.
2. If W is pre^* –I-open set, then $pre^*\delta\mathrm{Cl}^{\mathrm{I}}(\delta\mathrm{Int}^{\mathrm{I}}(W)) = \mathrm{Int}\left((\delta\mathrm{Cl}^{\mathrm{I}}(\delta\mathrm{Int}^{\mathrm{I}}(W)))\right)$.

Proof:

1. Assume W is S^* –I-open set in X. Thus, $W \subseteq \delta\mathrm{Int}^{\mathrm{I}}(\delta\mathrm{Cl}^{\mathrm{I}}(W))$. By Proposition 3.3, $S\delta\mathrm{Int}^{\mathrm{I}}\left(\delta\mathrm{Cl}^{\mathrm{I}}(W)\right) = W \cup \mathrm{Int}^{\mathrm{I}}(\delta\mathrm{Cl}^{\mathrm{I}}(W)) = \mathrm{Cl}(\delta\mathrm{Int}^{\mathrm{I}}(\delta\mathrm{Cl}^{\mathrm{I}}(W)))$.
2. Assume W be a e^* –I -open set in X. So, $W \subseteq \delta\mathrm{Cl}^{\mathrm{I}}(\delta\mathrm{Int}^{\mathrm{I}}(W))$. By Proposition 3.2, we have $pre^*\delta\mathrm{Cl}^{\mathrm{I}}(\delta\mathrm{Int}^{\mathrm{I}}(W)) = W \cup (\mathrm{Cl}^{\mathrm{I}}(\delta\mathrm{Int}^{\mathrm{I}}(W))) = \mathrm{Int}\left((\delta\mathrm{Cl}^{\mathrm{I}}(\delta\mathrm{Int}^{\mathrm{I}}(W)))\right)$.

Remark 2.5. The opposite of these consequences of Proposition 2.4 are not correct in particular as demonstrated by the below example:

Example 2.6. Assume $X = \{\xi, \mu, \zeta\}, \tau = \{\emptyset, X, \{\xi\}, \{\xi, \mu\}, \{\xi, \zeta\}\}$ $and\ I = \{\emptyset, \{\xi\}, \{\zeta\}, \{\xi, \zeta\}\}$. Thus, $S\delta\mathrm{Int}^{\mathrm{I}}\left(\delta\mathrm{Cl}^{\mathrm{I}}(W)\right) = \mathrm{Cl}(\delta\mathrm{Int}^{\mathrm{I}}(\delta\mathrm{Cl}^{\mathrm{I}}(W)))$ for $W = \{\mu, \zeta\}$, but W is not S^* –I-open. Furthermore

$pre^*\delta\mathrm{Cl}^{\mathrm{I}}(\delta\mathrm{Int}^{\mathrm{I}}(W)) = \mathrm{Int}\Big((\delta\mathrm{Cl}^{\mathrm{I}}(\delta\mathrm{Int}^{\mathrm{I}}(W)))\Big)$for $K = \{\xi, \varsigma\}$, but K is not pre^* –I-open.

Proposition 2.7. Let (X, τ, I) be an ideal topological space and $Q \subseteq X$. the subsequent characteristics occur:

1. If W is pre^* –I-closed set, then $pre^*\delta\mathrm{Cl}^{\mathrm{I}}(\delta\mathrm{Int}^{\mathrm{I}}(W)) = \mathrm{Int}\Big((\delta\mathrm{Cl}^{\mathrm{I}}(\delta\mathrm{Int}^{\mathrm{I}}(W)))\Big)$
2. If W is S^* –I-closed set, then $S\delta\mathrm{Int}^{\mathrm{I}}\Big(\delta\mathrm{Cl}^{\mathrm{I}}(W)\Big) = \mathrm{Cl}(\delta\mathrm{Int}^{\mathrm{I}}(\delta\mathrm{Cl}^{\mathrm{I}}(W)))$.

Proof:

1. Assume W is pre^* –I-closed set. So, $\delta\mathrm{Cl}^{\mathrm{I}}(\delta\mathrm{Int}^{\mathrm{I}}(W)) \subseteq W$. Thus, $pre^*\delta\mathrm{Cl}^{\mathrm{I}}(\delta\mathrm{Int}^{\mathrm{I}}(W)) = W \cap (\mathrm{Cl}^{\mathrm{I}}(\delta\mathrm{Int}^{\mathrm{I}}(W))) = \mathrm{Int}\Big((\delta\mathrm{Cl}^{\mathrm{I}}(\delta\mathrm{Int}^{\mathrm{I}}(W)))\Big)$.

Hence, $pre^*\delta\mathrm{Cl}^{\mathrm{I}}(\delta\mathrm{Int}^{\mathrm{I}}(W)) = \mathrm{Int}\left(\left(\delta\mathrm{Cl}^{\mathrm{I}}\left(\delta\mathrm{Int}^{\mathrm{I}}(W)\right)\right)\right)$.

2. Let W is S^* –I-closed set. So, $\delta\mathrm{Cl}^{\mathrm{I}}(\delta\mathrm{Int}^{\mathrm{I}}(W)) \subseteq W$. Thus, $S\delta\mathrm{Int}^{\mathrm{I}}\Big(\delta\mathrm{Cl}^{\mathrm{I}}(W)\Big) = W \cap (\mathrm{Int}^{\mathrm{I}}(\delta\mathrm{Cl}^{\mathrm{I}}(W))) = \mathrm{Cl}(\delta\mathrm{Int}^{\mathrm{I}}(\delta\mathrm{Cl}^{\mathrm{I}}(W)))$.

Hence, $S\delta\mathrm{Int}^{\mathrm{I}}\Big(\delta\mathrm{Cl}^{\mathrm{I}}(W)\Big) = \mathrm{Cl}(\delta\mathrm{Int}^{\mathrm{I}}(\delta\mathrm{Cl}^{\mathrm{I}}(W)))$.

Proposition 2.8.

The subset W for an ideal topological space (X, τ, I) is considered an e^* –I-closed set if and only if $W = pre^*\mathrm{Cl}^{\mathrm{I}}(\delta\mathrm{Int}^{\mathrm{I}}(W)) \cap S\delta\mathrm{Int}^{\mathrm{I}}\Big(\delta\mathrm{Cl}^{\mathrm{I}}(W)\Big)$.

Proof:

Suppose that W is an pre^* –I-closed set in X. This implies $pre^*\mathrm{Cl}^{\mathrm{I}}(\delta\mathrm{Int}^{\mathrm{I}}(W)) \cap S\delta\mathrm{Int}^{\mathrm{I}}\Big(\delta\mathrm{Cl}^{\mathrm{I}}(W)\Big) \subseteq W$. We have $\Big(\mathrm{W} \cup \mathrm{Cl}(\delta\mathrm{Int}^{\mathrm{I}}(\delta\mathrm{Cl}^{\mathrm{I}}(W)))\Big) \cap \left(\mathrm{W} \cup \mathrm{Int}\left(\left(\delta\mathrm{Cl}^{\mathrm{I}}\left(\delta\mathrm{Int}^{\mathrm{I}}(W)\right)\right)\right)\right) = W$. Thus, $W = pre^*\mathrm{Cl}^{\mathrm{I}}(\delta\mathrm{Int}^{\mathrm{I}}(W)) \cap S\delta\mathrm{Int}^{\mathrm{I}}\Big(\delta\mathrm{Cl}^{\mathrm{I}}(W)\Big)$.

Conversely, let $W = pre^*\mathrm{Cl}^{\mathrm{I}}(\delta\mathrm{Int}^{\mathrm{I}}(W)) \cap S\delta\mathrm{Int}^{\mathrm{I}}\Big(\delta\mathrm{Cl}^{\mathrm{I}}(W)\Big)$. Thus,

$pre^*\mathrm{Cl}^{\mathrm{I}}(\delta\mathrm{Int}^{\mathrm{I}}(W)) \cap S\delta\mathrm{Int}^{\mathrm{I}}\left(\delta\mathrm{Cl}^{\mathrm{I}}(W)\right) \subseteq \left(\mathrm{W} \cup \mathrm{Cl}(\delta\mathrm{Int}^{\mathrm{I}}(\delta\mathrm{Cl}^{\mathrm{I}}(W)))\right) \cap \left(\mathrm{W} \cup \mathrm{Int}\left(\left(\delta\mathrm{Cl}^{\mathrm{I}}\left(\delta\mathrm{Int}^{\mathrm{I}}(W)\right)\right)\right)\right)$. This implies that $\mathrm{Cl}(\delta\mathrm{Int}^{\mathrm{I}}(\delta\mathrm{Cl}^{\mathrm{I}}(W))) \cap \mathrm{Int}\left(\left(\delta\mathrm{Cl}^{\mathrm{I}}\left(\delta\mathrm{Int}^{\mathrm{I}}(W)\right)\right)\right) \subseteq W$. Therefore, W is an pre^* –I-closed set in X.

Corollary 2.9. Let (X,τ,I) be an ideal topological space and $W \subseteq X$. If W is an S^* –I open and pre^* –I -open, then $Cl(\mathrm{Int}^{\mathrm{I}}(Q)) = \mathrm{Cl}(\delta\mathrm{Int}^{\mathrm{I}}(\delta\mathrm{Cl}^{\mathrm{I}}(W))) \cap \mathrm{Int}\left(\left(\delta\mathrm{Cl}^{\mathrm{I}}\left(\delta\mathrm{Int}^{\mathrm{I}}(W)\right)\right)\right)$

Proof: By using Proposition 2.8. we obtain the result.

Remark 2.10: The opposite of these consequences of Corollary 2.9 are not correct in particular as demonstrated by the below example:

Example 2.11. Assume $X = \{\xi,\mu,\zeta\}, \tau = \{\emptyset, X, \{\xi\}, \{\xi,\mu\}, \{\mu\}, \{\xi,\zeta\}\}$ $and\ I = \{\emptyset, \{\xi\}, \{\zeta\}, \{\xi,\zeta\}\}$. Set $W = \{\mu,\xi\}$,Thus, $Cl(\mathrm{Int}^{\mathrm{I}}(W)) = \mathrm{Cl}(\delta\mathrm{Int}^{\mathrm{I}}(\delta\mathrm{Cl}^{\mathrm{I}}(W))) \cap \mathrm{Int}\left(\left(\delta\mathrm{Cl}^{\mathrm{I}}\left(\delta\mathrm{Int}^{\mathrm{I}}(W)\right)\right)\right)$but W is not S^* –I-open, but K is not pre^* –I -open.

Proposition 2.12. Assume (X,τ,I) be an ideal topological space and $W \subseteq X$. If W is S^* –I -closed and pre^* –I-closed, then $Int\left(\mathrm{Cl}^{\mathrm{I}}(W)\right) = \mathrm{Cl}\left(\delta\mathrm{Int}^{\mathrm{I}}\left(\delta\mathrm{Cl}^{\mathrm{I}}(W)\right)\right) \cup \mathrm{Int}\left(\left(\delta\mathrm{Cl}^{\mathrm{I}}\left(\delta\mathrm{Int}^{\mathrm{I}}(W)\right)\right)\right)$.

Proof: Assume W is a S^* –I-closed set and pre^* –I-closed set. So, By Proposition 2.7 $e^*\delta\mathrm{Cl}^{\mathrm{I}}\left(\delta\mathrm{Int}^{\mathrm{I}}(W)\right) = \mathrm{Int}\left(\left(\delta\mathrm{Cl}^{\mathrm{I}}\left(\delta\mathrm{Int}^{\mathrm{I}}(W)\right)\right)\right)$ and $S\delta\mathrm{Int}^{\mathrm{I}}\left(\delta\mathrm{Cl}^{\mathrm{I}}(W)\right) = \mathrm{Cl}(\delta\mathrm{Int}^{\mathrm{I}}(\delta\mathrm{Cl}^{\mathrm{I}}(W)))$Thus,

$Int\left(\mathrm{Cl}^{\mathrm{I}}(W)\right) = pre^*\delta\mathrm{Cl}^{\mathrm{I}}\left(\delta\mathrm{Int}^{\mathrm{I}}(W)\right) \cup S\delta\mathrm{Int}^{\mathrm{I}}\left(\delta\mathrm{Cl}^{\mathrm{I}}(W)\right) = \mathrm{Cl}\left(\delta\mathrm{Int}^{\mathrm{I}}\left(\delta\mathrm{Cl}^{\mathrm{I}}(W)\right)\right) \cup \mathrm{Int}\left(\left(\delta\mathrm{Cl}^{\mathrm{I}}\left(\delta\mathrm{Int}^{\mathrm{I}}(W)\right)\right)\right)$

.

3. Classifications and additional properties of continuity

Definition 3.1. A map $h:(X,\tau,I)\to(Y,\sigma)$ is considered follows:

1. $weakly^{*}$ δ^{I}-locally-continuous if the preimage $h^{-1}(W)$ is $weakly^{*}$ δ^{I}-locally closed for every open set W in Y.
2. S^{*} –I-continuous if the preimage $h^{-1}(W)$ is S^{*} –I-open for every open set W in Y.
3. pre^{*} –I-continuous if the preimage $h^{-1}(W)$ is pre^{*} –I-open for every open set W in Y.

Remark 3.2. For map $h:(X,\tau,I)\to(Y,\sigma)$ the subsequent characteristics are identical in (X,τ,I), a δ^{I}-extremally unconnected ideal space:

1. h is continuous,
2. h is S^{*} –I -continuous and weakly δ^{I}-locally-continuous,
3. h is pre^{*} –I -continuous and weakly δ^{I}locally-continuous.

Proof: This results simply via Proposition 3.4.

Definition 3.3. A subset W of an ideal topological space (X,τ,I) is considered to be:

1. Generalized pre^{*} –I -open if $P\subseteq Int\left(\mathrm{Cl}^{\mathrm{I}}(W)\right)$ whenever $M\subseteq W$ and P is a closed set in X.
2. Generalized pre^{*} –I -closed if and only if W^{c} is pre^{*} –I-open set in X.

Proposition 3.4. Assume (X,τ,I) be an ideal topological space and $W\subseteq X$. Then W is an e^{*} –I-closed set if and only if W is S^{*}δ-set and pre^{*} –I -closed set in X.

Proof: Suppose W is S^{*}δ-set and pre^{*} –I -closed set in X. Thus, $W=M\cap Cl(\mathrm{Int}^{\mathrm{I}}(W))$ for a δ^{I}-open set M in X. Because, $W\subseteq M$and W is pre^{*} –I-closed, so, $Cl(\mathrm{Int}^{\mathrm{I}}(W))\subseteq M$. Hence, $Cl(\mathrm{Int}^{\mathrm{I}}(W))\subseteq M\cap Cl(\mathrm{Int}^{\mathrm{I}}(W))$. Therefore, W is pre^{*} –I-open. Conversely, any pre^{*} –I -closed set is S^{*}δ-set and e^{*} –I -closed set, respectively, in X.

Proposition 3.5. Assume (X,τ,I) be an ideal topological space and $W\subseteq X$. Thus W is pre^{*} –I-closed set if and only if $Cl(\mathrm{Int}^{\mathrm{I}}(W))\subseteq M$ whenever M is an open set in X and $W \subseteq M$.

Proof: Let W is pre^* –I -closed set in X. Suppose that $W \subseteq M$ and M is an open set in X. This implies that W^c is pre^* –I -open set and M^c is a closed set in X. Because, W^c is pre^* –I -open set, $M^c \subseteq Int\left(\mathrm{Cl}^{\mathrm{I}}(W)\right)$. Hence, $Cl(\mathrm{Int}^{\mathrm{I}}(W)) = Int\left(Cl^{I}(W)\right)^c \subseteq M$, so $Cl(\mathrm{Int}^{\mathrm{I}}(W)) \subseteq M$. Proof of the opposite is similar.

4. Conclusion

This study explores and characterizes all two kinds of open subsets in ideal topological spaces: S^*-I-open sets and pre^*-I-open sets. We looked into the connection and contrasts between those sets, as well as the consequences for the framework for ideal topological spaces. Several propositions and lemmas were developed to explain these features, resulting in a better grasp of the fundamental topology. Furthermore, the work discusses the decomposition of continuous in this setting, which contributes to the larger subject of topology. The insights provided here not only increase theoretical understanding, but also have possible applications in other mathematical disciplines.

References

1. Ekici, E. and Noiri, T. On subsets and decompositions of continuity in ideal topological spaces, Arab. J. Sci. Eng. Sect. A Sci. 34, 165-177, (2009).

2. Hatir, E. On decompositions of continuity and complete continuity in ideal topological spaces, Eur. J. Pure Appl. Math. 6, no. 3, 352-362, (2013).

3. Al-Omeri, W. Noorani, M. and Al-Omari, A. On e-I-open sets, e-I-continuous functions and decomposition of continuity, J. Math. Appl. 38, 15-31, (2015).

4. Wadei, A.L., Noorani, M.S.M. and Ahmad, A.O., Weak open sets on simple extension ideal topological space, Ital. J. Pure Appl. Math. 33, 333-344, (2014).

5. Adhikari, A., & Adhikari, M. R. Basic Topology 1: Metric Spaces and
General Topology. Springer, (2022).

6. Jankovic, Mohammed, M. W., & Mohammed, A. A. Some Classes in Ideal Topological Spaces. *Journal of Education & Science*, *32*(2), (2023)..

7. Mukherjee, M. Bishwambhar, N. R. and Sen, R. On extension of topological spaces in terms of ideals, Topology and its Appl. 154, 3167-3172, (2007).

8. Arenas, F. Dontchev, G. J. and Puertas, M. L. Idealization of some weak
separation axioms, Acta Math. Hungar. 89, no. (1-2), 47- 53, (2000).

9. Nasef, A. A. and Mahmoud, R. A. Some applications via fuzzy ideals, Chaos Solitons Fractals. 13, 825-831, (2002).

10. Fathima, A. A., Maheswari, M., & Inthumathi, V. On δIJ. Bulletin of Pure and Applied
Sciences, 6, (2022).

11. Al-Omeri, W. Noiri, T.AGI∗ -sets, BGI∗ -sets and δβI-open sets in ideal
topological spaces, Int. J. Adv. Math. 2018, no.4 , 25-33, (2018).

12. Keskin, A., Noiri, T. and Yuksel, S. Decompositions of I-continuity and continuity, Commun. Fac. Sci. Univ. Ankara Series A1, 53, 67-75, (2004).

The effect of bio-prepared zinc nanoparticles from the fungus *Verticillium lecanii* on combating third-instar larvae of the date moth *Ephestia cautella*

[1] Doaa Abdulmajeed Mohamed

eduhm230154@uosamarra.edu.iq

[1,2] Department of Biology, College of Education - University of Samarra

Hisham naji hameed[2]

Hisham.n370@uosamarra.edu.iq

The effect of bio-prepared zinc nanoparticles from the fungus *Verticillium lecanii* on combating third-instar larvae of the date moth *Ephestia cautella*

[1] Doaa Abdulmajeed Mohamed

eduhm230154@uosamarra.edu.iq

[1,2] Department of Biology, College of Education - University of Samarra

[2]Hisham naji hameed

Hisham.n370@uosamarra.edu.iq

Abstract:

The study was conducted in the Department of Biology - College of Education - University of Samarra, which aims to combat the third instar larvae of the date moth *Ephestia cautella* using bio-prepared zinc nanoparticles from the fungus *Verticillium lecanii* and comparing it with the biomass of the fungus *Verticillium lecanii* and finding out which is most effective in eliminating the third instar of the date moth *Ephestia. cautella* and biomass concentrations were used (1, 1.5, 2) g / L.

Only distilled water was used in the control plants, with a time period of (24, 48, 72) hours for each concentration, Three concentrations of zinc nanoparticles were used: (0.250, 0.125, 0.62) ml / liter , and only distilled water was used in the control laboratories, with a period of time of (24, 48, 72) hours for each

concentration, and for each concentration, three replicates were used for each concentration, and 10 larvae of the date moth *Ephestia cautella* were placed in each replicate for each replicate of the experiment, and the results of each were given: Biomass had high killing results at a concentration of 2 ml/L after 72 hours, and nano zinc at a concentration of 0.250 ml/L after 72 hours.

Introduction:

The date moth is an insect with complete metamorphosis and has four stages: the egg, the larva, the pupa, and the adult. The female date moth lays her eggs in groups or individually on the outer surface of the date [1].

Although the female insect lives for approximately 14 days, The eggs laid by one female are approximately 135 eggs, and approximately 90% of the eggs are laid in the first four days. The eggs are characterized by containing prominent lines on the surface of the egg, both longitudinally and transversely, arranged in 24 irregular rows, with the length of one egg ranging from (0.33 - 0.38 mm).

Their width ranges between (0.22 - 0.32 mm), and the eggs are white when first laid by the adult insect, then they turn orange before the hatching process, with clear longitudinal and transverse elevations on the outer surface [2],The hatching process may take from 3-4 days after the female lays her eggs, the date moth, *Ephestia cautella*, is a polyphagous insect that infects different types of stored foodstuffs, most notably dates, whether they are on palm trees or fallen on the ground or in stores, as well as feeding on many stored foodstuffs such as dried figs, raisins, tarshana, and grains. And their products, legumes, nuts, oilseeds, cocoa and other food families[3].

Nanocomposites are materials to which nanoparticles are added during the manufacture of these materials. As a result, the nanomaterials show an improvement in their properties. Nanotechnology is considered a broad field of scientific research and opens up a wide field in various fields.

It is considered the main advantage of modern insecticides, as it has a useful pesticide effect to eliminate insects. It is not harmful to the main environmental components, and the word nano (Nanos) is originally a Greek word that means dwarf and is used to describe materials with small sizes from (1-100 nanometers). Nanobjects are bio-manufactured using microorganisms such as fungi, bacteria, viruses, and nano-extracts.

One of the advantages of this method is that it is cheap and does not require Energy, fast and at the same time environmentally friendly [4].

Fungi that infect insects and products derived from fungi have been used in biological control of targeted insects, The *Verticillum lecanii* fungus is one of the most common fungi on target insect families and is used to eliminate insects that cause economic damage [5].

Aim of the Study:

1- Evaluation of the effectiveness of biomass prepared from the fungus *Verticillum lecanii* on third-instar larvae of the date moth *Cautella Ephestia.*

2- The effectiveness of a nano-prepared biological preparation from the *Verticillum lecanii* fungus on eliminating the larvae of the date moth *Ephestia cautella*.

key words: *Verticillium lecanii,, Ephestia cautella* , PDA, ZnoNPs, nano

Materials and Methods:

Medium Solid Potato Dextrose Agar (PDA):

Prepare the medium according to the manufacturer's instructions, HIMEDIA, by dissolving 39 grams of potato medium in a liter of distilled water, placing it in a 1000 ml glass baker, shaking well, closing the nozzle with a cotton plug, then sterilizing with an autoclave at a temperature of 121°C and a pressure of 15 pounds/inch for 15 minutes, then Leave the medium to cool and before it hardens, pour it into sterilized dishes.

Liquid potato dextrose medium (PDB) Potato Dextrose Broth:

Prepare the medium according to the manufacturer's instructions by dissolving 24 grams of powdered medium in 1 liter of distilled water. Distribute the medium into conical flasks with a capacity of 250 ml and plug their nozzles with cotton plugs. Then sterilize with an autoclave at a temperature of 121 °C and a pressure of 15 pounds/in2 for 15 minutes, Prepare this medium to obtain the biomass of the *Verticillium lecanii* fungus.

Activation of the fungus *V. lecanii*

Activating the fungal isolate by replanting it on new PDA media 7-9 days before starting to produce biomass in order to use it in preparing biomass.

Preparation of *V. lecanii* biomass

To obtain biomass, the fungal isolate was grown in a sterile Petri dish containing sterile Potato Dextrose Agar medium, and incubated at a temperature of 2 ± 26 °C and a relative humidity of 5 ± 85% for 7 days.

After that, four discs were taken from the colonies growing on the medium. The solid food PDA, with a diameter of 5 mm, was multiplied on the sterile liquid medium placed in a 1000 ml glass container with the addition of 125 mg of tetracycline to ensure that bacteria did not grow, while continuing to move the glass containers incubated at a temperature of 2 ± 26 °C for 21 days with daily manual shaking. Biomass after 21 days of incubation by using a glass funnel and filter paper.

After that, the biomass was washed with distilled water three times, followed by washing it with deionized water twice to get rid of all residual nutrient medium. Weighed 10 grams of fungal biomass using a sensitive balance and transferred to 1000 ml glass containers containing 250 ml deionized water were also incubated under the same conditions above with daily shaking using a shaker for 120 hours.

After the expiration of the period, the fungal biomass was filtered using filters to obtain the fungal biomass filtrate. The filtrate was collected and incubated at a temperature of 26 ± 2 °C and a relative humidity of 5 ± 75% until use [6].

The biomass is then dried to obtain a powder for experiments on the third instar larvae of the date moth.

For fungal biomass, concentrations of (1, 1.5, and 2) grams were used, with three replicates for each concentration. The control factor in the experiment was used only distilled water for 24, 48, and 72 hours. The concentrations gave high rates of death.

Bio-prepared nanocomposite from *Verticillium lecanii*

The nanocomposite zinc oxide (ZnoNPs) that was used in the study was obtained from the Ministry of Science and Technology in Baghdad Governorate / Iraq. The compound was in the form of a white-yellowish powder, with a particle size of less than 5 micrometers with a purity of 99% , The Ministry prepared the compound in A plastic box containing 7 grams. It was received in the form of a nanopowder with a particle size of less than 100 nanometers.

Preparation of nanocomposites (ZnoNPs):

Silver nanoparticles were manufactured by crushing the mushroom extract using an ultrasound device for five minutes, after which the previously prepared zinc oxide solution was placed on a hot plate with a magnetic stirrer for 30 minutes, after which the mushroom extract was added to the oxide solution.

Zinc in drops, then placed in an ultrasound machine for 30 minutes, then mixed with a magnetic mixer without heat for 30 minutes [7].

An amount of nano-zinc oxide was weighed 0.5 grams of powder and a drop of concentrated nitric acid was placed on it and mixed with the powder, noting the rise of vapors from the powder after mixing it with nitric acid.

Then the homogeneous material was placed in a glass beaker containing 1000 ml of distilled water with continuous stirring for 10 minutes. To ensure that the nanocomposite dissolves with water, and thus we have the main stock concentration.

After that, we conduct several dilutions to reach the concentrations required in the experiment, which are a concentration of 0.250, 0.125, 0.062) and for a period of time of (24, 48, 72, 96), with three replicates for each concentration and a coefficient was used. The control in this experiment was only distilled water.

Statistical Analysis:

The results analyzed statistically by applying the statistical program (MINITAB VER.17) according to the Anova analysis test (Anova). The mathematical averages were compared according to the Duncuns Multiple Range test and at a possibility of $0.05 \geq p$ [8].

Results :

The results of the table (1) and the effect of the interaction of the different concentrations (0.062, 0.125, 0.250 mg/L) of the zinc oxide nano composite, as well as the time period for the death of the third instar of the date moth, showed that there were significant differences in the killing rates due to the interaction between the concentrations and the duration of exposure, as the highest percentage of killing was for the third instar larvae. The third was 96.7% at a concentration of 2500 after 96 hours of treatment, while the lowest killing percentage was 23.3% at a concentration of 0.062 after 24 hours of treatment, while averages of the killing percentage as a result of the concentrations showed that the highest killing percentage was at a concentration of 0.250 reaching 72.5%, while The lowest average kill rate at a concentration of 0.062 was 59.2%.

As for the average kill rate based on the duration of killing, the highest kill rate after 96 hours was 70.0%, and the lowest kill rate after 24 hours was 24.2%.

From the results it was shown that the percentage Larval killing increased with increasing concentration and duration of treatment. The results of the study were consistent with the findings of [9].

As they indicated that the zinc oxide nanocomposite had an effective effect in combating the red flour beetle T. castaneum compared to the pesticide malathion, as the results showed that there was a significant effect of the nanocomposite.

Zinc oxide affects the percentage of killing, productivity and weight loss of whole grains. These percentages increase with increasing concentration and duration of exposure, as these particles cause deformities and dehydration of the insect and provide protection for the grain by reducing the rate of the first generation of the insect T. castaneum and then reducing the percentage of weight loss in the grain. It was also similar The results of this study are based on the findings of [10].

Who indicated the effect of nano composites, including zinc oxide, in protecting grains from infection with the Khabra insect for a period of up to 40 days, where the percentage of weight loss was 0.67, 0.73, and 3.44%, while the percentage of weight loss was 3.44%.

The loss in the control treatment is 11.74%. Zinc oxide nanoparticles have been used to develop pesticides due to their antimicrobial, physical and some other properties [11]; [12].

Table (1) shows the effect of nano-zinc oxide (ZNPs) on the mortality rates of third-instar larvae of the date moth.

Concentration Average	**Time**				**Concentration ml /l**
	96 Hours	**72 Hours**	**48 Hours**	**24 Hours**	

7.25 A	**9.67 a**	**8.67 b**	**6.33 d**	**4.33 f**	**0.250**
6.25 B	**9.33 ab**	**7.33 c**	**5.33 e**	**3.00 g**	**0.125**
5.92 B	**9.00 b**	**7.33 c**	**5.00 e**	**2.33 h**	**0.062**
0.0 C	**0 i**	**0 i**	**0 i**	**0 i**	**Control**
	7.00 a	**5.83 b**	**4.17 c**	**2.42 d**	**Time average**

Small letters that are similar horizontally mean that there are no significant differences between them.

The results of the table (2) and the effect of the interaction of different concentrations (2, 1.5, 1) g/Lon biomass as well as the time period for the death of the third instar of the date moth showed that there were significant differences in the killing rates due to the interaction between the concentrations and the duration of exposure, as the highest percentage of killing for the third instar larvae was 93.3 % at concentration 2 after 72 hours of treatment, while the lowest killing rate was 23.3% at concentration 1 after 24 hours of treatment, while averages of the killing rate as a result of the concentrations showed that the highest killing rate was at concentration 2, reaching 72%, The lowest average kill rate at concentration 1 was 23.3%.

As for the average kill rate based on the duration of killing, the highest kill rate after 72 hours was 50.0%, and the lowest kill rate after 24 hours was 28.3%.

From the results it was shown that the percentage of Killing third instar larvae of date moth increased with increasing concentration and duration of treatment. The results of this study agreed with [13].

Through the use of suspensions of three types of chrysogenum fungi. *penicillium*, *V.lecanii, Aspergillus.niger*) in its effect on the larval stages of *C.quinquefasciatus* mosquitoes, as the insect-pathogenic fungus *V.lecanii* outperformed the rest of the fungi in influencing mosquito larvae with percentages of death reaching 20, 16.66, 13.33, and 10% after 48 hours of treatment and rose to 63.33), 60, 56.66 and 53.33 after 96 hours of treatment.

The high rate of death rates in the first larval ages with the last instar and adults is attributed to the incompleteness of the defense cells in the first larval ages, in addition to the lack of thickness of the cuticle layer, or it may be explained by changes in the biological and chemical composition of the insect's body wall, such as the presence of toxic compounds, which may To prevent the germination of fungal spores [14].

The results of other studies that are consistent with this study showed what was mentioned by [15].

that they were more sensitive to infection by *E. cautella*. The results showed that individuals of the first larval stages of the date moth were exposed to biological factors (bacteria and fungi) from later ages. The ability of the fungus to adhere to the body The insect, its structure, the germination tube and adhesion organ, and the amount of enzymes secreted by the fungus, such as chitinase, lipase, and protease enzymes, played a major role in destroying the insect's body.

The current study showed that increasing the concentration and duration of treatment of biologically prepared biomass from mushrooms has a significant impact on eliminating third–instar larvae of the date moth.

Table (2) shows the effect of biosynthetic mass from the fungus *V. lecanii*. On third instar larvae of the date moth *E. cautella*

Concentration Average	Time			Concentration ml /l
	72 Hours	48 Hours	24 Hours	
3.33 C	4.00 e	3.67 e	2.33 f	1
5.56 B	6.67 bc	6.33 c	3.67 e	1.5
7.22 A	9.33 a	7.00 b	5.33 d	2
0.0 D	0 g	0 g	0 g	Control
	5.00 a	4.25 b	2.83 c	Time average

Small letters that are similar horizontally mean that there are no significant differences between them.

Conclusion:

1-The fungus *V. lecanii* showed high efficiency in the biosynthesis of zinc oxide nanoparticles.

2- Biologically prepared nanoparticles have a promising future in controlling insect pests.

3. Treatment with zinc nanoparticles led to the killing of third-instar larvae of the date moth three days after treatment, with a direct relationship between concentrations and killing rates.

References:

1- **Arthington, A. H., Pearson, R. G., Connolly, N. M., James, C. S., Kennard, M. J., Loong, D., ... & Pusey, B. J. (2007).** Biological Indicators of Ecosystem Health in Wet Tropics Streams. *Catchment to Reef Research Program, CRC for Rainforest Ecology and Management and CRC for the Great Barrier Reef.(James Cook University, Townsville.)*.

2- **Abdul** Hussein, Ali. 1979. Palm trees and dates and their pests in Iraq. faculty of Agriculture . University of Basra. 190 pages.

3- **Aldawood,A.S.(2013)** Effect of covering dates fruit bunches on Ephestia cautella Walker (Lepidoptera: pyralidae)infestation: population dynamics studies in the field. Int. J. Agric. Appl. Sci. Vol. 5, No.1,:98-100.

4- **Ribeiro , L. P.; Blume, E.; Bogorni , P. C. ; Dequech , S. T.B.; Brand , S. C. and Junges,E.(2012)** Compatibility of *Beauveria bassiana* commercial isolate with botanical insecticides utilized in organic crops in southern Brazil. December 2012Biological Agriculture and Horticulture. 28(4):223-240.

5- **Kamalakannan** S. K. Vnaik kGChauhanA. **(2021)** .Sources of fungal bio-generated nano particies for potential control of mosquito –born diseases review.

6- **Al-Shammari,** Hazem Eidan (2015) The effect of the predator Dicrodiplosis manihoti Harris (Diptera: Cecidomyiidae) and silver nanoparticles prepared by biological methods on some biological aspects of the citrus mealybug Planococcus (Risso) Hemiptera: Pseudococcidae. Doctoral thesis. College of Agriculture, University of Baghdad.

7- Al-Naimi, MT. Hamdan, N.T. Abdel-Rahim, E., and Al-Janabi, .(2019).ZZ. Biodegradation of malathion pesticides by silver bioparticles from Bacillus licheniformis extracts. Research in Crops, 20. spl), (79-84.

8 -**Al-Rawi**, Khashi Mahmoud and Abdul Aziz Muhammad Khalaf Allah (1980). Design and analysis of agricultural experiments, Dar Al-Kutub Printing and Publishing Foundation, Ministry of Higher Education and Scientific Research, University of Mosul.

9 - Abd-El-Salam, S. A., Hamzah, A. M., & El-Taweelah, N. M. (2015). Aluminum and zinc oxides nanoparticles as a new method in controlling the red flour beetle, Tribolium castaneum (Herbest) compared to Malathion insecticide. *International Journal of Scientific Research in Agricultural Sciences*, *2*(Proceedings), 001-006.

10 - **Radhiu**, Ghadeer Abdul Jabbar. 2020. Evaluation of the efficiency of some commercial nanocomposites and alcoholic extracts of some plants in controlling the insect Trogodema granarium Evest 1898 (coleopteran): Dermestidae under laboratory conditions. Master's thesis. College of Agriculture, University of Kufa, Republic of Iraq. Issue (2) 1.

11 – **Akbar**, S., Tauseef, I., Subhan, F., Sultana, N., Khan, I., Ahmed, U., & Haleem, K. S. (2020). An overview of the plant-mediated synthesis of zinc oxide nanoparticles and their antimicrobial potential. *Inorganic and Nano-Metal Chemistry*, *50*(4), 257-271.

12 - **Akintelu**, S. A., & Folorunso, A. S. (2020). A review on green synthesis of zinc oxide nanoparticles using plant extracts and its biomedical applications. *BioNanoScience*, *10*(4), 848-863.

13- **Al-Fatlawi**, Ali Abdel Hamid Abdel Amir. (2021). Evaluating the effectiveness of biosynthetic silver nanoparticles using filtrate and suspensions of some fungal species in resisting mosquitoes. Master's thesis, College of Science, Al-Qadisiyah University. p. 134

14 - **Raduw, G. G., & Mohammed, A. A.** (2020). Insecticidal efficacy of three nanoparticles for the control of Khapra beetle (Trogoderma granarium) on different grains. *Journal of Agricultural and Urban Entomology*, *36* (1), 90-100.

15 - **Abdel Aoun**, Lara Sharif 2021. Evaluating the efficiency of some local isolates of the fungus Beauveria bassiana, the bio-commercial preparation

Naturalis-L, the pathogenic bacteria Bacillus thuringiensis, and nanocomposites SNPs, ANPs, and ZNPs in controlling the date (fig) moth Ephestia cautella in laboratory conditions. Master's thesis - College of Agriculture - University of Karbala. 176 pages.

تأثير جزيئات الزنك النانوية المحضرة حيويا من الفطر *Verticillium lecanii* في مكافحة يرقات العمر الثالث لفراشة التمر *Ephestia cautella*

1,2

[1,2]كلية التربية , قسم علوم الحياة – جامعة سامراء

دعاء عبدالمجيد محمد [1]

eduhm230154@uosamarra.edu.iq

هشام ناجي حميد [2]

Hisham.n370@uosamarra.edu.iq

المستخلص:

أجريت الدراسة في قسم علوم الحياة – كلية التربية – جامعة سامراء، وتهدف إلى مكافحة يرقات العمر الثالث لعثة التمر *Ephestia cautella* باستخدام جزيئات الزنك النانوية المحضرة حيوياً من فطر Verticillium lecanii ومقارنتها مع الكتلة الحيوية للفطر *Verticillium lecanii* ومعرفة أيهما أكثر فعالية في القضاء على العمر الثالث لعثة التمر *Ephestia*. واستخدمت تراكيز من النانو والكتلة الحيوية (1، 1.5، 2) غرام/لتر.

تم استخدام الماء المقطر فقط في محطات المراقبة وبمدة زمنية (24، 48، 72) ساعة لكل تركيز، وتم استخدام ثلاث تراكيز من جزيئات الزنك النانوية: (0.250، 0.125، 0.62) مل/لتر، والماء المقطر فقط. تم استخدام مختبرات المقارنة بفترة زمنية (24، 48، 72) ساعة لكل تركيز، ولكل تركيز تم استخدام

ثلاث مكررات لكل تركيز، وتم وضع 10 يرقات من فراشة التمر *Ephestia cautella* في مكررات للمقارنة.

تم إعطاء نتائج كل مكرر لكل مكرر للتجربة: أظهرت الكتلة الحيوية نتائج قتل عالية عند تركيز 2 مل/لتر بعد 72 ساعة، ونانو زنك بتركيز 0.250 مل/لتر بعد 72 ساعة.

الكلمات المفتاحيه: *Verticillium lecanii*, *Ephestia cautella* , PDA, ZnoNPs, nano

Study on the Existence of Solutions for Some Singular Nonlinear Equations on Exterior Domain

Mageed Hameed Ali[1], Othman Mahmood Alwan[2], Sinan Omar Ibrahim[3]

[1] College of Science, University of Kirkuk, Kirkuk, Iraq

[2,3]College of Education for Pure Sciences, Tikrit University, Salah AL-Dien, Iraq

[1]Email: mageedali@uokirkuk.edu.iq
[2]Email: othmanmahmood100@gmail.com
[3]Email: drsinan2001@gmail.com

Study on the Existence of Solutions for Some Singular Nonlinear Equations on Exterior Domain

Mageed Hameed Ali[1], Othman Mahmood Alwan[2], Sinan Omar Ibrahim[3]

[1] College of Science, University of Kirkuk, Kirkuk, Iraq

[2,3]College of Education for Pure Sciences, Tikrit University, Salah AL-Dien, Iraq

[1]Email: mageedali@uokirkuk.edu.iq
[2]Email: othmanmahmood100@gmail.com
[3]Email: drsinan2001@gmail.com

ABSTRACT. This paper focuses on investigating the presence of solutions for singular non-linear equations (1.1) in the exterior domain. $R > 0$ on the boundary where $N > 2$. $f(u) \sim \frac{-1}{|u|^{q-1}u}$ for $|u|$ small and $0 < q < 1$, and $f(u) \sim |u|^{p-1}u$, for $|u|$ large and where $0 < \mathrm{p} < 1$. also $\mathrm{K(x)} = |x|^{-\alpha}$ with $\alpha > 2(N-1)$.

Keywords: Existence, singular, exterior, non-linear

INTRODUCTION

This paper involves the examination of the equation:

$$\Delta u + K(x) f(u) = 0\,, \quad \text{for } R < |x| < \infty \tag{1.1}$$

$$u = 0 \quad on \quad R < |x| < \infty \tag{1.2}$$

$$u \to 0 \;\; as \;\; |x| \to \infty \tag{1.3}$$

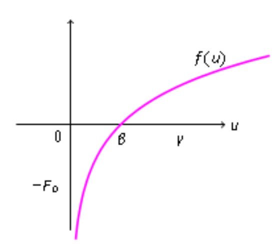

Where the Laplacian operator is denoted by Δ, the function

f: R\{0}→R, is locally Lipschitz. and : $\mathbb{R}^N \to \mathbb{R}$, $K(x) > 0$.

(H_1) f is odd, there exists $\beta > 0$ such that $f < 0$ on $(0, \beta)$, $f > 0$ on (β, ∞) and $\mathrm{f(\beta)} = 0$.

Graph 1.1. $f(u)$

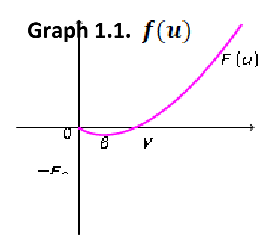

(H_2) $g_1 \colon R \to R$ *is* continuous and $f(u) = \frac{-1}{|u|^{q-1}u} + g_1(u)$ if u is small.

Where $0 < q < 1$ and $g_1(0) = 0$.

(H_3) $g_2 : R \to R$ is continuous and $f(u) = |u|^{p-1}u + g_2(u)$, if u is large. Where $0 < p < 1$. we let $F(u) = \int_0^u f(s)ds$. Since f is an odd function, it can be concludedthat F is an even function. Additionally, based on the assumption (H_2), it can be inferred that f is capable of being integrated into the vicinity of $u = 0$. This implies that F is a continuous function with a value of 0 at $u = 0$. Furthermore, F is bounded below by $-F_0$with $F_0 > 0$. Finally, from assumption (H_3), it can be determined that there exists a value of γ such that $0 < \beta < \gamma$.

Graph 1.2 . $F(u)$

(H_4) $F < 0$ on $(0, \gamma), F > 0$ on(γ, ∞), and $F > -F_0$ on $\mathbb{R}$, $F(\gamma) = 0$.

(H_5) The functions k and k' are characterized as having continuity on the interval $[R, \infty)$. It is also known that $k(r) > 0$, and that $k(r)$ is equal to $r - \alpha(2N - 1)$. Additionally, $2(N-1) + \frac{rk'}{k} < 0$. It is further assumed that α is greater than $2(N - 1)$, $\lim_{r\to\infty} rk'/k = -\alpha$.

(H_6) There exists $k_1, k_2 > 0$ such that $\frac{k_1}{r^\alpha} \leq k(r) \leq \frac{k_2}{r^\alpha}$.

Lemma 1 : Assuming that the given conditions are true, with $f\big(u(r)\big)$ defined as $\frac{-1}{u^q} + u^p$, where $0 < \mathrm{p}, \mathrm{q} < 1$, and $u\big(r_\beta\big) = \beta$ under the assumption H_1, it can be deduced that the value of $\beta = 1$

Proof: Suppose $f\big(u(r)\big) = \frac{-1}{u^q} + u^p$, Given that both $0 < p, q < 1$, it is necessary to make an estimation of r at r_β. This estimation is made based on the fact that $u\big(r_\beta\big) = \beta$.

$$0 = f(\beta) = \frac{-1}{\beta^q} + \beta^p$$

We obtain :

$$-1 + \beta^{p+q} = 0$$

implies that:

$\beta^{p+q} = 1$ then by taking the root $(p + q)$ of both sides :

thus $\beta = 1$. The end of the prove lemma 1.

Lemma 2: Let $F(u) = \frac{-u^{1-q}}{1-q} + \frac{u^{p+1}}{p+1}$ with $0 < \mathrm{p}, \mathrm{q} < 1$, and $u(r_\gamma) = \gamma$ then the value $= (\frac{p+1}{1-q})^{\frac{1}{q+p}}$.

Proof: Suppose $F(u) = \frac{-u^{1-q}}{1-q} + \frac{u^{p+1}}{p+1}$, where $0 < \text{p, q} < 1$ then we evaluate r at r_γ. We get :

$$0 = \frac{-\gamma^{1-q}}{1-q} + \frac{\gamma^{p+1}}{p+1}$$

$$0 = -(p+1)\gamma^{1-q} + (1-q)\gamma^{p+1}$$

Simplifying above we get:

$$\gamma^{p+q} = \frac{p+1}{1-q}$$

then by taking the root $(p+q)$of both sides. We obtain:

$$\gamma = \left(\frac{p+1}{1-q}\right)^{\frac{1}{p+q}}.$$

This completes the proof of lemma 2 .

Recent publications [1-10] regarding solutions of differential equations on the exterior domain piqued interest in the subject of this paper. this article is to study how the singular non-linear differential equation (1.1) behavior and to investigate the solutions that it produces. When $0 < p, q < 1$, and $\alpha > 2(N-1)$ are true. Additionally, in [1-10] the radial solutions were studied.

PRELIMINARIES

To study the existence of solutions for equations (1.1) through (1.3), it is necessary to make certain assumptions. Specifically, we assume that $r = |x|$, and that $u(r) = u(|x|)$, where $x \in R^N$.and satisfies

$$u''(r) + \frac{N-1}{r}u'(r) + K(|r|)f(u) = 0 \quad \text{On } (R, \infty) \tag{1.4}$$

$$\text{u(R)} = 0 \qquad \lim_{r\to\infty} u(r) = 0 \tag{1.5}$$

to prove the existing solution we change the variable

$$u(r) = v_a(r^{2-N}) \tag{1.6}$$

Therefore

$$u'(r) = v_a{}'(r^{2-N})(2-N)r^{1-N} \tag{1.7}$$

$$u''(r) = (2-N)(1-N)r^{-N}v'(r^{2-N}) + (2-N)^2 r^{2(1-N)}\, v_a{}''(r^{2-N}) \tag{1.8}$$

Letting $t = r^{2-N}$ and $r = t^{\frac{1}{2-N}}$ in $(1.4) - (1.5)$ we obtain:

$$v_a'' + h(t)f(v_a) = 0 \qquad \text{on } (0, R^{\tau}) \tag{1.9 }$$

$$v_a(R^{\tau}) = 0 \tag{1.10}$$

$$v_a'(R^{\tau}) = -a^{\tau} < 0 \tag{1.11}$$

where $R^{2-N} = R^{\tau}$and $a^{\tau} = \frac{aR^{N-1}}{N-2}$

Then where form $(H_4)$and (H_5) and suppose :

$h(t) = \frac{t^{\hat{\alpha}}}{(N-2)^2}$ where $\hat{\alpha} = \frac{\alpha-2(N-1)}{N-2} > 0$. Since $\alpha > 2(N-1)$, and $t \in (0, R^{\tau})$. Also from (1.7) and (1.8), This suggests that there are constants h_1 and h_2, where $0 \leq h_1 \leq h_2$, which implies that...

$$h(R^{\tau}) \geq h(t) \tag{1.12}$$

$$h'(t) > 0, h_1 t^{\hat{\alpha}} \leq h(t) \leq h_2 t^{\hat{\alpha}} \quad \text{on } (0, R^{\tau}). \tag{1.13}$$

Theorem 1.1. Suppose that $a > 0$, $\alpha > 2(N-1)$, where $N > 2$ and $(H_1) - (H_6)$ hold. then there exists a solution of the equations (1.9)-(1.11) on $(R^{\tau} - \epsilon,\ R^{\tau})$ for some $\epsilon > 0$.

Proof:

step (1):- Using the initial condition (1.10)-(1.11), we first integrate (1.9) on (t, R^{τ}), to obtain:

$$v_a(R^{\tau}) = 0,\ v_a'(R^{\tau}) = -a^{\tau} < 0$$

Integrating (1.9) on (t, R^{τ}) and using the initial condition we get:

$$-a^{\tau} - v_a'(t) = -\int_t^{R^{\tau}} h(t) f\big(v_a(s)\big)\, ds \tag{1.14}$$

$$v_a'(t) = -a^{\tau} + \int_t^{R^{\tau}} h(t) f\big(v_a(s)\big)\, ds \tag{1.15}$$

Also, integrating (1.15) on (t, R^{τ}) and with (1.11) we get :

$$-v_a(t) = v_a(R^{\tau}) - v_a(t) = -a^{\tau}(R^{\tau} - t) + \int_t^{R^{\tau}} \int_s^{R^{\tau}} h(x) f\big(v_a(x)\big) dx ds$$

$$v_a(t) = a^{\tau}(R^{\tau} - t) - \int_t^{R^{\tau}} \int_s^{R^{\tau}} h(x) f\big(v_a(x)\big) dx ds \tag{1.16}$$

Now, we let $D^\tau(t) = \frac{v_a(t)}{(R^\tau - t)}$ (1.17)

And $v_a(t) = D^\tau(t)\left(R^\tau - t\right)$ and using L'Hôpital's rule and we obtain:

$$\lim_{t\to(R^\tau)^-} \frac{v_a(t)}{(R^\tau - t)} = -v_a(R^\tau) = a^\tau$$

And rewriting the (1.16) and we get :

$$D^\tau(t) = a^\tau - \frac{1}{(R^\tau - t)} \int_t^{R^\tau} \int_s^{R^\tau} h(x) f((R^\tau - x)\ D^\tau(x)) dx ds \tag{1.18}$$

Step(2): We will use the fixed point method to solve equation (1.18). To do so, we must establish a set using the fixed-point method. and let, $a > 0, 0 < \epsilon < 1$, and then define:

$$A = \left\{ D^\tau \in C[R^\tau - \epsilon, R^\tau] \mid |D^\tau(t) - a^\tau| \le \frac{1}{2} a^\tau \text{on } [R^\tau - \epsilon, R^\tau] \right\}$$

Where $D^\tau(R^\tau) = a^\tau$and $C[R^\tau - \epsilon,\ R^\tau]$ is the set of real–valued continuous functions on $[R^\tau - \epsilon,\ R^\tau]$. Let :

$$\|D^\tau\| = \sup_{x\in[R^\tau - \epsilon,\ R^\tau]} |D^\tau(x)|.$$

Then $(A, \|.\|)$ is a Banach space.

Now let us define a map φ on A by $\varphi D^\tau(R^\tau) = a^\tau$ and :

$$\varphi D^\tau(t) = D^\tau(t) = a^\tau - \frac{1}{(R^\tau - t)} \int_t^{R^\tau} \int_s^{R^\tau} h(x) f((R^\tau - x) D^\tau(x)) dx ds \tag{1.19}$$

$\varphi: A \to A$, $R^\tau - \epsilon < t < R^\tau$. since $D^\tau(x) \in A$ and $0 < \epsilon < 1$ we have:

$$|D^\tau(t) - a^\tau| \le \frac{1}{2} a^\tau$$

$$-\frac{1}{2} a^\tau \le D^\tau(x) - a^\tau \le \frac{1}{2} a^\tau$$

$$a^\tau - \frac{1}{2} a^\tau \le D^\tau(x) \le \frac{1}{2} a^\tau + a^\tau$$

$$\frac{1}{2} a^\tau \le D^\tau \le \frac{3}{2} a^\tau \qquad \text{on } [R^\tau - \epsilon, R^\tau] \tag{1.20}$$

Now we estimate $f((R^\tau - x) D^\tau) = \frac{-1}{((R^\tau - x)^q D^{\tau q}} + g_1((R^\tau - x) D^\tau)$.

It follows form (1.20) that:

$$\left(\frac{1}{2}a^{\tau} \leq D^{\tau}(x) \leq \frac{3}{2}a^{\tau}\right)^{q} (R^{\tau}-x)^{q}$$

$$\frac{(R^{\tau}-x)^{q}}{2^{q}}a^{\tau q} \leq D^{\tau^{q}}(x)(R^{\tau}-x)^{q} \leq \left(\frac{3}{2}\right)^{q} a^{\tau q}(R^{\tau}-x)^{q}$$

$$\frac{2^{q}}{(R^{\tau}-x)^{q}a^{\tau q}} \geq \frac{1}{D^{\tau^{q}}(x)(R^{\tau}-x)^{q}} \geq \frac{1}{\left(\frac{3}{2}\right)^{q} a^{\tau q}(R^{\tau}-x)^{q}}$$

$$\frac{a^{\tau q}}{(R^{\tau}-x)^{q}2^{q}} \geq (R^{\tau}-x)^{-q}(D^{\tau}(x))^{-q} \geq \frac{2^{q}a^{\tau q}}{(R^{\tau}-x)^{q}3^{q}}$$

Now evaluate $\frac{-1}{(R^{\tau}-x)\, D^{\tau^{q}}(x)}$

$$\left|\frac{-1}{(R^{\tau}-x)^{q}((D^{\tau}(x))^{q}}\right| \leq \frac{2^{q}}{a^{\tau q}}(R^{\tau}-x)^{-q}\ . \qquad (1.21)$$

From H_2 we see $g_1(x)$ is locally Lipschitz, $0 < p < 1$, and $g_1(0) = 0$ therefore it follows that :

$$g_1((R^{\tau}-x)D^{\tau}(x)) \leq L|R^{\tau}-x||D^{\tau}(x)| \qquad (1.22)$$

$$g_1\big((R^{\tau}-x)D^{\tau}(x)\big) \leq L|R^{\tau}-x|\ \frac{3}{2}a^{\tau} = \frac{3}{2}a^{\tau}\ L|R^{\tau}-x|$$

Where L is the Lipschitz constant for g_1 on $[0,\frac{3}{2}a^{\tau}]$.

Using (1.11),(1.21) and (1.22). Since $h' > 0$, then $h(t) \leq h(R^{\tau})$ and $0 < \mathrm{p},\mathrm{q} < 1$ we see :

$$|h(x)f((R^{\tau}-x)D^{\tau}(x))| = \left|h(x)(\frac{-1}{(R^{\tau}-x)^{q}((D^{\tau}(x))^{q}} + g_1(R^{\tau}-x)D^{\tau}(x))\right|$$

$$\leq h(R^{\tau})[\left|\frac{2^{q}}{a^{\tau q}}(R^{\tau}-x)^{-q}\right| + L\left|(R^{\tau}-x)\frac{3}{2}a^{\tau}\right| \qquad (1.23)$$

Integrating on (t, R^{τ}) and using (1.23) we get:

$$\int_t^{R^{\tau}} |h(x)f((R^{\tau}-x)D^{\tau}(x))|dx \leq h(R^{\tau})\ [\frac{c_1}{a^{\tau q}}\ (R^{\tau}-t)^{1-q} + c_2 a^{\tau}(R^{\tau}-t)^{2}] \qquad (1.24)$$

Where $c_1 = \frac{2^{q}}{a^{\tau q}}\frac{1}{1-q}$ and $c_2 = \frac{3LR^{N-1}}{4}$. thus form (1.24)we see:

$$\int_t^{R^\tau} |h(x)f((R^\tau - x)D^\tau(x))|dx \to 0 \text{ as } t \to (R^\tau)^- \ . \quad (1.25)$$

Next, divide by $(R^\tau - t)$ and integrate (1.24) on (t, R^τ). we obtain :

$$\frac{1}{R^\tau - t}\int_t^{R^\tau}\int_s^{R^\tau} \left|h(x)f\big((R^\tau - x)D^\tau(x)\big)\right|dxds \le h(R^\tau)[\frac{c_3(R^\tau - t)^{1-q}}{a^{\tau q}} + a^\tau c_4(R^\tau - t)^2 \quad (1.26)$$

where $c_3 = \frac{c_1}{2-q}$ and $c_4 = \frac{c_2}{3}$ thus from(1.30)we see :

$$\lim_{t\to(R^\tau)^-}[\frac{1}{R^\tau - t}\int_t^{R^\tau}\int_s^{R^\tau}\left|h(x)f\big((R^\tau - x)D^\tau(x)\big)\right|dxds] = 0. \quad (1.27)$$

Now show that $\varphi: A \to A$ is a contraction mapping with $\varphi(D^\tau) \in A$ for each $D \in A$ if $\epsilon > 0$ is sufficiently small.

First, let $D^\tau \in A$ and so it follows from (1.26)-(1.27) that:

$$\frac{1}{R^\tau - t}\int_t^{R^\tau}\int_s^{R^\tau}\left|h(x)f\big((R^\tau - x)D^\tau(x)\big)\right|dxds$$

Is continuous on $[R^\tau - \epsilon, R^\tau]$.then from(1.18),(1.26) and(1.27) we see: $\lim_{t\to(R^\tau)^-} \varphi D^\tau(t) = a^\tau$,

$|\varphi D^\tau(t) - a^\tau| \le \frac{1}{2}a^\tau$ on $[R^\tau - \epsilon, R^\tau]$ and φD^τ continuous if $\epsilon > 0$ is sufficiently small.

Step(3): We need to prove that φ is a contraction mapping if ϵ is sufficiently small.

Let $D_1, D_2 \in A$ then:

$$\varphi D_1(t) - \varphi D_2(t) = \frac{-1}{R^\tau - t}\int_t^{R^\tau}\int_s^{R^\tau} h(x)\left[f\big((R^\tau - x)D_1(x)\big) - f\big((R^\tau - x)D_2(x)\big)\right]dxds \quad (1.28)$$

By (1.8) we have:

$$f\left((R^\tau - x)D^\tau(x)\right) = -(R^\tau - x)^{-q}D^{-q}(x) + g_1(R^\tau - x)D^\tau(x))$$

Where $0 < p, q < 1$.

Use (1.20) and (1.21).

We first estimate:

$$
\begin{aligned}
&\left|f\big((R^{\tau}-x)D_1\big) - f\big((R^{\tau}-x)D_2\big)\right| \\
&\qquad = \left|\frac{-1}{(R^{\tau}-x)^q}\left[\frac{1}{D_1^q}-\frac{1}{D_2^q}\right] + g_1\big((R^{\tau}-x)D_1\big) - g_1\big((R^{\tau}-x)D_2\big)\right| \\
&\qquad \le \frac{1}{(R^{\tau}-x)^q}\left|\frac{1}{D_1^q}-\frac{1}{D_2^q}\right| + L(R^{\tau}-x)|D_1-D_2| \qquad (1.29)
\end{aligned}
$$

Where L is the Lipschitz constant for g_1 on $[0,\frac{3}{2}a^{\tau}]$.

Next applying the mean value theorem, we see that the right-hand side of (1.29) is equal to

$$\frac{1}{(R^{\tau}-x)^q}\left[\frac{q}{D_3^{q+1}}|D_1-D_2|\right] + L(R^{\tau}-x)|D_1-D_2|$$

where D_3 is between D_1 and D_2.

since $D_i \in S$ for $i = 1,2,3$ and $|D_i - a^{\tau}| \le \frac{1}{2}a^{\tau}$ then $\frac{1}{2}a^{\tau} \le D_i \le \frac{3}{2}a^{\tau}$ on

$[R^{\tau}-\epsilon,\ R^{\tau}]$. Therefore it follows that $D_3^{q+1} \ge \left(\frac{1}{2}a^{\tau}\right)^{q+1}$ and so on$[R^{\tau}-\epsilon, R^{\tau}]$ we have:

$$
\begin{aligned}
&\left|f\big((R^{\tau}-x)D_1\big) - f\big((R^{\tau}-x)D_2\big)\right| \\
&\qquad \le |D_1-D_2|\left[\frac{q}{(R^{\tau}-x)^q}\left(\frac{2}{a^{\tau}}\right)^{q+1} + L(R^{\tau}-x)\right]. \qquad (1.30)
\end{aligned}
$$

From (1.12) $h(t) > 0$ is continuous and increasing on $(0, R^{\tau}]$ with $\alpha > 2(N-1)$ we see:

$$
\begin{aligned}
|\varphi D_1 - \varphi D_2| &\le \frac{h(R^{\tau})}{R^{\tau}-t}\int_t^{R^{\tau}}\int_s^{R^{\tau}} |D_1-D_2|\left[\frac{q\,2^{q+1}}{(R^{\tau}-x)^q\,(a^{\tau})^{q+1}} + L(R^{\tau}-x)\right]dxds \\
&\le \frac{h(R^{\tau})}{R^{\tau}-t}\|D_1-D_2\|\int_t^{R^{\tau}}\int_s^{R^{\tau}}\left[\frac{q\,2^{q+1}}{(R^{\tau}-x)^q\,(a^{\tau})^{q+1}} + L(R^{\tau}-x)\right]dxds
\end{aligned}
$$

$$\le\ h(R^{\tau})\|D_1-D_2\|\left[\frac{c_5\epsilon^{1-q}}{a^{q+1}} + c_6\epsilon^2\right] = c_7\|D_1-D_2\| \qquad (1.31)$$

Where. $c_5 = \frac{q}{(2-q)(1-q)}\left(\frac{2(N-2)}{R^{N-1}}\right)^{q+1}$, $c_6 = \frac{L}{6}$ and $c_7 = h(R^{2-N})\left[\frac{c_5\epsilon^{1-q}}{a^{q+1}} + c_6\epsilon^2\right]$ since:

$\lim_{\epsilon\to 0^+} c_7 = \lim_{\epsilon\to 0^+} h((R^{\tau})[\frac{c_5\epsilon^{1-q}}{a^{q+1}} + c_6\epsilon^2] = 0$ then for ϵ sufficiently small we see

$0 < c_7 < 1$ and therefore it follow (1.31) that φ is a contraction mapping Then by Contraction mapping principle on A we see there exists a unique solution. this complete proof of the theorem (1.1).

Now we define the energy equation of solution (1.9) –(1.11)

$$E_a(t) = \frac{1}{2}\frac{v_a'^2(t)}{h(t)} + F\big(v_a(t)\big) \tag{1.32}$$

Lemma1.2. The energy equation $E_a(t)$ is non-increasing.

Proof: from the energy equation (1.32), Differentiating $E_a(t)$ and using (1.14) :

$$E_a'(t) = \frac{1}{2}\left[\frac{h(t)\big(2v_a'(t)\big)v_a''(t) - v_a'^2(t)\, h'(t)}{h^2(t)}\right] + f\big(v_a(t)\big)\, v_a'(t)$$

$$E_a'(t) = [\frac{v_a'(t)\, v_a''(t)}{h} + f\big(v_a(t)\big)\, v_a'(t) - \frac{v_a'^2(t)\, h'(t)}{2h^2(t)}]$$

$$E_a'(t) = \frac{v_a'(t)}{h(t)}\,[v_a''(t) + h(t) v_a'(t)] - \frac{v_a'^2(t)\, h'(t)}{2h^2(t)}$$

and since we know from(1.12) that $h'(t) > 0$ and $v_a'^2 > 0$ then:

$$E_a'(t) = -\frac{v_a'^2(t)\, h'(t)}{2h^2(t)} \le 0 \tag{1.33}$$

Thus E_a' is non – increasing where it is defined for this t with $t < R^\tau$ then :

$$0 < \frac{1}{2}\frac{a^\tau}{h(R^\tau)} = E_a(R^\tau) \le E_a(t) = \frac{1}{2}\frac{v_a^2(t)}{h(t)} + F\big(v_a(t)\big)\,. \tag{1.33}$$

Thus $0 \le E(t)$.

Applications

In this passage, we will illustrate the primary outcome attained in theorem (1.1) through the use of an illustration. Let us examine the subsequent differential non-linear equation:
$v_a''(t) + h(t)(-v_a^{-q} + v_a^{\ p}) = 0.$

with the initial condition

$v_a(R^\tau) = 0, v_a'(R^\tau) = -a^\tau,$ to find the existence of solutions

Let $p = \frac{1}{2}, q = -\frac{1}{2}$ let $a^\tau = 2$ and $R^\tau = 2,$ therefore:

$$v_a''(t) + h(2)\left(-v_a^{-\frac{1}{2}} + v_a^{\frac{1}{2}}\right) = 0\,, \qquad \text{on } (0,2). \tag{1.34}$$

With initial condition:

$$v_a(2) = 0,\ v_a'(2) = -2 \tag{1.35}$$

Integrate the equation (1.34) on (t,2), we get :

$$v_a'(2) - v_a'(t) = -\int_t^2 h(2)(-v_a^{-\frac{1}{2}} + v_a^{\frac{1}{2}})dt$$

$$-v_a'(t) = 2 - \int_t^2 h(2)(-v_a^{-\frac{1}{2}} + v_a^{\frac{1}{2}})dt \tag{1.36}$$

Integrate (1.36) on $(t,2)$, we get :

$$v_a(t) = 2(2-t) - \int_t^2 \int_s^2 h(2)(-v_a^{-\frac{1}{2}} + v_a^{\frac{1}{2}})dsdt$$

And $D^\tau(t) = \frac{v_a(t)}{2-t}$ then $v_a(t) = (2-t)D^\tau(t)$

$\lim_{t\to 2} D^\tau(t) = \lim_{t\to 2}\frac{v_a(t)}{2-t}$ by L'Hôpital's rule then we get:

$$\lim_{t\to 2}\frac{v_a(t)}{2-t} = \frac{-2}{-1} = 2 = D^\tau(t)$$

let us define

$A = \{D^\tau(t) \in C[2-\epsilon,2] \,|\, |D^\tau(t) - 2| \le 1 \text{ on } (2-\epsilon,2)\}$ then $-1 \le D^\tau(t) - 2 \le 1$ and $1 \le D^\tau(t) \le 3$. Let $\|D^\tau(t)\| = \sup_{x\in[2-\epsilon,2]} |D^\tau(t)|$.

We will establish a mapping φ: A→A. Furthermore, given that f is locally Lipschitz then $|g_1(v_a(t))|$ on (0,2) then we get:

$$|g_1(v_a(t))| \le L|v_a(t)| \text{ then } |f| \le L(2-t)D^\tau(t)$$

$$\text{Also } h(t) \le h(2)\text{, since } h'(t) > 0$$

$|h(t)f| \le h(2)L(2-t)D^\tau(t)$

$|h(t)f| \le 3h(2)L(2-t) = C^*D^\tau$,where $1 < C^* < 1$

Let $D_1, D_2 \in A$ then $|\varphi D_1 - \varphi D_2| \le C|D_1 - D_2|$ on $(2-\epsilon, 2)$ then we obtain $0 < C < 1$

REFERENCES

[1] Ali, M., & Iaia, J. (2021). Existence and nonexistence for singular sublinear problems on exterior domains.

[2] Ali, M., & Iaia, J. (2021). Infinitely many solutions for a singular semilinear problem on exterior domains.

[3] Iaia, J. (2017). Existence of solutions for sublinear equations on exterior domains

[4] Iaia, J. (2019). Existence of infinitely many solutions for singular semilinear problems on exterior domains.

[5] McLeod, K., Troy, W. C., & Weissler, F. B. (1990). Radial solutions of Δu+ f (u)= 0 with prescribed numbers of zeros. *Journal of Differential Equations*, *83*(2), 368-378.

[6] Joshi, J., & Iaia, J. (2016). Existence of solutions for semilinear problems with a prescribed number of zeros on exterior domains. *Electronic Journal of Differential Equations, 112*, 1-11.

[7] Iaia, J. (2015). Loitering at the hilltop on exterior domains. *Electronic Journal of Qualitative Theory of Differential Equations*, *2015*(82), 1-11.

[8] Joshi, J. (2017). Existence and nonexistence of solutions for sublinear problems with prescribed number of zeros on exterior domains.

[9] Joshi, J., & Iaia, J. (2018). Infinitely many solutions for a semilinear problem on exterior domains with nonlinear boundary condition.

[10] Azeroual, B., & Zertiti, A. (2018). ON MULTIPLICITY OF RADIAL SOLUTIONS TO DIRICHLET PROBLEM INVOLVING THE $ p $-LAPLACIAN ON EXTERIOR DOMAINS. International Journal of Applied Mathematics, 31(1), 121-147.

Solve System of Nonlinear Fredholm Integro-Differential Equations of Second Kind by using Quintin B-Spline

Yusr Hamad Jassim[1], Borhan F. Jumaa[2] and Ghassan E. Arif[3]

[1,3]Department of Mathematics/ College of Education for Pure Sciences/ Tikrit University, Salah Al-din, Iraq.

[2]Computer Science Department, College of Computer Science and Information Technology, University of Kirkuk, Kirkuk, Iraq.

[1]yh230025pep@st.tu.edu.iq

[2]borhan_nissan@uokirkuk.edu.iq

[3]ghasanarif@tu.edu.iq

Solve System of Nonlinear Fredholm Integro–Differential Equations of Second Kind by using Quintin B–Spline

Yusr Hamad Jassim[1], Borhan F. Jumaa[2] and Ghassan E. Arif[3]

[1,3]Department of Mathematics/ College of Education for Pure Sciences/ Tikrit University, Salah Al–din, Iraq.

[2]Computer Science Department, College of Computer Science and Information Technology, University of Kirkuk, Kirkuk, Iraq.

[1]yh230025pep@st.tu.edu.iq

[2]borhan_nissan@uokirkuk.edu.iq

[3]ghasanarif@tu.edu.iq

Abstract

This paper investigates the numerical solution of systems of nonlinear Fredholm integro–differential equations of the second kind using the Quintic B–spline method. These equations are significant in various scientific fields, including fluid dynamics, biological models, and chemical kinetics, due to their complexity and widespread applications. Traditional analytical solutions are often impractical; hence, efficient numerical methods are essential. We extend the use of Quintic B–splines, previously applied to other types of integro–differential equations, to these systems. The method is described in detail, including the formulation of the integro–differential equations, the construction of Quintic B–spline interpolants, and the application of LU matrix factorization to solve the resulting system of equations. We present three numerical examples to demonstrate the accuracy and efficiency of the proposed method, comparing theoretical and numerical results using the maximum absolute error and least square error norms. The results show that the Quintic B–spline method provides a reliable and accurate approach for solving complex integro–differential equations.

Keywords: Quintic B−spline, Nonlinear Fredholm integro−differential equations, Numerical methods, Approximate solutions, LU matrix factorization, Fluid dynamics.

1. Introduction:

Mathematical modeling of real−life problems usually results in functional equations, like ordinary or partial differential equations, integral and integro−differential equations and stochastic equations. Many mathematical formulation of physical phenomena contain integro−differential equations. These equations arise in many fields like fluid dynamics, biological models and chemical kinetics. Integro−differential equations are usually difficult to solve analytically so it is required to obtain an efficient approximate solution [1]. In [3], some methods are showed for solving Integro−differential equations such as some methods are showed for solving

Integro−differential equations such as El−gendi's, Wollfe's and Galerkin methods.Recently, the first order linear Fredholm Integro−differential equation is solved by using rationalized Haar functions method [6]. In [2], [11] others methods can be seen to solve Integro−differential equation. In [10] use Quintic B−Spline Method for Solving Sharma Tasso Oliver Equation. In [12] On Solution of Fredholm Integro−differential Equations Using Composite Chebyshev Finite Difference Method. In [58] Cubic B−splines collocation method for a class of partial integro−differential equation. In [7] Use of Cubic B−Spline in Approximating Solutions of Boundary Value Problems. In [8] Exponentially Fitted Finite Difference Approximation for Singularly Perturbed Fredholm Integro−Differential Equation. In [9] Split−step quintic B−spline collocation methods for nonlinear Schrödinger Equations. In [4] Finite Difference with Quintic B−Splines for Solving a system of nonlinear Volterra Integro−Differential Equations of integer order.

In this paper examines the system of first and second−order multi−type Fredholm integro−differential equations of the second kind. The formulation below describes the unknown functions within and the derivative of the unknown function outside the integral sign. For $1,2,\ldots,m$

$$U_i^{(4)}(x)+\sum_{k=1}^{3}\mathcal{F}_{ik}(x)U_i^{(k)}(x)+\mathcal{F}_{i0}(x)U_i(x)=\mathcal{G}_i(x)+\mathcal{P}U_i(x) \quad (1.1)$$

where

$$\mathcal{P}U_i(x)=\sum_{j=1}^{m}\int_0^b\mathcal{K}_{ij}(x,t)\,\mathcal{V}(U_j(t))dt\ ,\ i=1,2,\ldots,m,\quad x\in[0,1]$$

With the initial conditions:

$$U_i^{(k)}(x_0)=U_{i0}^{k},\qquad k=0,1,2,3,\ i=1,2,\ldots,m \quad (1.2)$$

where $U_i(t)$ are unknown functions, $U^{(k)}{}_i(x)$ are the derivative of unknown function, Where $\mathcal{V}(U_j(t))$ is a nonlinear function of $U_j(t)$, the functions $\mathcal{G}_i(x),\mathcal{F}_{ik}(x)\ i=1,\ \ldots,m$ and kernels $\mathcal{K}_{ij}(x,t)$, $1\le i,j\le m$ These are real−valued functions defined on subsets of $\mathcal{R}^3\ and\ \mathcal{R}^1$, respectively..

2. Quintic B−Spline Interpolation:

The Quintic B−spline interpolation is a linear combination of the five order B−spline basis as follows:

$$QB(t)=\sum_{e=\ell-3}^{\ell+3}p_e B\mathbb{S}_e^5(t),\ \ \ell=0,1,2,\ldots,m \quad (1.3)$$

where p_e are unknown real coefficients and $B\mathbb{S}_e^5(t)$ are five−order B−spline functions

then,

$$\frac{d}{dt}QB(t)=\sum_{e=\ell-3}^{\ell+3}p_e\frac{d}{dt}B\mathbb{S}_e^5(t),\ \ \ell=0,1,2,\ldots,m \quad (1.4)$$

and

$$\frac{d^2}{dt^2}QB(t)=\sum_{e=\ell-3}^{\ell+3}p_e\frac{d^2}{dt^2}B\mathbb{S}_e^5(t),\ \ \ell=0,1,2,\ldots,m \quad (1.5)$$

and

$$\frac{d^3}{dt^3}QB(t)=\sum_{e=\ell-3}^{\ell+3}p_e\frac{d^3}{dt^3}B\mathbb{S}_e^5(t),\ \ \ell=0,1,2,\ldots,m \quad (1.6)$$

$$\frac{d^4}{dt^4}QB(t)=\sum_{e=\ell-3}^{\ell+3}p_e\frac{d^4}{dt^4}B\mathbb{S}_e^5(t),\ \ \ell=0,1,2,\ldots,m$$

According to the property of the quintic B−spline (1.3), can be simplified to

$$QB(t) = \mathcal{p}_{\ell-3} B\mathbb{S}^5_{\ell-3}(t_\ell) + \mathcal{p}_{\ell-2} B\mathbb{S}^5_{\ell-2}(t_\ell) + \mathcal{p}_{\ell-1} B\mathbb{S}^5_{\ell-1}(t_\ell) + \mathcal{p}_{\ell} B\mathbb{S}^5_{\ell}(t_\ell) + \mathcal{p}_{\ell+1} B\mathbb{S}^5_{\ell+1}(t_\ell) + \mathcal{p}_{\ell+2} B\mathbb{S}^5_{\ell+2}(t_\ell) + \mathcal{p}_{\ell+3} B\mathbb{S}^5_{\ell+3}(t_\ell) \quad (1.7)$$

By shifting the quintic B−spline to the right side by m's step, mathematically meaning:

$$B\mathbb{S}^5_{\ell-m}(t_\ell) B\mathbb{S}^5_{\ell}(t_{\ell+m})$$

Then can rewrite the equation (1.7) as

$$QB(t) = \mathcal{p}_{\ell-3} B\mathbb{S}^5_{\ell}(t_{\ell+3}) + \mathcal{p}_{\ell-2} B\mathbb{S}^5_{\ell}(t_{\ell+2}) + \mathcal{p}_{\ell-1} B\mathbb{S}^5_{\ell}(t_{\ell+1}) + \mathcal{p}_{\ell} B\mathbb{S}^5_{\ell}(t_\ell) + \mathcal{p}_{\ell+1} B\mathbb{S}^5_{\ell}(t_{\ell-1}) + \mathcal{p}_{\ell+2} B\mathbb{S}^5_{\ell}(t_{\ell-2}) + \mathcal{p}_{\ell+3} B\mathbb{S}^5_{\ell}(t_{\ell-3}) \quad (1.8)$$

Similarly, we can rewrite the equation (1.4), (1.5), (1.6) as following

$$\frac{d}{dt} QB(t) = \mathcal{p}_{\ell-3} \frac{d}{dt} B\mathbb{S}^5_{\ell}(t_{\ell+3}) + \mathcal{p}_{\ell-2} \frac{d}{dt} B\mathbb{S}^5_{\ell}(t_{\ell+2}) + \mathcal{p}_{\ell-1} \frac{d}{dt} B\mathbb{S}^5_{\ell}(t_{\ell+1}) + \mathcal{p}_{\ell} \frac{d}{dt} B\mathbb{S}^5_{\ell}(t_\ell) + \mathcal{p}_{\ell+1} \frac{d}{dt} B\mathbb{S}^5_{\ell}(t_{\ell-1}) + \mathcal{p}_{\ell+2} \frac{d}{dt} B\mathbb{S}^5_{\ell}(t_{\ell-2}) + \mathcal{p}_{\ell+3} \frac{d}{dt} B\mathbb{S}^5_{\ell}(t_{\ell-3}) \quad (1.9)$$

$$\frac{d^2}{dt^2} QB(t) = \mathcal{p}_{\ell-3} \frac{d^2}{dt^2} B\mathbb{S}^5_{\ell}(t_{\ell+3}) + \mathcal{p}_{\ell-2} \frac{d^2}{dt^2} B\mathbb{S}^5_{\ell}(t_{\ell+2}) + \mathcal{p}_{\ell-1} \frac{d^2}{dt^2} B\mathbb{S}^5_{\ell}(t_{\ell+1}) + \mathcal{p}_{\ell} \frac{d^2}{dt^2} B\mathbb{S}^5_{\ell}(t_\ell) + \mathcal{p}_{\ell+1} \frac{d^2}{dt^2} B\mathbb{S}^5_{\ell}(t_{\ell-1}) + \mathcal{p}_{\ell+2} \frac{d^2}{dt^2} B\mathbb{S}^5_{\ell}(t_{\ell-2}) + \mathcal{p}_{\ell+3} \frac{d^2}{dt^2} B\mathbb{S}^5_{\ell}(t_{\ell-3})$$

(1.10)

$$\frac{d^3}{dt^3} QB(t) = \mathcal{p}_{\ell-3} \frac{d^3}{dt^3} B\mathbb{S}^5_{\ell}(t_{\ell+3}) + \mathcal{p}_{\ell-2} \frac{d^3}{dt^3} B\mathbb{S}^5_{\ell}(t_{\ell+2}) + \mathcal{p}_{\ell-1} \frac{d^3}{dt^3} B\mathbb{S}^5_{\ell}(t_{\ell+1}) + \mathcal{p}_{\ell} \frac{d^3}{dt^3} B\mathbb{S}^5_{\ell}(t_\ell) + \mathcal{p}_{\ell+1} \frac{d^3}{dt^3} B\mathbb{S}^5_{\ell}(t_{\ell-1}) + \mathcal{p}_{\ell+2} \frac{d^3}{dt^3} B\mathbb{S}^5_{\ell}(t_{\ell-2}) + \mathcal{p}_{\ell+3} \frac{d^3}{dt^3} B\mathbb{S}^5_{\ell}(t_{\ell-3})$$

(1.11)

$$\frac{d^4}{dt^4} QB(t) = \mathcal{p}_{\ell-3} \frac{d^4}{dt^4} B\mathbb{S}^5_{\ell}(t_{\ell+3}) + \mathcal{p}_{\ell-2} \frac{d^4}{dt^4} B\mathbb{S}^5_{\ell}(t_{\ell+2}) + \mathcal{p}_{\ell-1} \frac{d^4}{dt^4} B\mathbb{S}^5_{\ell}(t_{\ell+1}) + \mathcal{p}_{\ell} \frac{d^4}{dt^4} B\mathbb{S}^5_{\ell}(t_\ell) + \mathcal{p}_{\ell+1} \frac{d^4}{dt^4} B\mathbb{S}^5_{\ell}(t_{\ell-1}) + \mathcal{p}_{\ell+2} \frac{d^4}{dt^4} B\mathbb{S}^5_{\ell}(t_{\ell-2}) + \mathcal{p}_{\ell+3} \frac{d^4}{dt^4} B\mathbb{S}^5_{\ell}(t_{\ell-3})$$

(1.12)

The following equations are formulated, by substituting the value of $B\mathbb{S}_\ell^5(t)$ at the Knots from table (1.1):

$$QB(t) = \wp_{\ell-2} + 26\wp_{\ell-1} + 66\wp_\ell + 26\wp_{\ell+1} + \wp_{\ell+2} \quad (1.13)$$

$$\frac{d}{dt}QB(t) = -\frac{5}{h}\wp_{\ell-2} - \frac{55}{h}\wp_{\ell-1} + \frac{55}{h}\wp_{\ell+1} + \frac{5}{h}\wp_{\ell+2} \quad (1.14)$$

$$\frac{d^2}{dt^2}QB(t) = \frac{20}{h^2}\wp_{\ell-2} + \frac{40}{h^2}\wp_{\ell-1} - \frac{120}{h^2}\wp_\ell + \frac{40}{h^2}\wp_{\ell+1} + \frac{20}{h^2}\wp_{\ell+2} \quad (1.15)$$

$$\frac{d^3}{dt^3}QB(t) = -\frac{60}{h^3}\wp_{\ell-2} + \frac{120}{h^3}\wp_{\ell-1} - \frac{120}{h^3}\wp_{\ell+1} + \frac{60}{h^3}\wp_{\ell+2} \quad (1.16)$$

$$\frac{d^4}{dt^4}QB(t) = \frac{120}{h^4}\wp_{\ell-2} - \frac{480}{h^4}\wp_{\ell-1} + \frac{720}{h^4}\wp_\ell - \frac{480}{h^4}\wp_{\ell+1} + \frac{120}{h^4}\wp_{\ell+2} \quad (1.17)$$

3. Description of the Method:

In this section, we study the use of Quintic B−splines to solve the system of first and second−order multi−type Fredholm integro−differential equations of the second kind.

$$\frac{d^4}{dt^4}U_i(t) + \mathcal{F}_{i3}(t)\frac{d^3}{dt^3}U_i(t) + \mathcal{F}_{i2}(t)\frac{d^2}{dt^2}U_i(t) + \mathcal{F}_{i1}(t)\frac{d}{dt}U_i(t) + \mathcal{F}_{i0}(t)U_i(t)$$
$$= \mathcal{G}_i(t) + \mathcal{P}U_i(t)\,, \quad i = 1,2,\ldots,m \quad (1.18)$$

where

$$\mathcal{P}U_i(t) = \sum_{j=1}^{m}\int_0^b \mathcal{K}_{ij}(t,x)\mathcal{V}(U_j(x))dt\,,\ i = 1,2,\ldots,m\,,\ t \in [0,1]$$

With the initial conditions:

$$\left.\begin{aligned} \frac{d^4}{dt^4}U_i(t_0) &= U_{i0}^4 \\ \frac{d^3}{dt^3}U_i(t_0) &= U_{i0}^3 \\ \frac{d^2}{dt^2}U_i(t_0) &= U_{i0}^2 \\ \frac{d}{dt}U_i(t_0) &= U_{i0}^1 \\ U_i(t_0) &= U_{i0} \end{aligned}\right\}$$

(1.19)

where $U_i(t)$ are unknown functions, $\frac{d^4}{dt^4}U_i(t)$, $\frac{d^3}{dt^3}U_i(t)$, $\frac{d^2}{dt^2}U_i(t)$, $\frac{d}{dt}U_i(t)$ are the derivative of unknown function, Where $\mathcal{V}(U_j(x))$ is a nonlinear function of $U_j(x)$, the functions $\mathcal{G}_i(x)$, $i = 1, \ldots, m$, $\mathcal{F}_{i3}(x)$, $\mathcal{F}_{i2}(x)$, $\mathcal{F}_{i1}(x)$, $\mathcal{F}_{i0}(x)$ and kernels $\mathcal{K}_{ij}(t,x),\ 1 \le i,j \le m$ These are real–valued functions defined on subsets of $\mathcal{R}^3\ and\ \mathcal{R}^1$, respectively.

We assume equally spaced knots, i.e., $h = t_{\ell+1} - t_\ell$. Let

$$U_i(t) = QB_i(t) = \mathcal{p}_{i\ell-2} + 26\mathcal{p}_{i\ell-1} + 66\mathcal{p}_{i\ell} + 26\mathcal{p}_{i\ell+1} + \mathcal{p}_{i\ell+2} \tag{1.20}$$

$$\frac{d}{dt}U_i(t) = \frac{d}{dt}QB_i(t) = -\frac{5}{h}\mathcal{p}_{i\ell-2} - \frac{55}{h}\mathcal{p}_{i\ell-1} + \frac{55}{h}\mathcal{p}_{i\ell+1} + \frac{5}{h}\mathcal{p}_{i\ell+2} \tag{1.21}$$

$$\frac{d^2}{dt^2}U_i(t) = \frac{d^2}{dt^2}QB_i(t) = \frac{20}{h^2}\mathcal{p}_{i\ell-2} + \frac{40}{h^2}\mathcal{p}_{i\ell-1} - \frac{120}{h^2}\mathcal{p}_{i\ell} + \frac{40}{h^2}\mathcal{p}_{i\ell+1} + \frac{20}{h^2}\mathcal{p}_{i\ell+2} \tag{1.22}$$

$$\frac{d^3}{dt^3}U_i(t) = \frac{d^3}{dt^3}QB_i(t) = -\frac{60}{h^3}\mathcal{p}_{i\ell-2} + \frac{120}{h^3}\mathcal{p}_{i\ell-1} - \frac{120}{h^3}\mathcal{p}_{i\ell+1} + \frac{60}{h^3}\mathcal{p}_{i\ell+2} \tag{1.23}$$

$$\frac{d^4}{dt^4}U_i(t) = \frac{d^4}{dt^4}QB_i(t)) = \frac{120}{h^4}\mathcal{p}_{i\ell-2} - \frac{480}{h^4}\mathcal{p}_{i\ell-1} + \frac{720}{h^4}\mathcal{p}_{i\ell} - \frac{480}{h^4}\mathcal{p}_{i\ell+1} + \frac{120}{h^4}\mathcal{p}_{i\ell+2} \tag{1.24}$$

be the approximating function, It is required that (1.20)–(1.24) satisfies our the system of first and second–order multi–type Fredholm integro–differential equations of the second kind (1.18) and (1.19) at $t = t_i$.

where t_i is an interior point. That is

$$\frac{d^4}{dt^4}QB_i(t) + \mathcal{F}_{i3}(t)\frac{d^3}{dt^3}QB_i(t) + \mathcal{F}_{i2}(t)\frac{d^2}{dt^2}QB_i(t) + \mathcal{F}_{i1}(t)\frac{d}{dt}QB_i(t) + \mathcal{F}_{i0}(t)QB_i(t) = \mathcal{G}_i(t) + \sum_{j=1}^{m}\int_0^b \mathcal{K}_{ij}(t,x)\mathcal{V}(QB_j(x))dt \tag{1.25}$$

i.e.

$$\frac{d^4}{dt^4}QB_1(t) + \mathcal{F}_{13}(t)\frac{d^3}{dt^3}QB_1(t) + \mathcal{F}_{12}(t)\frac{d^2}{dt^2}QB_1(t) + \mathcal{F}_{11}(t)\frac{d}{dt}QB_1(t) + \mathcal{F}_{10}(t)QB_1(t) = \mathcal{G}_1(t) + \sum_{j=1}^{m}\int_0^b \mathcal{K}_{1j}(t,x)\mathcal{V}(QB_j(x))dt \tag{1.26}$$

$$\frac{d^4}{dt^4}QB_2(t) + \mathcal{F}_{23}(t)\frac{d^3}{dt^3}QB_2(t) + \mathcal{F}_{22}(t)\frac{d^2}{dt^2}QB_2(t) + \mathcal{F}_{21}(t)\frac{d}{dt}QB_2(t) + \mathcal{F}_{20}(t)QB_2(t) = \mathcal{G}_2(t) + \sum_{j=1}^{m}\int_0^b \mathcal{K}_{2j}(t,x)\mathcal{V}(QB_j(x))dt \tag{1.27}$$

$$\vdots$$

$$\frac{d^4}{dt^4}QB_n(t) + \mathcal{F}_{n3}(t)\frac{d^3}{dt^3}QB_n(t) + \mathcal{F}_{n2}(t)\frac{d^2}{dt^2}QB_n(t) + \mathcal{F}_{n1}(t)\frac{d}{dt}QB_n(t) + \mathcal{F}_{n0}(t)QB_n(t) = \mathcal{G}_n(t) + \sum_{j=1}^{m}\int_0^b \mathcal{K}_{nj}(t,x)\mathcal{V}(QB_j(x))dt \tag{1.28}$$

B using the initial conditions (1.19), we get the following

$$\mathcal{p}_{i\ell-2} + 26\mathcal{p}_{i\ell-1} + 66\mathcal{p}_{i\ell} + 26\mathcal{p}_{i\ell+1} + \mathcal{p}_{i\ell+2} = U_{i0}$$
$$-\frac{5}{h}\mathcal{p}_{i\ell-2} - \frac{55}{h}\mathcal{p}_{i\ell-1} + \frac{55}{h}\mathcal{p}_{i\ell+1} + \frac{5}{h}\mathcal{p}_{i\ell+2} = U_{i0}^{1}$$
$$\frac{20}{h^2}\mathcal{p}_{i\ell-2} + \frac{40}{h^2}\mathcal{p}_{i\ell-1} - \frac{120}{h^2}\mathcal{p}_{i\ell} + \frac{40}{h^2}\mathcal{p}_{i\ell+1} + \frac{20}{h^2}\mathcal{p}_{i\ell+2} = U_{i0}^{2}$$
$$-\frac{60}{h^3}\mathcal{p}_{i\ell-2} + \frac{120}{h^3}\mathcal{p}_{i\ell-1} - \frac{120}{h^3}\mathcal{p}_{i\ell+1} + \frac{60}{h^3}\mathcal{p}_{i\ell+2} = U_{i0}^{3}$$
$$\frac{120}{h^4}\mathcal{p}_{i\ell-2} - \frac{480}{h^4}\mathcal{p}_{i\ell-1} + \frac{720}{h^4}\mathcal{p}_{i\ell} - \frac{480}{h^4}\mathcal{p}_{i\ell+1} + \frac{120}{h^4}\mathcal{p}_{i\ell+2} = U_{i0}^{4}$$

We can write the above system as the matrix

$$AP = U$$

(1.29)

Where

$$A = \begin{bmatrix} 1 & 26 & 66 & 26 & 1 \\ -5 & -55 & 0 & 55 & 5 \\ 20 & 40 & -120 & 40 & 20 \\ -60 & 120 & 0 & -120 & 60 \\ 120 & -480 & 720 & -480 & 120 \end{bmatrix} \quad P = \begin{bmatrix} \mathcal{p}_{i\ell-2} \\ \mathcal{p}_{i\ell-1} \\ \mathcal{p}_{i\ell} \\ \mathcal{p}_{i\ell+1} \\ \mathcal{p}_{i\ell+2} \end{bmatrix} \quad U = \begin{bmatrix} U_{i0} \\ hU_{i0}^{1} \\ h^2U_{i0}^{2} \\ h^3U_{i0}^{3} \\ h^4U_{i0}^{4} \end{bmatrix}$$

And use LU matrix factorization to solve this system to evaluate the value of the coefficients $\mathcal{p}_{i\ell-2}, \mathcal{p}_{i\ell-1}, \mathcal{p}_{i\ell}, \mathcal{p}_{i\ell+1}, \mathcal{p}_{i\ell+2}$ at $t = t_0 = 0$

And use the equations $(1.25)-(1.28)$ to find the value of the coefficients $\mathcal{p}_{i\ell-1}$, $\mathcal{p}_{i\ell}, \mathcal{p}_{i\ell+1}, \mathcal{p}_{i\ell+2}$ at $t = t_1, t_2, \ldots, t_n$.

and the approximate solution $U_i, i = 1,2,3,\ldots,n$ can be found from

$$U_i(t) = \sum_{e=-3}^{+3} \mathcal{p}_e B\mathbb{S}_e^5(t) .$$

4. Numerical Methods

In this section, we address three examples of the second type of nonlinear system of multi-type Fredholm integro-differential equations using a Quintic B-splines method. To analyze the numerical performance of the given method, we use two error measurements, that is, the maximum absolute error L_∞ and $L.S.E.$ error norm which are defined by

$$L_\infty = \|U(exact) - U(approximate)\|_\infty$$
$$= \max_i |U_i(exact) - U_i(approximate)|$$

$L.S.E. = \sum_{i=1}^{m}(U_i(exact) - U_i(approximate))^2$

Example (1):

$$\left.\begin{aligned} u'(t) + 3u(t) &= 3t^2 - \frac{31}{15}t - \frac{11}{6} + \int_0^1 (t+y)\,[u^2(y) + v^2(y)]dy \\ v'(t) + 2v(t) &= \frac{32}{15}t^2 + 4t + \frac{11}{12} + \int_0^1 (t^2 - y)\,[u(y)v(y)]dy \end{aligned}\right\} \quad (1.30)$$

where $\quad u(0) = 0, v(0) = 0 \quad (1.31)$

The exact solution $\quad u(t) = t^2 - t \quad$ and $\quad v(x) = t^2 + t$

Suppose that

$$u(t) = QB_1(t) = \wp_{1,\ell-2} + 26\wp_{1,\ell-1} + 66\wp_{1,\ell} + 26\wp_{1,\ell+1} + \wp_{1,\ell+2} \quad (1.32)$$

$$\frac{d}{dt}u(t) = \frac{d}{dt}QB_1(t) = -\frac{5}{h}\wp_{1,\ell-2} - \frac{55}{h}\wp_{1,\ell-1} + \frac{55}{h}\wp_{1,\ell+1} + \frac{5}{h}\wp_{1,\ell+2} \quad (1.33)$$

$$v(t) = QB_2(t) = \wp_{2,\ell-2} + 26\wp_{2,\ell-1} + 66\wp_{2,\ell} + 26\wp_{2,\ell+1} + \wp_{2,\ell+2} \quad (1.34)$$

$$\frac{d}{dt}v(t) = \frac{d}{dt}QB_2(t) = -\frac{5}{h}\wp_{2,\ell-2} - \frac{55}{h}\wp_{2,\ell-1} + \frac{55}{h}\wp_{2,\ell+1} + \frac{5}{h}\wp_{2,\ell+2} \quad (1.35)$$

$$u^2(t) = (QB_1(t))^2 = \left(\wp_{1,\ell-2} + 26\wp_{1,\ell-1} + 66\wp_{1,\ell} + 26\wp_{1,\ell+1} + \wp_{1,\ell+2}\right)^2 \quad (1.36)$$

$$v^2(t) = (QB_2(t))^2 = \left(\wp_{2,\ell-2} + 26\wp_{2,\ell-1} + 66\wp_{2,\ell} + 26\wp_{2,\ell+1} + \wp_{2,\ell+2}\right)^2 \quad (1.37)$$

And $\quad \int_0^1 (t+y)\,dy = t + \frac{1}{2} \;,\quad \int_0^1 (t^2 - y)\,dy = t^2 - \frac{1}{2}$

Substation the equations (1.32) $-(1.37)$ in to system (1.30), we obtain

$$-\frac{5}{h}\wp_{1,\ell-2} - \frac{55}{h}\wp_{1,\ell-1} + \frac{55}{h}\wp_{1,\ell+1} + \frac{5}{h}\wp_{1,\ell+2} + 3(\wp_{1,\ell-2} + 26\wp_{1,\ell-1} + 66\wp_{1,\ell} + 26\wp_{1,\ell+1} + \wp_{1,\ell+2}) = 3t^2 - \frac{31}{15}t - \frac{11}{6} + \left(t + \frac{1}{2}\right)\left(\left(\wp_{1,\ell-2} + 26\wp_{1,\ell-1} + 66\wp_{1,\ell} + 26\wp_{1,\ell+1} + \wp_{1,\ell+2}\right)^2 \left(\wp_{2,\ell-2} + 26\wp_{2,\ell-1} + 66\wp_{2,\ell} + 26\wp_{2,\ell+1} + \wp_{2,\ell+2}\right)^2\right)$$

(1.38)

$-\frac{5}{h}p_{2,\ell-2}-\frac{55}{h}p_{2,\ell-1}+\frac{55}{h}p_{2,\ell+1}+\frac{5}{h}p_{2,\ell+2}+2(p_{2,\ell-2}+26p_{2,\ell-1}+66p_{2,\ell}+26p_{2,\ell+1}+p_{2,\ell+2})=\frac{32}{15}t^2+4t+\frac{11}{12}+(t^2-\frac{1}{2})(p_{1,\ell-2}+26p_{1,\ell-1}+66p_{1,\ell}+26p_{1,\ell+1}+p_{1,\ell+2})(p_{2,\ell-2}+26p_{2,\ell-1}+66p_{2,\ell}+26p_{2,\ell+1}+p_{2,\ell+2})$

(1.39)

We rewrite the equations (1.38),(1.39) as the system of matrix, and use LU matrix factorization to solve this system to evaluate the value of the coefficients $p_{i\ell-2}, p_{i\ell-1}, p_{i\ell}, p_{i\ell+1}, p_{i\ell+2}$ at $t=t_0,t_1,\dots,t_{10}$, where $i=1,2$ and the approximate solution $u(t)$ and $v(t)$ can be found from

$u(t)=\sum_{e=-3}^{+3}p_{1,e}B\mathbb{S}_e^5(t)$ and $v(t)=\sum_{e=-3}^{+3}p_{2,e}B\mathbb{S}_e^5(t)$

Table (1.1) displays a comparison between the theoretical and numerical results obtained using QBS for $u(t)$ in example 1, based on the least square error with h=0.1.

T	Exact	QBS	Error(L_∞)
0.000000000000000	0.000000000000000	0.000000000000000	0.000000000000000
0.100000000000000	-0.090000000000000	-0.090132114993877	0.000132114993877
0.200000000000000	-0.160000000000000	-0.159431408530056	0.000568591469944
0.300000000000000	-0.210000000000000	-0.210800614669086	0.000800614669086
0.400000000000000	-0.240000000000000	-0.239746786881128	0.000253213118872
0.500000000000000	-0.250000000000000	-0.250226656277407	0.000226656277407
0.600000000000000	-0.240000000000000	-0.239622362429794	0.000377637570206
0.700000000000000	-0.210000000000000	-0.209066242146599	0.000933757853401
0.800000000000000	-0.160000000000000	-0.159176289356898	0.000823710643102
0.900000000000000	-0.090000000000000	-0.090255344092533	0.000255344092533
1.000000000000000	0.000000000000000	-0.000418721162904	0.000418721162904
L.S.E	3.030765535946593e-006		

Table (1.2) displays a comparison between the theoretical and numerical results obtained using QBS for $v(t)$ in example 1, based on the least square error with h=0.1.

T	Exact	QBS	Error(L_∞)
0.000000000000000	0.000000000000000	0.000000000000000	0.000000000000000
0.100000000000000	0.110000000000000	0.110808583826749	0.000808583826749
0.200000000000000	0.240000000000000	0.239708009140380	0.000291990859620
0.300000000000000	0.390000000000000	0.390990917371084	0.000990917371084
0.400000000000000	0.560000000000000	0.560889732752114	0.000889732752114

0.500000000000000	0.750000000000000	0.749860377538571	0.000139622461429
0.600000000000000	0.960000000000000	0.959888259874967	0.000111740125033
0.700000000000000	1.190000000000000	1.189601614041920	0.000398385958080
0.800000000000000	1.440000000000000	1.439436750659063	0.000563249340937
0.900000000000000	1.710000000000000	1.709732509734401	0.000267490265599
1.000000000000000	2.000000000000000	1.999991161087142	0.000008838912858
L.S.E.	3.092178720991963e-006		

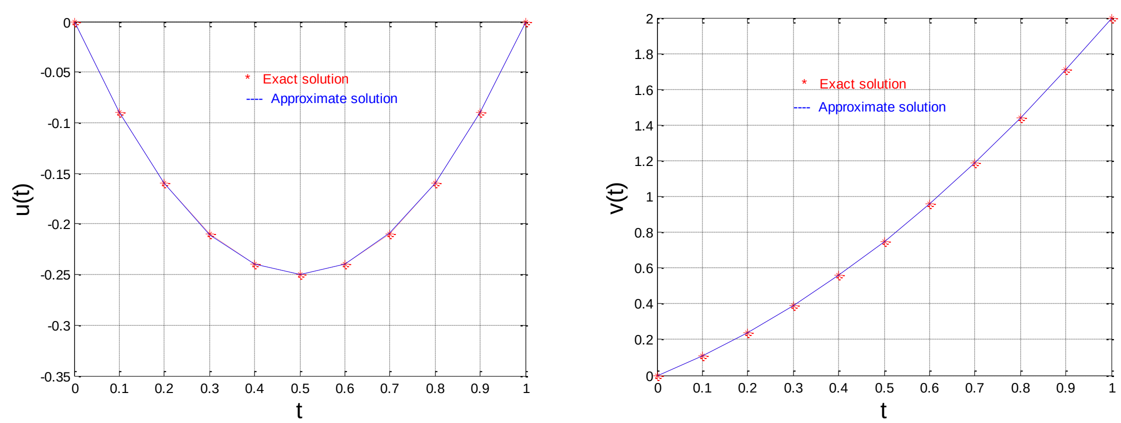

Fig.(1.1) displays a comparison between the exact and numerical solutions obtained using QBS for $u(t)$ and $v(t)$ in example 1, based on the least square error with h=0.1

Example (2)

Consider the following system of multi−type three nonlinear Fredholm integro−differential equations of the second kind.

$$\left.\begin{aligned} u'(t) + t^2u(t) &= (t^2+1)e^t - e^{(t+1)} + \int_0^1 \left[e^{(t-3y)}v^2(y) + e^{(t-6y)}w^2(y)\right] dy \\ v'(t) + tv(t) &= (t+2)e^{2t} - 2e^t + \int_0^1 \left[e^{(t-6y)}w^2(y) + e^{(t-2y)}u^2(y)\right] dy \\ w'(t) + 2tw(t) &= (2t+3)e^{3t} - 2e^t + \int_0^1 \left[e^{(t-2y)}u^2(y) + e^{(t-4y)}v^2(y)\right] dy \end{aligned}\right\} \quad (1.40)$$

where $u(0) = 1, v(0) = 1, w(0) = 1$ (1.41)

The exact solution are $u(t) = e^t$, $v(t) = e^{2t}$ and $w(t) = e^{3t}$

Suppose that

$$u(t) = QB_1(t) = p_{1,\ell-2} + 26p_{1,\ell-1} + 66p_{1,\ell} + 26p_{1,\ell+1} + p_{1,\ell+2} \quad (1.42)$$

$$\frac{d}{dt}u(t) = \frac{d}{dt}QB_1(t) = -\frac{5}{h}p_{1,\ell-2} - \frac{55}{h}p_{1,\ell-1} + \frac{55}{h}p_{1,\ell+1} + \frac{5}{h}p_{1,\ell+2} \quad (1.43)$$

$$v(t) = QB_2(t) = p_{2,\ell-2} + 26p_{2,\ell-1} + 66p_{2,\ell} + 26p_{2,\ell+1} + p_{2,\ell+2} \quad (1.44)$$

$$\frac{d}{dt}v(t) = \frac{d}{dt}QB_2(t) = -\frac{5}{h}p_{2,\ell-2} - \frac{55}{h}p_{2,\ell-1} + \frac{55}{h}p_{2,\ell+1} + \frac{5}{h}p_{2,\ell+2} \quad (1.45)$$

$$w(t) = QB_3(t) = p_{3,\ell-2} + 26p_{3,\ell-1} + 66p_{3,\ell} + 26p_{3,\ell+1} + p_{3,\ell+2} \quad (1.46)$$

$$\frac{d}{dt}w(t) = \frac{d}{dt}QB_3(t) = -\frac{5}{h}p_{3,\ell-2} - \frac{55}{h}p_{3,\ell-1} + \frac{55}{h}p_{3,\ell+1} + \frac{5}{h}p_{3,\ell+2} \quad (1.47)$$

$$u^2(t) = (QB_1(t))^2 = \left(p_{1,\ell-2} + 26p_{1,\ell-1} + 66p_{1,\ell} + 26p_{1,\ell+1} + p_{1,\ell+2}\right)^2 \quad (1.48)$$

$$v^2(t) = (QB_2(t))^2 = \left(p_{2,\ell-2} + 26p_{2,\ell-1} + 66p_{2,\ell} + 26p_{2,\ell+1} + p_{2,\ell+2}\right)^2 \quad (1.49)$$

$$w^2(t) = (QB_3(t))^2 = \left(p_{3,\ell-2} + 26p_{3,\ell-1} + 66p_{3,\ell} + 26p_{3,\ell+1} + p_{3,\ell+2}\right)^2 \quad (1.50)$$

And $\int_0^1 e^{(t-2y)}\,dy = \frac{1}{2}(e^t - e^{t-2})$, $\int_0^1 e^{(t-3y)}\,dy = \frac{1}{3}(e^t - e^{t-3})$, $\int_0^1 e^{(t-4y)}\,dy = \frac{1}{4}(e^t - e^{t-4})$, and $\int_0^1 e^{(t-6y)}\,dy = \frac{1}{6}(e^t - e^{t-6})$

Substation the equations (1.42) $-(1.50)$ in to system (1.40), we obtain

$$-\frac{5}{h}p_{1,\ell-2} - \frac{55}{h}p_{1,\ell-1} + \frac{55}{h}p_{1,\ell+1} + \frac{5}{h}p_{1,\ell+2} + t^2(= p_{1,\ell-2} + 26p_{1,\ell-1} + 66p_{1,\ell} + 26p_{1,\ell+1} + p_{1,\ell+2}) = (t^2+1)e^t - e^{(t+1)} + \frac{1}{3}(e^t - e^{t-3})\left(\left(p_{2,\ell-2} + 26p_{2,\ell-1} + 66p_{2,\ell} + 26p_{2,\ell+1} + p_{2,\ell+2}\right)^2\right) + \frac{1}{6}(e^t - e^{t-6})\left(\left(p_{3,\ell-2} + 26p_{3,\ell-1} + 66p_{3,\ell} + 26p_{3,\ell+1} + p_{3,\ell+2}\right)^2\right) \quad (1.51)$$

$$p_{2,\ell-2} + 26p_{2,\ell-1} + 66p_{2,\ell} + 26p_{2,\ell+1} + p_{2,\ell+2} + t\left(-\frac{5}{h}p_{2,\ell-2} - \frac{55}{h}p_{2,\ell-1} + \frac{55}{h}p_{2,\ell+1} + \frac{5}{h}p_{2,\ell+2}\right) = (t+2)e^{2t} - 2e^t + \frac{1}{3}(e^t - e^{t-3})\left(\left(p_{2,\ell-2} + 26p_{2,\ell-1} + 66p_{2,\ell} + 26p_{2,\ell+1} + p_{2,\ell+2}\right)^2\right) + \frac{1}{2}(e^t - e^{t-2})\left(\left(p_{1,\ell-2} + 26p_{1,\ell-1} + 66p_{1,\ell} + 26p_{1,\ell+1} + p_{1,\ell+2}\right)^2\right) \quad (1.52)$$

$\mathcal{p}_{3,\ell-2} + 26\mathcal{p}_{3,\ell-1} + 66\mathcal{p}_{3,\ell} + 26\mathcal{p}_{3,\ell+1} + \mathcal{p}_{3,\ell+2} + 2t\left(-\frac{5}{h}\mathcal{p}_{3,\ell-2} - \frac{55}{h}\mathcal{p}_{3,\ell-1} + \frac{55}{h}\mathcal{p}_{3,\ell+1} + \frac{5}{h}\mathcal{p}_{3,\ell+2}\right) = (2t+3)e^{3t} - 2e^{t} + \frac{1}{2}(e^{t} - e^{t-2})\left((\mathcal{p}_{1,\ell-2} + 26\mathcal{p}_{1,\ell-1} + 66\mathcal{p}_{1,\ell} + 26\mathcal{p}_{1,\ell+1} + \mathcal{p}_{1,\ell+2})^2\right) + \frac{1}{4}(e^{t} - e^{t-4})\left((\mathcal{p}_{2,\ell-2} + 26\mathcal{p}_{2,\ell-1} + 66\mathcal{p}_{2,\ell} + 26\mathcal{p}_{2,\ell+1} + \mathcal{p}_{2,\ell+2})^2\right)$

(1.53)

We rewrite the equations (1.51),(1.52), and (1.53) as the system of matrix, and use LU matrix factorization to solve this system to evaluate the value of the coefficients $\mathcal{p}_{i\ell-2}, \mathcal{p}_{i\ell-1}, \mathcal{p}_{i\ell}, \mathcal{p}_{i\ell+1}, \mathcal{p}_{i\ell+2}$ at $t = t_0, t_1, \ldots, t_{10}$, where $i = 1,2,3$

and the approximate solution $u(t), v(t)$ and $w(t)$ can be found from

$$u(t) = \sum_{e=-3}^{+3} \mathcal{p}_{1,e} B\mathbb{S}_e^5(t)\ ,\ \ v(t) = \sum_{e=-3}^{+3} \mathcal{p}_{2,e} B\mathbb{S}_e^5(t),$$

And $$w(t) = \sum_{e=-3}^{+3} \mathcal{p}_{3,e} B\mathbb{S}_e^5(t)$$

Table (1.3) displays a comparison between the theoretical and numerical results obtained using QBS for $u(t)$ in example 2, based on the least square error with h=0.1.

T	Exact	QBS	Error(L_∞)
0.000000000000000	**1.000000000000000**	**1.000000000000000**	**0.000000000000000**
0.100000000000000	**1.105170918075648**	**1.104900957561066**	**0.000269960514582**
0.200000000000000	**1.221402758160170**	**1.222125206739247**	**0.000722448579077**
0.300000000000000	**1.349858807576003**	**1.350539390043863**	**0.000680582467860**
0.400000000000000	**1.491824697641270**	**1.492437774258060**	**0.000613076616790**
0.500000000000000	**1.648721270700128**	**1.648381658786630**	**0.000339611913498**
0.600000000000000	**1.822118800390509**	**1.820439905729760**	**0.001678894660749**
0.700000000000000	**2.013752707470477**	**2.017347962194445**	**0.003595254723968**
0.800000000000000	**2.225540928492468**	**2.223355111546455**	**0.002185816946012**
0.900000000000000	**2.459603111156950**	**2.461017574917845**	**0.001414463760895**
1.000000000000000	**2.718281828459046**	**2.717811462129567**	**0.000470366329478**
L.S.E.	**2.429349406261739e-005**		

Table (1.4) displays a comparison between the theoretical and numerical results obtained using QBS for $v(t)$ in example 2, based on the least square error with h=0.1.

T	Exact	QSB	Error(L_∞)
0.000000000000000	**1.000000000000000**	**1.000000000000000**	**0.000000000000000**

0.100000000000000	1.221402758160170	1.221161823831211	0.000240934328959
0.200000000000000	1.491824697641270	1.491745850755535	0.000078846885736
0.300000000000000	1.822118800390509	1.821572806401336	0.000545993989173
0.400000000000000	2.225540928492468	2.225052017055391	0.000488911437077
0.500000000000000	2.718281828459046	2.718816030039497	0.000534201580451
0.600000000000000	3.320116922736547	3.319632060587300	0.000484862149247
0.700000000000000	4.055199966844675	4.054557695600595	0.000642271244080
0.800000000000000	4.946032424395115	4.945279966426286	0.000752457968829
0.900000000000000	6.049647464412947	6.048318518614160	0.001328945798787
1.000000000000000	7.389056098930650	7.387994461123630	0.001061637807013
L.S.E.	4.993749759327024e-006		

Table (1.5) displays a comparison between the theoretical and numerical results obtained using QBS for $w(t)$ in example 2, based on the least square error with h=0.1.

T	Exact	QSB	Error(L_∞)
0.000000000000000	1.000000000000000	1.000000000000000	0.000000000000000
0.100000000000000	1.349858807576003	1.349189511673419	0.000669295902584
0.200000000000000	1.822118800390509	1.821181422992235	0.000937377398274
0.300000000000000	2.459603111156949	2.458607905325421	0.000995205831528
0.400000000000000	3.320116922736548	3.320381755679806	0.000264832943257
0.500000000000000	4.481689070338065	4.481350878900778	0.000338191437287
0.600000000000000	6.049647464412945	6.049296683322290	0.000350781090655
0.700000000000000	8.166169912567646	8.165421823233722	0.000748089333925
0.800000000000000	11.023176380641605	11.023457084168742	0.000280703527138
0.900000000000000	14.879731724872837	14.876492940363732	0.003238784509104
1.000000000000000	20.085536923187668	20.094819415426169	0.009282492238501
L.S.E.	9.991744472469092e-005		

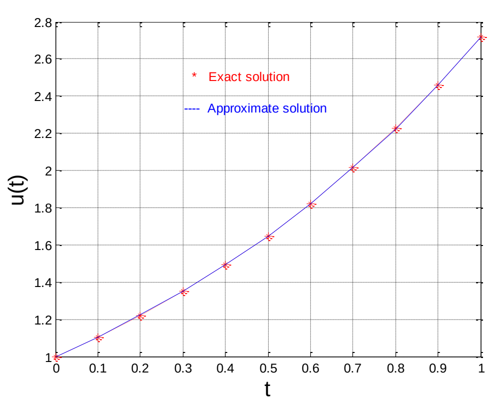

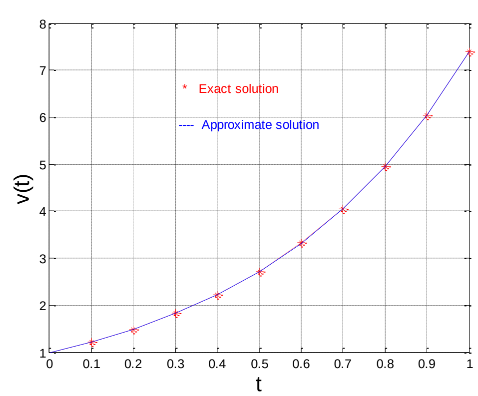

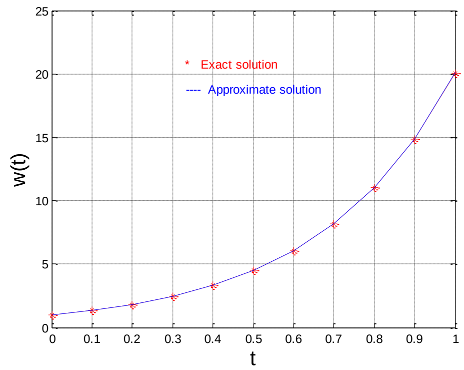

Fig.(1.2) displays a comparison between the exact and numerical solutions obtained using QBS for $u(t), v(t),$ and $w(t)$ in example 2, based on the least square error with h=0.1

Example (3):

Consider the following system of multi−type two nonlinear Fredholm integro−differential equations of the second kind.

$$\left.\begin{aligned} u''(t) + u'(t) + tu(t) &= tcos(t) + (t-6)sin(t) + \int_0^{\pi} cos(t-y)[u^2(y) + v^2(y)]dy \\ v''(t) + v'(t) + 3v(t) &= 5cos(t) - 3sin(t) + \int_0^{\pi} sin(t-y)[u^2(y) + v^2(y)]dy \end{aligned}\right\} \quad (1.54)$$

where $u(0) = 1, u'(0) = 1, v(0) = 1, v'(0) = -1$ (1.55)

The exact solution are $u(t) = cos(t) + sin(t)$ and $v(t) = cos(t) - sin(t)$

$$u(t) = QB_1(t) = p_{1,\ell-2} + 26p_{1,\ell-1} + 66p_{1,\ell} + 26p_{1,\ell+1} + p_{1,\ell+2} \quad (1.56)$$

$$\frac{d}{dt}u(t) = \frac{d}{dt}QB_1(t) = -\frac{5}{h}p_{1,\ell-2} - \frac{55}{h}p_{1,\ell-1} + \frac{55}{h}p_{1,\ell+1} + \frac{5}{h}p_{1,\ell+2} \quad (1.57)$$

$$\frac{d^2}{dt^2}u(t) = \frac{d^2}{dt^2}QB_1(t) = \frac{20}{h^2}p_{1\ell-2} + \frac{40}{h^2}p_{1\ell-1} - \frac{120}{h^2}p_{1\ell} + \frac{40}{h^2}p_{1\ell+1} + \frac{20}{h^2}p_{1\ell+2} \quad (1.58)$$

$$v(t) = QB_2(t) = p_{2,\ell-2} + 26p_{2,\ell-1} + 66p_{2,\ell} + 26p_{2,\ell+1} + p_{2,\ell+2} \quad (1.59)$$

$$\frac{d}{dt}v(t) = \frac{d}{dt}QB_2(t) = -\frac{5}{h}p_{2,\ell-2} - \frac{55}{h}p_{2,\ell-1} + \frac{55}{h}p_{2,\ell+1} + \frac{5}{h}p_{2,\ell+2} \quad (1.60)$$

$$\frac{d^2}{dt^2}v(t) = \frac{d^2}{dt^2}QB_2(t) = \frac{20}{h^2}p_{2\ell-2} + \frac{40}{h^2}p_{2\ell-1} - \frac{120}{h^2}p_{2\ell} + \frac{40}{h^2}p_{2\ell+1} + \frac{20}{h^2}p_{2\ell+2} \quad (1.61)$$

$$u^2(t) = (QB_1(t))^2 = \left(p_{1,\ell-2} + 26p_{1,\ell-1} + 66p_{1,\ell} + 26p_{1,\ell+1} + p_{1,\ell+2}\right)^2$$

(1.62)

$$v^2(t) = (QB_2(t))^2 = \left(p_{2,\ell-2} + 26p_{2,\ell-1} + 66p_{2,\ell} + 26p_{2,\ell+1} + p_{2,\ell+2}\right)^2$$

(1.63)

And $\int_0^\pi \cos(t-y)\,dy = [-\sin(t-y)]_0^\pi = -sin(t-\pi) + sin(t)$

$\int_0^\pi \sin(t-y)\,dy = [\cos(t-y)]_0^\pi = cos(t-\pi) - cos(t)$

Substation the equations (1.56)−(1.63)in to system (1.54), we obtain

$$\frac{20}{h^2}p_{1\ell-2} + \frac{40}{h^2}p_{1\ell-1} - \frac{120}{h^2}p_{1\ell} + \frac{40}{h^2}p_{1\ell+1} + \frac{20}{h^2}p_{1\ell+2} - \frac{5}{h}p_{1,\ell-2} - \frac{55}{h}p_{1,\ell-1} + \frac{55}{h}p_{1,\ell+1} + \frac{5}{h}p_{1,\ell+2} + t\left(p_{1,\ell-2} + 26p_{1,\ell-1} + 66p_{1,\ell} + 26p_{1,\ell+1} + p_{1,\ell+2}\right) = tcos(t) + (t-6)sin(t) + (-sin(t-\pi) + sin(t))\left(\left(p_{1,\ell-2} + 26p_{1,\ell-1} + 66p_{1,\ell} + 26p_{1,\ell+1} + p_{1,\ell+2}\right)^2 + \left(p_{2,\ell-2} + 26p_{2,\ell-1} + 66p_{2,\ell} + 26p_{2,\ell+1} + p_{2,\ell+2}\right)^2\right)$$

(1.64)

$$\frac{20}{h^2}p_{2\ell-2} + \frac{40}{h^2}p_{2\ell-1} - \frac{120}{h^2}p_{2\ell} + \frac{40}{h^2}p_{2\ell+1} + \frac{20}{h^2}p_{2\ell+2}) - \frac{5}{h}p_{2,\ell-2} - \frac{55}{h}p_{2,\ell-1} + \frac{55}{h}p_{2,\ell+1} + \frac{5}{h}p_{2,\ell+2} + 3\left(p_{2,\ell-2} + 26p_{2,\ell-1} + 66p_{2,\ell} + 26p_{2,\ell+1} + p_{2,\ell+2}\right) = 5cos(t) - 3sin(t) + (cos(t-\pi) - cos(t))\left(\left(p_{1,\ell-2} + 26p_{1,\ell-1} + 66p_{1,\ell} + 26p_{1,\ell+1} + p_{1,\ell+2}\right)^2 + \left(p_{2,\ell-2} + 26p_{2,\ell-1} + 66p_{2,\ell} + 26p_{2,\ell+1} + p_{2,\ell+2}\right)^2\right)$$

(1.65)

We rewrite the equations (1.64) and (1.65) as the system of matrix, and use LU matrix factorization to solve this system to evaluate the value of the coefficients $p_{i\ell-2}$, $p_{i\ell-1}$, $p_{i\ell}$, $p_{i\ell+1}$, $p_{i\ell+2}$ at $t = t_0, t_1, \dots, t_{10}$, where $i = 1,2$

and the approximate solution $u(t)$ and $v(t)$ can be found from

$u(t) = \sum_{e=-3}^{+3} p_{1,e} B\mathbb{S}_e^5(t)$

and $v(t) = \sum_{e=-3}^{+3} p_{2,e} B\mathbb{S}_e^5(t)$,

Table (1.6) displays a comparison between the theoretical and numerical results obtained using QBS for $u(t)$ in example 3, based on the least square error with h=0.1.

T	Exact	QBS	Error(L_∞)
0.000000000000000	1.000000000000000	1.000000000000000	0.000000000000000
0.100000000000000	1.094837581924854	1.095225180862248	0.000387598937394
0.200000000000000	1.178735908636303	1.178236451287586	0.000499457348717
0.300000000000000	1.250856695786946	1.250585492328722	0.000271203458224
0.400000000000000	1.310479336311536	1.310378573446287	0.000100762865249
0.500000000000000	1.357008100494576	1.356978305314501	0.000029795180075
0.600000000000000	1.389978088304714	1.390126019033501	0.000147930728787
0.700000000000000	1.409059874522180	1.409314225311100	0.000254350788920
0.800000000000000	1.414062800246688	1.413961269551550	0.000101530695138
0.900000000000000	1.404936877898148	1.404893674699979	0.000043203198169
1.000000000000000	1.381773290676036	1.382470898082720	0.000697607406683
L.S.E.	1.069691719567815e-006		

Table (1.7) displays a comparison between the theoretical and numerical results obtained using QBS for $v(t)$ in example 3, based on the least square error with h=0.1.

T	Exact	QBS	Error(L_∞)
0.000000000000000	1.000000000000000	1.000000000000000	0.000000000000000
0.100000000000000	0.895170748631198	0.895198065056720	0.000027316425522
0.200000000000000	0.781397247046180	0.781456916778587	0.000059669732406
0.300000000000000	0.659816282464266	0.659866532975597	0.000050250511331
0.400000000000000	0.531642651694235	0.531681429161264	0.000038777467030
0.500000000000000	0.398157023286170	0.398146653018486	0.000010370267683
0.600000000000000	0.260693141514643	0.259878893460428	0.000814248054215
0.700000000000000	0.120624500046797	0.120751445614610	0.000126945567813
0.800000000000000	-0.020649381552357	-0.020555383172683	0.000093998379674
0.900000000000000	-0.161716941356819	-0.161422266230619	0.000294675126200
1.000000000000000	-0.301168678939757	-0.300406575408598	0.000762103531159
L.S.E.	1.364029000926428e-006		

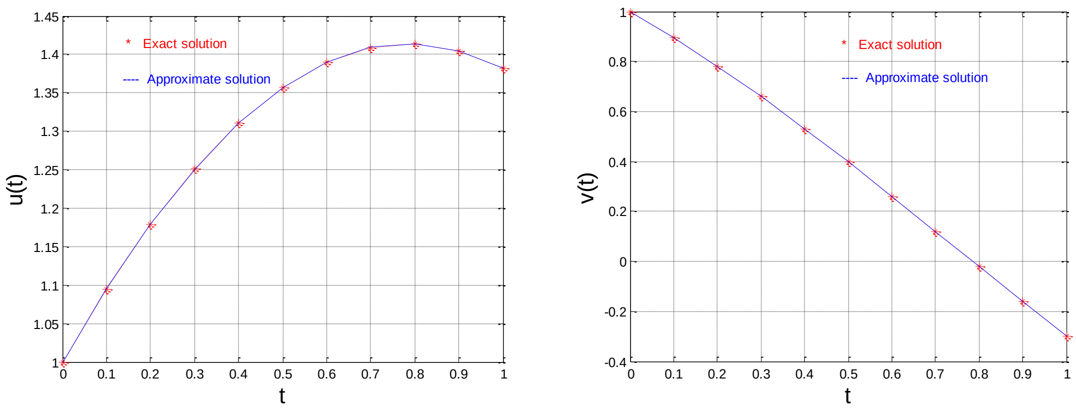

Fig.(1.3) displays a comparison between the exact and numerical solutions obtained using QBS for $u(t)$, and $v(t)$ in example 3, based on the least square error with h=0.1

5. Conclusions:

In this study, we successfully applied the Quintic B-spline method to solve systems of nonlinear Fredholm integro-differential equations of the second kind. The method was validated through three numerical examples, demonstrating high accuracy and efficiency. The comparison between theoretical and numerical solutions using maximum absolute error and least square error norms confirms the reliability of the Quintic B-spline approach. The method's ability to handle complex integro-differential equations makes it a valuable tool for various applications in scientific and engineering fields. The results highlight the potential of Quintic B-splines in providing precise numerical solutions where analytical methods are challenging to apply.

6. Recommendations:

1. Further Research: Future studies should explore the application of the Quintic B-spline method to other types of integro-differential equations and investigate its performance with different boundary and initial conditions.
2. Software Implementation: Developing software tools that incorporate the Quintic B-spline method can make this technique more accessible to researchers and engineers, facilitating its use in practical applications.

3. Comparison with Other Methods: Conducting comparative studies with other numerical methods, such as finite element and finite difference methods, can provide deeper insights into the strengths and limitations of the Quintic B-spline approach.
4. Higher-Dimensional Problems: Extending the method to solve higher-dimensional integro-differential equations can open new avenues for its application in more complex real-world problems.
5. Adaptive Algorithms: Developing adaptive algorithms that adjust the B-spline parameters based on the problem's complexity can enhance the method's efficiency and accuracy.
6. By addressing these recommendations, the potential and applicability of the Quintic B-spline method in solving complex integro-differential equations can be further realized and optimized.

References

[1] Batiha, B., Noorani, M. S. M., & Hashim, I. (2008). Numerical solutions of the nonlinear integro-differential equations. *International Journal of Open Problems in Computer Science and Mathematics. IJOPCM*, *1*(1), 34-42.

[2] Chuong, N. M., & Tuan, N. V. (1995). Spline collocation methods for Fredholm integro-differential equations of second order. *Acta Math. Vietnamica*, *20*(1), 85-98.

[3] Delves, L. M., & Mohamed, J. L. (1985). *Computational methods for integral equations*. CUP Archive.

[4] Jumaa, B. F. (2024). Finite Difference with Quintic B-Splines for Solving a system of nonlinear Volterra Integro-Differential Equations of integer order. *Wasit Journal for Pure sciences*, *3*(2), 8-21.

[5] Gholamian, M., & Saberi-Nadjafi, J. (2018). Cubic B-splines collocation method for a class of partial integro-differential equation. *Alexandria engineering journal*, *57*(3), 2157-2165.

[6] Maleknejad, K., Mirzaee, F., & Abbasbandy, S. (2004). Solving linear integro-differential equations system by using rationalized Haar functions method. *Applied mathematics and computation*, *155*(2), 317-328.

[7] Munguia, M., & Bhatta, D. (2015). Use of cubic b-spline in approximating solutions of boundary value problems. *Applications and Applied Mathematics: An International Journal (AAM)*, *10*(2), 7.

[8] Alam, M., & Pandey, R. K. (2024). Exponentially Fitted Finite Difference Approximation for Singularly Perturbed Fredholm Integro-Differential Equation. *arXiv preprint arXiv:2401.16379*.

[9] Wang, S. (2023). Split-step quintic B-spline collocation methods for nonlinear Schrödinger equations. *AIMS Mathematics*, *8*(8), 19794-19815.

[10] Eldanaf, T. S., Elsayed, M., Eissa, M. A., & Abd Alaal, F. E. E. (2022). Quintic B-Spline Method for Solving Sharma Tasso Oliver Equation. *Journal of Applied Mathematics and Physics*, *10*(12), 3920-3936.

[11] Yalçinbaş, S., & Sezer, M. (2000). The approximate solution of high-order linear Volterra–Fredholm integro-differential equations in terms of Taylor polynomials. *Applied Mathematics and Computation*, *112*(2-3), 291-308.

[12] Pashazadeh Atabakan, Z., Kazemi Nasab, A., & Kılıçman, A. (2013). On solution of Fredholm integrodifferential equations using composite Chebyshev finite difference method. In *Abstract and Applied Analysis* (Vol. 2013, No. 1, p. 694043). Hindawi Publishing Corporation.

Some Properties on Infra Soft Nano α −Open(Closed) Sets

L[1]eqaa M. Saeed Hussein, E[2,*] kram A. Saleh, S[3]abih W. Askandar

[1] Department of Mathematics College of Basic Education, , University of Telafer, Mosul, Iraq

[2] Department of Mathematics College of Computer Sciences and Mathematics, University of Mosul, Mosul, Iraq

[3] Department of Mathematics College of Education for Pure Science, University of Mosul, Mosul, Iraq

[1]Leqaa.m.saeed@uotelafer.edu.iq

[2],*ekram.math@uomosul.edu.iq,

[3]sabihqaqos@uomosul.edu.iq

Some Properties on Infra Soft Nano α −Open(Closed) Sets

L[1]eqaa M. Saeed Hussein, E[2,*] kram A. Saleh, S[3]abih W. Askandar

[1] Department of Mathematics College of Basic Education, , University of Telafer, Mosul, Iraq

[2] Department of Mathematics College of Computer Sciences and Mathematics, University of Mosul, Mosul, Iraq

[3] Department of Mathematics College of Education for Pure Science, University of Mosul, Mosul, Iraq

[1]Leqaa.m.saeed@uotelafer.edu.iq

[2],*ekram.math@uomosul.edu.iq,

[3]sabihqaqos@uomosul.edu.iq

Abstract: In this paper, we explained a soft nano closed (open) set , referred to as an infra soft nano α closed (open) set and infra soft nano semi closed (open) and establish some fundamental features of this set. The connection between the infra soft nano-open(closed)set and other soft nano topological closed (open) sets is investigated. The findings mentioned in this study are preliminary and serve as and in the study are preliminary and serve as an introduction to more advanced research in theoretical and practical areas.

keywords: Nano soft open (closed)set, Nano soft topological space, Infra Nano soft topology, Infra Nana Soft α-open (closed) sets.

Introduction

In 1999, Molodtsov [13] developed custom soft sets, a novel mathematical approach to soft topology. He studied the union operator of open intersections and the difference and complement functions of two soft sets. However, Ali et al. found significant flaws in their definition. In 2003 [14] began to explore the basic principles and concepts of soft set theory . [7] developed new operators and methods to preserve many features and conclusions of soft set theory .In 2011 [8] and [18] defended the use of soft open sets in soft topological spaces (STS). There is a large body of research on topological terms in soft topology [1-3], [9] Many SOS(soft open set) and SCS (soft closed sets) are described in terms of parameter sets μ on some universe *U*. They are then extended to related soft topologies and their properties are examined. [4] introduced the concept of soft open sets in nano topological spaces, with are called nano-soft topological spaces. The separation axiom for NanoZ-topological space [11] defines soft NanoZ-open sets using NanoZ-topological space (SNZ) [10]. Soft topology has been extended to various structures with weaker or stronger topologies, one of which is the fundamental soft topological space (STS). Subsoft α-open sets on subsoft topological spaces have also been studied [4–7], [15–18]. Terms such as subsoft connectivity, subsoft local connectivity, and subsoft compactness are used in these studies.

In this paper, we study infra soft nano $\alpha -$ interior $(\mathrm{ISN}_{\alpha} - \mathrm{int})$ infra soft nano α- closure $(\mathrm{ISN}_{\alpha} - \mathrm{cl})$ infra soft nano $\alpha - o$pen(ISN_{α}OS) infra soft nano α – closed (ISN_{α}-CS) sets, and establish some of their basic characteristics.

.

This means that the infra nano soft topological spaces (INSTS)are flexible for discussing topological spaces and investigating the relationships between them. in INSTS many aspects of nano soft topological spaces are still valid valid, making it easier to establish specific links between certain topological notions. In this paper, we define Infra Soft Nano Topological Space (ISNTS) and Infra soft Nano α −interior (ISN_{α} −int), infra Soft Nano α-closure (ISN_{α} -cl) with some examples and investigate many of their basic properties. we introduce the ideal of ISN_{α}-OS which form a class of ISOS. We give some characterizations of ISN_{α}-OS and ISN_{α}-CS and establish

some of their properties. Additionally, we demonstrate that this class of Soft Nano sets is closed under arbitrary unions and identity the conditions under which it is closed under finite intersection.

2.Preliminaries

Definition2.1 The group of soft parameters. In order to be able to define the soft group, the availability of primitive elements and an E group for the parameter are required. By assuming the existence of the set of all features of the primitive elements, and denoted it as P(U) , the existence of a nonempty subset of the parameter E. The ordered pair (F,A) means a soft set on the primitive elements, where F is a function defined by i.e.any soft set on p is a feature family of subsets. p, which shows that any soft group is not necessarily a grop.see[17]

Definition2.2 This definition dealt with a non-empty set of soft equivalence rows. Through it, the soft upper sets were defined, which include the union of all the soft equivalence rows that are part of the original set, so that if they intersect with the subset of the space, they are a non-empty set. As for the soft lower sets, they are the union of all soft parity rows that are part of the space group. As for the specified soft region, the resultant will be the difference between the upper soft sums and the soft lower sums, see[17]

Definition 2.3 In any soft nano topological space, the largest soft open set of the parameter can defined by finding the union of all the soft open sets of the parameter (A,E) or in short (A, E)the largest partial open soft nano group of the parameter(A,E), see[17]

Definition2.4 A family Ω of soft sets over A with bas a parameter set is said to be an infra soft topology on A if it is closed under finite intersection and Φ is a member of Ω. The triple ðA, Ω,BÞ is called an infra soft topological space (briefly, ISTS). We called a member of Ω an infra soft open set and called its complement an infra soft closed set. We called ðA, Ω, BÞ stable if all its infra soft open sets are stable and called finite (resp., countable) if A is finite (resp., countable). Proposition 15 (see [17]). Let ðA, Ω, BÞ be an ISTS. The.

Definition 2.5[10]

Let $(U,\tau_R^Z(X),\mathfrak{E})$ or $(U,\tau_R^Z(X_{\mathfrak{E}}))$ be a Soft Nano topological space then subset ϖ of U is said soft Nano-z open set if ϖ satisfices the following conditions:

$1 - \forall a \in \varpi,\mathfrak{E})\exists\ SNO\ G_{\mathfrak{E}}$ or $(G.\mathfrak{E})$ such that $a \in G_{\mathfrak{E}} \sqsubseteq SNCl(\varpi,\mathfrak{E})$.

$2 - G_{\mathfrak{E}}$ or $(G,\mathfrak{E})\ U_{\mathfrak{E}} \Leftrightarrow (\varpi,\mathfrak{E}) = (U,\mathfrak{E})$.

3. Infra Soft Nano α −open(closed) sets

Definition3.1 A Nano Soft $(N_{\mathrm{E}},\mathrm{F})$ of universal set U with parameter F is said to be ISN$_\alpha$-OS (ISN$_\alpha$-CS)set if $(N_{\mathrm{E}},\mathrm{F}) \subseteq$N int $(Ncl^*(N\ int(N_{\mathrm{E}},\mathrm{F})\ )$ ([$(Ncl\ (N\ int^*\big(Ncl(N_{\mathrm{E}},\mathrm{F})\big)] \subseteq\ (N_{\mathrm{E}},\mathrm{F})$ The class of all ISN$_\alpha$-OS (ISN$_\alpha$-CS)sets in U_F will be denoted as ISN$_\alpha$-OS (U_F) [ISN$_\alpha$-CS (U_F)]

Definition3.2 Let us consider two Nano soft sets $(N_{\mathrm{E}},Z)\ and\ (N_{\mathrm{E}},\mathrm{F})$, we can then define nano soft closure and Nano soft interior over Universal set U with parameter K. In the following way

$*$ ISN$_\alpha cl(N_{\mathrm{E}},\mathrm{F}) =\cap \{(N_{\mathrm{E}},Z) : (N_{\mathrm{E}},Z) \supseteq (N_{\mathrm{E}},\mathrm{F}), (N_{\mathrm{E}},Z)$ is an ISN$_\alpha$–CS of U }called an ISN$_\alpha$–cl.

$*$ ISN$_\alpha - \ int(N_{\mathrm{E}},\mathrm{F}) =\cup \{\ \{(N_{\mathrm{E}},Z) : (N_{\mathrm{E}},Z)\ \subseteq (N_{\mathrm{E}},\mathrm{F}), (N_{\mathrm{E}},Z)$ is an ISN$_\alpha$ -OS in U}is called on (ISN$_\alpha$ −int)

$*$ ISN$_S\ cl(N_{\mathrm{E}},\mathrm{F}) =\cap \{(N_{\mathrm{E}},Z) : (N_{\mathrm{E}},Z)\ \supseteq (N_{\mathrm{E}},\mathrm{F}), (N_{\mathrm{E}},Z)$

Is an ISN_S CS of U is called an Infra Nano soft semi closure.

$*$ IS$N_S - \ int(N_{\mathrm{E}},\mathrm{F}) =\cup \{(N_{\mathrm{E}},Z) : (N_{\mathrm{E}},Z)\ \subseteq (N_{\mathrm{E}},Z), (N_{\mathrm{E}},\mathrm{F})$ is an ISN_S OS in U is called an Infra Nano soft semi interior

Theorem3.3 A Nano soft$(N_\Upsilon,\mathcal{r})$ set is ISN$_\alpha$–OS (U_F) if and only if there exise a NSOS(N_Υ,F) such that

$$(N_\Upsilon,F) \subseteq (N_\Upsilon,\mathcal{r})\ \subseteq int(cl^*(N_\Upsilon,F))$$

proof: If $(N_\Upsilon,\mathcal{r}) \in$ ISN$_\alpha$– OS (U_F)then $(N_\Upsilon,\mathcal{r}) \subseteq Nint\Big(Ncl^*\big(Nint(N_\Upsilon,\mathcal{r})\big)\Big)$,

put $(N_\Upsilon,F) = Nint(N_\Upsilon,\mathcal{r})$ then

(N_Υ, r) is NSOS and $(N_\Upsilon, F) \subseteq (N_\Upsilon, r) \subseteq Nint(Ncl^*(N_\Upsilon, F))$. In other way , let (N_Υ, F)be a NSOS such that $(N_\Upsilon, F) \subseteq (N_\Upsilon, r) \subseteq Nint(Ncl^*(N_\Upsilon, F))$ therefore

$Nint(Ncl^*(N_\Upsilon, F)) \subseteq Nint(Ncl^*(Nint(N_\Upsilon, r)))$. then $(N_\Upsilon, r) \subseteq Nint(Ncl^*(Nint(N_\Upsilon, r)))$

Theorem 3.4 A Nano soft set (N_Υ, F) is $\text{ISN}_\alpha - \text{OS}\ (U_F)$ if and only if a NSCS (N_Υ, r) such that $Ncl(N\,int^*(N_\Upsilon, r)) \subseteq (N_\Upsilon, F) \subseteq Ncl(N_\Upsilon, r)$.

Proof: If (N_Υ, F) is $\text{ISN}_\alpha\text{CS}\ (U_F)$ ther $Ncl(N\,int^*(Ncl(N_\Upsilon, F))) \subseteq (N_\Upsilon, \text{F})$. Put $(N_\Upsilon, B) = Ncl(N_\Upsilon, F)$ then $(N_\Upsilon, r)$is NSCS and $Ncl(N\,int^*(N_\Upsilon, r)) \subseteq (N_\Upsilon, \text{F})$. In other way . let (N_Υ, r) be a NSCS such that $Ncl(N\,int^*(N_\Upsilon, r)) \subseteq (N_\Upsilon, \text{F}) \subseteq (N_\Upsilon, r)$. This indicates that $Ncl(N\,int^*(Ncl(N_\Upsilon, \text{F})) \subseteq Ncl(N\,int^*(N_\Upsilon, r))$ then $Ncl(N\,int^*(N_\Upsilon, \text{F})) \subseteq Ncl(N_\Upsilon, \text{F})$.

Theorem3.5 Let (N_Υ, μ) be a Nano soft set over universe U and parameter set μ . then the following properties are true

$*$ $\text{INS}_s\ int(N_\Upsilon, \mu) = (N_\Upsilon, \mu) \cap N\,cl(Nint(N_\Upsilon, \mu)$.

$**$ $\text{INS}_s\ cl(N_\Upsilon, \mu) = (N_\Upsilon, \mu) \cup N\,int^*(Ncl(N_\Upsilon, \mu)$.

proof : * By the definition of $\text{INS}_s\ int$ is infra nano soft-semi open(INSSOS)) then $\text{INS}_s - int(N_\Upsilon, \mu) \subseteq Ncl^*(Nint(\text{INS}_s - int(N_\Upsilon, \mu)) \subseteq Ncl^*(Nint(N_\Upsilon, \mu))$, also $\text{INS}_s - int(N_\Upsilon, \mu) \subseteq (N_\Upsilon, \mu) \subseteq Ncl^*(Nint((N_\Upsilon, \mu)) \Rightarrow (1)$

we have $Nint(N_\Upsilon, \mu) \subseteq (N_\Upsilon, \mu) \cap Ncl^*(Nint(N_\Upsilon, \mu)) \subseteq Ncl^*(Nint(N_\Upsilon, \mu))$. by def. 3.2 $(N_\Upsilon, \mu) \cap Ncl^*(Nint(N_\Upsilon, \mu))$ is an INSSOS and $(N_\Upsilon, \mu) \cap Ncl^*(Nint(N_\Upsilon, \mu))$,then $(N_\Upsilon, \mu) \cap Ncl^*(Nint(N_\Upsilon, \mu)) \subseteq \text{INS}_s - int(N_\Upsilon, \mu) \Rightarrow (2)$from (1) &(2) we get (*).

** Similar to the above proof (*).

Theorem 3.7 Let us consider the Nano soft subset $(N_\Upsilon, \text{F})$of a nano Soft space NSS(U_F), the following statements are hold:

$*$) If $(N_\Upsilon, \text{F}) \subseteq (N_\Upsilon, E) \subseteq Nint(Ncl^*((N_\Upsilon, F) \in \text{ISN}_\alpha\text{OS}(U_F)$ then $(N_\Upsilon, E) \in \text{ISN}_\alpha\text{OS}(U_F)$

$**$)if $N\,cl(Nint^*(N_\Upsilon, \text{F}) \subseteq (N_\Upsilon, E) \subseteq (N_\Upsilon, F)\ then\ (N_\Upsilon, F) \in \text{ISN}_\alpha\text{CS}(U_F)$ then $(N_\Upsilon, E) \in \text{ISN}_\alpha\text{CS}(U_F)$

proof: $*$)Let $(N_\Upsilon, \text{F}) \in \text{ISN}_\alpha\text{OS}(U_F)$then $\exists(N_\Upsilon, H)$ an SNOS such that $(N_\Upsilon, H) \subseteq (N_\Upsilon, \text{F}) \subseteq Nint(Ncl^*((N_\Upsilon, H)$ this implies that $(N_\Upsilon, H) \subseteq (N_\Upsilon, r)\ and\ (N_\Upsilon, F) \subseteq Nint(Ncl^*((N_\Upsilon, H)$.

$\Rightarrow\ Nint(Ncl^*((N_\Upsilon,F) \subseteq\ Nint(Ncl^*((N_\Upsilon,H)$ and $(N_\Upsilon,H) \subseteq (N_\Upsilon,\mathscr{r}) \subseteq\ Nint(Ncl^*((N_\Upsilon,H)$ then $(N_\Upsilon,\mathscr{r}) \in \mathrm{ISN}_\alpha\mathrm{OS}(U_F)$

$**$)Same as the proof of $*$

Proposition3.8 Let (N_Υ,F) and (N_Υ,E)be two nana soft sets in (U_k) and $(N_\Upsilon,\mathrm{F}) = (N_\Upsilon,E)$then the following statements are true:

1. $\mathrm{ISN}_\alpha -\ int(N_\Upsilon,F)$ is the largest $\mathrm{ISN}_\alpha\mathrm{OS}$ Contained in (N_Υ,F)
2. $\mathrm{ISN}_\alpha -\ int(N_\Upsilon,F) \subseteq (N_\Upsilon,F)$
3. $\mathrm{ISN}_\alpha -\ int(N_\Upsilon,F) \subseteq \mathrm{ISN}_\alpha -\ int(N_\Upsilon,E)$
4. $\mathrm{ISN}_\alpha -\ int(\mathrm{ISN}_\alpha -\ int(N_\Upsilon,F)) = \mathrm{ISN}_\alpha -\ int(N_\Upsilon,F)$
5. $(N_\Upsilon,F) \in\ \mathrm{ISN}_\alpha\mathrm{OS}(U_F)$ iff $\mathrm{ISN}_\alpha -\ int(N_\Upsilon,F) = (N_\Upsilon,F)$

proposition3:9 Let $(N_\Upsilon,F)$of Jand (N_Υ,E)be two nano soft sets in $\mathrm{NSS}(U_F)$ and $(N_\Upsilon,F) \subseteq (N_\Upsilon,F)$then the following statements are true:

1. $\mathrm{ISN}_\alpha cl(N_\Upsilon,F)$is the smallest $\mathrm{ISN}_\alpha CS$ containing (N_Υ,F)
2. $(N_\Upsilon,F) \subseteq\ \mathrm{ISN}_\alpha cl(N_\Upsilon,F)$
3. $\mathrm{ISN}_\alpha cl(N_\Upsilon,F) \subseteq\ \mathrm{ISN}_\alpha cl(N_\Upsilon,E)$
4. $\mathrm{ISN}_\alpha cl\big(\mathrm{ISN}_\alpha cl(N_\Upsilon,F)\big) = \mathrm{ISN}_\alpha cl(N_\Upsilon,F)$
5. $(N_\Upsilon,F) \in\ \mathrm{ISN}_\alpha\mathrm{cl}(U_F)$ iff $\mathrm{ISN}_\alpha cl(N_\Upsilon,F) = (N_\Upsilon,F)$

Theorem3.10 Let (N_Υ,F)be a nano soft set of NSS (U_F) then the following

assertions are true:

1. $(\mathrm{ISN}_\alpha int(N_\Upsilon,F)^c = \mathrm{ISN}_\alpha cl(N_\Upsilon,F)$
2. $(\mathrm{ISN}_\alpha cl(N_\Upsilon,F)^c = \mathrm{ISN}_\alpha int(N_\Upsilon,F)$
3. $\mathrm{ISN}_\alpha int(N_\Upsilon,F) \subseteq (N_\Upsilon,F) \cap Nint(Ncl^*(Nint(N_\Upsilon,F)$
4. $\mathrm{ISN}_\alpha cl(N_\Upsilon,F) \supseteq (N_\Upsilon,F) \cup Ncl(Nint^*(Ncl(N_\Upsilon,F)$

Proof:

1. $(\mathrm{ISN}_\alpha int(N_\Upsilon,F)^c = \cup \{(N_\Upsilon,E): (N_\Upsilon,E) \subseteq (N_\Upsilon,F)\ , (N_\Upsilon,E)$ is an $\mathrm{ISN}_\alpha\mathrm{OS}$ of $(U_F)^c$ $= \mathrm{ISN}_\alpha cl(N_\Upsilon,F)$
2. Similarly of 1
3. Since $(N_\Upsilon,F) \supseteq \mathrm{ISN}_\alpha int(N_\Upsilon,F)$ and $\mathrm{ISN}_\alpha int(N_\Upsilon,F)$ is an $\mathrm{ISN}_\alpha\mathrm{OS}$. Hence $Nint(Ncl^*(Nint(N_\Upsilon,F) \supseteq\ \mathrm{ISN}_\alpha int(N_\Upsilon,F)$ then $\mathrm{ISN}_\alpha int(N_\Upsilon,F) \subseteq (N_\Upsilon,F)\ \cap\ Nint(Ncl^*(Nint(N_\Upsilon,F))$
4. Similarly of 3

Corollary3.11 Let (N_Υ, F)be a nano soft set of NSS (U_F). then the following assertions are true:

•)If $(N_\Upsilon, F)$is a NSOS, then $\text{ISN}_\alpha int(N_\Upsilon, F) \subseteq Nint(Ncl^*(Nint(N_\Upsilon, F)).$

••) If $(N_\Upsilon, F)$is a NSCS, then $\text{ISN}_\alpha cl(N_\Upsilon, F) \supseteq Ncl(Nint^*(Ncl(N_\Upsilon, F))$

Theorem 3.12 *)The arbitrary Union of an $\text{ISN}_\alpha OS$ is $\text{ISN}_\alpha OS$

**) The arbitrary intersection of an $\text{ISN}_\alpha CS$ is $\text{ISN}_\alpha CS$

Proof: Let $\{(N_\Upsilon, D)\}$ be a family of $\text{ISN}_\alpha OS$. then for every j ,

$(N_\Upsilon, F)_j \subseteq Nint(Ncl^*(Nint(N_\Upsilon, F)_j)$ $and \cup (N_\Upsilon, F)_j \cup (Nint\left(Ncl^*(Nint(N_\Upsilon, F)_j)\right)) \subseteq$ $(Nint\left(Ncl^*(Nint(N_\Upsilon, F)_j)\right))$

Hence $(N_\Upsilon, F)_j$ is $\text{ISN}_\alpha OS$.

**) Similarly *)

Theorem 3.13 Let (Z_Υ, μ) be a nano soft set over the universes U parameter μ. then $Nint^*(Z_\Upsilon, \mu) \subseteq \text{ISN}_\alpha int(Z_\Upsilon, \mu) \subseteq (Z_\Upsilon, \mu) \subseteq \text{ISN}_\alpha cl(Z_\Upsilon, \mu) \subseteq \text{N}cl^*(Z_\Upsilon, \mu)$

proof: Since $Nint^*(Z_\Upsilon, \mu) \subseteq (Z_\Upsilon, \mu)$ this continues that $\text{ISN}_\alpha int(\text{ISN}_\alpha int^*(Z_\Upsilon, \mu) \subseteq \text{ISN}_\alpha int(Z_\Upsilon, \mu)$. then $\text{ISN}_\alpha int(\text{N}int^*(Z_\Upsilon, \mu) = \text{N}int^*(Z_\Upsilon, \mu)$ also $\text{N}int^*(Z_\Upsilon, \mu) \subseteq \text{ISN}_\alpha int(Z_\Upsilon, \mu) \ldots\ldots\ldots\ldots.*$

So using result $(Z_\Upsilon, \mu) \subseteq \text{N}cl^*(Z_\Upsilon, \mu)$, this $\text{ISN}_\alpha cl(Z_\Upsilon, \mu) \subseteq \text{ISN}_\alpha cl(\text{N}cl^*(Z_\Upsilon, \mu))$.then

$\text{ISN}_\alpha cl(\text{N}cl^*(Z_\Upsilon, \mu)) = \text{N}cl^*(Z_\Upsilon, \mu), so\ \text{ISN}_\alpha cl(Z_\Upsilon, \mu) \subseteq \text{N}cl^*(Z_\Upsilon, \mu)$ ……….**

from$*$ & $**$we will get

$Nint^*(Z_\Upsilon, \mu) \subseteq \text{ISN}_\alpha int(Z_\Upsilon, \mu) \subseteq (Z_\Upsilon, \mu) \subseteq \text{ISN}_\alpha cl(Z_\Upsilon, \mu) \subseteq \text{N}cl^*(Z_\Upsilon, \mu)$.

Theorem 3.14 Let (N_Υ, F) be a nano soft set of $(U, \lambda, \mathcal{F})$ then the following assertions hold:-

1- If (N_Υ, F) is an $\text{ISN}_\alpha OS(\text{ISN}_\alpha CS)$than (N_Υ, F) is a $\text{SN}_\alpha OS(\text{SN}_\alpha CS)$

2-If (N_Υ, F) is an $\text{ISN}_\alpha OS(\text{ISN}_\alpha CS)$,then (N_Υ, F) is a nano soft α^* open (Supra nano soft α-open) a nano soft α^* closed (Supra nano soft α- closed) set.

3- If (N_Υ, F) is an $\text{ISN}_\alpha OS(\text{ISN}_\alpha CS)$ then (N_Υ, F) is a nano soft Pre^*open (supra nano soft-preopen) (nano soft Pre^* closed (supra nano soft precloseal) set.

4-If (N_{Υ}, F) is an ISN$_{\alpha}OS$(ISN$_{\alpha}CS$) then (N_{Υ}, F) is a nano soft semi open (ISN_sOS) (nano soft semi* closed (ISN_sCS).

5- If (N_{Υ}, F) is a N SOS(NSCS) then (N_{Υ}, F) is ISN_sOS (ISN_sCS).

proof: By the definitions 2.1 , 2.2 and 3.1 and basic relationships with other nano soft sets, we can prove above results..

Remark3.15 Any NSOS ⇒is supra nano soft α openset, ISN_{α}OS⇒ SN_{α}OS,

, SN_{α}OS⇒ SSN_{α}OS , SN_{α}OS⇒ SSN_{α}OS & S pre-OS, ISN_{α}OS⇒ $ISSN_{\square}$OS and SSN_{pre}OS, SN_{pre}OS ⇒ SSN_{pre}OS , $ISSN_{o}$S ⇒ SSN_{o}S . there is no connections between $ISSN_{o}S$ *and* $SSN_{\text{pre}}S$

The following examples will show that the converses of remark need not to be true.

Example 316 Let $U = \{z, h, l, f\}$,$\mu = \{e_1, e_2, e_3\}$,
$(\kappa, \mu) = \{(e_1, \{z\}), (\{e_2, l\}), (\{e_3, \{h, l\}\})\}$ be a soft set over U and $X = \{z, h\} \subseteq U$then
$U/R = \{\{z\}, \{l\}, \{h, l\}\}$ and Nano soft sets
$=$
$\{\sigma_{\mu}, U_{\mu}, (\{e_1, \kappa_1\}), (\{e_2, \kappa_1\}), (\{e_3, \kappa_1\}), (\{e_1, \kappa_{11}\}), (\{e_2, \kappa_{11}\}), (\{e_3, \kappa_{11}\}), (\{e_1, \kappa_8\}), (\{e_2, \kappa_8\}$
with $(\kappa_1, \mu) = \{(\{e_1, \{z\}), (\{e_2, \{\kappa_1\}\}), (\{e_3, \{\kappa_1\}\})\}$,
$(\kappa_2, \mu) = \{(\{\mu, \{h\}\})\}, (\kappa_3, \mu) = \{(\mu, \{l\})\}, (\kappa_4, \mu) = \{\mu, \{f\}\}, (\kappa_5, \mu) = \{\mu, \{z, h\}\}, (\kappa_6, \mu) = \{\mu, \{z, l\}\}, (\kappa_7, \mu) = \{\mu, \{z, f\}\}, (\kappa_8, \mu) = \{\mu, \{h, l\}\}$
, $(\kappa_9, \mu) = \{\mu, \{h, f\}\}, (\kappa_{10}, \mu) = \{\mu, \{l, f\}\}$
, $(\kappa_{11}, \mu) = \{\mu, (\{z, h, l\})\}$, , $(\kappa_{12}, \mu) = \{\mu, (\{z, h, f\})\}$, $(\kappa_{13}, \mu) = \{\mu, (\{h, l, f\})\}$
, $(\kappa_{14}, \mu) = \{\mu, (\{z, l, f\})\}$

(κ_7, μ) is ISS NOS but it is not $SSN_{\text{pre}} - \text{OS}$.

(κ_9, μ) is ISSNOS but it is not a SNOS

(κ_{11}, μ) is a $SSN_{\text{pre}} - \text{OS}$ set but it is not ISSNOS.

(κ_{12}, μ) is $SSN_{\text{pre}} - \text{OS}$ but it is not (SNOS.

(κ_{12}, μ) is $SSN_{\text{pre}} - \text{OS}$ but it is not ISN_{α}OS

(κ_9, μ) is ISSNOS but it is not ISN_{α}OS

Example 3.17 Let $U = \{z, l, r\}, \mu = \{e_1, e_2\}, \{\kappa, \mu\} = (e_1, \{l\}), (e_2, \{l, r\})$ be a soft set of U and $X = \{h, r\} \subseteq U$ with $U/R = \{\{l\}, \{z, r\}\}$ nano soft sets $(\tau_R(x)\mu) = \{\sigma_\mu, U_\mu, (e_1, \{h\}), (e_2, \{h\})\}$ with $(\kappa_1, \mu) = \{(\mu, \{h\})\}$, $(\kappa_2, \mu) = \{(\mu, \{l, r\})\}$

(κ_2, μ) is SSN_αOS but it is not ISN_αOS.

(κ_2, μ) is SSN_αOS but it is not SN_OS.

(κ_2, μ) is SN_αOS but it is not ISN_αOS.

(κ_2, μ) is SSN_OS but it is not ISN_αOS.

(κ_2, μ) is SN_{pre}OS but it is not ISN_αOS.

References

[1] D. Andrijevic, "Semi-preopen sets," Mathematics Vesnik, vol. 38, no. 1, pp. 24-32, 1986.

[2] M. Akdag and A. Ozkan, "Soft α-open sets and soft α-continuous functions," Abstract and Applied Analysis, vol. 2014, Article ID 891341, 7 pages, 2014

[3] M. Akdag and A. Ozkan, "Soft β -open sets and soft β-continuous functions," Hindawi Publishing corporations, The Scient. World Journal, vol. 2014, Article ID 843456, 6 pages, 2014

[4] T. M. Al-shami, "New soft structure: infra soft topological spaces, " Mathematical Problems in Engineering, vol. 2021, Article ID 3361604, p. 12, 2021.

[5] T. M. Al-shami, "Infra soft compact spaces and application to fixed point theorem," Journal of Function Spaces, vol. 2021, Article ID 3417096, 9 pages, 2021.

[6] T. M. Al-shami and E. A. Abo-Tabl, "Connectedness and local connectedness on infra soft topological spaces," Mathematics. vol. 9, no. 15, 2021

[7] M. I. Ali, F. Feng, X. Liu, W.K. Min and M. Shabir " On some new operations in soft set theory", Computers and Mathematies with Applications, Vol5,no.9, pp 1547-1553,2009

[8] N. Çağman, S. Karataş, and S. Enginoğlu, "Soft topology," Computer and Mathematics with Applications, vol. 62, no. 1. pp. 351-358, 2011.

[9] B. Chen, "Soft Semi-open sets and related properties in soft topological spaces," Applied Mathematics and Information Sciences, vol. 7, no. 1, pp. 287-294, 2013.

[10] S.A.Ekram,F.M.Ahmad and Umit "Soft Nano-Z-Topological Spaces" Baghdad sciences journal, accepted ,2024

[11] S.A.Ekram "Separation axioms of nano-z-topological space" 2nd International Conference of Mathematics, Applied Sciences, Information and Communication Technology AIP Conf. Proc. 2834, 080018-1–080018-6;2023 https://doi.org/10.1063/5.0161580 Published by AIP Publishing. 978-0-7354-4715-8/$30.00.

[12] M John Peter and R Manoharan Infra Soft α-Open (Closed) Sets on Infra Soft Topological pace" International journal of Mechanical, Vol.7 no.2,2022 p.380-385.

[13] D. Molodtsov, "Soft set theory-first results," Computers and Mathematics with Applications, vol. 37, no. 4-5, pp. 19-31, 1999.

[14] P. K. Maji, R. Biswas, and A. R. Roy, "Soft set theory," Computers and Mathematics with Applications, vol. 45, no. 4-5, pp. 555- 562,2003

[15] H. A. Othman, On Fuzzy supra-preopen sets, Ann. Fuzzy Math. Inform., 12, No. 3 (2016) 361-371.

[16] H. A. Othman and Md. Hanif. Page, On an Infra-a-Open Sets, Global Journal of Mathematical Analysis, 4, No. 3 (2016) 12- 16.

[17] P.G.Patil, Nivedita Kabbur and J. Pradeepkumar, Weaker forms on soft nano open set, journal of Computer and Mathematics Sciences. 2017

[18] M. Shabir and M. Naz, "On soft topological spaces," Computers and Mathematics with Applications, vol. 61, no. 7, pp. 1786-1799,2011.

[19] M. Tareq Al-shami and A.A.Azzam, " Infra soft semiopen sets and Infra soft semicontinuity" Journal of Function Spaces, vol. 2021, Article ID 5716876, 11 pages,